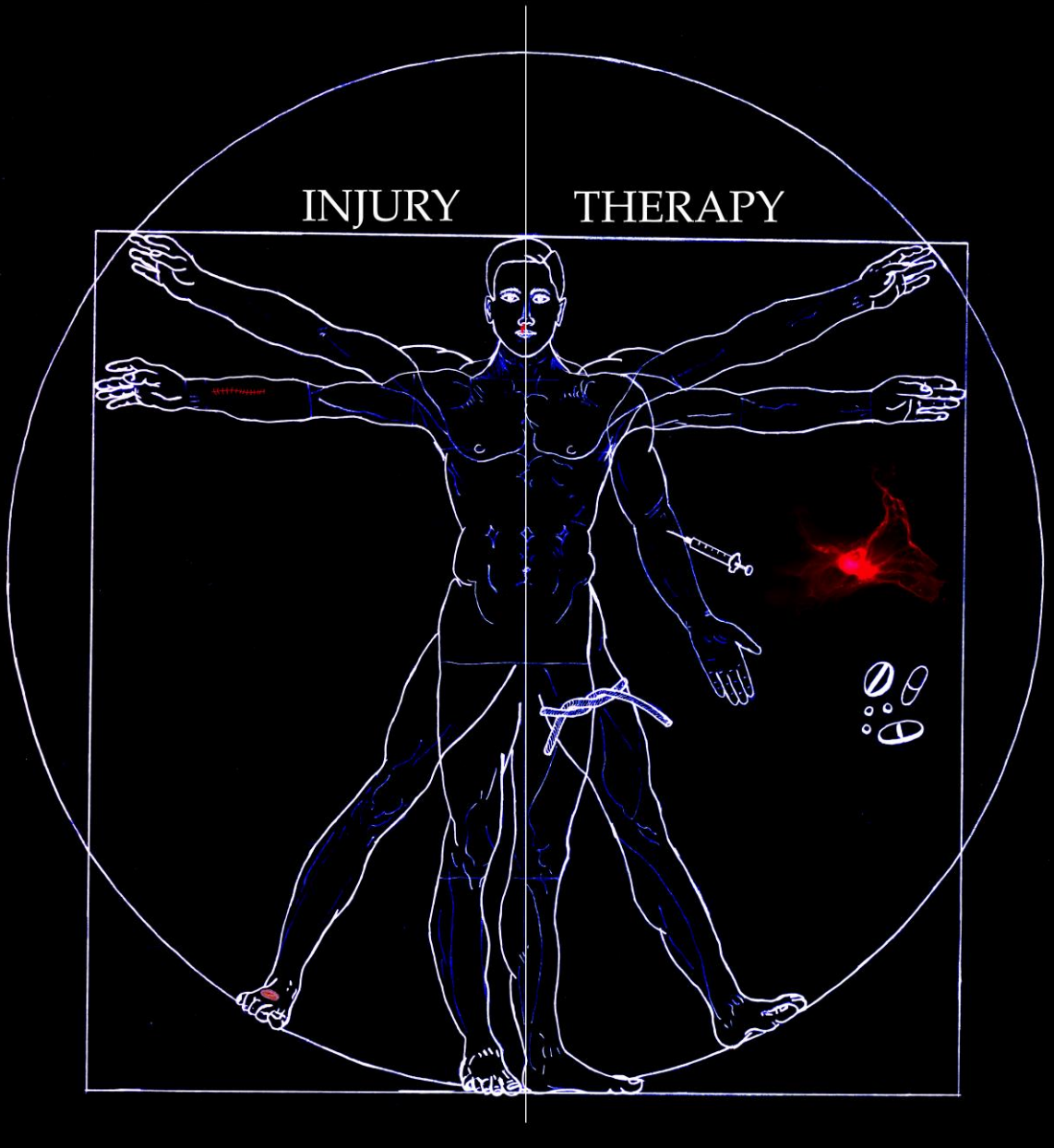


Cytoprotective mechanisms, palatogenesis, and wound repair



Niels A.J. Cremers

Cytoprotective mechanisms, palatogenesis, and wound repair

Niels A.J. Cremers

Colofon

ISBN: 978-94-6380-255-0

The research described in this thesis was performed at the laboratory of Orthodontics and Craniofacial Biology, Department of Dentistry, Radboud university medical center, Radboud Institute for Molecular Life Sciences, Nijmegen, the Netherlands. The work was in part supported by the Dutch Burns Foundation (Brandwondenstichting, grant 09.110) and the Radboud university medical center.

Printing: proefschriftmaken.nl

Cover Design: Niels A.J. Cremers

Layout: proefschriftmaken.nl

Copyright ©: Niels A.J. Cremers

All rights reserved. No parts of this publication may be reported or transmitted, in any form or by any means, without permission of the author.

Cytoprotective mechanisms, palatogenesis, and wound repair

Proefschrift

ter verkrijging van de graad van doctor

aan de Radboud Universiteit Nijmegen

op gezag van de rector magnificus prof. dr. J.H.J.M. van Krieken,

volgens besluit van het College van Decanen

in het openbaar te verdedigen op maandag 18 maart 2019

om 16.30 uur precies

door

Niels Antonius Johannes Cremers

geboren op 27 juli 1985

te Venray

Promotoren:

Prof. dr. C.E.L. Carels

Prof. dr. A.M. Kuijpers-Jagtman

Copromotor:

Dr. F.A.D.T.G. Wagener

Manuscriptcommissie:

Prof. dr. G.J. Meijer

Prof. dr. E. Middelkoop (VU)

Dr. H.A.M. Mutsaers (Aarhus University)

Cytoprotective mechanisms, palatogenesis, and wound repair

Doctoral Thesis

to obtain the degree of doctor

from Radboud University Nijmegen

on the authority of the Rector Magnificus prof. dr. J.H.J.M. van Krieken,

according to the decision of the Council of Deans

to be defended in public on Monday, March 18, 2019

at 16.30 hours

by

Niels Antonius Johannes Cremers

Born on July 27, 1985

in Venray (the Netherlands)

Supervisors:

Prof. dr. C.E.L. Carels

Prof. dr. A.M. Kuijpers-Jagtman

Co-supervisor:

Dr. F.A.D.T.G. Wagener

Doctoral Thesis Committee:

Prof. dr. G.J. Meijer

Prof. dr. E. Middelkoop (VU)

Dr. H.A.M. Mutsaers (Aarhus University)

Printing of this thesis was financially supported by:

Radboud University



Radboudumc
university medical center

Institute for Molecular Life Sciences
Radboudumc

Contents

Chapter 1 General introduction

PART I: Decreased protective mechanisms hamper tissue repair and craniofacial development

Chapter 2 Delayed cutaneous wound closure in heme oxygenase-2 deficient mice despite normal heme oxygenase-1 expression. *J Cell Mol Med.* 2014;18:2488-98.

Chapter 3 Chemokine signaling during midline epithelial seam disintegration facilitates palatal fusion. *Front Cell Dev Biol.* 2017;5:94.

Chapter 4 Mechanical stress changes the complex interplay between heme oxygenase-1, inflammation and fibrosis during excisional wound repair. *Front Med (Lausanne).* 2015;2:86.

PART II: Activation of protective mechanisms to enhance tissue regeneration

Chapter 5 Curcumin-induced heme oxygenase-1 expression prevents H₂O₂-induced cell death in wild type and heme oxygenase-2 knockout adipose-derived mesenchymal stem cells. *Int J Mol Sci.* 2014;15:17974-99.

Chapter 6 Effects of remote ischemic preconditioning on heme oxygenase-1 expression and cutaneous wound repair. *Int J Mol Sci.* 2017;18:438.

Chapter 7 Heme scavenging discriminates between tissue survival and immune activation. *Submitted, 2018.*

PART III: General discussion and Summary

Chapter 8 General discussion and future perspectives

Chapter 9 Summary

Chapter 10 Samenvatting

Dankwoord

Curriculum Vitae

List of publications

PhD portfolio

Chapter 1

General introduction

Abbreviations

CCR2	C-C chemokine receptor type 2
CL/P	Cleft lip and/ or palate
CO	Carbon monoxide
CXCL10	C-X-C motif chemokine 10
ECM	Extracellular matrix
EMT	Epithelial to mesenchymal transition
HO	Heme oxygenase
IL-8	Interleukin-8
IPC	Ischemic preconditioning
IRI	Ischemia-reperfusion injury
MCP-1	Monocyte chemoattractant protein-1
MES	Midline epithelial seam
MSC	Mesenchymal stem cells
nrf2	Nuclear-related factor-2
RIPC	Remote ischemic preconditioning
ROS	Reactive oxygen species
TGF- β	Transforming growth factor-beta
VEGF	Vascular endothelial growth factor

1.1 Introduction

Cleft lip and/ or palate (CL/P) is the most common developmental craniofacial disorder affecting the upper lip, the alveolus and the roof of the mouth (1, 2). The prevalence of CL/P is 1:500-1:1000 per newborn with ethnic and geographic variation (3). CL/P can be classified in different phenotypes, and be limited to one side (unilateral) or be a double-sided (bilateral) cleft of the lip, with or without a cleft of the alveolus and/ or palate, and can also occur as an isolated cleft palate only (4, 5). Figure 1.1 shows some common types of orofacial clefts and subsequent scar formation following CLP surgery. The most severe form is a complete bilateral cleft with a cleft in both the soft and the hard tissues of the palate (6).

Around thirty percent of the CL/Ps are syndromic and have additional phenotypic abnormalities, such as Pierre Robin, and Van der Woude syndrome, whereas seventy percent are non-syndromic and caused by a combination of genetic and environmental factors (7). Diverse genes are associated with the development of CL/P in humans, including deletions and mutations in P63, PVRL1, CLPTM1, TBX22, IRF6 (van der Woude syndrome), and SOX9 (Pierre Robin syndrome) (8). More details on genetic factors concerning CL/P are reviewed in (7, 9). Environmental factors to which pregnant mothers are exposed and are associated with an increased risk for CL/P include smoking, alcohol, anti-epileptic drugs, diabetes, infections, age >40 years, folate deficiency, zinc deficiency and contact to teratogens, such as chemical solvents, pesticides, valproic acid, phenytoin, and retinoic acid (10).

Nutritional guidelines for pregnant women and women who plan to have a baby as prevention for getting babies with CL/P include sufficient intake of folic acid and certain vitamins, and keeping a healthy lifestyle shortly before and during pregnancy (11, 12). Unfortunately, despite these guidelines CL/P development cannot be prevented completely as a result of the interplay between genetic predispositions and environmental factors. Therefore, more insight into the molecular mechanisms leading to CL/P and scar formation is necessary.

1.2 Sequelae of the presence of an orofacial cleft

The presence of an orofacial cleft leads to functional, esthetic, and psychosocial problems (Figure 1.1) (1, 13). Well-known functional problems in children with CL/P are sucking and feeding problems, hearing impairment, and speech problems. Surgical intervention is needed to repair the cleft (14, 15).

There are many different protocols used in the world to repair CL/P (16). In the Radboudumc, Nijmegen, the Netherlands, CL/P patients normally undergo their first surgery at an early age of 6-12 months to close the lip and soft palate, and the second surgery at three years to close the hard palate. Patients with CL/P require care by a multidisciplinary team of specialists, including a plastic and reconstructive surgeon, maxillofacial surgeon, orthodontist, otolaryngologist, speech therapist, pediatrician, geneticist, and sometimes a psychologist (17, 18).

Despite the surgical closure of the cleft, scar formation at the lip and the palate may further contribute to the morbidity (Figure 1.1) (19, 20). The scarring impairs subsequent maxillofacial growth and interferes with the development of the dentition.

Inadequate repair of the soft palate can lead to velopharyngeal insufficiency (21, 22). Ten to thirty percent of the treated patients remain unable to achieve adequate velopharyngeal function and develop complications (23, 24).

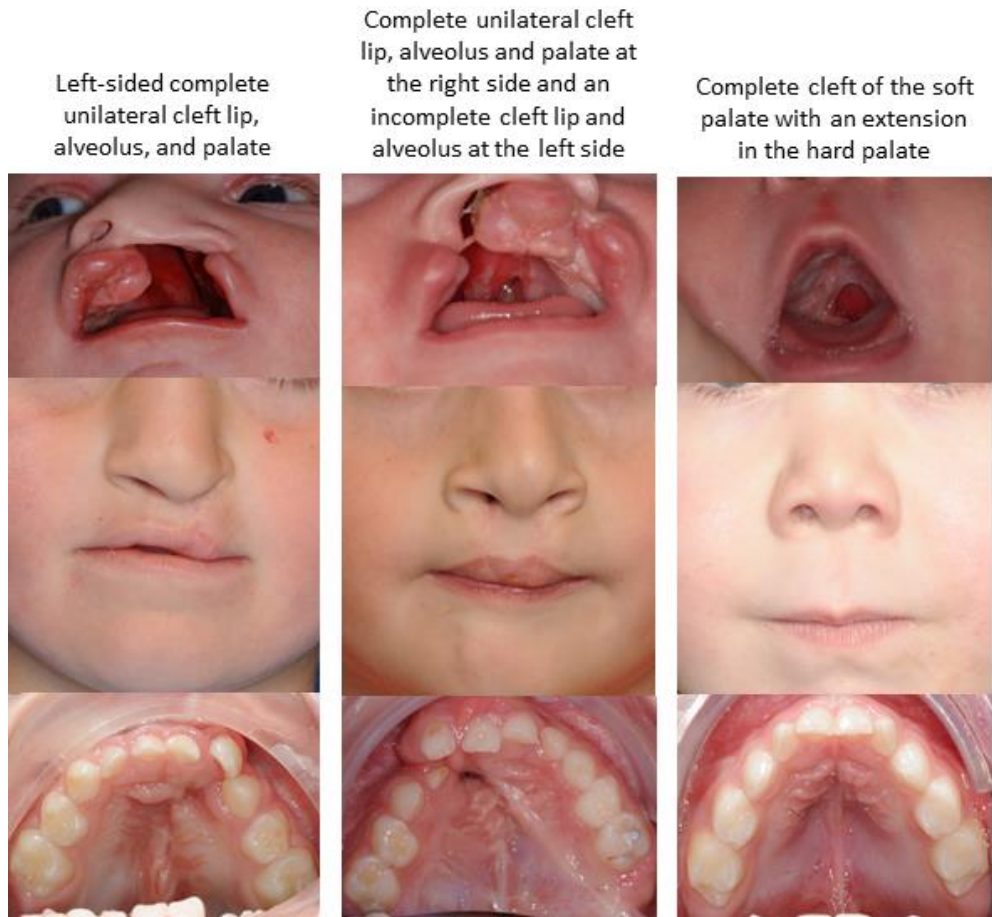


Figure 1.1: Different types of orofacial clefts before and after operation

On the top row, extra-oral pictures before surgery at the age of 2-4 weeks. The photos in the middle row represent the same persons as above at the age of 5 years, after CL/P surgery showing scar formation of the lip and deformation of the nose as a result of the repaired cleft (only first and second picture from the left). The intra-oral pictures of the maxilla on the bottom row show scar formation of the palate. *(Pictures are courtesy of Maarten Suttorp, and are shown with the informed consent of the patients' representative).*

Following tissue injury, for instance, due to surgery, inflammation is initiated to destroy invading pathogens and to eliminate injurious agents and damaged cells (25). Although inflammation is a protective and necessary process, the inflammatory process needs to be tightly controlled to prevent chronic inflammation (26, 27). Extended excessive oxidative and inflammatory stress may overwhelm adaptive protective mechanisms and aggravate tissue damage (28, 29). Processes that are important during embryological development play a similar role during wound repair (30). However, in contrast to adult wound repair,

inflammation during early embryological wound repair is attenuated, subsequently resulting in reduced scar formation (30-32).

Resolution of inflammation is important to restore tissue homeostasis, to allow a smooth wound repair and to minimize scar formation (29, 33). Controlling the pro-oxidative and pro-inflammatory stressors by induction of cytoprotective mechanisms that regulate inflammation and tissue repair may thus be necessary to promote tissue regeneration (34). For example, excessive levels of the pro-inflammatory and pro-oxidative free heme that get released during tissue injury may lead to pathological wound repair (35). Targeting protective mechanisms that neutralize free heme molecules by administration of heme-binding proteins (e.g., hemopexin) or promoting enzymatic degradation by heme oxygenase (HO) may provide therapeutic potential (36, 37). Since the surgeries in CL/P patients to close the cleft are planned, this offers a therapeutic window for preconditioning strategies whereby induction of cytoprotective genes such as nuclear-related factor-2 (nrf2), HO-1, hemopexin, and biliverdin reductase before surgery may protect against subsequent harmful stressors (38-42).

This thesis aims to better explore the molecular and cellular mechanisms that discriminate between tissue repair and tissue regeneration and proof the hypothesis that the induction of cytoprotective pathways leads to improved wound repair. Hereto, we focused on novel therapeutic strategies that harness inflammation and promote wound regeneration.

What is the difference between tissue repair and tissue regeneration?

Tissue repair is the restoration of damaged tissue and allows some functionality, but the deposition of connective tissue during this process leads to various degrees of scar formation. Tissue regeneration is the successful renewal of the tissue to its original state without scars and no hampered functionality. While wound repair is also often used to define the wound healing process itself, wound regeneration usually refers to the end state of wound repair.

The etiology of scar formation following cleft surgery is not entirely understood. However, mechanical tension on the healing wound by facial growth and excessive inflammation further exacerbates scar formation (43). The scars on the palate may restrict normal midfacial growth and impair dento-alveolar development (44). Besides functional problems caused by the scars, cosmetic and psychological problems may occur in CL/P patients (45, 46). It has been shown that in individuals with a cleft that never had cleft surgery, such as in less developed countries and isolated habitats, midfacial growth is within normal limits (47, 48). However, not performing surgery strongly worsens speech development while functional, esthetic, and social problems remain (31, 49). This underscores the need for novel strategies to attenuate scar formation after surgery.

A paradigm within regenerative biology is that molecular and cellular pathways controlling tissue generation during embryonic development often also control wound repair (30). Therefore, mechanisms regulating developmental processes during palatogenesis are likely to provide critical insights into tissue repair and its influence on homeostasis following palatal injury. Often mesenchymal-epithelial cross-talk orchestrates processes as migration, proliferation, and apoptosis. Better insight into the etiology of CL/P

may eventually thus also lead to novel preventive and therapeutic strategies for scar formation.

1.3 Disturbed palatogenesis and the etiology of CL/P compared with wound repair

The palate consists of two distinct regions, the bony and immobile hard palate, and the mobile posterior fibro-muscular soft palate (7). The palate of humans and other mammals is formed by the fusion of the primary palate, which includes the alveolar arch, and the secondary palate that consists of the hard and soft palate (50).

Development of the palate in humans starts the fourth week after conception, and is a sequential process that involves vertical palatal shelf growth (week 7)(Figure 1.2A), shelf elevation (week 8) and formation of the midline epithelial seam (MES) by attachment of the palatal shelves (weeks 9-12) (Figure 1.2B), and the subsequent disappearance of the MES and fusion of the mesenchyme (11, 51). Several mechanisms have been postulated to explain the disappearance of the MES: cell migration, apoptosis, and epithelial to mesenchymal transition (EMT) (Figure 1.2C) (52, 53). Failure of MES disintegration results in cleft palate. However, the etiology of clefting remains still mostly unclear and is complex and multifactorial (9).

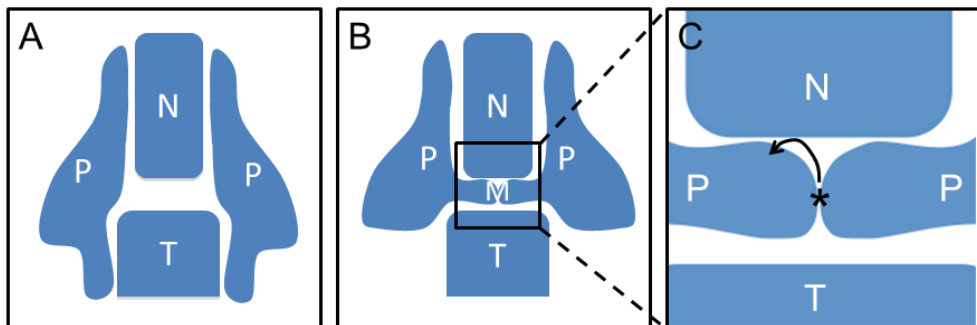


Figure 1.2: Palatogenesis and the disappearance of the midline epithelial seam (MES)

A). The bilateral palatal shelves (P) aligned next to the nose (N) grow down vertically along the sides of the tongue (T). B). The tongue develops downwards together with the growth of the mandible making space for the elevation of the palatal shelves to grow horizontally and form the midline epithelial seam (M) at the place where the palatal shelves connect. C). Magnification of the attachment of the palatal shelves leading to the MES formation; the asterisk depicts epithelial cells that may either go into apoptosis, differentiate into other cells, or migrate from the MES towards the side of the palate as depicted by the arrow.

Palatogenesis has much in common with the wound repair process. During wound repair, different cell types are recruited to the site of injury where they proliferate, differentiate, and synthesize extracellular matrix (ECM) to restore the lost tissue. Inflammatory and damaged cells go into apoptosis, and re-epithelialization occurs by proliferation of epithelial cells and keratinocytes and migration of these cells towards each other at the wound edges, after which structural re-organization follows (20, 30). These processes can be compared with the elongation of the palatal shelves towards each other, the formation of the MES, and the migration and apoptosis of cells during the disappearance of the MES, palatal fusion and the re-organization of ECM to regenerate the tissue (20). Moreover, from the top 35 genes associated with CL/P selected by Biggs *et al.*, about 50% share a known role in

craniofacial development and wound repair, confirming strong similarities between these two processes (20). For example, patients with Van der Woude syndrome have mutations in the IRF6 gene, and this leads to more and major wound complications following CL/P surgical repair (54). A role for IRF6 in wound healing is further supported by its effects on differentiation, proliferation, and migration of epithelial cells (54-57). In this thesis, we will mainly focus on genes involved in the inflammatory response and cytoprotective pathways.

1.4 Wound repair and scar formation

The skin's main function is to maintain homeostasis, to regulate the temperature, electrolyte balance and to act as a barrier against external harmful agents, including radiation and pathogens (58). The skin of the body consists of several layers; the epidermis, dermis, and hypodermis, which further comprise different layers. The lip, in addition, has a deeper muscle layer (*m. orbicularis oris*) and oral mucosa on the inside. It is important to connect these different layers correctly during reconstructive CL/P surgery because this affects the function of the lip during speech and laugh, and its esthetics. The hard and soft palate are involved in different functions that include speech, hearing, sucking and swallowing (48, 59). Surgical cleft palate repair aims to close the cleft and to reconstruct the velopharyngeal musculature to improve velopharyngeal function. However, this leads to the formation of scar tissue that interferes with normal growth and functioning.

Wound healing is a dynamic and precisely coordinated process of sequential cellular, molecular and biochemical events, which are aimed to restore the integrity of the injured tissue as quickly as possible (60-63). Following hemostasis, the healing process is divided into three distinct, but overlapping phases: inflammation, proliferation, and remodeling (Figure 1.3) (61, 64, 65).

First, blood components leak into the site of injury and platelets aggregate together with fibrin (66). The platelets release growth factors and cytokines, initiating the inflammatory phase and attract granulocytes, macrophages, and lymphocytes (65). The granulocytes will clear the wound from invading pathogens and cellular debris (67). At the wound site monocytes differentiate into macrophages and play different roles (68, 69). Here, a pro-inflammatory subset of macrophages initially promotes the inflammatory phase by attracting additional leukocytes via pro-inflammatory cytokines and chemokines, such as IL-8, MCP-1, CCR2, and CXCL10 (70). Later, anti-inflammatory macrophages promote resolution of inflammation by clearing apoptotic cells and producing anti-inflammatory cytokines, such as IL-10, TGF- β , and VEGF (25, 71). These cytokines stimulate keratinocytes, fibroblasts, and endothelial cells to promote tissue regeneration (72).

The proliferative phase is characterized by the replacement of the provisional matrix with newly formed granulation tissue (re-epithelialization) (73). The cellularity of the wound increases as fibroblasts, epithelial cells, and vascular endothelial cells migrate to the site of injury and start to proliferate, restoring the structure and function of the injured tissue (74). A proper vascular structure is of additional importance for supplying oxygen and nutrients, and quick tissue repair (75). Moreover, wound sizes are decreased by myofibroblasts that through the interactions with surrounding ECM and the expression of smooth muscle actin contract the wound (76). Myofibroblasts continue to produce ECM and then usually go into apoptosis (77).

The remodeling phase begins about a week after injury and may continue for years (31, 72). The dense fibers of collagen, which are produced by (myo-) fibroblasts during the earlier phases of wound healing, undergo remodeling (76). The aim of this remodeling is to create greater tensile strength. Tensile strength is restored to 20% of its original strength after three weeks and gradually increases to a maximum of 80% in approximately one year (60, 78). Under optimal situations, this leads to the formation of an acellular scar (79).

However, during pathologic wound healing in the abundance of oxidative, inflammatory, and mechanical stressors, these efficient and well-coordinated processes of wound repair are disturbed and can result in excessive scarring (Figure 1.3).

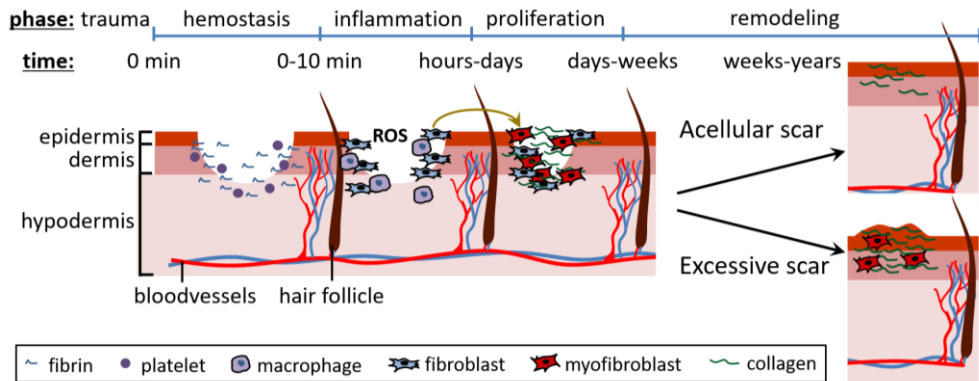


Figure 1.3: Wound repair may result in scar formation.

Platelets and fibrin clot together to advance hemostasis, during which pro-inflammatory cytokines and reactive oxygen species (ROS) are produced that attract inflammatory cells, including granulocytes and macrophages, or normal skin cells, such as fibroblasts and keratinocytes, to form new tissue. Fibroblasts differentiate into myofibroblasts and contract the wounds to protect against external pathogens and for a quicker wound repair. During the proliferation phase, there is an increase in skin cells and secretion of extracellular matrix (ECM), which is mainly caused by the myofibroblasts. During normal wound repair, myofibroblasts go into apoptosis, and wound remodeling leads to an acellular scar, however under pathological conditions myofibroblasts fail to die and continue contraction and the production of ECM, leading to excessive scar formation.

1.5 Mechanical, oxidative, and inflammatory stress promote excessive scar formation

Hampered wound repair can lead to chronic non-healing wounds and severe scar formation, e.g., hypertrophic or keloid scars, and may result in loss of function, itching, and cosmetic malformations (33, 80-84). Keloids have a genetic linkage and contain thick collagen fibers, whereas hypertrophic scars contain thin collagen fibers, which are organized into nodules (85, 86). The quality of the wound healing process is determined by the cause and severity of the trauma, environmental factors and individual conditions, like age (87), weight (88), nutritional status (60, 89), hydration status, comorbidities (88), and medication (62, 72). In most chronic wounds, the healing process gets stuck in the inflammatory or proliferative phase (90, 91). In acute and chronic wounds, growth factors, cytokines, proteases, and ECM molecules play important roles in the different stages of the healing process (61). Alterations in one or more of these components could lead to impaired wound repair. The vital role of a good working vasculature structure is supported by diabetic and elderly

patients, which often suffer from bad healing ulcers due to the lack of good blood supply (92). In addition, ischemia and oxidative damage by reactive oxygen species (ROS) may have an important role in the non-healing nature of chronic wounds and scar development in acute wounds (93). Myofibroblasts speed up wound healing by contraction and by secreting ECM molecules. When these cells fail to go into apoptosis, myofibroblasts continue to produce ECM (77, 84, 94). These persisting myofibroblasts can lead to mechanical stress on the wound and scar formation (Figure 1.3) (76). Also, since babies with a cleft are still growing, this leads to extra mechanical stress on the healing wound and may promote excessive scar formation (13).

Under pathologic conditions, such as prolonged inflammation and elevated levels of ROS, defective wound repair can develop into chronically inflamed open wounds and/or excessive scarring (33, 81). Patients with increased oxidative stress and inflammation, such as diabetic, obese, and elderly people are more prone to develop pathologically healing wounds, fibrosis, and scar formation, and their progeny have increased incidence in congenital abnormalities, such as CL/P, despite current therapies (95-100). Impaired wound healing should be addressed with suitable and effective therapies, for example by the inhibition of the inflammatory response in injured tissues (27). Proper wound care stands at the basis of wound repair as it determines the outcome of the regenerating tissue. Wound repair strategies have evolved for millennia, but the repair process is still not completely understood.

1.6 Evolution of wound repair strategies throughout history

Throughout history, humans have been exposed to injuries and challenged to prevent blood loss and infection. One of the oldest medical manuscripts describing wound care is a Sanskrit clay tablet (Persia) dating back to 2200 BC (101). The tablet describes three healing procedures that still exist today: washing the wound (cleansing), making plasters (topical therapy), and bandaging the wounds (dressings) (102). Plasters consisted of mixtures of substances including mud or clay, molded bread, meat, oil, plants, and herbs, and were applied to wounds to achieve hemostasis and provide protection (103).

Egyptians used honey, *Aloe vera*, animal fat, and lint as described in the Smith and Ebers papyri in circa 1600 BC and 1500 BC, respectively (104, 105). Although the Egyptians closed the wounds mainly to prevent evil spirits from invading, it also had functional effects. The lint probably aided wound drainage, the fat provided a barrier to environmental pathogens, molded bread led to the production of penicillin, and the honey served as a natural antibiotic, and thereby together preventing infection (106). The use of honey for wound therapy was also used in India more than two millennia ago and is still part of modernly advanced wound dressings (107, 108).

The Greeks stressed the importance of cleanliness and washed the wounds with clean (first boiled) water, vinegar (acetic acid), and wine as described by Hippocrates (400 BC) (103, 109). In addition, they applied cold or a tourniquet to stop bleeding and used a tin pipe (syringe) for drainage of pus (110). They also acknowledged the importance of rapid wound closure and discriminated between acute (fresh) and chronic (non-healing) wounds (103).

The Roman Celsus (25BC- 50AD) focused, in addition to controlling hemorrhage, also on inflammation, and was the first to describe four fundamental signs of infection: rubor, tumor, calor, and dolor (redness, swelling, heat, and pain) (110, 111).

Two centuries later, the Greek surgeon Galen of Pergamum (200 BC), who served Roman gladiators, made large contributions to the fields of anatomy and physiology and postulated different treatments to stop hemorrhage (112). He acknowledged the importance of maintaining wound-site moisture, applied styptics, used silk to tie off bleeding vessels, and believed in blood-letting (113, 114). During the Middle Ages and until the Renaissance, Galen's theories were considered the sole truth. Except for the progress in anatomy and the discovery of the circulatory system attributed to Leonardo Da Vinci (1452-1519), Andreas Vesalius (1514-1564), and William Harvey (1578-1657), there were limited advances in wound therapy besides using hot iron/ oil, egg yolk, and turpentine, maggot therapy, or silver nitrate to aid wounds (110).

Profound advances were made in the 19th century with the development of microbiology and the "cell theory" that described the formation, proliferation, and regeneration of cells (115, 116). In 1858, Rudolf Virchow added the fifth sign of inflammation being 'function loss' (functio laesa) (117, 118).

The interaction of the cells with micro-organisms and the relation with "diseases" was made by Louis Pasteur (germ theory of diseases) (119), and antiseptic treatments made advances: Ignaz Semmelweis (hand washing) (120), Joseph Lister (sterilization of surgical gauze with carbolic acid/ phenol as anti-septic agent) (121), and Robert Wood Johnson (co-founder of Johnson and Johnson: sterilization of gauze and wound dressings with dry heat, steam and pressure) (110).

The discovery of penicillin by Alexander Fleming (1928), and oral antibiotics (1940) revolutionized clinical therapy and helped control infections and decreased mortality (122). The last decades more insights into the inflammatory process were gained, and wound dressings were further optimized using different materials, and loaded with substances as honey, iodide, silver, antibiotics, (stem) cells, and growth factors (123, 124).

Conventional and novel therapies, such as wound irrigation (125), the use of dressings, bandages and bioengineered skin (58, 126), silicone sheets (80), topical application of antibiotics and growth factors (87, 127), pressure therapy (126), (hyperbaric) oxygen therapy (67, 128), and steroid injections (129), to reduce hypertrophic scarring have improved wound repair.

Unfortunately, these therapies are still of limited success and urge for alternative adjuvant wound therapies (82, 130). A better understanding of the injurious and cytoprotective factors involved during wound repair is necessary to target the decisive factors that determine wound regeneration.

1.7 The levels of injurious and cytoprotective factors determine scar formation

Following injury, as presently following CL/P surgery, pro-oxidative and pro-inflammatory stimuli, such as heme, ROS, and pro-inflammatory cytokines are released. This may lead to extended survival of myofibroblasts and subsequently promote excessive scar formation.

Wound repair in early embryos is fast, efficient and scarless, an ability that is lost as development proceeds (30, 131, 132). A major difference between embryonic and adult wound repair is the strong presence of an inflammatory response at sites of adult wound

repair, whereas in embryos the inflammatory response is strongly attenuated (30, 131, 133, 134).

A swift resolution of acute inflammation or better protection against these injurious stressors seems thus crucial to protect from chronic inflammation, collateral damage and excessive scarring. In order to ameliorate wound repair, the balance of injurious and protective factors should thus be shifted towards an enhanced cytoprotective microenvironment. For this thesis, different strategies to harness inflammation and oxidative stress and to improve wound repair and regeneration were therefore probed.

Protective mechanisms that can be triggered to improve wound repair are using preconditioning strategies, inducing the cytoprotective HO system, and administration of stem cells. We will next introduce these subjects in more detail.

1.8 Preconditioning

Preconditioning is the phenomenon that exposure to a substance or little stressor in advance to a more harmful stressor reduces tissue damage by inducing cytoprotective responses (135). Different preconditioning strategies have been demonstrated to protect against oxidative or inflammatory stress in a variety of conditions, such as ischemia-reperfusion injury (IRI), surgery, and organ transplantation (136-138). Several forms of preconditioning exist such as pharmacological and ischemic preconditioning (IPC). Pharmacological preconditioning may include medicinal treatments such as administration of the anticoagulant heparin to prevent thrombosis and embolisms, or inducers of the cytoprotective enzyme HO, which has shown to improve cell survival and to avoid tissue damage. IPC is mediated by (repeated) short cycles of ischemia-reperfusion to an organ and has shown to protect this organ against subsequent stronger stress. With remote IPC (RIPC) not the target organ is subjected to this first stress but a remote organ, e.g., a limb (139, 140). RIPC has shown promising effects in several settings.

1.9 The heme oxygenase system

One of the most important examples of cytoprotective pathways forms the HO system. HO is the rate-limiting enzyme breaking down heme into biliverdin, free iron (Fe^{2+}) and carbon monoxide (CO). Biliverdin is rapidly converted into the anti-oxidant bilirubin by biliverdin reductase (141, 142). Two distinct isoforms (HO-1 and HO-2) have been identified. HO-2 is constitutively expressed, whereas HO-1 is an inducible form and can be induced by a variety of pathophysiological stimuli, such as heme, cytokines, endotoxins, hypoxia and oxidative stress (143). HO-activity has major effects on the different phases of wound healing, and HO-induction leads to an improved and enhanced wound healing, whereas inhibition or lack of HO leads to a slower wound repair (144, 145). HO-1 induction is considered to be an adaptive cellular response that resolves inflammation enabling inflamed tissues to return to homeostasis (146).

HO-activity improves many aspects that are hampered during tissue repair creating a less hostile environment. It suppresses oxidative stress, inflammation, and the formation of myofibroblasts from fibroblasts, promotes myofibroblast apoptosis, cell proliferation, and angiogenesis, and modulates cytokine expression, probing other protective responses (147, 148). HO-activity is important in counteracting various pathological conditions by

creating an antioxidant environment that overcomes injurious stressors and hence improving the outcome of tissue repair. Choosing the right therapy for specific wounds and improving the outcome of wound repair without resulting in function loss and scar formation is the next challenge.

1.10 Stem cells

Stem cells can differentiate into different cell types and are crucial during embryogenesis, palatogenesis, and repair of injured tissue. Stem cells are stored in niches, and upon activation by injury, these cells are mobilized to the site of injury where they can differentiate into any cell type necessary for wound repair (149-152). In addition, these stem cells produce cytoprotective and anti-inflammatory factors that help to create a micro-environment permissive for regeneration (96, 149, 153-158). Stem cell therapy is clinically used in diverse pathologies, such as leukemia and rheumatoid arthritis, and forms a promising novel adjuvant treatment in wound repair to prevent scarring (96, 123, 150, 159-161). Wound repair can be improved by inducing re-epithelialization and angiogenesis, but also by inhibiting oxidative and inflammatory responses (96, 153, 154, 162-170). The cytoprotective environment created by the stem cells inhibits the formation of myofibroblasts from fibroblasts and prevents fibrosis and hypertrophic scarring (78, 96, 150, 159, 160, 171). Whether the differentiation potential of the stem cells or their paracrine effects plays the major role in wound repair is still point of discussion. Since stem cells die quickly after administration to an injury and conditioned media derived from stem cells by itself can improve wound repair, it is suggested that the paracrine effects play the major role (172-176). In line with this, unilateral administration of stem cells to two-sided excisional wounds improved wound repair on both sides, further supporting a role for systemic paracrine effects (177). Even when stem cells administered to wounds do not differentiate, they can still produce protective paracrine factors, and thus increasing the survival of stem cells during therapy may further support their efficacy.

Many studies are showing that administration of mesenchymal stem cells (MSCs) in wound healing is effective and contributes to an enhanced wound repair and proper skin restoration during all phases of wound healing in both rodents and humans, (151, 153-155, 164, 165, 178-182). This has been extensively reviewed by Chen *et al.* (183), Jackson *et al.* (78, 184), and Maxson *et al.* (185).

1.11 Objectives and research questions

The purpose of this thesis is to explore several protective strategies to better understand the decisive factors determining between tissue repair and damage by studying developmental, inflammatory, and wound healing processes. We postulate that decreased activity of protective pathways (Part I) will impair wound repair and palatogenesis, whereas induction of protective signaling cascades (Part II), will provide a regenerative environment that improves wound repair and promotes regeneration (Figure 1.4).

Part I

Decreased protective mechanisms:

- ROS
- Inflammation
- Deficient protective factors
- Mechanical stress

Part II

Induction of protective pathways:

- HO
- Stem cells
- RIPC

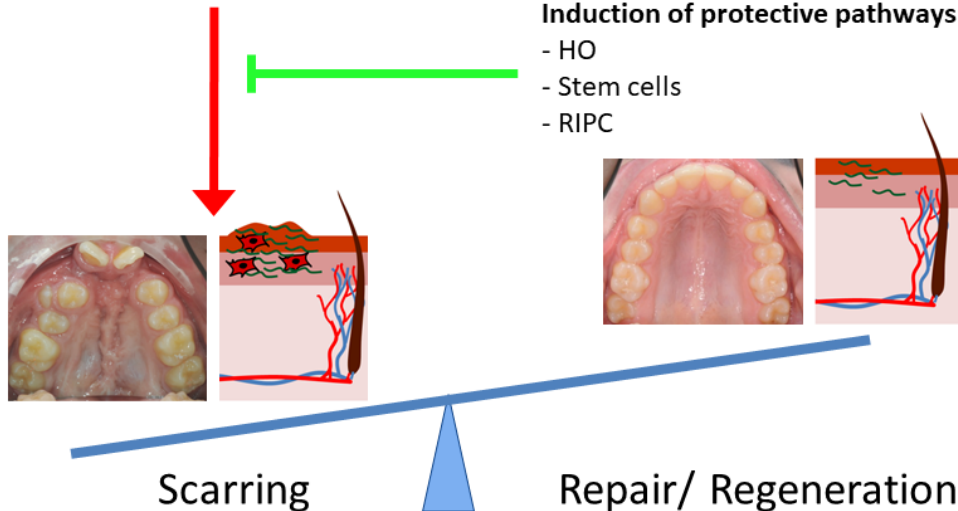


Figure 1.4: Summary of the strategies in this thesis to harness inflammatory and oxidative stress

Reactive oxygen species (ROS), inflammation, mechanical stress, and decreased protective molecules and mechanisms promote excessive scar formation (part I). We postulate that inducing protective pathways (part II), such as the heme oxygenase (HO) system, administration of stem cells, and applying remote ischemic preconditioning (RIPC) will skew the balance towards the formation of a minimal acellular scar. We expect that these strategies will neutralize ROS and inflammation, attenuate myofibroblast formation or induce myofibroblast apoptosis, stimulate angiogenesis and homeostasis.

Research question 1: How do decreased protective factors contribute to impaired palatogenesis and wound repair?

Genetic components play a large role in the etiology of CL/P. Some of these genes may affect protective factors that regulate the levels of oxidative and inflammatory signals. A lack of protective signaling pathways most probably will result in hampered wound repair. In this thesis, we will investigate the contribution of reduced protective signaling on palatogenesis and wound repair using mouse models with mutations that specifically knockout protective genes, or apply constant mechanical stress such as also is experienced on the wounds of a growing patient after CL/P surgery.

Research question 2: How to harness oxidative and inflammatory stress to facilitate wound repair and regeneration?

Inflammation needs to be controlled to prevent chronic non-healing wounds or excessive scar formation. Resolution of acute inflammation is mediated and controlled by endogenous antioxidant and anti-inflammatory regulators and pathways. Together these protective factors are crucial for preventing excessive tissue damage, chronic inflammation,

and allowing normal wound repair. The inflammatory resolution will attenuate the influx of activated leukocytes and edema formation into the wounded tissues and thereby form a regenerative environment. Therefore, pro-inflammatory chemokines, cytokines, and cell adhesion molecules need to be reduced by upregulating cytoprotective pathways.

1.12 Outline of the thesis

In **Part I**, we investigated the effect of diminished protective pathways:

- during excisional wound repair; using knockout mice lacking the constitutively expressed cytoprotective enzyme HO-2 (**Chapter 2**),
- during embryogenesis; using HO-2 deficient mice, in order to better understand the process of embryonic development and palatogenesis, and to unravel novel therapeutic targets to prevent CL/P formation and improve wound repair (**Chapter 3**),
- as experienced during excisional wound repair under constant mechanical stress, such as experienced in growing patients with CL/P after surgery, using a splinted excisional wound model; the natural physiological role of HO-1 during this process will be evaluated (**Chapter 4**).

In **Part II**, the induction of protective mechanisms will be studied as potential preconditioning strategy to improve cutaneous wound repair and protection against stem cell apoptosis, in specific

- if the induction of HO-1 can prevent oxidative stress-induced mesenchymal stem cell (MSC) death (**Chapter 5**),
- whether remote ischemic preconditioning (RIPC) can improve cutaneous wound repair via an HO-1 dependent mechanism (**Chapter 6**),
- how danger signals and tissue survival factors can discriminate between immune activation and tissue protection (**Chapter 7**).

In **Part III**, our main findings will be discussed, and future perspectives are proposed (**Chapter 8**). Summaries are given in English (**Chapter 9**) and Dutch (**Chapter 10**).

References

1. Bartzela TN, Carels CE, Bronkhorst EM, Ronning E, Rizell S, Kuijpers-Jagtman AM. Tooth agenesis patterns in bilateral cleft lip and palate. *Eur J Oral Sci.* 2010;118(1):47-52.
2. Carvajal Monroy PL, Grefte S, Kuijpers-Jagtman AM, Wagener FA, Von den Hoff JW. Strategies to improve regeneration of the soft palate muscles after cleft palate repair. *Tissue engineering Part B, Reviews.* 2012;18(6):468-77.
3. Gritli-Linde A. Molecular control of secondary palate development. *Developmental biology.* 2007;301(2):309-26.
4. Luijsterburg AJ, Rozendaal AM, Vermeij-Keers C. Classifying common oral clefts: a new approach after descriptive registration. *The Cleft palate-craniofacial journal : official publication of the American Cleft Palate-Craniofacial Association.* 2014;51(4):381-91.
5. McBride WA, McIntyre GT, Carroll K, Mossey PA. Subphenotyping and Classification of Orofacial Clefts: Need for Orofacial Cleft Subphenotyping Calls for Revised Classification. *The Cleft palate-craniofacial journal : official publication of the American Cleft Palate-Craniofacial Association.* 2015.
6. Kerameddin S, Namipashaki A, Ebrahimi S, Ansari-Pour N. IRF6 Is a Marker of Severity in Nonsyndromic Cleft Lip/Palate. *Journal of dental research.* 2015;94(9 Suppl):226S-32S.
7. Levi B, Brugman S, Wong VW, Grova M, Longaker MT, Wan DC. Palatogenesis: engineering, pathways and pathologies. *Organogenesis.* 2011;7(4):242-54.
8. Funato N, Nakamura M, Yanagisawa H. Molecular basis of cleft palates in mice. *World journal of biological chemistry.* 2015;6(3):121-38.
9. Kohli SS, Kohli VS. A comprehensive review of the genetic basis of cleft lip and palate. *Journal of oral and maxillofacial pathology : JOMFP.* 2012;16(1):64-72.
10. Wyszynski DF, Beaty TH. Review of the role of potential teratogens in the origin of human nonsyndromic oral clefts. *Teratology.* 1996;53(5):309-17.
11. Shkookani MA, Chen M, Vong A. Cleft lip - a comprehensive review. *Frontiers in pediatrics.* 2013;1:53.
12. Oginni FO, Adenekan AT. Prevention of oro-facial clefts in developing world. *Annals of maxillofacial surgery.* 2012;2(2):163-9.
13. Cremers NA, Suttorp M, Gerritsen MM, Wong RJ, van Run-van Breda C, van Dam GM, et al. Mechanical Stress Changes the Complex Interplay Between HO-1, Inflammation and Fibrosis, During Excisional Wound Repair. *Front Med (Lausanne).* 2015;2:86.
14. Kummer AW. Speech therapy for errors secondary to cleft palate and velopharyngeal dysfunction. *Seminars in speech and language.* 2011;32(2):191-8.
15. Pearson GD, Kirschner RE. Surgery for cleft palate and velopharyngeal dysfunction. *Seminars in speech and language.* 2011;32(2):179-90.
16. Hopper RA, Tse R, Smartt J, Swanson J, Kinter S. Cleft palate repair and velopharyngeal dysfunction. *Plastic and reconstructive surgery.* 2014;133(6):852e-64e.
17. Kosowski TR, Weathers WM, Wolfswinkel EM, Ridgway EB. Cleft palate. *Seminars in plastic surgery.* 2012;26(4):164-9.
18. Kuijpers-Jagtman AM. The orthodontist, an essential partner in CLP treatment. *B-Ent.* 2006;2 Suppl 4:57-62.
19. Nollet PJ, Katsaros C, Van't Hof MA, Kuijpers-Jagtman AM. Treatment outcome in unilateral cleft lip and palate evaluated with the GOSLON yardstick: a meta-analysis of 1236 patients. *Plastic and reconstructive surgery.* 2005;116(5):1255-62.
20. Biggs LC, Goudy SL, Dunnwald M. Palatogenesis and cutaneous repair: A two-headed coin. *Dev Dyn.* 2015;244(3):289-310.
21. Li J, Johnson CA, Smith AA, Salmon B, Shi B, Brunski J, et al. Disrupting the intrinsic growth potential of a suture contributes to midfacial hypoplasia. *Bone.* 2015;81:186-95.
22. Brouwer KM, Lundvig DM, Middelkoop E, Wagener FA, Von den Hoff JW. Mechanical cues in orofacial tissue engineering and regenerative medicine. *Wound Repair Regen.* 2015;23(3):302-11.
23. Morris HL. Velopharyngeal competence and primary cleft palate surgery, 1960-1971: a critical review. *The Cleft palate journal.* 1973;10:62-71.
24. Marrinan EM, LaBrie RA, Mulliken JB. Velopharyngeal function in nonsyndromic cleft palate: relevance of surgical technique, age at repair, and cleft type. *The Cleft palate-craniofacial journal : official publication of the American Cleft Palate-Craniofacial Association.* 1998;35(2):95-100.
25. Koh TJ, DiPietro LA. Inflammation and wound healing: the role of the macrophage. *Expert Rev Mol Med.* 2011;13:e23.
26. Medzhitov R. Origin and physiological roles of inflammation. *Nature.* 2008;454(7203):428-35.

27. Wagener FA, Carels CE, Lundvig DM. Targeting the redox balance in inflammatory skin conditions. *International journal of molecular sciences*. 2013;14(5):9126-67.
28. Nathan C, Ding A. Nonresolving inflammation. *Cell*. 2010;140(6):871-82.
29. Papathanasiou E, Trotman CA, Scott AR, Van Dyke TE. Current and Emerging Treatments for Postsurgical Cleft Lip Scarring: Effectiveness and Mechanisms. *Journal of dental research*. 2017;96(12):1370-7.
30. Martin P, Parkhurst SM. Parallels between tissue repair and embryo morphogenesis. *Development*. 2004;131(13):3021-34.
31. Gurtner GC, Werner S, Barrandon Y, Longaker MT. Wound repair and regeneration. *Nature*. 2008;453(7193):314-21.
32. Degen KE, Gourdie RG. Embryonic wound healing: a primer for engineering novel therapies for tissue repair. *Birth defects research Part C, Embryo today : reviews*. 2012;96(3):258-70.
33. Lundvig DM, Immenschuh S, Wagener FA. Heme oxygenase, inflammation, and fibrosis: the good, the bad, and the ugly? *Front Pharmacol*. 2012;3:81.
34. Nathan C. Points of control in inflammation. *Nature*. 2002;420(6917):846-52.
35. Wagener FA, Eggert A, Boerman OC, Oyen WJ, Verhofstad A, Abraham NG, et al. Heme is a potent inducer of inflammation in mice and is counteracted by heme oxygenase. *Blood*. 2001;98(6):1802-11.
36. Immenschuh S, Iwahara S, Satoh H, Nell C, Katz N, Muller-Eberhard U. Expression of the mRNA of heme-binding protein 23 is coordinated with that of heme oxygenase-1 by heme and heavy metals in primary rat hepatocytes and hepatoma cells. *Biochemistry*. 1995;34(41):13407-11.
37. Wagener FA, Volk HD, Willis D, Abraham NG, Soares MP, Adema GJ, et al. Different faces of the heme-heme oxygenase system in inflammation. *Pharmacol Rev*. 2003;55(3):551-71.
38. Murry CE, Jennings RB, Reimer KA. Preconditioning with ischemia: a delay of lethal cell injury in ischemic myocardium. *Circulation*. 1986;74(5):1124-36.
39. Lai IR, Chang KJ, Chen CF, Tsai HW. Transient limb ischemia induces remote preconditioning in liver among rats: the protective role of heme oxygenase-1. *Transplantation*. 2006;81(9):1311-7.
40. Barbagallo I, Galvano F, Frigiola A, Cappello F, Riccioni G, Murabito P, et al. Potential therapeutic effects of natural heme oxygenase-1 inducers in cardiovascular diseases. *Antioxidants & redox signaling*. 2013;18(5):507-21.
41. Keyse SM, Tyrrell RM. Heme oxygenase is the major 32-kDa stress protein induced in human skin fibroblasts by UVA radiation, hydrogen peroxide, and sodium arsenite. *Proceedings of the National Academy of Sciences of the United States of America*. 1989;86(1):99-103.
42. Hancock WW, Buelow R, Sayegh MH, Turka LA. Antibody-induced transplant arteriosclerosis is prevented by graft expression of anti-oxidant and anti-apoptotic genes. *Nature medicine*. 1998;4(12):1392-6.
43. van Beurden HE, Von den Hoff JW, Torensma R, Maltha JC, Kuijpers-Jagtman AM. Myofibroblasts in palatal wound healing: prospects for the reduction of wound contraction after cleft palate repair. *Journal of dental research*. 2005;84(10):871-80.
44. Wagener FA, van Beurden HE, von den Hoff JW, Adema GJ, Figdor CG. The heme-heme oxygenase system: a molecular switch in wound healing. *Blood*. 2003;102(2):521-8.
45. Sousa AD, Devare S, Ghanshani J. Psychological issues in cleft lip and cleft palate. *Journal of Indian Association of Pediatric Surgeons*. 2009;14(2):55-8.
46. Ohannessian P, Berggren A, Abdiu A. The cleft lip evaluation profile (CLEP): a new approach for postoperative nasolabial assessment in patients with unilateral cleft lip and palate. *Journal of plastic surgery and hand surgery*. 2011;45(1):8-13.
47. Chen ZQ, Wu J, Chen RJ. Sagittal maxillary growth pattern in unilateral cleft lip and palate patients with unrepaired cleft palate. *The Journal of craniofacial surgery*. 2012;23(2):491-3.
48. Sinno H, Tahiri Y, Thibaudeau S, Izadpanah A, Christodoulou G, Lin SJ, et al. Cleft lip and palate: an objective measure outcome study. *Plastic and reconstructive surgery*. 2012;130(2):408-14.
49. Eming SA, Martin P, Tomic-Canic M. Wound repair and regeneration: mechanisms, signaling, and translation. *Sci Transl Med*. 2014;6(265):265sr6.
50. Bush JO, Jiang R. Palatogenesis: morphogenetic and molecular mechanisms of secondary palate development. *Development*. 2012;139(2):231-43.
51. Stanier P, Moore GE. Genetics of cleft lip and palate: syndromic genes contribute to the incidence of non-syndromic clefts. *Human molecular genetics*. 2004;13 Spec No 1:R73-81.
52. Meng L, Bian Z, Torensma R, Von den Hoff JW. Biological mechanisms in palatogenesis and cleft palate. *Journal of dental research*. 2009;88(1):22-33.
53. Dudas M, Li WY, Kim J, Yang A, Kaartinen V. Palatal fusion - where do the midline cells go? A review on cleft palate, a major human birth defect. *Acta histochemica*. 2007;109(1):1-14.

54. Jones JL, Canady JW, Brookes JT, Wehby GL, L'Heureux J, Schutte BC, et al. Wound complications after cleft repair in children with Van der Woude syndrome. *The Journal of craniofacial surgery*. 2010;21(5):1350-3.
55. Biggs LC, Rhea L, Schutte BC, Dunnwald M. Interferon regulatory factor 6 is necessary, but not sufficient, for keratinocyte differentiation. *J Invest Dermatol*. 2012;132(1):50-8.
56. Biggs LC, Naridze RL, DeMali KA, Lusche DF, Kuhl S, Soll DR, et al. Interferon regulatory factor 6 regulates keratinocyte migration. *J Cell Sci*. 2014;127(Pt 13):2840-8.
57. Kwa MQ, Nguyen T, Huynh J, Ramnath D, De Nardo D, Lam PY, et al. Interferon regulatory factor 6 differentially regulates Toll-like receptor 2-dependent chemokine gene expression in epithelial cells. *J Biol Chem*. 2014;289(28):19758-68.
58. Metcalfe AD, Ferguson MW. Tissue engineering of replacement skin: the crossroads of biomaterials, wound healing, embryonic development, stem cells and regeneration. *Journal of the Royal Society, Interface / the Royal Society*. 2007;4(14):413-37.
59. Fakh-Gomez N, Sanchez-Sanchez M, Iglesias-Martin F, Garcia-Perla-Garcia A, Belmonte-Caro R, Gonzalez-Perez LM. Repair of complete bilateral cleft lip with severely protruding premaxilla performing a premaxillary setback and vomerine osteotomy in one stage surgery. *Medicina oral, patologia oral y cirugia bucal*. 2015;20(4):e500-7.
60. Stechmiller JK. Understanding the role of nutrition and wound healing. *Nutrition in clinical practice : official publication of the American Society for Parenteral and Enteral Nutrition*. 2010;25(1):61-8.
61. Diegelmann RF, Evans MC. Wound healing: an overview of acute, fibrotic and delayed healing. *Frontiers in bioscience : a journal and virtual library*. 2004;9:283-9.
62. Wild T, Rahbarnia A, Kellner M, Sobotka L, Eberlein T. Basics in nutrition and wound healing. *Nutrition*. 2010;26(9):862-6.
63. Singer AJ, Clark RA. Cutaneous wound healing. *The New England journal of medicine*. 1999;341(10):738-46.
64. Reinke JM, Sorg H. Wound repair and regeneration. *European surgical research Europäische chirurgische Forschung Recherches chirurgicales europeennes*. 2012;49(1):35-43.
65. Broughton G, 2nd, Janis JE, Attinger CE. The basic science of wound healing. *Plastic and reconstructive surgery*. 2006;117(7 Suppl):12S-34S.
66. Golebiewska EM, Poole AW. Platelet secretion: From haemostasis to wound healing and beyond. *Blood reviews*. 2015;29(3):153-62.
67. Rodriguez PG, Felix FN, Woodley DT, Shim EK. The role of oxygen in wound healing: a review of the literature. *Dermatologic surgery : official publication for American Society for Dermatologic Surgery [et al]*. 2008;34(9):1159-69.
68. Wynn TA, Vannella KM. Macrophages in Tissue Repair, Regeneration, and Fibrosis. *Immunity*. 2016;44(3):450-62.
69. Minutti CM, Knipper JA, Allen JE, Zaiss DM. Tissue-specific contribution of macrophages to wound healing. *Seminars in cell & developmental biology*. 2016.
70. Mahdavian Delavary B, van der Veer WM, van Egmond M, Niessen FB, Beelen RH. Macrophages in skin injury and repair. *Immunobiology*. 2011;216(7):753-62.
71. Sindrilaru A, Scharffetter-Kochanek K. Disclosure of the Culprits: Macrophages-Versatile Regulators of Wound Healing. *Advances in wound care*. 2013;2(7):357-68.
72. Guo S, Dipietro LA. Factors affecting wound healing. *Journal of dental research*. 2010;89(3):219-29.
73. Landen NX, Li D, Stahle M. Transition from inflammation to proliferation: a critical step during wound healing. *Cellular and molecular life sciences : CMLS*. 2016;73(20):3861-85.
74. Kasuya A, Tokura Y. Attempts to accelerate wound healing. *Journal of dermatological science*. 2014;76(3):169-72.
75. Klopper J, Lindenmaier W, Fiedler U, Mehlhorn A, Stark GB, Finkenzeller G. High efficient adenoviral-mediated VEGF and Ang-1 gene delivery into osteogenically differentiated human mesenchymal stem cells. *Microvascular research*. 2008;75(1):83-90.
76. Darby IA, Laverdet B, Bonte F, Desmouliere A. Fibroblasts and myofibroblasts in wound healing. *Clinical, cosmetic and investigational dermatology*. 2014;7:301-11.
77. Hinz B, Phan SH, Thannickal VJ, Prunotto M, Desmouliere A, Varga J, et al. Recent developments in myofibroblast biology: paradigms for connective tissue remodeling. *The American journal of pathology*. 2012;180(4):1340-55.
78. Jackson WM, Nesti LJ, Tuan RS. Mesenchymal stem cell therapy for attenuation of scar formation during wound healing. *Stem cell research & therapy*. 2012;3(3):20.

79. Stroncek JD, Reichert WM. Overview of Wound Healing in Different Tissue Types. In: Reichert WM, editor. *Indwelling Neural Implants: Strategies for Contending with the In Vivo Environment*. Boca Raton (FL)2008.
80. Bloemen MC, van der Veer WM, Ulrich MM, van Zuijlen PP, Niessen FB, Middelkoop E. Prevention and curative management of hypertrophic scar formation. *Burns : journal of the International Society for Burn Injuries*. 2009;35(4):463-75.
81. van der Veer WM, Bloemen MC, Ulrich MM, Molema G, van Zuijlen PP, Middelkoop E, et al. Potential cellular and molecular causes of hypertrophic scar formation. *Burns : journal of the International Society for Burn Injuries*. 2009;35(1):15-29.
82. Aarabi S, Longaker MT, Gurtner GC. Hypertrophic scar formation following burns and trauma: new approaches to treatment. *PLoS Med*. 2007;4(9):e234.
83. Rhett JM, Ghatnekar GS, Palatinus JA, O'Quinn M, Yost MJ, Gourdie RG. Novel therapies for scar reduction and regenerative healing of skin wounds. *Trends in biotechnology*. 2008;26(4):173-80.
84. Sarrazy V, Billet F, Micallef L, Coulomb B, Desmoulière A. Mechanisms of pathological scarring: Role of myofibroblasts and current developments. *Wound Repair and Regeneration*. 2011;19:s10-s5.
85. Ehrlich HP, Desmoulière A, Diegelmann RF, Cohen IK, Compton CC, Garner WL, et al. Morphological and immunochemical differences between keloid and hypertrophic scar. *The American journal of pathology*. 1994;145(1):105-13.
86. Verhaegen PD, van Zuijlen PP, Pennings NM, van Marle J, Niessen FB, van der Horst CM, et al. Differences in collagen architecture between keloid, hypertrophic scar, normotrophic scar, and normal skin: An objective histopathological analysis. *Wound Repair Regen*. 2009;17(5):649-56.
87. Miller MC, Nanchahal J. Advances in the modulation of cutaneous wound healing and scarring. *BioDrugs : clinical immunotherapeutics, biopharmaceuticals and gene therapy*. 2005;19(6):363-81.
88. Seitz O, Schürmann C, Hermes N, Müller E, Pfeilschifter J, Frank S, et al. Wound Healing in Mice with High-Fat Diet- or ob Gene-Induced Diabetes-Obesity Syndromes: A Comparative Study. *Experimental Diabetes Research*. 2010;2010:1-15.
89. Wei L, Fraser JL, Lu ZY, Hu X, Yu SP. Transplantation of hypoxia preconditioned bone marrow mesenchymal stem cells enhances angiogenesis and neurogenesis after cerebral ischemia in rats. *Neurobiology of disease*. 2012;46(3):635-45.
90. Snyder RJ. Treatment of nonhealing ulcers with allografts. *Clinics in dermatology*. 2005;23(4):388-95.
91. Taylor JE, Laity PR, Hicks J, Wong SS, Norris K, Khunkamchoo P, et al. Extent of iron pick-up in deferoxamine-coupled polyurethane materials for therapy of chronic wounds. *Biomaterials*. 2005;26(30):6024-33.
92. Krock BL, Skuli N, Simon MC. Hypoxia-induced angiogenesis: good and evil. *Genes & cancer*. 2011;2(12):1117-33.
93. Mustoe T. Understanding chronic wounds: a unifying hypothesis on their pathogenesis and implications for therapy. *American journal of surgery*. 2004;187(5A):65S-70S.
94. Klingberg F, Hinz B, White ES. The myofibroblast matrix: implications for tissue repair and fibrosis. *The Journal of pathology*. 2013;229(2):298-309.
95. Shaw TJ, Kishi K, Mori R. Wound-associated skin fibrosis: mechanisms and treatments based on modulating the inflammatory response. *Endocrine, metabolic & immune disorders drug targets*. 2010;10(4):320-30.
96. Meyer M, Muller AK, Yang J, Sulcova J, Werner S. The role of chronic inflammation in cutaneous fibrosis: fibroblast growth factor receptor deficiency in keratinocytes as an example. *The journal of investigative dermatology Symposium proceedings / the Society for Investigative Dermatology, Inc [and] European Society for Dermatological Research*. 2011;15(1):48-52.
97. Spilson SV, Kim HJ, Chung KC. Association between maternal diabetes mellitus and newborn oral cleft. *Ann Plast Surg*. 2001;47(5):477-81.
98. Stott-Miller M, Heike CL, Kratz M, Starr JR. Increased risk of orofacial clefts associated with maternal obesity: case-control study and Monte Carlo-based bias analysis. *Paediatr Perinat Epidemiol*. 2010;24(5):502-12.
99. Bille C, Skyttøe A, Vach W, Knudsen LB, Andersen AM, Murray JC, et al. Parent's age and the risk of oral clefts. *Epidemiology*. 2005;16(3):311-6.
100. Shahrukh Hashmi S, Gallaway MS, Waller DK, Langlois PH, Hecht JT, National Birth Defects Prevention S. Maternal fever during early pregnancy and the risk of oral clefts. *Birth Defects Res A Clin Mol Teratol*. 2010;88(3):186-94.
101. Saber A. Ancient Egyptian surgical heritage. *Journal of investigative surgery : the official journal of the Academy of Surgical Research*. 2010;23(6):327-34.

102. Hsieh S, Maranda EL, Salih T, Nguyen A, Marsh AM, Jimenez JJ. The Power to Heal. *JAMA dermatology*. 2016;152(8):954.
103. Shah JB. The history of wound care. *The journal of the American College of Certified Wound Specialists*. 2011;3(3):65-6.
104. Sanchez GM, Burr ridge AL. Decision making in head injury management in the Edwin Smith Papyrus. *Neurosurgical focus*. 2007;23(1):E5.
105. Ali FR, Finlayson AE. Pharaonic trichology: the Ebers Papyrus. *JAMA dermatology*. 2013;149(8):920.
106. Murray CK, Hinkle MK, Yun HC. History of infections associated with combat-related injuries. *The Journal of trauma*. 2008;64(3 Suppl):S221-31.
107. Dorai AA. Wound care with traditional, complementary and alternative medicine. *Indian journal of plastic surgery : official publication of the Association of Plastic Surgeons of India*. 2012;45(2):418-24.
108. Stewart JA, McGrane OL, Wedmore IS. Wound care in the wilderness: is there evidence for honey? *Wilderness & environmental medicine*. 2014;25(1):103-10.
109. Johnston CS, Gaas CA. Vinegar: medicinal uses and antiglycemic effect. *MedGenMed : Medscape general medicine*. 2006;8(2):61.
110. Broughton G, 2nd, Janis JE, Attinger CE. A brief history of wound care. *Plastic and reconstructive surgery*. 2006;117(7 Suppl):6S-11S.
111. Rather LJ. Disturbance of function (functio laesa): the legendary fifth cardinal sign of inflammation, added by Galen to the four cardinal signs of Celsus. *Bulletin of the New York Academy of Medicine*. 1971;47(3):303-22.
112. Daunton CK, S.; Smith, L.; Steele D. A history of materials and practices for wound management. *Wound Practice and Research*. 2012;20(4):174-86.
113. Sarabahi S. Recent advances in topical wound care. *Indian journal of plastic surgery : official publication of the Association of Plastic Surgeons of India*. 2012;45(2):379-87.
114. Papavramidou N, Thomaidis V, Fiska A. The ancient surgical bloodletting method of arteriotomy. *Journal of vascular surgery*. 2011;54(6):1842-4.
115. Clarke PG, Clarke S. Nineteenth century research on cell death. *Experimental oncology*. 2012;34(3):139-45.
116. Wolpert L. Evolution of the cell theory. *Philos Trans R Soc Lond B Biol Sci*. 1995;349(1329):227-33.
117. Heidland A, Klassen A, Rutkowski P, Bahner U. The contribution of Rudolf Virchow to the concept of inflammation: what is still of importance? *J Nephrol*. 2006;19 Suppl 10:S102-9.
118. Medzhitov R. Inflammation 2010: new adventures of an old flame. *Cell*. 2010;140(6):771-6.
119. Smith KA. Louis pasteur, the father of immunology? *Frontiers in immunology*. 2012;3:68.
120. Stewardson A, Allegranzi B, Sax H, Kilpatrick C, Pittet D. Back to the future: rising to the Semmelweis challenge in hand hygiene. *Future microbiology*. 2011;6(8):855-76.
121. Jessney B. Joseph Lister (1827-1912): a pioneer of antiseptic surgery remembered a century after his death. *Journal of medical biography*. 2012;20(3):107-10.
122. Bush K. The coming of age of antibiotics: discovery and therapeutic value. *Annals of the New York Academy of Sciences*. 2010;1213:1-4.
123. Cerqueira MT, Pirraco RP, Marques AP. Stem Cells in Skin Wound Healing: Are We There Yet? *Adv Wound Care (New Rochelle)*. 2016;5(4):164-75.
124. Dhivya S, Padma VV, Santhini E. Wound dressings - a review. *BioMedicine*. 2015;5(4):22.
125. Fernandez R, Griffiths R. Water for wound cleansing. *Cochrane database of systematic reviews*. 2012;2:CD003861.
126. Murphy PS, Evans GR. Advances in wound healing: a review of current wound healing products. *Plastic surgery international*. 2012;2012:190436.
127. Stinner DJ, Noel SP, Haggard WO, Watson JT, Wenke JC. Local antibiotic delivery using tailorable chitosan sponges: the future of infection control? *Journal of orthopaedic trauma*. 2010;24(9):592-7.
128. Eskes A, Ubbink DT, Lubbers M, Lucas C, Vermeulen H. Hyperbaric oxygen therapy for treating acute surgical and traumatic wounds. *Cochrane database of systematic reviews*. 2010(10):CD008059.
129. Mustoe TA, Cooter RD, Gold MH, Hobbs FD, Ramelet AA, Shakespeare PG, et al. International clinical recommendations on scar management. *Plastic and reconstructive surgery*. 2002;110(2):560-71.
130. Tziotzios C, Profyris C, Sterling J. Cutaneous scarring: Pathophysiology, molecular mechanisms, and scar reduction therapeutics Part II. Strategies to reduce scar formation after dermatologic procedures. *J Am Acad Dermatol*. 2012;66(1):13-24; quiz 5-6.
131. Redd MJ, Cooper L, Wood W, Stramer B, Martin P. Wound healing and inflammation: embryos reveal the way to perfect repair. *Philosophical transactions of the Royal Society of London Series B, Biological sciences*. 2004;359(1445):777-84.

132. Nodder S, Martin P. Wound healing in embryos: a review. *Anat Embryol (Berl)*. 1997;195(3):215-28.
133. Eming SA, Krieg T, Davidson JM. Inflammation in wound repair: molecular and cellular mechanisms. *J Invest Dermatol*. 2007;127(3):514-25.
134. Borena BM, Martens A, Broeckx SY, Meyer E, Chiers K, Duchateau L, et al. Regenerative Skin Wound Healing in Mammals: State-of-the-Art on Growth Factor and Stem Cell Based Treatments. *Cell Physiol Biochem*. 2015;36(1):1-23.
135. Platt JL, Nath KA. Heme oxygenase: protective gene or Trojan horse. *Nature medicine*. 1998;4(12):1364-5.
136. Narayanan SV, Dave KR, Perez-Pinzon MA. Ischemic preconditioning and clinical scenarios. *Curr Opin Neurol*. 2013;26(1):1-7.
137. Jaeschke H, Woolbright BL. Current strategies to minimize hepatic ischemia-reperfusion injury by targeting reactive oxygen species. *Transplantation reviews*. 2012;26(2):103-14.
138. Rao J, Qin J, Qian X, Lu L, Wang P, Wu Z, et al. Lipopolysaccharide preconditioning protects hepatocytes from ischemia/reperfusion injury (IRI) through inhibiting ATF4-CHOP pathway in mice. *PLoS one*. 2013;8(6):e65568.
139. Souza Filho MV, Loiola RT, Rocha EL, Simao AF, Gomes AS, Souza MH, et al. Hind limb ischemic preconditioning induces an anti-inflammatory response by remote organs in rats. *Braz J Med Biol Res*. 2009;42(10):921-9.
140. Hausenloy DJ, Yellon DM. Remote ischaemic preconditioning: underlying mechanisms and clinical application. *Cardiovasc Res*. 2008;79(3):377-86.
141. Gozzelino R, Jeney V, Soares MP. Mechanisms of cell protection by heme oxygenase-1. *Annu Rev Pharmacol Toxicol*. 2010;50:323-54.
142. Morse D, Choi AM. Heme oxygenase-1: from bench to bedside. *Am J Respir Crit Care Med*. 2005;172(6):660-70.
143. Wagener FA, Scharstuhl A, Tyrrell RM, Von den Hoff JW, Jozkowicz A, Dulak J, et al. The heme-heme oxygenase system in wound healing; implications for scar formation. *Curr Drug Targets*. 2010;11(12):1571-85.
144. Grochot-Przeczek A, Lach R, Mis J, Skrzypek K, Gozdecka M, Sroczynska P, et al. Heme oxygenase-1 accelerates cutaneous wound healing in mice. *PLoS One*. 2009;4(6):e5803.
145. Lundvig DM, Scharstuhl A, Cremers NA, Pennings SW, te Paske J, van Rheden R, et al. Delayed cutaneous wound closure in HO-2 deficient mice despite normal HO-1 expression. *J Cell Mol Med*. 2014;18(12):2488-98.
146. Immenschuh S, Ramadori G. Gene regulation of heme oxygenase-1 as a therapeutic target. *Biochemical pharmacology*. 2000;60(8):1121-8.
147. Toriseva M, Ala-aho R, Peltonen S, Peltonen J, Grenman R, Kahari VM. Keratinocyte growth factor induces gene expression signature associated with suppression of malignant phenotype of cutaneous squamous carcinoma cells. *PLoS one*. 2012;7(3):e33041.
148. Herrmann JL, Abarbanell AM, Weil BR, Manukyan MC, Poynter JA, Brewster BJ, et al. Optimizing Stem Cell Function for the Treatment of Ischemic Heart Disease. *Journal of Surgical Research*. 2011;166(1):138-45.
149. Sasaki M, Abe R, Fujita Y, Ando S, Inokuma D, Shimizu H. Mesenchymal stem cells are recruited into wounded skin and contribute to wound repair by transdifferentiation into multiple skin cell type. *Journal of immunology*. 2008;180(4):2581-7.
150. Butler KL, Goverman J, Ma H, Fischman A, Yu YM, Bilodeau M, et al. Stem cells and burns: review and therapeutic implications. *Journal of burn care & research : official publication of the American Burn Association*. 2010;31(6):874-81.
151. Fu X, Fang L, Li X, Cheng B, Sheng Z. Enhanced wound-healing quality with bone marrow mesenchymal stem cells autografting after skin injury. *Wound Repair Regen*. 2006;14(3):325-35.
152. Liu ZJ, Zhuge Y, Velazquez OC. Trafficking and differentiation of mesenchymal stem cells. *Journal of cellular biochemistry*. 2009;106(6):984-91.
153. Wu Y, Chen L, Scott PG, Tredget EE. Mesenchymal stem cells enhance wound healing through differentiation and angiogenesis. *Stem cells*. 2007;25(10):2648-59.
154. Rustad KC, Wong VW, Sorkin M, Glotzbach JP, Major MR, Rajadas J, et al. Enhancement of mesenchymal stem cell angiogenic capacity and stemness by a biomimetic hydrogel scaffold. *Biomaterials*. 2012;33(1):80-90.
155. Dash NR, Dash SN, Routray P, Mohapatra S, Mohapatra PC. Targeting nonhealing ulcers of lower extremity in human through autologous bone marrow-derived mesenchymal stem cells. *Rejuvenation research*. 2009;12(5):359-66.

156. Wu Y, Wang J, Scott PG, Tredget EE. Bone marrow-derived stem cells in wound healing: a review. *Wound Repair Regen.* 2007;15 Suppl 1:S18-26.
157. McFarlin K, Gao X, Liu YB, Dulchavsky DS, Kwon D, Arbab AS, et al. Bone marrow-derived mesenchymal stromal cells accelerate wound healing in the rat. *Wound Repair Regen.* 2006;14(4):471-8.
158. Kim WS, Park BS, Sung JH. The wound-healing and antioxidant effects of adipose-derived stem cells. *Expert opinion on biological therapy.* 2009;9(7):879-87.
159. Leung A, Crombleholme TM, Keswani SG. Fetal wound healing: implications for minimal scar formation. *Current opinion in pediatrics.* 2012;24(3):371-8.
160. Chen FM, Wu LA, Zhang M, Zhang R, Sun HH. Homing of endogenous stem/progenitor cells for in situ tissue regeneration: Promises, strategies, and translational perspectives. *Biomaterials.* 2011;32(12):3189-209.
161. Teng M, Huang Y, Zhang H. Application of stems cells in wound healing--an update. *Wound Repair Regen.* 2014;22(2):151-60.
162. Rubina K, Kalinina N, Efimenko A, Lopatina T, Melikhova V, Tsokolaeva Z, et al. Adipose stromal cells stimulate angiogenesis via promoting progenitor cell differentiation, secretion of angiogenic factors, and enhancing vessel maturation. *Tissue engineering Part A.* 2009;15(8):2039-50.
163. Nambu M, Kishimoto S, Nakamura S, Mizuno H, Yanagibayashi S, Yamamoto N, et al. Accelerated wound healing in healing-impaired db/db mice by autologous adipose tissue-derived stromal cells combined with atelocollagen matrix. *Ann Plast Surg.* 2009;62(3):317-21.
164. Javazon EH, Keswani SG, Badillo AT, Crombleholme TM, Zoltick PW, Radu AP, et al. Enhanced epithelial gap closure and increased angiogenesis in wounds of diabetic mice treated with adult murine bone marrow stromal progenitor cells. *Wound Repair Regen.* 2007;15(3):350-9.
165. Badiavas EV, Falanga V. Treatment of chronic wounds with bone marrow-derived cells. *Archives of dermatology.* 2003;139(4):510-6.
166. Nie C, Yang D, Xu J, Si Z, Jin X, Zhang J. Locally administered adipose-derived stem cells accelerate wound healing through differentiation and vasculogenesis. *Cell transplantation.* 2011;20(2):205-16.
167. Ma K, Liao S, He L, Lu J, Ramakrishna S, Chan CK. Effects of nanofiber/stem cell composite on wound healing in acute full-thickness skin wounds. *Tissue engineering Part A.* 2011;17(9-10):1413-24.
168. Burr SP, Dazzi F, Garden OA. Mesenchymal stromal cells and regulatory T cells: the Yin and Yang of peripheral tolerance? *Immunology and cell biology.* 2013;91(1):12-8.
169. Wang ZS, Wu LQ, Yi X, Geng C, Li YJ, Yao RY, et al. [CK19 can be used to predict the early recurrence and prognosis of HBV-related hepatocellular carcinoma patients with low AFP serum concentration after R0 radical hepatectomy]. *Zhonghua zhong liu za zhi [Chinese journal of oncology].* 2012;34(10):753-8.
170. Kuo YR, Chen CC, Goto S, Lin PY, Wei FC, Chen CL. Mesenchymal stem cells as immunomodulators in a vascularized composite allotransplantation. *Clinical & developmental immunology.* 2012;2012:854846.
171. Stoff A, Rivera AA, Sanjib Banerjee N, Moore ST, Michael Numnum T, Espinosa-de-Los-Monteros A, et al. Promotion of incisional wound repair by human mesenchymal stem cell transplantation. *Experimental dermatology.* 2009;18(4):362-9.
172. Madrigal M, Rao KS, Riordan NH. A review of therapeutic effects of mesenchymal stem cell secretions and induction of secretory modification by different culture methods. *Journal of translational medicine.* 2014;12:260.
173. Spees JL, Lee RH, Gregory CA. Mechanisms of mesenchymal stem/stromal cell function. *Stem cell research & therapy.* 2016;7(1):125.
174. Lee DE, Ayoub N, Agrawal DK. Mesenchymal stem cells and cutaneous wound healing: novel methods to increase cell delivery and therapeutic efficacy. *Stem cell research & therapy.* 2016;7:37.
175. Arno AI, Amini-Nik S, Blit PH, Al-Shehab M, Belo C, Herer E, et al. Human Wharton's jelly mesenchymal stem cells promote skin wound healing through paracrine signaling. *Stem cell research & therapy.* 2014;5(1):28.
176. Yew TL, Hung YT, Li HY, Chen HW, Chen LL, Tsai KS, et al. Enhancement of wound healing by human multipotent stromal cell conditioned medium: the paracrine factors and p38 MAPK activation. *Cell transplantation.* 2011;20(5):693-706.
177. Shin L, Peterson DA. Human mesenchymal stem cell grafts enhance normal and impaired wound healing by recruiting existing endogenous tissue stem/progenitor cells. *Stem cells translational medicine.* 2013;2(1):33-42.
178. Nakagawa H, Akita S, Fukui M, Fujii T, Akino K. Human mesenchymal stem cells successfully improve skin-substitute wound healing. *The British journal of dermatology.* 2005;153(1):29-36.

179. Huang S, Lu G, Wu Y, Jirigala E, Xu Y, Ma K, et al. Mesenchymal stem cells delivered in a microsphere-based engineered skin contribute to cutaneous wound healing and sweat gland repair. *Journal of dermatological science*. 2012;66(1):29-36.
180. Kwon DS, Gao X, Liu YB, Dulchavsky DS, Danyluk AL, Bansal M, et al. Treatment with bone marrow-derived stromal cells accelerates wound healing in diabetic rats. *International wound journal*. 2008;5(3):453-63.
181. Yoshikawa T, Mitsuno H, Nonaka I, Sen Y, Kawanishi K, Inada Y, et al. Wound therapy by marrow mesenchymal cell transplantation. *Plastic and reconstructive surgery*. 2008;121(3):860-77.
182. Falanga V, Iwamoto S, Chartier M, Yufit T, Butmarc J, Koultab N, et al. Autologous bone marrow-derived cultured mesenchymal stem cells delivered in a fibrin spray accelerate healing in murine and human cutaneous wounds. *Tissue engineering*. 2007;13(6):1299-312.
183. Chen JS, Wong VW, Gurtner GC. Therapeutic potential of bone marrow-derived mesenchymal stem cells for cutaneous wound healing. *Frontiers in immunology*. 2012;3:192.
184. Jackson WM, Nesti LJ, Tuan RS. Concise review: clinical translation of wound healing therapies based on mesenchymal stem cells. *Stem cells translational medicine*. 2012;1(1):44-50.
185. Maxson S, Lopez EA, Yoo D, Danilkovitch-Miagkova A, Leroux MA. Concise review: role of mesenchymal stem cells in wound repair. *Stem cells translational medicine*. 2012;1(2):142-9.

PART I:

DECREASED PROTECTIVE MECHANISMS HAMPER TISSUE
REPAIR AND CRANIOFACIAL DEVELOPMENT

Chapter 2

Delayed cutaneous wound closure in heme oxygenase-2 deficient mice despite normal heme oxygenase-1 expression.

Lundvig DM*, Scharstuhl A*, **Cremers NA**, Pennings SW, te Paske J, van Rheden R, van Run-van Breda C, Regan RF, Russel FG, Carels CE, Maltha JC, Wagener FA.

*contributed equally

J Cell Mol Med. 2014 Dec;18(12):2488-98.

Abstract

Impaired wound healing can lead to scarring, and esthetical and functional problems. The cytoprotective heme oxygenase (HO) enzymes degrade heme into iron, biliverdin and carbon monoxide. HO-1 deficient mice suffer from chronic inflammatory stress and delayed cutaneous wound healing, while corneal wound healing in HO-2 deficient mice is impaired with exorbitant inflammation and absence of HO-1 expression. This study addresses the role of HO-2 in cutaneous excisional wound healing using HO-2 knockout (KO) mice. Here, we show that HO-2 deficiency also delays cutaneous wound closure compared to WT controls. In addition, we detected reduced collagen deposition and vessel density in the wounds of HO-2 KO mice compared to WT controls. Surprisingly, wound closure in HO-2 KO mice was accompanied by an inflammatory response comparable to WT mice. HO-1 induction in HO-2 deficient skin was also similar to WT controls and may explain this protection against exaggerated cutaneous inflammation but not the delayed wound closure. Proliferation and myofibroblast differentiation were similar in both two genotypes. Next, we screened for candidate genes to explain the observed delayed wound closure and detected delayed gene and protein expression profiles of the chemokine (C-X-C) ligand-11 (CXCL-11) in wounds of HO-2 KO mice. Abnormal regulation of CXCL-11 has been linked to delayed wound healing and disturbed angiogenesis. However, whether aberrant CXCL-11 expression in HO-2 KO mice is caused by or is causing delayed wound healing needs to be further investigated.

Keywords: heme oxygenase, wound healing, skin.

Abbreviations

α SMA	Alpha-smooth muscle actin
ColIV	Collagen IV
CXCL-11	Chemokine (C-X-C) ligand 11
CXCR3	Chemokine (C-X-C) receptor 3
Gr-1	Granulocyte receptor antigen-1
HO	Heme oxygenase
HPF	High power field
KO	Knockout
MMP	Matrix metalloproteinase
ROS	Reactive oxygen species
WT	Wild-type

Introduction

Cutaneous wound repair occurs in temporally coordinated and overlapping phases: inflammation, granulation tissue formation and remodelling (1). The timely progression of the different phases is coordinated by cytokines and growth factors, and each phase is characterized by the presence of specific cell types (2). Both clinical and experimental studies have confirmed the importance for a well-regulated inflammatory resolution for proper wound healing, since prolonged inflammatory and oxidative stress may cause non-healing, chronic wounds or excessive scarring (3, 4).

Heme oxygenases (HO) are enzymes that degrade heme into biliverdin, carbon monoxide and iron. Biliverdin is then converted into the antioxidant bilirubin by biliverdin reductase. HO-1 is highly inducible by a wide range of stresses, including inflammatory and oxidative stress, whereas HO-2 is mainly constitutively expressed (5, 6). The HO system is important in the resolution of inflammation (7, 8). The cytoprotective effects of the stress-induced HO-1 are evident in various pathological models and settings, whereas the constitutive HO-2 is important for physiological maintenance of the heme pool (9).

HO-1 deficient humans and mice demonstrate chronic inflammatory stress accompanied by increased leukocyte recruitment (10, 11). Moreover, genetic or pharmacologic ablation of HO-1 expression and activity in mice results in slower cutaneous wound closure (12). Also, HO-2 deficient mice show delayed wound healing and an exaggerated inflammatory response after corneal epithelial wounding (13, 14) which was associated with impaired HO-1 induction and function (13). Notably, HO-2 levels have been suggested to regulate HO-1 expression and function in a cell and tissue-specific manner (15), and compensatory HO-1 expression in HO-2 deficient tissue has been reported (16, 17). Moreover, genetic or pharmacological HO-1 induction as well as administration of HO effector molecules biliverdin/bilirubin down-regulate the inflammatory response and restore wound healing in HO-1 deficient skin (12, 18) and HO-2 deficient cornea (14, 19). On the other hand, HO-1 has pro-angiogenic effects via regulating VEGF synthesis (20, 21). Wound healing in HO-1 KO mice occurs with reduced neovascularization in the skin (12) whereas exaggerated angiogenesis was found in HO-2 deficient corneas (19). Application of biliverdin ameliorated this pathologic angiogenesis occurring after corneal wounding in HO-2 KO mice (19).

Because of the described intricate involvement of both HO-1 and HO-2 in wound healing and regulation of inflammatory responses, this study focused on exploring the possible role of HO-2 in cutaneous wound healing using a full-thickness excisional wound model and HO-2 KO mice.

Methods and materials

Animals

Homozygote HO-2 KO mice generated by targeted disruption of the HO-2 gene (22) and WT mice were bred in-house on a mixed 129Sv x C57BL/6 background. Mice were provided with food and water ad libitum and maintained on a 12h light/dark cycle and specific pathogen-free conditions. All experiments and protocols were approved by the institutional Radboud University Nijmegen animal experimentation committee.

Excisional wound model

Prior to wounding 6–12 weeks old female mice were shaved using an electrical clipper. The following day four full-thickness wounds were made on the back including the *m. panniculus carnosus* using a sterile disposable 4-mm biopsy punch (Kai Medical, Seki City, Japan) and the mice were left uncovered to heal (n = 18/genotype). At day 2 after wounding mice were killed, and the remaining mice (n = 9/genotype) were followed until day 7 (n = 9/genotype). For gene transcript analysis mice were wounded (n = 12/genotype) and killed at day 2 (n = 6/genotype) and day 5 (n = 6/genotype) after wounding. Punched out tissue at day 0 was collected as control. Wounds were collected using a disposable 6-mm biopsy punch (Kai Medical) allowing collection of the complete wound together with the surrounding normal tissue.

Wound size analysis

Wounds were digitally documented on different days with a ruler placed next to the wounds for size normalization. Wound area was measured at least twice by a blinded investigator using ImageJ (NIH) v1.44p software.

Immunohistochemistry

Tissue samples were fixed for 24h in 4% paraformaldehyde and further processed for routine paraffin embedding. Sections were deparaffinized using Histosafe and rehydrated using an alcohol range. Endogenous peroxidase activity was quenched with 3% H₂O₂ in methanol for 20 min., and immunohistochemical stainings were performed and photographed as previously described (23). Photographs were taken on a Carl Zeiss Imager Z.1 system (Carl Zeiss Microimaging GmbH, Jena, Germany). For antibodies and antigen retrievals used, see Table 2.1.

Table 2.1. Antibodies used for immunohistochemistry

Antibody	Specificity	Dilution	Antigen retrieval	Source
SPA-895	HO-1	1:800	A	Stressgen, Victoria, BC, USA
OSA-200	HO-2	1:800	A	Stressgen
MCA497R	F4/80	1:200	A	AbD Serotec, Kidlington, UK
2233PCO	Collagen IV	1:200	A	Euro-Diagnostica, Malmo, Sweden
Sc-34785	CXCL-11	1:100	B	Santa Cruz Biotechnology, CA, USA
A2547	αSMA	1:600	A	Sigma Aldrich, St. Louis, MO, USA

A: 10 mM citrate buffer 70°C for 10 min, followed by trypsin digestion for 7 min.

B: 10 mM citrate buffer RT, 120 min.

Semi-quantitative scoring of immunohistochemical sections

HO-1 and F4/80 immunoreactivity were evaluated as the number of positive cells (based on the percentage of positive staining) and staining intensity of four sections per animal. Extent was scored as: 0, ≤5%; 1, 6–25%; 2, 26–50%; 3, >50%. Intensity was scored as: 0, weak; 1, moderate; 2, strong. Intensity was designated as weak when only barely detectable. To correlate extent and intensity on the staining, a composite score was calculated by multiplying the individual scores of extent by intensity. Scoring was done three times by a blinded investigator. CXCL-11 immunoreactivity was evaluated by scoring a single section per animal by two independent investigators as previously described (24). To assess αSMA immunoreactivity four sections per animal were scored twice as earlier described (25).

Vascularization was assessed twice on five high-power fields (HPF; 400x magnification) on four sections per animal as previously described (26). A mean score per animal was used for further analysis.

Collagen deposition

Collagen deposition in AZAN stained wound sections (1–4 sections/ mouse) was determined by image analysis using a macro built in Image J (27). The wound area was manually defined before running the macro using the edges of the *m. panniculus carnosus* and epithelium as boundaries. Measurements were performed twice, and mean intensity/mm² per mouse was used for further analysis.

Assessment of mRNA expression by quantitative real-time PCR

Total RNA was extracted from skin and wound samples by using Trizol (Invitrogen, Carlsbad, CA, USA) and a RNeasy Mini kit (Qiagen, Hilden, Germany), and cDNA was produced using the iScript cDNA synthesis kit (Bio-Rad, Hercules, CA, USA). To screen for differences in gene expression profiles of wound associated genes in HO-2 KO and WT mice, pooled cDNAs synthesized from individual wounds of HO-2 KO and WT mice isolated at day 5 were tested on a Mouse Wound Healing RT2 Profiler™ PCR Array according to the manufacturer's instructions (SABiosciences, Frederick, MD, USA). Individual cDNAs from all time-points were subsequently analyzed for genes up- or down-regulated more than two-fold using custom-designed primers (Table 2.2) and iQ SYBR Green Supermix (Invitrogen) in a CFX96 Real-Time PCR system (Bio-Rad). Relative gene expression values were evaluated using the 2^{-ΔΔCt} method using GAPDH as housekeeping gene (28). Fold changes were normalized to WT mean day 0.

Table 2.2. Murine primers used for qPCR

Gene	Fw primer (5'→3')	Rv primer (5'→3')	Reference
HO-1	CAACATTGAGCTGTTTGAGG	TGGCTTTGTGTTCTCTGTC	-
HO-2	AAGGAAGGGACCAAGGAAG	AGTGGTGGCCAGCTTAAATAG	-
TNF	CTCTTCTATTCTGCTTG	GAATTGTCATCTGGCATAAC	-
CXCL-11	CACGCTGCTCAAGGCTTCCTTATG	TGTCGCAGCCGTTACTCGGGT	-
Gr-1	TGGACTCTCACAGAAGCAAAG	GCAGAGGTCTTCTCCAACA	-
F4/80	AATCCTGTGAAGATGTGG	GAGTGTTGATGCAAATGAAG	-
ACTA2	CAGGCATGGATGGCATCAATCAC	ACTCTAGCTGTGAAGTCAGTGTCG	(29)
GAPDH	GGCAAATTCACGGCACA	GTTAGTGGGGTCTCGCTCCTG	-

Western blotting

Protein was extracted from homogenized 4-mm skin biopsies in 100 μl lysis buffer (1 mM EDTA, 0.5% Triton X-100, complete protease inhibitor cocktail (Roche, Penzberg, Germany), 100 μM PMSF), and Western blotting using primary antibodies against HO-1 and HO-2 (SPA-895 and OSA-200, 1:5000; Stressgen, Victoria, BC, USA) was performed as previously described (30).

Statistical analysis

Statistical analysis was performed with GraphPad Prism 4.03 software. Normal data distribution was assessed using the Kolmogorov–Smirnov test. In case of non-normality, data were transformed. Statistical differences in qPCR data, wound closure and collagen

deposition were determined using Student's t-test with Bonferroni-correction in case of multiple testing. Semi-quantitative scores were analyzed with non-parametric Mann-Whitney U test or Kruskal-Wallis test with Dunn's post hoc test. Collagen deposition, wound closure and qPCR data are presented as mean \pm SD. Semi-quantitative scores are presented as box-and-whisker plots of median with 10–90 percentiles. $p < 0.05$ was considered statistically significant.

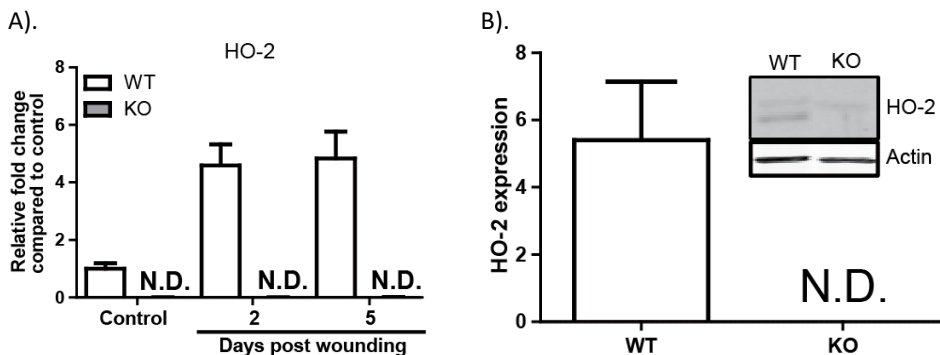
Results

Delayed cutaneous wound closure in HO-2 deficient mice

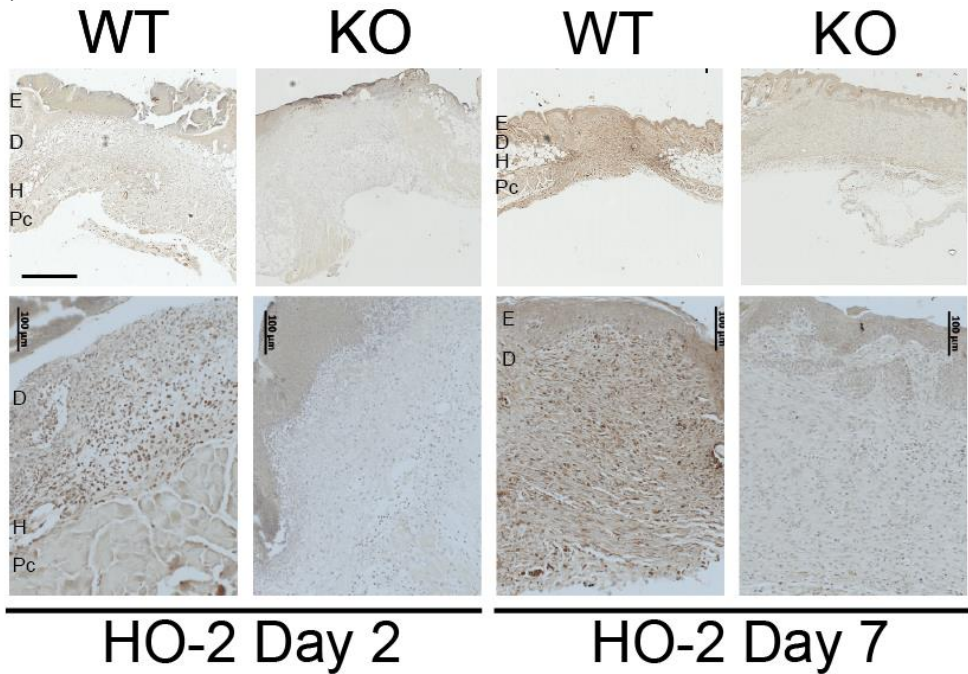
Prior to experimental start, we verified that HO-2 KO mice indeed were devoid of HO-2 mRNA and protein expression (Figure S2.1). To investigate the role of HO-2 in cutaneous wound closure, full-thickness wounds were made on the backs of HO-2 KO and WT mice and monitored in time (Figure 2.1). Wound area assessment demonstrated significantly larger wounds in HO-2 KO mice compared to WT controls at day 2 [$6.9 \pm 1.8 \text{ mm}^2$ versus $5.1 \pm 1.1 \text{ mm}^2$ ($n = 18/\text{genotype}$); $p < 0.01$], day 5 [$4.9 \pm 1.6 \text{ mm}^2$ versus $2.3 \pm 0.4 \text{ mm}^2$ ($n = 9/\text{genotype}$); $p < 0.001$] and day 7 [$2.1 \pm 0.6 \text{ mm}^2$ versus $1.1 \pm 0.3 \text{ mm}^2$ ($n = 9/\text{genotype}$); $p < 0.001$] after wounding.

Normal inflammatory response in HO-2 KO mice after cutaneous wounding

To determine whether delayed cutaneous wound healing in HO-2 KO mice is because of an exaggerated inflammatory response as observed after corneal injury, we compared gene expression profiles of different inflammatory factors and cell markers in skin of HO-2 KO and WT mice at day 2 and 5 (Figure 2.2). The pro-inflammatory cytokine TNF and the stress-induced enzyme COX-2 demonstrated an injury-induced increase in transcript levels compared to unwounded skin in both WT and HO-2 KO mice, however, we did not detect any differences between the two genotypes at any of the investigated time points (Figure 2.2A and B). Furthermore, granulocyte marker receptor antigen-1, Gr-1 and macrophage marker F4/80 both demonstrated an injury-induced increase in transcript levels compared to unwounded skin, however, no differences between HO-2 KO and WT mice were evident (Figure 2.2C and D). This was also reflected at the protein level, as semi-quantitative assessment of F4/80 immunoreactivity in wound sections demonstrated no significant differences between HO-2 KO and WT mice at day 2 and day 7 after wounding (Figure 2.2E and F).



C).



Supplemental Figure S2.1. Cutaneous HO-2 expression in WT and HO-2 KO mice.

(A) HO-2 gene transcript levels in WT (white bars) and HO-2 KO (grey bars) mice in time presented as mean \pm SD. Controls represent samples collected at day 0, and data was normalized to WT mean day 0. (B) Western blot (insert) of cutaneous HO-2 protein expression in unwounded skin of WT (white bar) and HO-2 KO (grey bar) mice. Band intensity was normalized to housekeeping protein β -actin. Data is presented as mean \pm SD. (C) Immunohistochemical staining of HO-2 in skin sections of WT and HO-2 KO mice at day 2 and day 7 after wounding. Anatomical indications by E, epidermis; D, dermis; H, hypodermis; Pc, panniculus carnosus. Bars, 500 μ m (upper panel), 100 μ m (lower panel).

A).



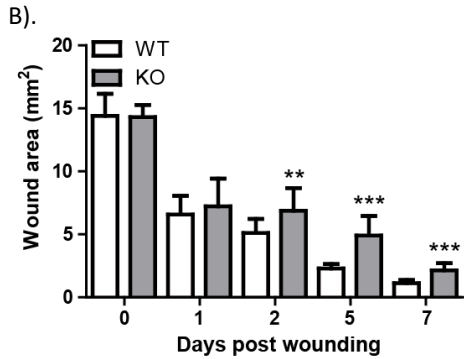
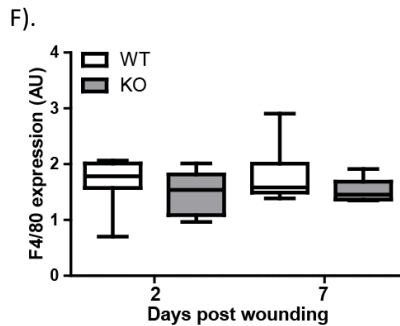
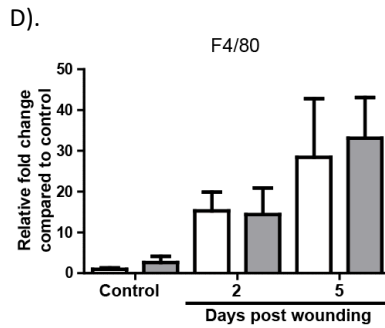
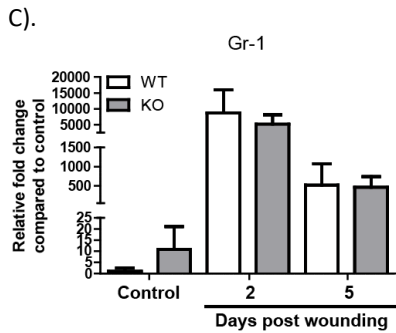
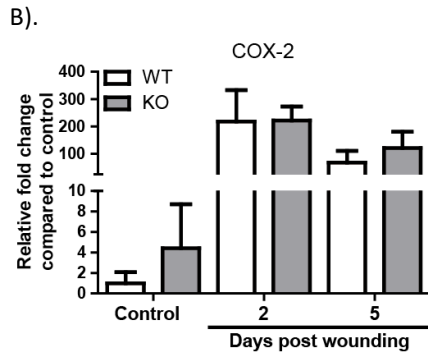
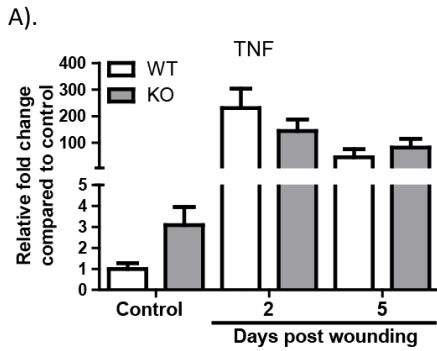


Figure 2.1 Slower cutaneous wound closure in HO-2 KO after excisional wounding. (A) Wound closure in WT (upper panel) and HO-2 KO (lower panel) mice in time; bar, 5 mm. (B) Wound area (mm²) reduction in WT (white bars) and HO-2 KO (grey bars) mice in time presented as mean \pm SD. ** p <0.01, *** p <0.001.



E).

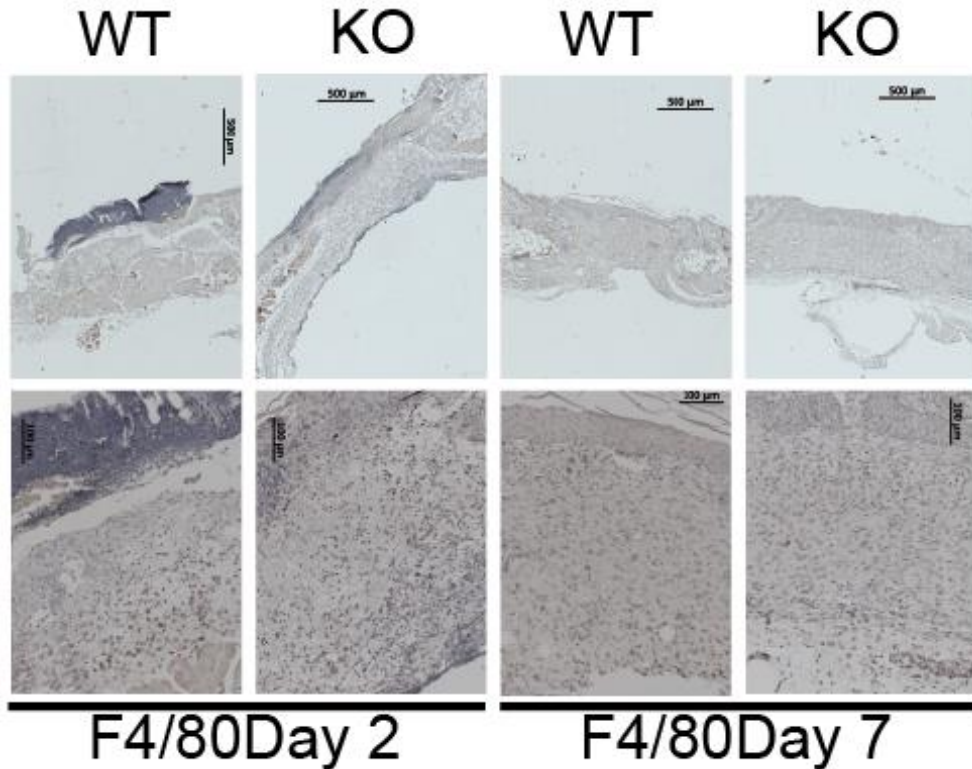


Figure 2.2 HO-2 KO mice demonstrate a normal inflammatory response after wounding. Gene transcript levels of pro-inflammatory proteins (A) TNF and (B) COX-2 and inflammatory cell markers (C) Gr-1, and (D) F4/80 in WT (white bars) and HO-2 KO (grey bars) mice in time presented as mean \pm SD. Controls are tissue biopsies collected at day 0, and data were normalized to WT mean day 0. (E) Box-and-whisker plot with 10–90 percentiles of semi-quantitative assessment of F4/80 immunoreactivity in (F). (F) F4/80 immunoreactivity in representative wound sections of WT and HO-2 KO mice at day 2 and 7 after wounding. Anatomical indications by E, epidermis; D, dermis; H, hypodermis; Pc, panniculus carnosus; bars, 500 μ m (upper panel), 100 μ m (lower panel).

Injury-induced HO-1 expression in both HO-2 KO and WT mice

In contrast to HO-2 deficient cornea (13) we detected both HO-1 mRNA transcript and protein in the skin of HO-2 KO mice (Figure 2.3). Similar levels of HO-1 protein were detected in unwounded skin of HO-2 KO and WT mice (6.9 ± 3.2 and 9.3 ± 6.7 , respectively; Figure 2.3A). Also, a comparable injury-induced increase in HO-1 transcript levels was evident in both HO-2 KO and WT mice (Figure 2.3B). Furthermore, injury-induced HO-1 protein expression was detected in both WT and HO-2 KO skin (Figure 2.3C). HO-1 positive cells were present at high numbers both in the wound area and in the surrounding tissue at day 2, while at day 7 HO-1 positive cells were predominantly found in the wound area (Figure 2.3C). Semi-quantitative assessment of HO-1 immunoreactivity demonstrated a significant reduction in HO-1 expression at day 7 compared to day 2 in both WT and HO-2 KO wounds ($P < 0.05$ for both genotypes), however, no significant differences between the genotypes were detected (Figure 2.3D).

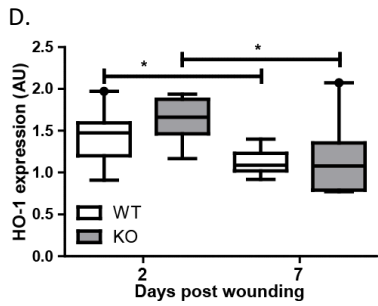
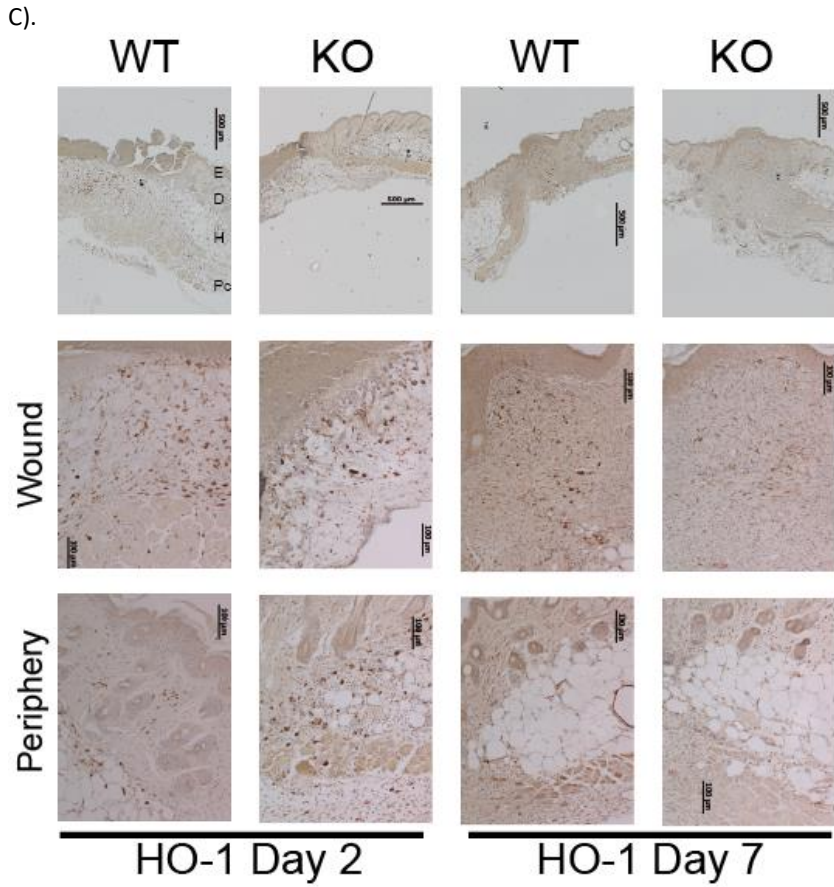
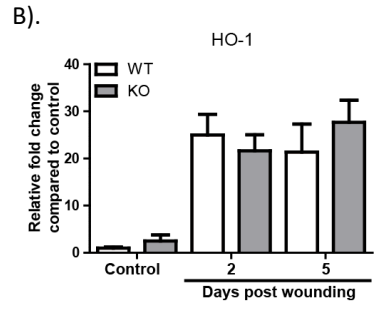
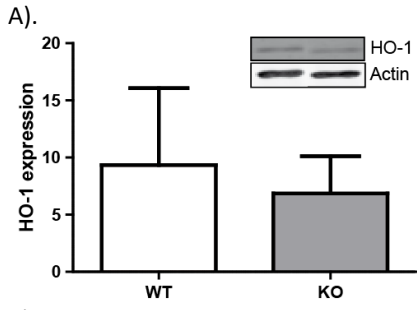


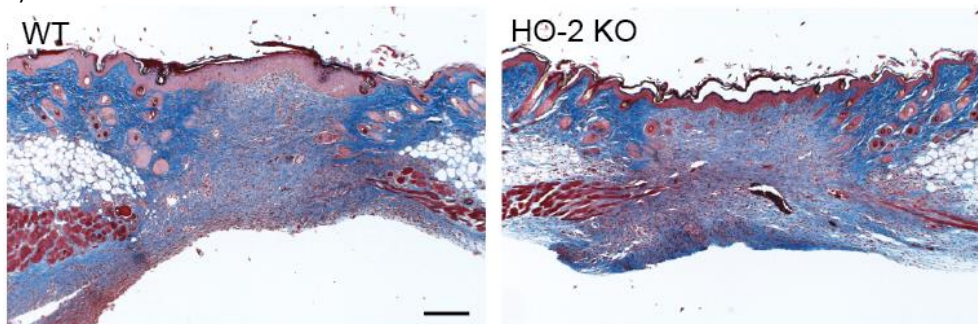
Figure 2.3 HO-2 KO mice induce cutaneous HO-1 expression after wounding. (A) Western blot (insert) of cutaneous HO-1 expression in unwounded skin in WT (white bar) and HO-2 KO (grey bar) mice. Band intensity was normalized to housekeeping protein β -actin. Data are presented as mean \pm SD. (B) HO-1 gene transcript levels in WT (white bars) and HO-2 KO (grey bars) mice in time as represented as mean \pm SD. Controls represent biopsies collected at day 0, and data were normalized to WT mean day 0. (C) HO-1 immunoreactivity in representative wound sections of WT and HO-2 KO mice at day 2 and day 7 after wounding. Anatomical indications by E, epidermis; D, dermis; H, hypodermis; Pc, panniculus carnosus; bars, 500 μ m (upper panel), 100 μ m (wound, periphery). (D) Semi-quantitative scores of HO-1 immunoreactivity in (C) presented as box-and-whisker plot with 10–90 percentiles. * $p < 0.05$.

Reduced collagen deposition and lower vessel density in HO-2 KO wounds

HO-2 KO mice demonstrated no abnormalities compared to WT mice with respect to the inflammatory phase. We therefore questioned whether the delayed wound healing was a result of a dysregulated granulation phase. Assessment of collagen deposition in wound sections of HO-2 KO and WT mice using an Image J macro demonstrated a significant lower percentage collagen deposition per area in HO-2 KO wounds compared to WT controls at day 7 after wounding ($8.8 \pm 4.2\%/mm^2$ versus $29.8 \pm 10.8\%/mm^2$, $p < 0.001$; Figure 2.4A and B). Also, we investigated the degree of vascularization in the wound areas of HO-2 KO and WT mice by semi-quantitative scoring of wound sections stained for collagen IV, a basement membrane protein found in the walls of blood vessels (31). We detected a significant lower density of vessels per HPF in wound sections of HO-2 KO mice compared to WT mice at day 7 after wounding ($p < 0.05$; Figure 2.4C and D). We wondered if the delayed wound healing could be related to a lower cell proliferation capacity in HO-2 deficient cells, and we therefore assessed the mRNA levels of Ki67, a marker of actively cycling cells (32). We detected a time-dependent increase in Ki67 mRNA levels consistent with an increased influx and proliferation of wound repair associated cells; however, no differences between HO-2 KO and WT mice were evident at any of the investigated time-points (Figure 2.5A).

During the granulation phase keratinocytes dominate epithelization and (myo)fibroblasts produce ECM such as collagen and close the wound (33). We therefore investigated whether the presence of less (myo)fibroblasts could be an explanation for the reduced collagen deposition. We detected similar mRNA levels of ACTA2, the murine counterpart of myofibroblast marker α SMA, at all examined time-points (Figure 2.5B). Moreover, we did not detect any difference in α SMA protein immunoreactivity level at day 7 after wounding as evaluated by semi-quantitative scoring (Figure 2.5C and D).

A).



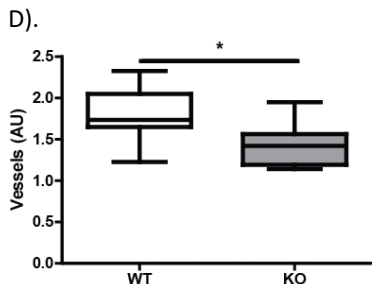
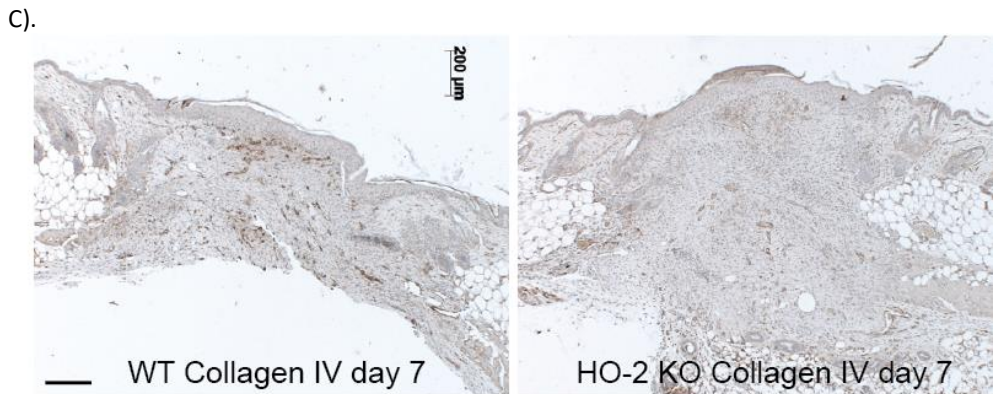
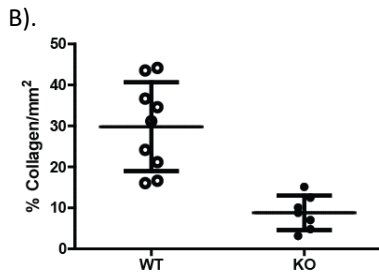
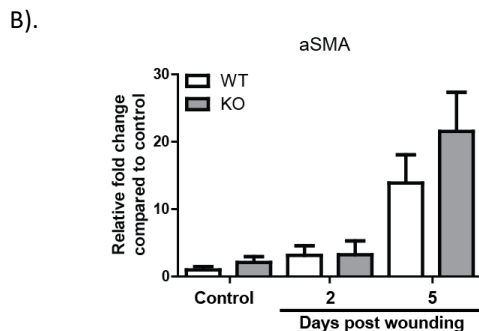
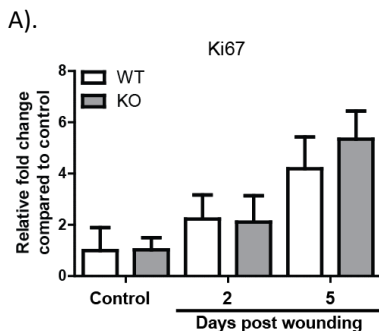
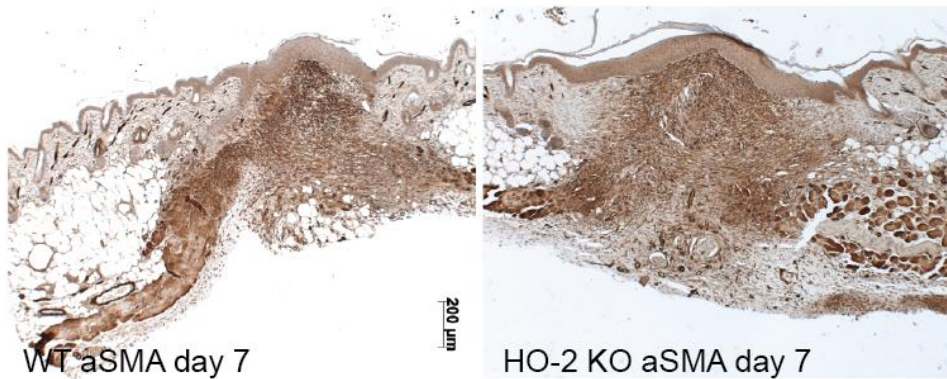


Figure 2.4 Reduced collagen deposition and vessel density in HO-2 KO mice. (A) Representative images of AZAN stained wound sections of WT and HO-2 KO mice at day 7 after wounding; bar, 200 μ m. (B) Collagen deposition in WT (open circles) and HO-2 KO (closed circles) mice at day 7 after wounding. (C) Representative images of collagen IV immunoreactivity, a common blood vessel marker, in WT and HO-2 KO mice at day 7 after wounding; bar, 200 μ m. (D) Semi-quantitative scoring of high-power fields of (C). Data are represented as box-and-whisker plot with 10–90 percentiles. * $p < 0.05$, *** $p < 0.001$.



C).



D).

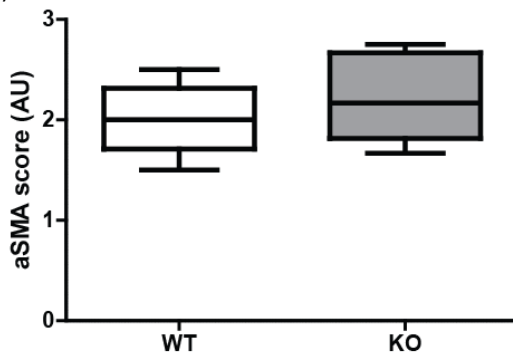


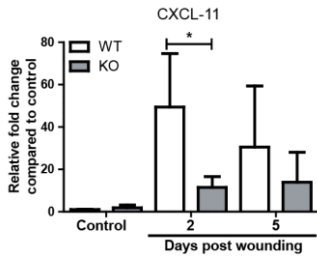
Figure 2.5 Myofibroblast differentiation occurs in HO-2 KO mice. Ki67 (A) and ACTA2 (B) gene transcript levels in WT (white bars) and HO-2 KO (grey bars) mice in time as represented as mean \pm SD. Controls represent biopsies collected at day 0, and data were normalized to WT mean day 0. (C) Representative images of α SMA immunoreactivity in wounds of WT and HO-2 KO mice at day 7 after wounding; bar, 200 μ m. (D) Semi-quantitative scoring of α SMA in (C) presented as box-and-whisker plot with 10–90 percentiles.

Different expression levels of CXCL-11 in WT and HO-2 KO mice after wounding

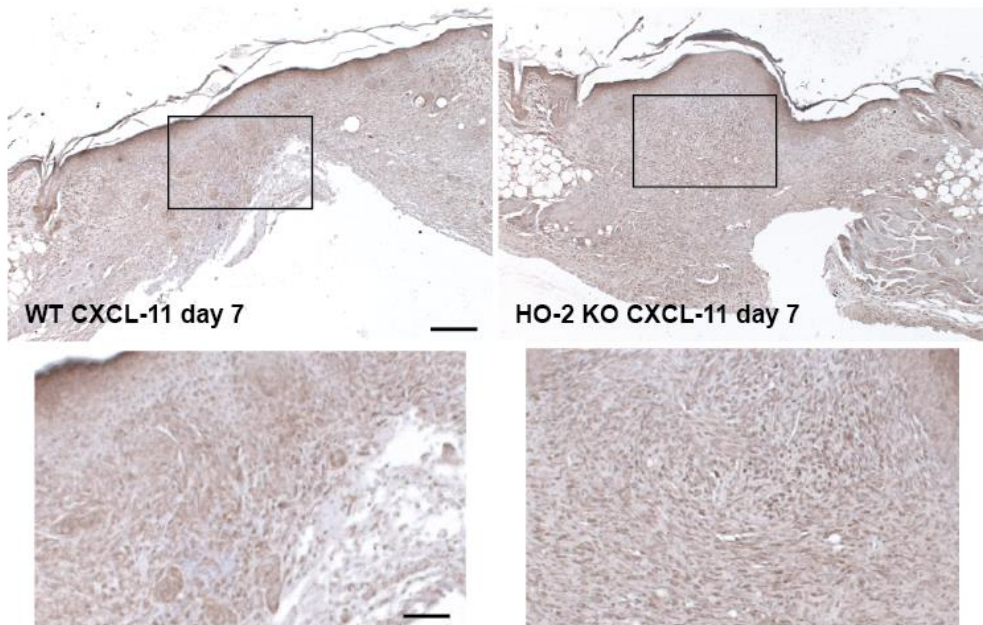
HO-1 deficiency is linked to delayed wound healing and impaired angiogenesis after injury. However, HO-2 deficient skin demonstrates injury-induced HO-1 expression, and we therefore wondered which genes could be explanatory for the reduced collagen deposition and lower vessel density observed in HO-2 KO mice. First, we compared gene expression profiles of pooled cDNAs isolated from day 5 wound tissue of HO-2 KO and WT mice using a PCR wound healing array, followed by validation by custom-designed primers and individual cDNAs. Unexpectedly, after individual validation we only detected significant differences between HO-2 KO and WT mice in the expression profile of a single gene out of 84 screened genes, namely CXCL-11 (Figure 2.6A, data not shown). Injury-induced CXCL-11 gene transcription observed in WT mice was absent in HO-2 KO mice at day 2 (49.4 ± 25.3 versus 11.5 ± 5.1 ; $p < 0.05$). However, at day 5 after wounding we detected similar CXCL-11 gene transcription levels in WT and HO-2 KO mice, which was mainly because of a down-regulation of gene transcription in WT mice (Figure 2.6A). In contrast, immunohistochemical staining and semi-quantitative scoring of wound tissue isolated from HO-2 KO and WT mice

7 days after wounding showed a markedly higher level of CXCL-11 positive cells in the wounds of HO-2 KO mice compared to WT controls ($p=0.0503$; Figure 2.6B and C).

A).



B).



C).

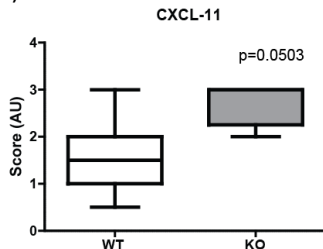


Figure 2.6 Different CXCL-11 expression in HO-2 KO and WT mice after injury. (A) CXCL-11 gene transcript levels in WT (white bars) and HO-2 KO (grey bars) mice in time presented as mean \pm SD. Controls represent biopsies collected at day 0, and data were normalized to WT mean day 0. (B) Semi-quantitative scoring of CXCL-11 immunoreactivity in (C) of WT (white) and HO-2 KO (grey) wounds presented as box-and-whisker plot with 10–90 percentiles. $*p<0.05$. (C) Representative images of CXCL-11 immunoreactivity in wound tissue of WT and HO-2 KO mice at day 7 after wounding; bar, 200 μ m. Insert represent magnified boxed area; bar, 70 μ m.

Discussion

In this study, we investigated the role of HO-2 in cutaneous wound closure using HO-2 KO mice and a full-thickness excisional wound model. High levels of HO-2 in the skin have been suggested to be a first line of defense against acute injury (34). Following excisional wounding we observed significantly slower cutaneous wound closure accompanied by reduced collagen deposition and lower vessel density in HO-2 KO mice compared to WT controls at day 7. The most pronounced difference in wound healing rates between HO-2 KO and WT seems to be during the first days of wound healing.

Cutaneous wounding is followed by hemolysis and free heme release leading to local oxidative stress and inflammation. HO-1 is rapidly induced after wounding (35, 36) and promotes inflammatory resolution by down-regulating inflammatory mediators and attenuating infiltration of inflammatory cells (37, 38). Moreover, pharmacologic induction or overexpression of HO-1 accelerates both corneal and cutaneous wound healing (12, 39). On the contrary, HO-1 deficiency in man and mice leads to a chronic inflammatory state (10, 11). Also, pharmacologic or genetic inhibition of HO-1 slows down cutaneous wound closure via suppressed re-epithelialization and neovascularization in murine models (12). In HO-2 KO mice impaired corneal wound healing is associated with exaggerated inflammation (13, 40). We therefore have been suggested that also the delayed cutaneous wound closure observed in HO-2 KO mice results from an exaggerated inflammatory response.

Unexpectedly, we did not detect significant differences in the mRNA or protein expression level of the pro-inflammatory proteins, such as TNF and COX-2 and markers for granulocytes and macrophages. This rules out that exaggerated inflammation is the underlying cause of delayed cutaneous wound closure in HO-2 KO mice. The exaggerated corneal inflammatory response was associated with impaired HO-1 induction and function (13). The importance of HO-activity was further supported by amelioration of corneal inflammatory resolution after application of biliverdin in HO-2 KO mice (14, 19).

HO-2 can regulate HO-1 induction and function in a tissue- and cell-specific manner (15, 17). Increased HO-1 expression has been suggested to be a compensatory mechanism in HO-2 deficient lung and myocardium (16, 41). We detected similar levels of both HO-1 mRNA and protein expression in unwounded skin and injury-induced HO-1 up-regulation after wounding of HO-2 KO and WT mice, explaining the normal inflammatory resolution in both genotypes. Cell-type-specific compensatory HO-1 expression likely dampens the inflammatory response after cutaneous wounding, as we observed a normal inflammatory phenotype in HO-1 expressing skin compared to the exaggerated inflammatory response in HO-1 deficient corneal tissue in HO-2 KO mice (13, 40, 42). Notably, delayed cutaneous wound closure in HO-1 KO mice is also not accompanied by an uncontrolled inflammatory response following excisional wounding (12).

We next turned our focus to the granulation phase of cutaneous wound healing that is dominated by migration, proliferation and differentiation of fibroblasts, keratinocytes and endothelial cells in the wound area. Differential expression of HO-1 and HO-2 in keratinocytes and fibroblasts has been demonstrated (43). This difference is critical for different sensitivities towards UV-induced oxidative stress (15, 44). This could also have consequences in a more complex setting, such as during wound repair. However, we did not observe any differences between HO-2 KO and WT mice with respect to the proliferation marker Ki67 or expression of the myofibroblast marker α SMA during the time course of wound healing.

Angiogenesis is a crucial process for proper wound healing, and disturbed blood vessel formation leads to delayed wound healing. Pro-angiogenic properties of HO-1 have been demonstrated (20, 21). Both diabetic db/db mice having weaker injury-induced HO-1 expression and HO-1 deficient mice demonstrate impaired vascularization and delayed wound closure which could be restored with HO-1 gene transfer (12). Here, we also observed lower vessel density in the wounds of HO-2 KO mice despite normal HO-1 expression. This may restrict the blood supply to the healing tissue and set back wound healing.

To probe the molecular mechanism responsible for the delayed cutaneous wound closure in HO-2 KO mice, we used a PCR array containing 84 wound healing associated genes. Surprisingly, we only detected significant differences between HO-2 KO and WT mice in the expression profile of a single gene, namely CXCL-11. CXCL-11 is a versatile cytokine that via interaction with its receptor CXCR3 is thought to modulate several cell types important during several phases of cutaneous wound repair (45). Decreased CXCL-11 or CXCR3 expression leads to delayed re-epithelialization, impaired epidermis maturation and is associated with altered angiogenesis (46-49). CXCL-11 is also an antagonist for C-C chemokine receptor type 5 (CCR5) (50). CCR5 KO mice have delayed wound closure, impaired neovascularization and reduced collagen production following excisional wounding (51). In contrast to WT controls, we did not detect any injury-induced up-regulation of CXCL-11 mRNA in HO-2 KO mice at day 2 after wounding. But, surprisingly, more CXCL-11 positive cells were present in the wounds of HO-2 KO mice compared to WT controls at day 7 after wounding. These observations imply that there is a slight delay in the expression of CXCL-11 gene and protein in HO-2 KO mice compared to WT controls. However, whether this is a consequence or a causing factor of the delayed cutaneous wound closure in HO-2 KO mice warrants further investigation. Summarizing, we demonstrated delayed dermal wound closure, decreased vascularization and reduced collagen deposition in HO-2 KO mice independent from inflammation and HO-1 expression. These data indicate a tissue-specific role for HO-2, as HO-2 seems to play a pivotal role in corneal, but not cutaneous, wound healing. This is directly linked to the regulation of injury-induced HO-1 expression. Furthermore, we report differences in the expression of the cytokine CXCL-11 between HO-2 KO and WT mice during wound repair. Whether this difference is causative or caused by the observed delay in cutaneous wound closure needs to be further investigated.

References

1. Martin P. Wound healing--aiming for perfect skin regeneration. *Science*. 1997;276(5309):75-81.
2. Buganza Tepole A, Kuhl E. Systems-based approaches toward wound healing. *Pediatric research*. 2013;73(4 Pt 2):553-63.
3. Sidgwick GP, Bayat A. Extracellular matrix molecules implicated in hypertrophic and keloid scarring. *JEurAcadDermatolVenereol*. 2012;26(2):141-52.
4. Grice EA, Segre JA. Interaction of the microbiome with the innate immune response in chronic wounds. *Advances in experimental medicine and biology*. 2012;946:55-68.
5. Otterbein LE, Choi AM. Heme oxygenase: colors of defense against cellular stress. *American journal of physiology Lung cellular and molecular physiology*. 2000;279(6):L1029-37.
6. Maines MD, Trakshel GM, Kutty RK. Characterization of two constitutive forms of rat liver microsomal heme oxygenase. Only one molecular species of the enzyme is inducible. *The Journal of biological chemistry*. 1986;261(1):411-9.
7. Grochot-Przeczek A, Dulak J, Jozkowicz A. Haem oxygenase-1: non-canonical roles in physiology and pathology. *ClinSci(Lond)*. 2012;122(3):93-103.
8. Willis D, Moore AR, Frederick R, Willoughby DA. Heme oxygenase: a novel target for the modulation of the inflammatory response. *NatMed*. 1996;2(1):87-90.
9. Abraham NG, Kappas A. Pharmacological and clinical aspects of heme oxygenase. *PharmacolRev*. 2008;60(1):79-127.
10. Yachie A, Niida Y, Wada T, Igarashi N, Kaneda H, Toma T, et al. Oxidative stress causes enhanced endothelial cell injury in human heme oxygenase-1 deficiency. *The Journal of clinical investigation*. 1999;103(1):129-35.
11. Kapturczak MH, Wasserfall C, Brusko T, Campbell-Thompson M, Ellis TM, Atkinson MA, et al. Heme oxygenase-1 modulates early inflammatory responses: evidence from the heme oxygenase-1-deficient mouse. *AmJPathol*. 2004;165(3):1045-53.
12. Grochot-Przeczek A, dLach R, Mis J, Skrzypek K, Gozdecka M, Sroczyńska P, et al. Heme oxygenase-1 accelerates cutaneous wound healing in mice. *PLoSOne*. 2009;4(6):e5803.
13. Seta F, Bellner L, Rezzani R, Regan RF, Dunn MW, Abraham NG, et al. Heme oxygenase-2 is a critical determinant for execution of an acute inflammatory and reparative response. *AmJPathol*. 2006;169(5):1612-23.
14. Bellner L, Wolstein J, Patil KA, Dunn MW, Laniado-Schwartzman M. Biliverdin Rescues the HO-2 Null Mouse Phenotype of Unresolved Chronic Inflammation Following Corneal Epithelial Injury. *Investigative ophthalmology & visual science*. 2011;52(6):3246-53.
15. Zhong JL, Raval C, Edwards GP, Tyrrell RM. A role for Bach1 and HO-2 in suppression of basal and UVA-induced HO-1 expression in human keratinocytes. *Free radical biology & medicine*. 2010;48(2):196-206.
16. Dennery PA, Spitz DR, Yang G, Tatarov A, Lee CS, Shegog ML, et al. Oxygen toxicity and iron accumulation in the lungs of mice lacking heme oxygenase-2. *The Journal of clinical investigation*. 1998;101(5):1001-11.
17. Ding Y, Zhang YZ, Furuyama K, Ogawa K, Igarashi K, Shibahara S. Down-regulation of heme oxygenase-2 is associated with the increased expression of heme oxygenase-1 in human cell lines. *The FEBS journal*. 2006;273(23):5333-46.
18. Ahanger AA, Prawez S, Leo MD, Kathirvel K, Kumar D, Tandan SK, et al. Pro-healing potential of hemin: an inducer of heme oxygenase-1. *EurJPharmacol*. 2010;645(1-3):165-70.
19. Bellner L, Vitto M, Patil KA, Dunn MW, Regan R, Laniado-Schwartzman M. Exacerbated corneal inflammation and neovascularization in the HO-2 null mice is ameliorated by biliverdin. *ExpEye Res*. 2008;87(3):268-78.
20. Bussolati B, Ahmed A, Pemberton H, Landis RC, Di Carlo F, Haskard DO, et al. Bifunctional role for VEGF-induced heme oxygenase-1 in vivo: induction of angiogenesis and inhibition of leukocytic infiltration. *Blood*. 2004;103(3):761-6.
21. Bussolati B, Mason JC. Dual role of VEGF-induced heme-oxygenase-1 in angiogenesis. *Antioxidants & redox signaling*. 2006;8(7-8):1153-63.
22. Poss KD, Tonegawa S. Reduced stress defense in heme oxygenase 1-deficient cells. *Proceedings of the National Academy of Sciences of the United States of America*. 1997;94(20):10925-30.
23. Tan SD, Xie R, Klein-Nulend J, van Rheden RE, Bronckers AL, Kuijpers-Jagtman AM, et al. Orthodontic force stimulates eNOS and iNOS in rat osteocytes. *J Dent Res*. 2009;88(3):255-60.
24. Gal P, Toporcer T, Vidinsky B, Mokry M, Novotny M, Kilik R, et al. Early changes in the tensile strength and morphology of primary sutured skin wounds in rats. *Folia biologica*. 2006;52(4):109-15.

25. Faragalla HF, Marcon NE, Yousef GM, Streutker CJ. Immunohistochemical staining for smoothelin in the duplicated versus the true muscularis mucosae of Barrett esophagus. *The American journal of surgical pathology*. 2011;35(1):55-9.
26. Park SS, Yang JI, Kim SK, Lee KC. Positive Effects of Orally Administered Sildenafil on Skin Wound Healing of Rats. *Tissue Engineering and Regenerative Medicine*. 2010;7(4):425-31.
27. Hadi AM, Mouchaers KT, Schalij I, Grunberg K, Meijer GA, Vonk-Noordegraaf A, et al. Rapid quantification of myocardial fibrosis: a new macro-based automated analysis. *Cell Oncol (Dordr)*. 2011;34(4):343-54.
28. Livak KJ, Schmittgen TD. Analysis of relative gene expression data using real-time quantitative PCR and the 2⁻(Delta Delta C(T)) Method. *Methods*. 2001;25(4):402-8.
29. Wang H, Yan S, Chai H, Riha GM, Li M, Yao Q, et al. Shear stress induces endothelial transdifferentiation from mouse smooth muscle cells. *Biochemical and biophysical research communications*. 2006;346(3):860-5.
30. Scharstuhl A, Mutsaers HA, Pennings SW, Szarek WA, Russel FG, Wagener FA. Curcumin-induced fibroblast apoptosis and in vitro wound contraction are regulated by antioxidants and heme oxygenase: implications for scar formation. *JCell MolMed*. 2009;13(4):712-25.
31. Barsky SH, Baker A, Siegal GP, Togo S, Liotta LA. Use of anti-basement membrane antibodies to distinguish blood vessel capillaries from lymphatic capillaries. *Am J Surg Pathol*. 1983;7(7):667-77.
32. Gerdes J, Lemke H, Baisch H, Wacker HH, Schwab U, Stein H. Cell cycle analysis of a cell proliferation-associated human nuclear antigen defined by the monoclonal antibody Ki-67. *J Immunol*. 1984;133(4):1710-5.
33. Eming SA, Krieg T, Davidson JM. Inflammation in wound repair: molecular and cellular mechanisms. *J Invest Dermatol*. 2007;127(3):514-25.
34. Wagener FA, Volk HD, Willis D, Abraham NG, Soares MP, Adema GJ, et al. Different faces of the heme-heme oxygenase system in inflammation. *Pharmacol Rev*. 2003;55(3):551-71.
35. Kampfer H, Kolb N, Manderscheid M, Wetzler C, Pfeilschifter J, Frank S. Macrophage-derived heme-oxygenase-1: expression, regulation, and possible functions in skin repair. *MolMed*. 2001;7(7):488-98.
36. Hanselmann C, Mauch C, Werner S. Haem oxygenase-1: a novel player in cutaneous wound repair and psoriasis? *The Biochemical journal*. 2001;353(Pt 3):459-66.
37. Wagener FA, da Silva JL, Farley T, de WT, Kappas A, Abraham NG. Differential effects of heme oxygenase isoforms on heme mediation of endothelial intracellular adhesion molecule 1 expression. *JPharmacolExpTher*. 1999;291(1):416-23.
38. Wagener FA, van Beurden HE, von den Hoff JW, Adema GJ, Figdor CG. The heme-heme oxygenase system: a molecular switch in wound healing. *Blood*. 2003;102(2):521-8.
39. Patil K, Bellner L, Cullaro G, Gotlinger KH, Dunn MW, Schwartzman ML. Heme oxygenase-1 induction attenuates corneal inflammation and accelerates wound healing after epithelial injury. *Invest OphthalmolVisSci*. 2008;49(8):3379-86.
40. Marrazzo G, Bellner L, Halilovic A, Li Volti G, Drago F, Dunn MW, et al. The role of neutrophils in corneal wound healing in HO-2 null mice. *PLoS one*. 2011;6(6):e21180.
41. Adachi T, Ishikawa K, Hida W, Matsumoto H, Masuda T, Date F, et al. Hypoxemia and blunted hypoxic ventilatory responses in mice lacking heme oxygenase-2. *Biochemical and biophysical research communications*. 2004;320(2):514-22.
42. Bellner L, Martinelli L, Halilovic A, Patil K, Puri N, Dunn MW, et al. Heme oxygenase-2 deletion causes endothelial cell activation marked by oxidative stress, inflammation, and angiogenesis. *JPharmacolExpTher*. 2009;331(3):925-32.
43. Applegate LA, Noel A, Vile G, Frenk E, Tyrrell RM. Two genes contribute to different extents to the heme oxygenase enzyme activity measured in cultured human skin fibroblasts and keratinocytes: implications for protection against oxidant stress. *Photochemistry and photobiology*. 1995;61(3):285-91.
44. Zhong JL, Edwards GP, Raval C, Li H, Tyrrell RM. The role of Nrf2 in ultraviolet A mediated heme oxygenase 1 induction in human skin fibroblasts. *Photochemical & photobiological sciences : Official journal of the European Photochemistry Association and the European Society for Photobiology*. 2010;9(1):18-24.
45. Davidson JM. Can scarring be turned off? *Am J Pathol*. 2010;176(4):1588-91.
46. Dale DC, Boxer L, Liles WC. The phagocytes: neutrophils and monocytes. *Blood*. 2008;112(4):935-45.
47. Yates CC, Whaley D, A YC, Kulesekaran P, Hebda PA, Wells A. ELR-negative CXC chemokine CXCL11 (IP-9/I-TAC) facilitates dermal and epidermal maturation during wound repair. *Am J Pathol*. 2008;173(3):643-52.

48. Yates CC, Whaley D, Hooda S, Hebda PA, Bodnar RJ, Wells A. Delayed reepithelialization and basement membrane regeneration after wounding in mice lacking CXCR3. *Wound repair and regeneration : official publication of the Wound Healing Society [and] the European Tissue Repair Society.* 2009;17(1):34-41.
49. Yates CC, Whaley D, Kulasekeran P, Hancock WW, Lu B, Bodnar R, et al. Delayed and deficient dermal maturation in mice lacking the CXCR3 ELR-negative CXC chemokine receptor. *Am J Pathol.* 2007;171(2):484-95.
50. Petkovic V, Moghini C, Paoletti S, Ugucioni M, Gerber B. I-TAC/CXCL11 is a natural antagonist for CCR5. *J Leukoc Biol.* 2004;76(3):701-8.
51. Ishida Y, Kimura A, Kuninaka Y, Inui M, Matsushima K, Mukaida N, et al. Pivotal role of the CCL5/CCR5 interaction for recruitment of endothelial progenitor cells in mouse wound healing. *J Clin Invest.* 2012;122(2):711-21.

Chapter 3

Chemokine signaling during midline epithelial seam disintegration facilitates palatal fusion.

Suttorp CM, **Cremers NA**, van Rheden R, Regan RF, Helmich P, van Kempen S, Kuijpers-Jagtman AM, Wagener FADTG.

Front Cell Dev Biol, 2017 Oct 30;5:94.

Abstract

Disintegration of the midline epithelial seam (MES) is crucial for palatal fusion, and failure results in cleft palate. Palatal fusion and wound repair share many common signaling pathways related to epithelial-mesenchymal cross-talk. We postulate that chemokine CXCL11, its receptor CXCR3, and the cytoprotective enzyme heme oxygenase (HO), which are crucial during wound repair, also play a decisive role in MES disintegration. Fetal growth restriction and craniofacial abnormalities were present in HO-2 knockout (KO) mice without effects on palatal fusion. CXCL11 and CXCR3 were highly expressed in the disintegrating MES in both wild-type and HO-2 KO animals. Multiple apoptotic DNA fragments were present within the disintegrating MES and phagocytized by recruited CXCR3-positive wt and HO-2 KO macrophages. Macrophages located near the MES were HO-1-positive, and more HO-1-positive cells were present in HO-2 KO mice compared to wild-type. This study of embryonic and palatal development provided evidence that supports the hypothesis that the MES itself plays a prominent role in palatal fusion by orchestrating epithelial apoptosis and macrophage recruitment via CXCL11-CXCR3 signaling.

Keywords: Embryology, cleft palate, chemokine, chemokine receptor, CXCL11, CXCR3, macrophage, heme oxygenase, cytoprotective enzymes, cell migration, apoptosis.

Abbreviations

ABC	avidin-biotin peroxidase complex
AP	Alkaline phosphatase
BCIP	5-bromo-4-chloro-3'-indolyphosphate
CLP	Cleft palate with cleft lip
CPO	Cleft palate without cleft lip
CO	Carbon monoxide
CXCL11	Chemokine (C-X-C) ligand 11
CXCR3	Chemokine (C-X-C) receptor 3
DAB	diaminobenzidine-peroxidase
E0	Embryonic day 0
EMT	Epithelial-to-mesenchymal transformation
FragEL	Fragment End Labeling
HE	Haematoxylin and eosin
HO	Heme oxygenase
KO	Knockout
KS-test	Kolmogorov-Smirnov test
MEE	Midline epithelial edge
MES	Midline epithelial seam
NBT	Nitro-blue tetrazolium
PBSG	Phosphate-buffered saline with glycine
ROS	Reactive oxygen species
TdT	Terminal deoxynucleotidyl Transferase
WT	Wild-type

Introduction

Formation of the secondary palate requires adhesion by the midline epithelial edge (MEE) of both palatal shelves, formation of the transient midline epithelial seam (MES), disintegration of the MES, and fusion of the palatal shelves (1). Only after disintegration of the MES the mesenchyme of the palatal shelves can fuse to form the secondary palate. Failure of epithelial adhesion between both palatal shelves (2) or a lack of MES disintegration (3, 4) will result in cleft palate with (CLP) or without cleft lip (CPO). Multiple mechanisms have been proposed to explain the disappearance of the MES. The main hypotheses underlying MES disintegration involve epithelial cell migration to the oral or nasal epithelium (5), epithelial-to-mesenchymal transformation (EMT) (6), epithelial cell apoptosis (7-10), or a combination of these events (3).

CLP is the most common congenital facial malformation in humans and occurs in approximately 1/700 live births (11). However, CPO is the rarest form of oral clefting, with an incidence ranging from 1.3 to 25.3/10,000 live births (12). Although the exact biological mechanisms underlying orofacial clefting are not completely understood (13), a combination of genetic and environmental factors is thought to play a role. Approximately 50% of children born with CPO have a genetic syndrome (14), compared to 30% with CLP (15). Notably, maternal smoking, diabetes, and infections have been shown to strongly increase the risk for babies with orofacial clefts (13, 16), suggesting that control of oxidative and inflammatory stress is important.

Accumulating data suggest that the heme-degrading antioxidative enzyme heme oxygenase (HO) is a key regulator during embryological development (17-19). HO facilitates placentalization, fetal growth, and -development by restricting excessive free heme levels. Heme promotes oxidative and inflammatory stress (20, 21) and may lead to intrauterine fetal growth restriction and fetal loss (17). HO protects against this inflammatory stress by degrading heme and generating free iron/ferritin, carbon monoxide (CO), and biliverdin/bilirubin (22). These HO effector molecules regulate vasodilation and anti-apoptotic signaling, inhibit platelet aggregation, reduce leukocyte adhesion, and reduce pro-inflammatory cytokines (22, 23). Two functional isoforms of HO have been described, HO-1 and HO-2. HO-1 has low basal levels but is strongly inducible, whereas HO-2 is largely constitutively expressed. HO-2 is highly expressed in the brain, testes, and blood vessels (24). Interestingly, the cytoprotective HO-1 and HO-2 enzymes are both strongly expressed in the placenta during embryonic development and in neural crest cells that form the craniofacial tissues in mice and humans (18, 25). Elevated inflammatory, oxidative, and angiogenic factors have been demonstrated in the endothelial cells of HO-2 knockout (KO) mice (26). During pregnancy, down-regulation of both HO-1 (27) and HO-2 (18) in the placenta is associated with pregnancy failure. Spontaneous abortion, pre-eclampsia, or fetal growth retardation are associated with lower HO-2 protein levels compared to healthy pregnant controls (18).

Palatal fusion and wound repair are regenerative processes that share common signaling pathways and gene regulatory networks (28). Epithelial-mesenchymal cross-talk is essential in both processes. Decreased signaling between the versatile CXCL11 and its receptor CXCR3 on epithelial cells leads to delayed re-epithelialization and impaired epidermis maturation during wound repair (29). Moreover, CXCR3 KO mice present excessive scar formation following injury (30). Macrophages are important in regenerative and embryonic developmental processes (31-34), and blocking the CXCL11-CXCR3 axis

suppresses macrophage infiltration (35, 36). Recently, slower wound closure and delayed CXCL11 expression in wounds was observed in HO-2 KO mice (37). Interestingly, HO-2 deficiency was shown to result in impaired macrophage function (38). Although CXCL11-CXCR3 signaling regulates diverse cellular functions, including influx of immune cells during inflammation (39, 40) and wound repair (29, 41), little is known about its role during palatal fusion.

We postulate that palatal fusion is hampered in HO-2 KO mice by disruption of epithelial cell and macrophage cross-talk in the MES due to hampered CXCL11-CXCR3 signaling. In the present study, MES disintegration is investigated in relation to chemokine signaling and the effects of HO-2 deficiency on embryonic development and palatal fusion.

Materials and Methods

Animals used for the study

To obtain fetuses for this study, 8-week-old female wild-type (wt) (n=7) and HO-2 KO (n=8) mice were mated with respectively wt and HO-2 KO male mice. Homozygote HO-2 KO mice generated by targeted disruption of the HO-2 gene (26, 42), and wt mice, both of a mixed 129Sv x C57BL/6 background, were bred and maintained in our animal facility. The animals were housed under normal laboratory conditions with 12 h light/dark cycle and *ad libitum* access to water and powdered rodent chow (Sniff, Soest, The Netherlands) and were allowed to acclimatize for at least 1 week before the start of the experiment. Ethical permission for the study was obtained according to the guidelines of the Board for Animal Experiments of the Radboud University Nijmegen (RU-DEC 2012-166).

Hormone administration before mating

Preliminary experiments (RU-DEC 2009-160) demonstrated that young animals (8-10 weeks old), that were mated for the first time, often did not carry fetuses. This was demonstrated for both wt mice and HO-2 KO mice. The chance of pregnancy was therefore enhanced using the hormones Folligonan (Genadotropin serum, Intervet Nederland B.V., Boxmeer, The Netherlands) and Pregnyl (Human chorionic gonadotropin, N.V. Organon, Oss, The Netherlands). Because there is a lag time period of approximately 13 days between hormone application and palatal formation, we expected minor influence on the experimental outcome. At day -3 at 4.00 p.m. Folligonan (6E in 30 μ l) and at day -1 at 4.00 p.m. Pregnyl (6E in 30 μ l) was administered by intraperitoneal injection.

Plugging day and obtaining wt and HO-2 KO fetuses

The presence of a vaginal copulation plug, indicating that mating has occurred, was taken as day 0 of pregnancy (embryonic day 0; E0) (43). 1 wt mouse and 2 HO-2 KO mice demonstrated no plugged status. These animals were mated again 4 weeks later, and all demonstrated then a plugged status.

Since the palatal shelves fuse between embryonic day E14.5 and E15.5 in wt mice (44) we presumed that fetuses of E15 were suitable for our study. At embryonic day E15, 7 wt and 7 HO-2 KO animals were killed by CO₂/O₂ inhalation for 10 minutes. Only 3 out of 7 plugged wt mice, and 4 out of 7 plugged HO-2 KO mice carried fetuses. In total, 16 wt fetuses of E15 and 11 HO-2 KO fetuses of E15 were obtained.

In order to monitor the growth restriction found in HO-2 KO fetuses in more detail, we also analyzed the body size of E16 HO-2 KO fetuses. Therefore, 1 pregnant HO-2 KO mouse was killed at embryonic day 16, resulting in 12 HO-2 KO fetuses of E16.

Implantation rate

The uterus and fetuses were photographed (Figure 3.1). For the fetus carrying mice the mean implantation rate was analyzed by calculating the percentage of fetuses to the total number of embryonic implantations (fetuses+non-viable or hemorrhagic embryonic implantations).

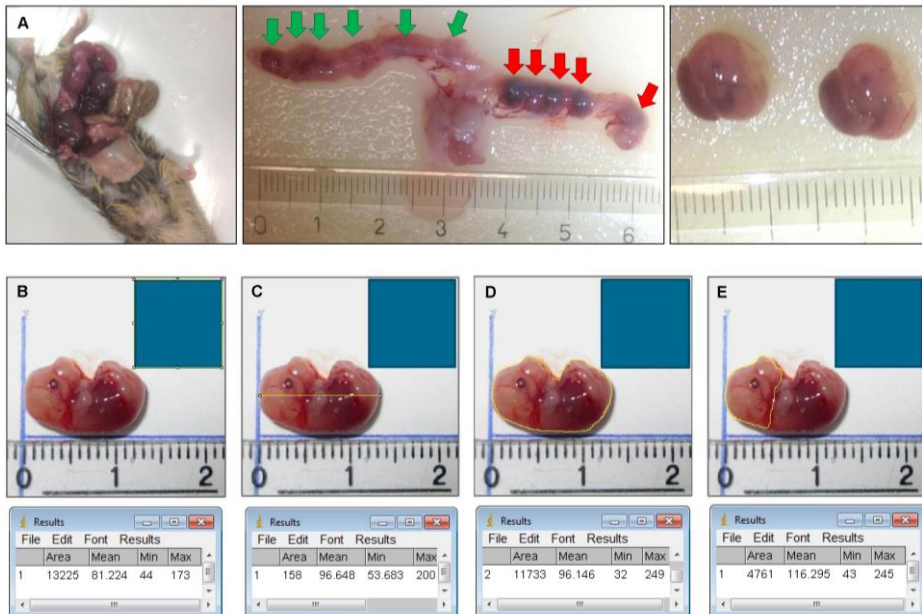


Figure 3.1: A: Isolation of the fetuses and measurement of body length, body surface, head surface. Plugged mouse (e.g., HO-2 KO at E15) was sacrificed by CO₂ inhalation for 10 minutes, the uterus and organs were removed. Fetuses were isolated from the uterus. Location of the 6 fetuses in the uterus before they were removed (green arrows). Location of the 5 non-viable/hemorrhagic embryonic implantations (red arrows). **B:** A square scale bar was drawn in each photograph of 10 x 10 mm (1 cm²) and the total number of pixels within the square was determined (e.g., 13225 pixels). **C:** A line in the length of the body of the fetus was drawn and the number of pixels was recorded (e.g., 158 pixels). The length was calculated (e.g., 158/√13225 = 13,7 mm). **D:** The outline of the total body surface of the fetus was drawn and the number of pixels was recorded (e.g., 11733 pixels). The total body surface was calculated (e.g., 11733/13225 = 0,89 cm²). **E:** The outline of the head surface was drawn and the number of pixels was recorded (e.g., 4761 pixels). The head surface was calculated (e.g., 4761/13225 = 0,36 cm²).

The wt and HO-2 KO fetuses compared for weight, length and body surface

The weight and size of wt fetuses (E15) and HO-2 KO fetuses (E15/E16) was measured. Severely malformed fetuses (n=2) were excluded for weight and size analysis. The body length, body surface and head surface of the fetuses were measured from photographs using ImageJ (1.48v) software (National institutes of health, Bethesda, MD, USA) and used for statistical analysis, for details see Figure 3.1.

Assessment of mRNA expression of HO-2, CXCL11, CXCR3 and HO-1 in fetus head samples by quantitative real-time PCR

To screen for differences in gene expression between HO-2 KO and wt fetuses, cDNAs were synthesized from samples from heads of wt (E15; n=5) and HO-2 KO (E15; n=4) fetuses. Fetuses were decapitated and total RNA was extracted using Trizol (Invitrogen, Carlsbad, CA, USA) and a RNeasy Mini kit (Qiagen, Hilden, Germany), and cDNA was produced using the iScript cDNA synthesis kit (Bio-Rad, Hercules, CA, USA). cDNAs were analyzed for gene expression of HO-1, HO-2, CXCL11 and CXCR3, using custom-designed primers (Table 3.1) and iQ SYBR Green Supermix (Invitrogen, Carlsbad, CA, USA) in a CFX96 real-time PCR system (Bio-Rad, Hercules, CA, USA). Relative gene expression values were evaluated with the $2^{-\Delta\Delta Ct}$ method using GAPDH as housekeeping gene (45).

Table 3.1: Custom-designed mouse primers used for assessment of mRNA expression of GAPDH, HO-1, HO-2, CXCL11 and CXCR3 in fetus head samples by quantitative real-time PCR.

Marker	Gene name	Forward primer (5'-3')	Reverse primer (5'-3')
Reference gene	<i>Gapdh</i>	GGCAAATTC AACGGCACA	GTTAGTGGGGTCTCGCTCCTG
Cytoprotection	<i>Hmox1</i>	CAACATTGAGCTGTTTGAGG	TGGTCTTTGTGTTCTCTGTGTC
Cytoprotection	<i>Hmox2</i>	AAGGAAGGGACCAAGGAAG	AGTGGTGGCCAGCTTAAATAG
Chemokine	<i>Cxcl11</i>	CACGCTGCTCAAGGCTTCTTATG	TGTCGCAGCCGTTACTCGGGT
Chemokine receptor	<i>Cxcr3</i>	CAGCTGAACCTTGACAGAACCT	GCAGCCCCAGCAAGAAGA

Haematoxylin-Eosin staining of transversal sections through the secondary palate

Mouse tissue samples were fixed for 24h in 4% paraformaldehyde and further processed for routine paraffin embedding. Paraffin sections were deparaffinized using Xylol, rehydrated using an alcohol range (100%-70%), and used for immunohistochemistry and FragEL™ analysis. Serial transversal sections through the secondary palate region of 5 µm thickness mounted on Superfrost Plus slides (Menzel-Gläser, Braunschweig, Germany) were routinely stained with Haematoxylin and Eosin (HE) for general tissue survey. The exact location of the fusing palatal shelves was determined per individual fetus. The HE stainings were subdivided into the four stages of palatogenesis based on the anatomy of the palatal shelves: elevation, horizontal, midline adhesion and fusion, according to Dudas et al. (44) and screened for anatomical abnormalities. These series were used as reference to obtain transversal sections containing palatal shelves in midline adhesion and fusion for immunohistochemical staining (Figure 3.2).

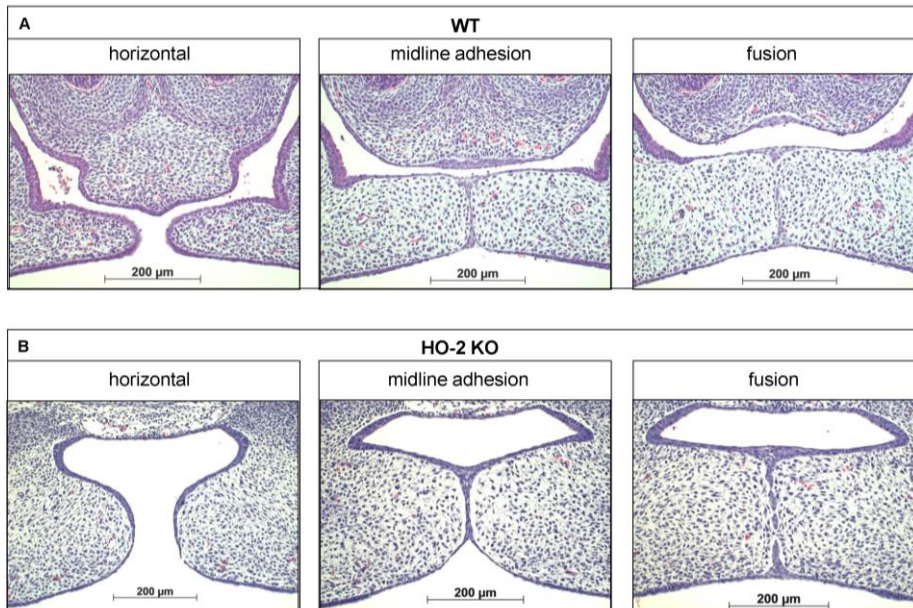


Figure 3.2: Palatal fusion observed in both wt and HO-2 KO fetuses at E15. HE stainings demonstrated horizontal orientation of the palatal shelves, midline adhesion and fusion within the same fetus. **A:** wt fetus at E15 (magnification: x100). Palatal shelves in a later stage of the palatal fusion increased in size. The MES changed from a multi-cell-layer into a continuous one-single-cell-layer, to a disintegrating MES, during which islands of epithelium in the midline were observed. **B:** HO-2 KO fetus at E15 (magnification: x100). Palatal shelves in a later stage of the palatal fusion increased to some extent in size. Several islands of epithelium in the midline were observed.

Immunohistochemistry

Selected paraffin embedded sections were deparaffinized using Xylo and rehydrated using an alcohol range (100%-70%). Endogenous peroxidase activity was quenched with 3% H₂O₂ in methanol for 20 min, and immunohistochemical stainings for HO-1, CXCL11, CXCR3 and macrophage marker F4/80 were performed as previously described (46). In brief, tissue sections were incubated for 60 min with a biotin-labeled secondary antibody (Table 3.2). Next, the sections washed with PBSG (phosphate-buffered saline with glycine) and treated with avidin-biotin peroxidase complex (ABC) for 45 min in the dark. After extensive washing with PBSG, diaminobenzidine-peroxidase (DAB) staining was performed for 10 min for the HO-1, CXCL11 and CXCR3 stainings.

Analysis of apoptosis and recruited F4/80 positive macrophages in the palate

For studying apoptosis in the MES, transversal sections containing palatal shelves in midline contact and fusion stage of wt and HO-2 KO fetuses were selected. During apoptosis, cellular endonucleases cleave nuclear DNA between nucleosomes, producing specific DNA fragments with free 3'-OH groups at the end. These 3' OH group can be labeled using Fragment End Labeling (FragEL™, Calbiochem, San Diego, CA, USA) allowing detection of apoptotic DNA fragments at the individual cell level as previously described (47). The procedure was performed according to the protocol of the manufacturer (Calbiochem, San Diego, CA, USA). In brief, rehydrated paraffin sections were subjected to proteinase K

digestion (0,5 µg/ml) for 10 min. Endogenous peroxidase activity was quenched with 3% H₂O₂ in methanol for 20 min. TdT (Terminal deoxynucleotidyl Transferase) added biotin labeled deoxynucleotides to the end of these DNA fragments. After addition of ABC, DAB was added and incubated at room temperature for 10 min. For the F4/80 staining + AP (alkaline phosphatase) + NBT (nitro-blue tetrazolium) + BCIP (5-bromo-4-chloro-3'-indolyphosphate) was used. For used antibodies and antigen retrievals, see table 3.2 and 3.3. Photographs were taken using a Carl Zeiss Imager Z.1 system (Carl Zeiss Microimaging GmbH, Jena, Germany) with AxioVision (4.8v) software (Zeiss, Göttingen, Germany).

Table 3.2: Antibodies and antigen retrievals used for immunohistochemical stainings for HO-1, CXCL11, CXCR3, F4/80 and apoptotic DNA fragments.

Antibody	Specificity	Dilution	Antigen retrieval	Source
SPA-895	HO-1	1:600	Combi: Citrate buffer 70°C for 10 min Trypsin digestion in PBS 0,015% 37°C for 5 min	Stressgen
Sc-34785	CXCL11	1:200	Citrate buffer 70°C for 2 hrs	Santa Cruz Biotechnology, Santa Cruz, CA, USA
NB100-56404	CXCR3	1:50	Citrate buffer 70°C for 2 hrs	Novus Biologicals, Littleton, USA
BM8	F4/80	1:400	Combi: Citrate buffer 70°C for 10 min Trypsin digestion in PBS 0,015% for 5 min	eBioscience

Table 3.3: Secondary antibodies used for HO-1, CXCL11, CXCR3, apoptotic DNA fragments immunohistochemical staining, and F4/80 with apoptotic DNA fragments/CXCR3/HO-1 double stainings. Antigen retrieval used for double stainings: Combi = Citrate buffer 70°C for 10 min + Trypsin digestion in PBS 0,075% 37°C for 5 min.

Secondary antibody	Specificity	Dilution	Color	Source
A11008	goat anti-rabbit AlexaFluor-488	1:500	Green	Invitrogen Thermofisher scientific
145-712-065-153 in combination with S-11226	donkey anti-rat Biotin	1:500	-	Jackson Immunoresearch Europe LTD
	Streptavidin AlexaFluor-568	1:500	Red	Invitrogen Thermofisher scientific
715-065-151	donkey anti-rabbit Biotin+ABC+DAB	1:500	Brown	Jackson Immunoresearch Europe LTD
	donkey anti-rabbit Biotin+ABC+AP+nbt/bcip	1:500	Blue	Calbiochem, San Diego, CA, USA

Quantification of CXCL11, CXCR3 and HO-1 immunoreactivity within the epithelium of the palatal shelves

Transversal sections through the secondary palate of wt and HO-2 KO fetuses were screened. For quantification sections were selected following the inclusion criteria: transversal sections containing palatal shelves in midline adhesion and fusion with at least the presence of a part of the MES.

The immunostained sections were first categorized into two categories based on their palatal morphology (palatal morphology classification): fusing palatal shelves, and fusing palatal shelves with adhesion to the nasal septum, see Figure 3.3.

Within each section the epithelium of the palatal shelves was then subdivided into three separate regions (Figure 3.3) according to morphological characteristics (Epithelium region classification): epithelium of the palatal shelves from the edge, including the MES, to the half of the width of the shelves (in RED), epithelium of the lateral half of the palatal shelves (in BLUE), epithelium of the lateral wall of the nasal cavity, this region is positioned outside the palatal shelves and served as a control region (in YELLOW), see Figure 3.3.

CXCL11, CXCR3 and HO-1 immunoreactivity was evaluated by two observers, by blindly scoring, independently of each other. The epithelial regions per single section were semi-quantitatively scored according to the immunoreactivity scoring scale in three categories (HIGH, MODERATE and LOW). For each individual fetus the modus of the scoring per epithelial region was used for further statistical analysis. For details see Figure 3.3. To determine the inter-examiner reliability, 10 sections were measured by the two observers and acceptable coefficient of determination (R^2) scores > 0.80 were obtained for immunoreactivity scoring.

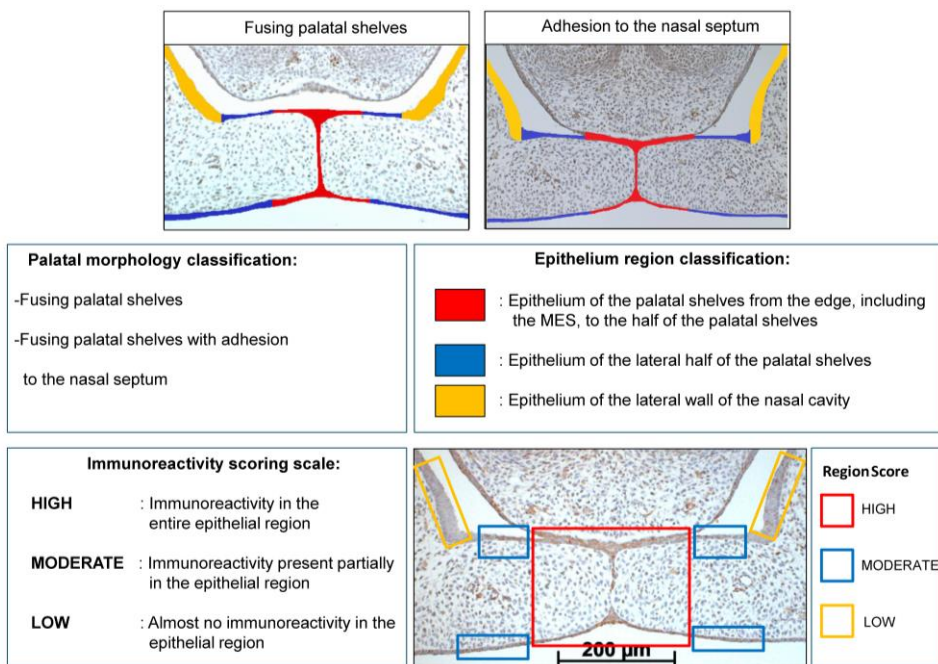


Figure 3.3: Palatal morphology classification: The CXCL11, CXCR3 and HO-1 immunostained sections were categorized in two stages according to their morphological characteristics: fusing palatal shelves, and fusing palatal shelves with adhesion to the nasal septum. **Epithelium region classification:** For each section epithelial layers were subdivided in 3 regions of interest according to morphological characteristics: epithelium of the palatal shelves from the edge, including the MES, to half of the width of the shelves (in RED), epithelium of the lateral half of the palatal shelves (in BLUE), epithelium of the lateral wall of the nasal cavity, this region is positioned outside the palatal shelves and served as a control region (in YELLOW). **Immunoreactivity scoring scale:** Semi-quantitative scoring of CXCL11, CXCR3 and HO-1 immunoreactivity in epithelium of the palatal shelves. Each epithelial region was semi-quantitatively scored according to the following scale: (HIGH) Immunoreactivity present in the entire epithelial region, (MODERATE) Immunoreactivity present only partially in the epithelial region, (LOW) Almost no

immunoreactivity present in the epithelial region. **Right lower panel:** Immunoreactivity scored for the 3 epithelial locations in a CXCL11 immunostained section (e.g., wt fetus, E15, section with adhesion of the palatal shelves and adhesion to the nasal septum). RED region was scored as HIGH, BLUE region was scored as MODERATE, YELLOW region was scored as LOW for CXCL11 immunoreactivity.

Quantification of CXCL11, CXCR3 and HO-1 positive cells in the mesenchyme of the palatal shelves

The immunostained sections, wt and HO-2 KO, were first categorized based on their morphology (Palatal morphology classification, Figure 3.3). Since a significant variance in the size of the palatal shelves was present, expression was adjusted to surface area. The individual surface of each pair of shelves was measured using ImageJ (1.48v) software (Zeiss, Göttingen, Germany). Then, the number of CXCL11, CXCR3 and HO-1 positive cells within the outline of the mesenchyme of the palatal shelves was counted. For details see Figure 3.4. For each section the number of positive mesenchymal cells/mm² was calculated. Cell counting was performed twice, by two blinded observers independently of each other, and the mean value of positive cells/mm² per fetus was calculated and used for statistical analysis. To determine the inter-examiner reliability, 10 sections were measured by the two observers and acceptable coefficient of determination (R^2) scores > 0.80 were obtained for cell counting.

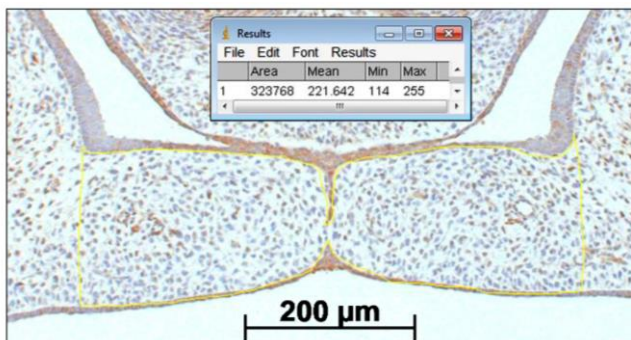


Figure 3.4: Palatal shelf surface measurement for determining the number of CXCL11, CXCR3 and HO-1 positive immunostained cells cells/mm² within the mesenchyme of the palatal shelves. A square scale bar was drawn in the microscopic picture (magnification: x100) of the section of 1000µm x 1000µm (1 mm²) and the total number of pixels within the square was determined (e.g., 1 mm² = 3442880 pixels). The contour of the mesenchyme of the shelves was drawn (yellow line). The number of pixels for this area was determined by the ImageJ (1.48v) software (323768 pixels). The number of positive immunostained cells within this mesenchymal area of the palatal shelves were counted by direct observation using the Zeiss microscope (e.g., 52 CXCL11 positive cells). The number of cells/mm² was calculated (3442880/323768) x 52 = 553 cells/mm².

Apoptotic DNA fragments in macrophages

Transversal sections containing palatal shelves in midline adhesion and fusion of wt and HO-2 KO fetuses were selected for the F4/80-immuno staining - FragEL™ DNA fragmentation kit combination. The F4/80 surface receptor is considered as one of the best markers for mature macrophages (48). The proximity of macrophages to apoptotic DNA fragments within the MES and the presence of apoptotic DNA fragments within the F4/80 positive macrophages were studied. For used antibodies and antigen retrievals, see tables 3.2 and 3.3.

CXCR3 and HO-1 expression in macrophages studied by immunofluorescence microscopy

Double staining for F4/80 with CXCR3/HO-1 were performed on paraffin sections of wt and HO-2 KO fetuses. Tissue samples were fixed for 24h in 4% paraformaldehyde and further processed for routine paraffin embedding. Sections were deparaffinized using Histosafe and rehydrated using an alcohol range (100%-70%). Fluorescent immunohistochemical double stainings for F4/80 with CXCR3, and F4/80 with HO-1 were performed. Nuclear staining was performed with DAPI. For antibodies used, see tables 3.2 and 3.3.

Statistical analysis

The data for the implantation rate, fetus weight, fetus length, fetus surface, fetus head surface and the PCR data for the mRNA expression of HO-1, HO-2, CXCL11, and CXCR3 showed a normal distribution as evaluated by the Kolmogorov-Smirnov test (KS-test).

To compare differences in implantation rate between the wt group and HO-2 KO group the Independent-Samples T-test was performed.

To analyze the fetus weight, fetus length, fetus surface, fetus head surface for the wt E15 group, the HO-2 KO E15 group and the HO-2 KO E16 group the ANOVA and Tukey's multiple comparison *post hoc* test were used.

The HO-1, CXCL11 and CXCR3 immunoreactivity in the epithelium regions was semi-quantitatively scored and analyzed using the non-parametric Kruskal-Wallis ANOVA on ranks test and Dunn's Multiple Comparison *post hoc* test to compare differences between the wt group and HO-2 KO group.

The data from quantification of the number of HO-1 positive cells in the mesenchyme showed a non-normal distribution as measured by the KS-test and the non-parametric Mann-Whitney U test was used to compare differences between the wt group and HO-2 KO group.

Quantification data of the number of CXCL11 and CXCR3 positive cells in the mesenchyme showed a normal distribution as measured by the KS-test. Independent-Samples T-test was performed to compare differences between the wt group and HO-2 KO group.

To determine the inter-examiner reliability, the coefficient of determination (R^2) was calculated by the square of the Pearson correlation coefficient for the quantitative data, and calculated by the square of the Spearman correlation coefficient for the semi-quantitative data.

Differences were considered to be significant if $p < 0.05$. All statistical analyses were performed using Graphpad Prism 5.03 software (GraphPad Software, San Diego, CA, USA).

Results

Fetal growth restriction and malformations occur in the absence of HO-2 expression

Quantitative real-time PCR confirmed the genotypes of mice by showing that HO-2 mRNA was only present in samples from wild-type (wt) fetuses, and not in HO-2 KO fetuses ($p < 0.001$, Figure 3.5A). Hemorrhagic embryonic implantations were found in both wt and HO-2 KO animals (Figure 3.1A). No significance difference in the mean implantation rate was found between pregnant wt and HO-2 KO mice (46% versus 52%, $p = 0.79$). At E15, HO-2 KO fetuses weighed significantly less ($p < 0.05$, Figure 3.5B) with a significantly smaller body surface than wt fetuses ($p < 0.01$, Figure 3.5C). The differences fetus length ($p = 0.25$, Figure 3.5D) and in head/body surface ratio ($p = 0.97$, Figure 3.5E) for both genotypes were not

significantly different at E15. To monitor the restriction of fetal growth in HO-2 KO fetuses in more detail, we also analyzed the body size of E16 HO-2 fetuses. No significant difference was found between the E15 wt fetuses and E16 HO-2 KO fetuses in regards to weight (Figure 3.5B) and body surface (Figure 3.5C). No malformations or craniofacial anomalies were found in the wt fetuses (Figure 3.5F). Among the 15 HO-2 KO fetuses (E15 and E16), 1 E16 fetus had severe malformations (Figure 3.5I), 1 E16 fetus exhibited a craniofacial anomaly (Figure 3.5J), and 1 E15 fetus appeared to be the smallest fetus without anomalies (Figure 3.5K).

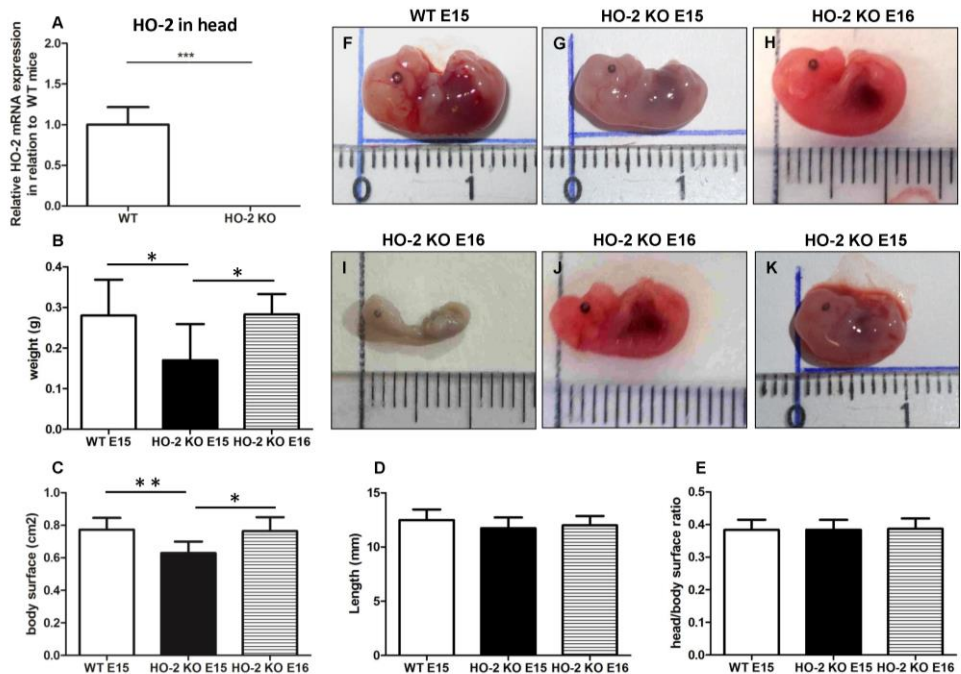


Figure 3.5: Fetal growth restriction and malformations occur in the absence of HO-2 expression. A: HO-2 mRNA was not found in HO-2 KO fetuses. HO-2 mRNA was observed in wt fetuses E15 (n=5), but not in HO-2 KO fetuses E15 (n=4). wt fetuses (E15; n=15), HO-2 KO fetuses (E15; n=4) and HO-2 KO fetuses (E16; n=11) were compared for B: weight, C: body surface and D: length (p=0.25), E: head/body surface ratio (p=0.97). Data present mean \pm SD. (*=p<0.05; **=p<0.01), (***=p<0.001). F: wt fetus at E15 (0,28g; 12,9mm). G: HO-2 KO fetus at E15 (0,13g; 12,5mm). H: HO-2 KO fetus at E16 (0,31g; 12,4mm). I: HO-2 KO fetus at E16 demonstrating severe malformations (0,065g; 10mm). J: HO-2 KO fetus at E16 demonstrating a craniofacial anomaly (0,20g, 12,2mm). K: HO-2 KO fetus at E15 appeared to be the smallest fetus without anomalies (0,10g, 10,3mm).

Palatal fusion observed in both wt and HO-2 KO fetuses at E15

Though the HO-2 KO fetuses were smaller in size, no difference in the adhesion and fusion of the palatal shelves was observed between the sections from wt and HO-2 KO fetuses at E15. In 2 wt fetuses and 2 HO-2 KO fetuses at E15, the palatal shelves were not yet elevated. In both genotypes, different phases of palatogenesis were observed in histological sections from the same fetus. The MES changes from a multi-cell layer into a continuous single-cell layer, to a disintegrating MES, during which islands of epithelium are observed. For more details, see Figure 3.2.

CXCL11 expression in the MES and mesenchyme

Because CXCL11 plays an important role in wound repair, we investigated the mRNA expression of chemokine CXCL11 in fetal head samples. CXCL11 mRNA was observed in samples from both wt and HO-2 KO fetuses without reaching a significant difference between the two genotypes ($p=0.88$, Figure 3.6).

Next, we investigated the cellular expression of CXCL11 during palatal fusion. CXCL11 protein was significantly higher expressed in the epithelium of the MES compared to the other epithelial layers of the fusing palatal shelves and the epithelium of the nasal cavity in both wt ($p<0.001$) and HO-2 KO fetuses ($p<0.001$)(Figure 3.6B, C, F-H). No significant difference was found between the genotypes. High CXCL11 protein expression was also found within the epithelium of the tips of the palatal shelves lacking midline adhesion, in sections of both genotypes (data not shown). CXCL11-positive cells were also observed in the mesenchyme of the palatal shelves, but no significant difference in the number of CXCL11-positive cells/mm² was found between the wt and HO-2 KO groups ($p=0.97$, Figure 3.6D) or in the samples with fusing palatal shelves with adhesion to the nasal septum ($p=0.47$, Figure 3.6E).

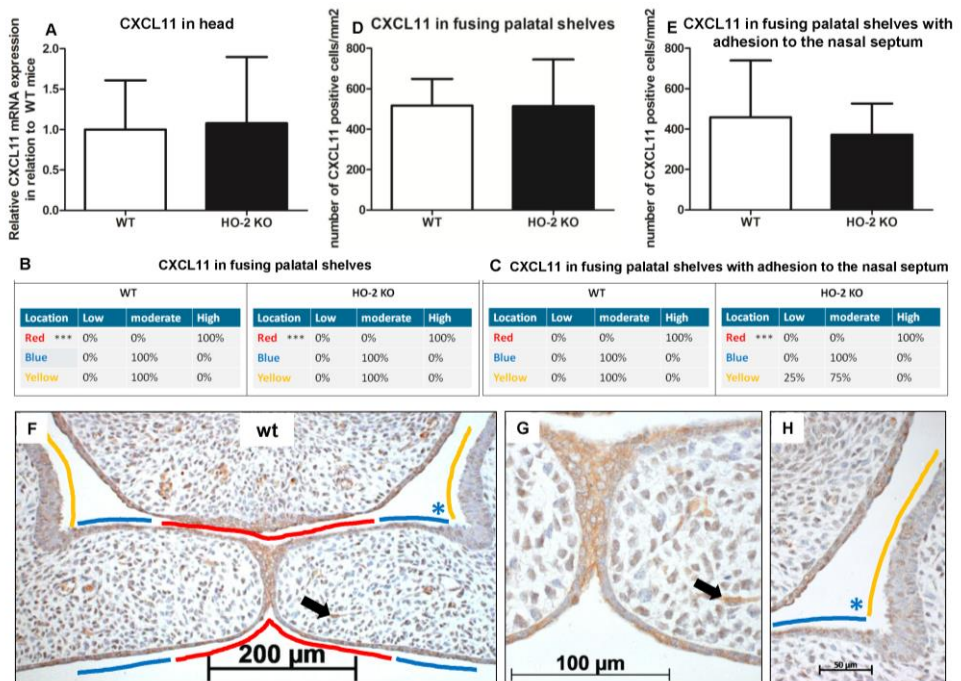


Figure 3.6: CXCL11 expression in the MES and mesenchyme in both wt and HO-2 KO fetuses. **A:** CXCL11 mRNA expression was both present in wt ($n=5$) and in HO-2 KO E15 fetuses ($n=4$)($p=0.88$). Data present mean \pm SD. CXCL11 overexpression in the MES in wt and HO-2 KO fetuses. Scoring was performed according to figure 3.3. **B:** Significant higher CXCL11 expression was observed in the MES (in RED)(***= $p<0.001$) compared to the other epithelial regions in the fusing palatal shelves (in BLUE) and the nasal cavity (in YELLOW) in the wt group and HO-2 KO group. **C:** Significant higher CXCL11 expression was observed in the MES (in RED)(***= $p<0.001$) compared to the BLUE region and YELLOW region in the HO-2 KO sections with fusing palatal shelves with adhesion to the nasal septum. **D:** No significant difference in the number of CXCL11 positive cells/mm² in the mesenchyme of the fusing palatal shelves was found between the wt and HO-2 KO fetuses($p=0.97$). Data present mean \pm SD. **E:** No significant

difference in the number of CXCL11 positive cells/mm² was found in the mesenchyme between the wt and HO-2 KO group in the sections with fusing palatal shelves with adhesion to the nasal septum ($p=0.97$). Data present mean \pm SD. **F:** Representative CXCL11 immunostaining in fusing palatal shelves without adhesion to the nasal septum of a wt fetus (E15) (magnification: x100). The MES (in RED) was highly CXCL11 positive compared to the other epithelial regions; epithelium of the lateral half of the palatal shelves (in BLUE) and epithelium of the lateral wall of the nasal cavity (in YELLOW). **G:** Several CXCL11 positive cells in the mesenchyme were observed (e.g., black arrow indicates a CXCL11 positive cell in the mesenchyme) (magnification: x400). This was found in both wt and HO-2 KO fetuses. **H:** Moderate CXCL11 expression in the epithelium of the lateral half of the palatal shelf (in BLUE), and in the epithelium of the lateral wall of the nasal cavity (in YELLOW) (magnification: x400).

CXCR3 expression in the MES and mesenchyme

Next, we investigated the expression of CXCL11 receptor CXCR3 at the mRNA level. In samples from heads of wt and HO-2 KO fetuses, CXCR3 mRNA expression was observed but with no significant difference between the groups ($p=0.16$, Figure 3.7).

CXCR3 protein expression was significantly higher in the epithelium of the MES than the other epithelial layers of the palatal shelves and the epithelium of the nasal cavity in the fusing palatal shelves of the wt fetuses ($p<0.05$, Figure 3.7B, F-H). Higher CXCR3 protein expression in the epithelium of the MES was also observed in the fusing palatal shelves with adhesion to the nasal septum from the HO-2 KO fetuses ($p<0.001$, Figure 3.7C).

Interestingly, CXCR3-positive cells were also observed in the mesenchyme of the palatal shelves. No significant difference in the number of CXCR3-positive cells/mm² was found between the wt and HO-2 KO groups in the fusing palatal shelves ($p=0.96$, Figure 3.7D) or the fusing palatal shelves with adhesion to the nasal septum ($p=0.20$, Figure 3.7E).

CXCR3-positive macrophages were located near the MES and phagocytized apoptotic cell fragments of the MES

CXCR3-positive cells are suspected of being macrophages based on morphology and because macrophages have been shown to be positive for CXCR3 (35, 36). Therefore, we investigated whether CXCR3-positive macrophages are present within the fusing palate using immunofluorescence microscopy. F4/80-CXCR3 double-positive macrophages were observed in the fusing palatal shelves, with some located near the disintegrating MES, in both wt and HO-2 KO fetuses (Figure 3.8).

In both wt and HO-2 KO fetuses, multiple apoptotic DNA fragments were present in the epithelial cells of the disintegrating MES. No apoptotic cell fragments were observed in the other epithelial regions. To assess whether the recruited macrophages phagocytose these apoptotic cell fragments, we stained for both apoptotic fragments and macrophages (FragEL™ DNA fragmentation assay in combination with F4/80). Macrophages located near the MES did phagocytose apoptotic DNA fragments (Figure 3.9A, B, C). Other macrophages were observed in the mesenchyme closely localized near the apoptotic DNA fragments within the disintegrating MES (Figure 3.9B).

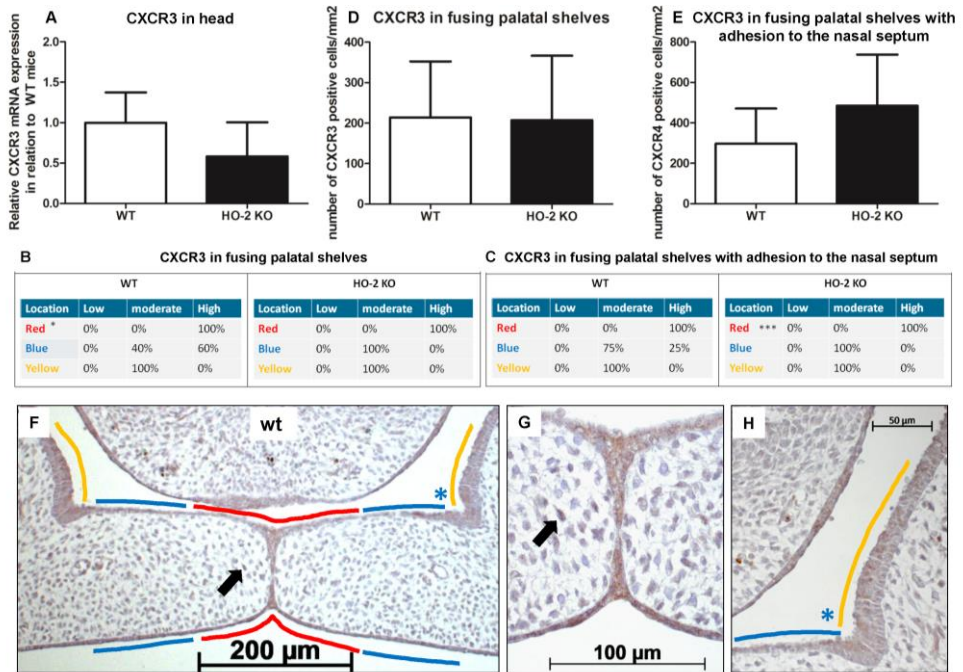


Figure 3.7: CXCR3 expression in the MES and mesenchyme in both wt and HO-2 KO fetuses. **A:** CXCR3 mRNA expression was found in wt fetuses E15 (n=5) and in HO-2 KO fetuses E15 (n=4)(p=0.16). Data present mean \pm SD. **B:** Statistically significant higher CXCR3 expression was observed in the wt group in the MES (in RED)(*= $p < 0.05$) compared to the YELLOW region. **C:** Significant higher CXCR3 expression was observed in the MES (in RED) (**= $p < 0.001$) compared to the BLUE region and YELLOW region in the HO-2 KO sections with adhesion of the palatal shelves and adhesion to the nasal septum. **D:** No significant difference in the number of CXCR3 positive cells/mm² in the mesenchyme of the fusing palatal shelves was found between the wt and HO-2 KO fetuses)(p=0.96). Data present mean \pm SD. **E:** No significant difference in the number of CXCR3 positive cells/mm² in the mesenchyme was found between the wt and HO-2 KO group of the sections with adhesion of the palatal shelves and adhesion to the nasal septum(p=0.47). Data present mean \pm SD. **F:** Representative CXCR3 immunostaining of fusing palatal shelves without adhesion to the nasal septum of a wt fetus (E15) (magnification: x100). The MES (in RED) had higher CXCR3 expression compared to the other epithelial regions (in BLUE) and (in YELLOW). **G:** Some CXCR3 positive cells in the mesenchyme were observed. This was found for the wt sections and HO-2 KO sections (black arrow indicates a CXCR3 positive cell in the mesenchyme) (magnification: x400). **H:** Moderate CXCR3 expression in the epithelium of the lateral half of the palatal shelf (in BLUE), and in the epithelium of the lateral wall of the nasal cavity (in YELLOW) (magnification: x400).

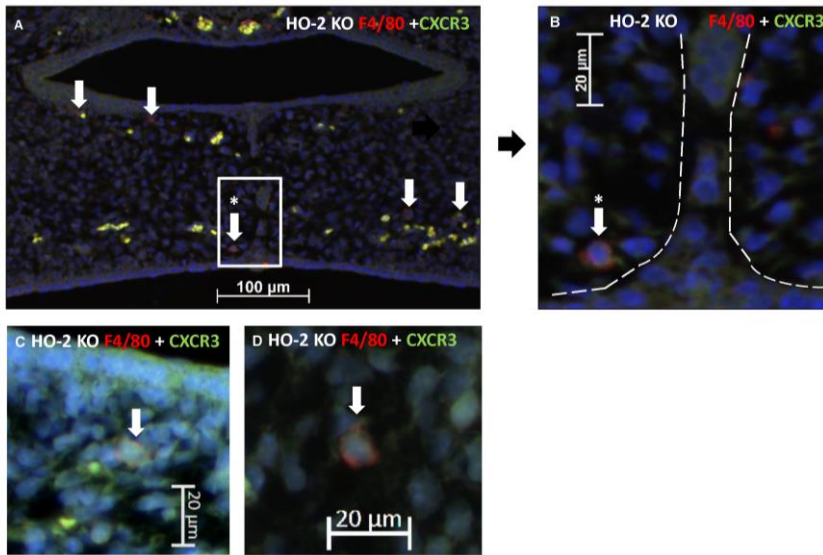
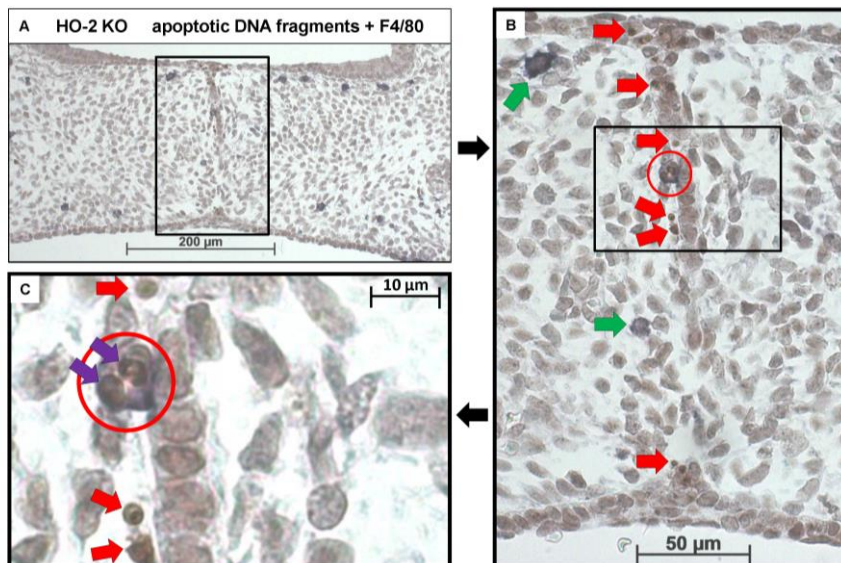


Figure 3.8: CXCR3 positive macrophages were located near the MES. **A:** Representative immunofluorescent histochemical double staining for F4/80 (red) with CXCR3 (green) in HO-2 KO section (E16). Nuclear staining with DAPI (Blue). The mesenchyme demonstrates the presence of a F4/80 positive HO-2 KO macrophages, which also express CXCR3 (white arrows) (magnification: x200). One CXCR3 F4/80 positive HO-2 KO macrophage was located near the disintegrating MES (white arrow within the white square). **B:** Magnification of a F4/80 positive HO-2 KO macrophage located near the MES (area between the dotted white lines) (magnification: x400). **C:** Magnification of a F4/80 positive HO-2 KO macrophage located in the mesenchyme of the palate shelf (magnification: x400). **D:** Magnification of a F4/80 positive HO-2 KO macrophage located outside the palatal shelf (magnification: x400).



3.9: Macrophages located near the MES phagocytose apoptotic cell fragments.

A: Representative FragEL™ DNA fragmentation assay (brown) in combination with F4/80 (dark blue) macrophage staining. Fusing palatal shelves in a HO-2 KO fetus (E16) (magnification: x100). Multiple macrophages were observed in the mesenchyme of the palatal shelves. **B:** Magnification of the disintegrating MES (magnification: x400, black square). Multiple apoptotic DNA fragments are observed within the MES (Red arrows). The only

Figure

apoptotic DNA fragments in the palatum outside the MES are in macrophages that had taken up epithelial cells seen. Two macrophages were located near the MES (green arrows), one macrophage was in close contact with the MES (red circle). **C:** Magnification of the macrophage in close contact with the MES (black square). In this macrophage (red circle), two apoptotic cell fragments within its cell body are present (purple arrows). Apoptotic DNA fragments near the macrophage were observed (red arrows). These findings were representative for both wt and HO-2 KO sections.

More HO-1-positive cells are found in palatal shelves from HO-2 KO fetuses

As macrophages can express the cytoprotective enzyme HO-1 during the digestion of cellular debris (49, 50), we studied whether HO-1-positive macrophages are present within the fusing palate. HO-1 mRNA was observed in samples from the heads of both wt and HO-2 KO fetuses without reaching a significant difference between the two genotypes ($p=0.35$, Figure 3.10A). Double immunostaining for macrophage marker F4/80 and HO-1 showed that many F4/80-positive macrophages were positive for HO-1. F4/80 and HO-1-positive cells were observed in the fusing palatal shelves and near the disintegrating MES in both wt and HO-2 KO fetuses (Figure 3.10B, C).

The number of HO-1-positive cells in the mesenchyme of the fusing palatal shelves was significantly higher in the HO-2 KO group than in the wt group ($p=0.02$, Figure 3.10D-G). Almost no HO-1 expression was observed in the epithelium of the palatal shelves in the wt and HO-2 KO groups.

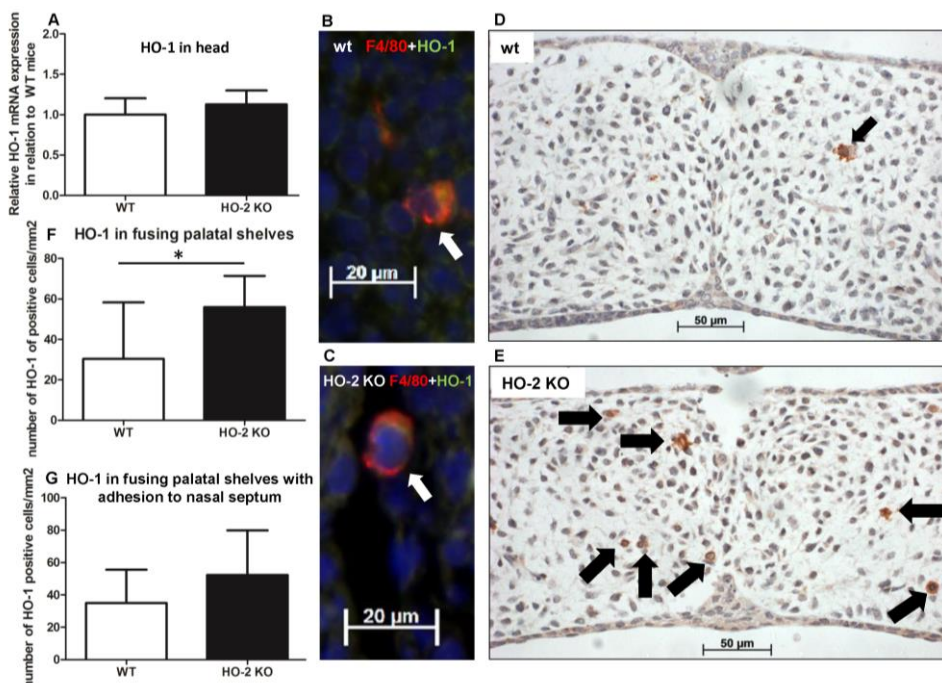


Figure 3.10: More HO-1-positive cells are found in palatal shelves from HO-2 KO fetuses. **A:** HO-1 mRNA expression was similar in wt fetuses E15 (n=5) and in HO-2 KO fetuses E15 (n=4) ($p=0.35$). Data present mean \pm SD. **B:** Representative fluorescent immunohistochemical double staining for F4/80 and HO-1 of fusing palatal shelves with adhesion to the nasal septum of a wt fetus (E15) (magnification: x400). A part of the mesenchyme around the MES, showing a F4/80 positive macrophage (red) expressing HO-1 (green) located (white arrow). Nuclear staining with DAPI (Blue). **C:** Representative fluorescent immunohistochemical double staining for F4/80 with HO-1 of

fusing palatal shelves with adhesion to the nasal septum of a HO-2 KO fetus (E16) (magnification: x400). A F4/80 positive HO-2 KO macrophage (red) expressing HO-1 (green) located near the MES (white arrow). Nuclear staining with DAPI (Blue). **D:** Representative HO-1 immunostaining of palatal shelves of a wt fetus (E15) (magnification: x400). This part of the mesenchyme demonstrates the presence of one HO-1 positive cell (black arrow). **E:** Representative HO-1 immunostaining of fusing palatal shelves of a HO-2 KO fetus (E16) (magnification: x400). This part of the mesenchyme demonstrates the presence of seven HO-1 positive cells (black arrows). **F:** Significant higher numbers of HO-1 positive cells/mm² were observed in the HO-2 KO fetuses compared to the wt fetuses in the fusing palatal shelves (p=0.02). Data present mean ± SD. **G:** Numbers of HO-1 positive cells/mm² in the mesenchyme of wt and HO-2 KO fetuses in the fusing palatal shelves with adhesion to the nasal septum (p=0.60). Data present mean ± SD.

Discussion

Although deletion of HO-2 expression in mice leads to fetal growth restriction, severe malformations, and craniofacial anomalies, we found no evidence of disruption of palatal fusion in HO-2 KO fetuses. We showed that multiple apoptotic DNA fragments were exclusively present in the MES of both genotypes, supporting earlier findings that apoptosis of epithelial cells drives MES disintegration (8). We demonstrated that both CXCR3 and its ligand, the chemokine CXCL11, were highly expressed by epithelial cells in the MES, suggesting that chemokine signaling acts via an autocrine loop to initiate processes involved in its own disintegration. Although, probably also other downstream mechanisms play a role in this process, such as caspases, other enzymes and apoptotic DNA fragments. We demonstrated that apoptotic DNA fragments from the MES were phagocytized by both wt and HO-2 KO macrophages. It is likely that CXCR3-positive macrophages were recruited via CXCL11 expression by the MES (Figure 3.11). However, we cannot exclude that additionally, other mechanisms can in a later phase facilitate macrophage recruitment. For example, apoptotic nucleotide fragments derived from the MES have been demonstrated to promote macrophage contributed to this recruitment (51). Macrophages near the disintegrating MES were positive for HO-1 in both wt and HO-2 KO fetuses, but more HO-1-positive cells were found in the palate mesenchyme from HO-2 KO fetuses. Although HO-2 KO macrophages have been shown to be dysfunctional in a mouse corneal epithelial debridement model (38), HO-2 KO macrophages phagocytosis of apoptotic DNA fragments still function, possibly with help of HO-1 overexpression.

Adult HO-2-deficient mice are morphologically indistinguishable from wt mice (42), but only full-grown mice have been studied thus far. To the best of our knowledge, this is the first study of HO-2 KO embryonic development. Down-regulation of HO-2 is associated with spontaneous abortion in humans (18). We did not find that the absence of HO-2 expression resulted in an increased fetal loss rate or decreased implantation rate in mice. However, non-viable and hemorrhagic embryonic implantations were frequently observed in both genotypes. Homozygote HO-2 KO mice were recently demonstrated to be viable (37), though they demonstrated delayed wound repair (37, 52) and an exaggerated inflammatory response after corneal epithelial wounding (53). Fetal growth retardation is associated with down-regulation of HO-2 in human pathologic pregnancies (18), which is in line with our findings that HO-2 deletion leads to a developmental growth delay at E15 of approximately 1 day. Among the HO-2 KO fetuses, one was severely malformed and another presented a head anomaly, but no anomalies or malformations were found in wt fetuses.

Chemokine signaling during MES disintegration facilitates palatal fusion

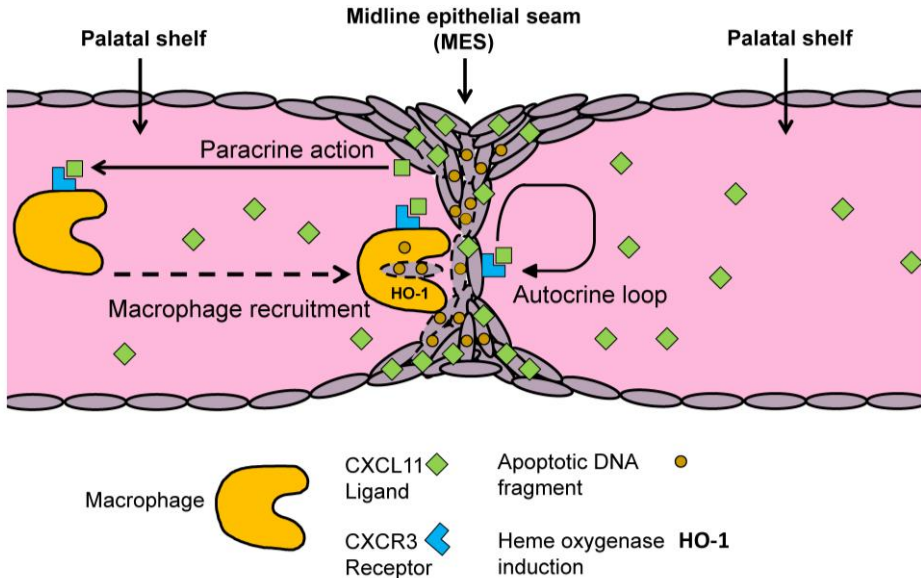


Figure 3.11: MES mediated chemokine signaling facilitates MES disintegration and palatal fusion.

Conceptual model: Autocrine and paracrine MES signaling facilitates palatal fusion. CXCL11/CXCR3 autocrine signaling controls migration and/or apoptosis of epithelial cells during disintegration of the MES. CXCL11-CXCR3 paracrine signaling recruits macrophages to clean up the MESs. HO-2 KO macrophages are still able to phagocytize apoptotic DNA fragments from the MES due to induction of HO-1.

Environmental factors, such as maternal diabetes, oxidative stress, and infections can have a disturbing influence on palatal fusion and lead to clefting of the lip and palate (16). HO-2 is essential for regulating physiological levels of reactive oxygen species (ROS) (54, 55). Although we found growth restriction and morphological anomalies in HO-2 KO fetuses, proper fusion of the palatal shelves was observed. In the absence of additional stresses, HO-2 KO fetuses can thus develop into mice with a normal palate, possibly due to compensation by elevated HO-1 expression. Next, we studied palatogenesis in HO-2 KO mice in more detail.

We demonstrated increased expression of chemokine CXCL11 and its receptor CXCR3 within the disintegrating MES in both genotypes. CXCR3-CXCL11 signaling serves as a coordinator in wound repair (56, 57) and is involved in the process of re-epithelialization and epidermis maturation (37). In keratinocytes, CXCR3 signaling activated μ -calpain to loosen the adhesions for migration (29). Scars in CXCR3 KO mice exhibited hyperkeratosis and hypercellularity (30), features that are also observed in hypertrophic scar formation in humans (56). CXCR3 plays a key role in coordinating the switch from regeneration of the epithelial compartment towards maturation (58) and modulates cell proliferation and apoptosis (59, 60). In the disintegrating MES CXCL11-CXCR3 signaling is therefore likely involved in controlling processes, such as migration and apoptosis of epithelial cells.

We found many apoptotic DNA fragments throughout the disintegrating MES, supporting apoptosis as a driving mechanism in MES disintegration (7-10). No apoptotic

DNA fragments were found in the other epithelial regions of the palatal shelves or the mesenchyme of the palatal shelves. Blocking cell death with z-VAD, an inhibitor of caspases, leads to persistence of the MES structure, which interferes with fusion of the palatal shelves *in vitro* (61), suggesting that this could lead to cleft palate. However, a role of epithelial migration in MES disintegration cannot be excluded.

In addition to CXCR3 expression in the epithelial MES layer, we also demonstrated CXCR3 expression in the mesenchyme of the fusing palatal shelves. We found CXCR3-positive and phagocytosing macrophages near the disintegrating MES, suggesting that macrophages are actively recruited by CXCL11. This demonstrates that the MES actively participates in its disintegration via chemokine signaling. However, we cannot exclude that other mechanisms play a role, such as caspases, other enzymes and enzyme inhibitors. Recruitment of CXCR3-positive macrophages by CXCL11 paracrine signaling was demonstrated previously also in other models (35, 36).

Although HO-2 deletion impaired macrophage function in corneal epithelial wound repair (38), in our study both wt and HO-2 KO macrophages phagocytosed apoptotic DNA fragments and, thus, were still functional. Although impairment of macrophage function by HO-2 deletion was found in a wound repair study in adult mice (38), we studied macrophage function in a non-pathological environment during embryonic development. However, our findings contradict another wound healing study, demonstrating that HO-2 deletion was associated with impaired HO-1 induction (52). Significantly more HO-1-positive cells were found in the palatal mesenchyme of HO-2 KO fetuses compared to wt fetuses, in which HO-1-positive cells were scarce. We suggest that the higher HO-1 expression during embryonic development is a compensating mechanism for HO-2 deletion in recruited macrophages in the fusing palatal shelves. An increased HO-1 induction could explain in part the discrepancy in function between HO-2 KO macrophages in adult and embryonic mice.

A limitation of the present study was the relatively small number of fetuses. However, among the 23 HO-2 KO fetuses, one demonstrated severe malformations and another viable fetus had a craniofacial anomaly, suggesting that HO-2 supports fetal growth and development.

In conclusion, we determined that HO-2 deletion leads to fetal growth restriction and craniofacial anomalies. In contrast to our hypothesis, no disturbance was observed in palatal fusion in HO-2 KO fetuses. However, CXCL11 and CXCR3 were highly expressed in the disintegrating MES in both wt and HO-2 KO animals. Both wt and HO-2 KO CXCR3-positive macrophages were functional since apoptotic cells from the disintegrating MES were phagocytosed. Increased numbers of HO-1-positive cells were found within the mesenchyme of the fusing palatal shelves of the HO-2 KO fetuses. It is tempting to speculate that HO-2 deletion leads to up-regulation of HO-1 expression in macrophages, protecting them from oxidative stress following ingestion of apoptotic epithelial fragments from the disintegrating MES. Our data supports the hypothesis that chemokine signaling by the MES orchestrates its disintegrating by epithelial apoptosis and macrophage recruitment via CXCL11-CXCR3 signaling. However, also alternative pathways may have contributed to these processes. Further research is needed to investigate whether hampered palatal fusion can be the result of disrupted chemokine signaling and whether reduced protection against oxidative and inflammatory stresses promote craniofacial malformations.

References

1. Ackermans MM, Zhou H, Carels CE, Wagener FA, Von den Hoff JW. Vitamin A and clefting: putative biological mechanisms. *Nutrition reviews*. 2011;69(10):613-24.
2. Dudas M, Kim J, Li WY, Nagy A, Larsson J, Karlsson S, et al. Epithelial and ectomesenchymal role of the type I TGF-beta receptor ALK5 during facial morphogenesis and palatal fusion. *Developmental biology*. 2006;296(2):298-314.
3. Iseki S. Disintegration of the medial epithelial seam: is cell death important in palatogenesis? *Development, growth & differentiation*. 2011;53(2):259-68.
4. Gritli-Linde A. Molecular control of secondary palate development. *Developmental biology*. 2007;301(2):309-26.
5. Jin JZ, Ding J. Analysis of cell migration, transdifferentiation and apoptosis during mouse secondary palate fusion. *Development*. 2006;133(17):3341-7.
6. Nawshad A. Palatal seam disintegration: to die or not to die? that is no longer the question. *Developmental dynamics : an official publication of the American Association of Anatomists*. 2008;237(10):2643-56.
7. Vukojevic K, Kero D, Novakovic J, Kalibovic Govorko D, Saraga-Babic M. Cell proliferation and apoptosis in the fusion of human primary and secondary palates. *European journal of oral sciences*. 2012;120(4):283-91.
8. Lan Y, Xu J, Jiang R. Cellular and Molecular Mechanisms of Palatogenesis. *Curr Top Dev Biol*. 2015;115:59-84.
9. Xu X, Han J, Ito Y, Bringas P, Jr., Urata MM, Chai Y. Cell autonomous requirement for *Tgfr2* in the disappearance of medial edge epithelium during palatal fusion. *Developmental biology*. 2006;297(1):238-48.
10. Vaziri Sani F, Hallberg K, Harfe BD, McMahon AP, Linde A, Gritli-Linde A. Fate-mapping of the epithelial seam during palatal fusion rules out epithelial-mesenchymal transformation. *Developmental biology*. 2005;285(2):490-5.
11. Brown NL, Sandy JR. Tails of the unexpected: palatal medial edge epithelium is no more specialized than other embryonic epithelium. *Orthod Craniofac Res*. 2007;10(1):22-35.
12. Burg ML, Chai Y, Yao CA, Magee W, 3rd, Figueiredo JC. Epidemiology, Etiology, and Treatment of Isolated Cleft Palate. *Front Physiol*. 2016;7:67.
13. Mossey PA, Little J, Munger RG, Dixon MJ, Shaw WC. Cleft lip and palate. *Lancet*. 2009;374(9703):1773-85.
14. Watkins SE, Meyer RE, Strauss RP, Aylsworth AS. Classification, epidemiology, and genetics of orofacial clefts. *Clin Plast Surg*. 2014;41(2):149-63.
15. Drew SJ. Clefting syndromes. *Atlas Oral Maxillofac Surg Clin North Am*. 2014;22(2):175-81.
16. Brocardo PS, Gil-Mohapel J, Christie BR. The role of oxidative stress in fetal alcohol spectrum disorders. *Brain research reviews*. 2011;67(1-2):209-25.
17. Zenclussen ML, Casalis PA, El-Mousleh T, Rebelo S, Langwisch S, Linzke N, et al. Haem oxygenase-1 dictates intrauterine fetal survival in mice via carbon monoxide. *The Journal of pathology*. 2011;225(2):293-304.
18. Zenclussen AC, Lim E, Knoeller S, Knackstedt M, Hertwig K, Hagen E, et al. Heme oxygenases in pregnancy II: HO-2 is downregulated in human pathologic pregnancies. *Am J Reprod Immunol*. 2003;50(1):66-76.
19. Zenclussen ML, Linzke N, Schumacher A, Fest S, Meyer N, Casalis PA, et al. Heme oxygenase-1 is critically involved in placentation, spiral artery remodeling, and blood pressure regulation during murine pregnancy. *Front Pharmacol*. 2014;5:291.
20. Wagener FA, Eggert A, Boerman OC, Oyen WJ, Verhofstad A, Abraham NG, et al. Heme is a potent inducer of inflammation in mice and is counteracted by heme oxygenase. *Blood*. 2001;98(6):1802-11.
21. Wagener FA, Abraham NG, van Kooyk Y, de Witte T, Figdor CG. Heme-induced cell adhesion in the pathogenesis of sickle-cell disease and inflammation. *Trends Pharmacol Sci*. 2001;22(2):52-4.
22. Wagener FA, Volk HD, Willis D, Abraham NG, Soares MP, Adema GJ, et al. Different faces of the heme-heme oxygenase system in inflammation. *Pharmacol Rev*. 2003;55(3):551-71.
23. Grochot-Przeczek A, Dulak J, Jozkowicz A. Haem oxygenase-1: non-canonical roles in physiology and pathology. *Clinical science*. 2012;122(3):93-103.
24. Ewing JF, Maines MD. Regulation and expression of heme oxygenase enzymes in aged-rat brain: age related depression in HO-1 and HO-2 expression and altered stress-response. *Journal of neural transmission*. 2006;113(4):439-54.

25. Shi J, Mei W, Yang J. Heme metabolism enzymes are dynamically expressed during *Xenopus* embryonic development. *Biocell : official journal of the Sociedades Latinoamericanas de Microscopia Electronica et al.* 2008;32(3):259-63.
26. Bellner L, Martinelli L, Halilovic A, Patil K, Puri N, Dunn MW, et al. Heme oxygenase-2 deletion causes endothelial cell activation marked by oxidative stress, inflammation, and angiogenesis. *The Journal of pharmacology and experimental therapeutics.* 2009;331(3):925-32.
27. Sollwedel A, Bertoja AZ, Zenclussen ML, Gerlof K, Lisewski U, Wafula P, et al. Protection from abortion by heme oxygenase-1 up-regulation is associated with increased levels of Bag-1 and neuropilin-1 at the fetal-maternal interface. *Journal of immunology.* 2005;175(8):4875-85.
28. Biggs LC, Goudy SL, Dunnwald M. Palatogenesis and cutaneous repair: A two-headed coin. *Developmental dynamics : an official publication of the American Association of Anatomists.* 2015;244(3):289-310.
29. Satish L, Blair HC, Glading A, Wells A. Interferon-inducible protein 9 (CXCL11)-induced cell motility in keratinocytes requires calcium flux-dependent activation of mu-calpain. *Molecular and cellular biology.* 2005;25(5):1922-41.
30. Yates CC, Krishna P, Whaley D, Bodnar R, Turner T, Wells A. Lack of CXC chemokine receptor 3 signaling leads to hypertrophic and hypercellular scarring. *The American journal of pathology.* 2010;176(4):1743-55.
31. Epelman S, Lavine KJ, Randolph GJ. Origin and functions of tissue macrophages. *Immunity.* 2014;41(1):21-35.
32. Epelman S, Liu PP, Mann DL. Role of innate and adaptive immune mechanisms in cardiac injury and repair. *Nature reviews Immunology.* 2015;15(2):117-29.
33. Roszser T. Understanding the Mysterious M2 Macrophage through Activation Markers and Effector Mechanisms. *Mediators of inflammation.* 2015;2015:816460.
34. Mass E, Ballesteros I, Farlik M, Halbritter F, Gunther P, Crozet L, et al. Specification of tissue-resident macrophages during organogenesis. *Science.* 2016;353(6304).
35. Kakuta Y, Okumi M, Miyagawa S, Tsutahara K, Abe T, Yazawa K, et al. Blocking of CCR5 and CXCR3 suppresses the infiltration of macrophages in acute renal allograft rejection. *Transplantation.* 2012;93(1):24-31.
36. Torraca V, Cui C, Boland R, Bebelman JP, van der Sar AM, Smit MJ, et al. The CXCR3-CXCL11 signaling axis mediates macrophage recruitment and dissemination of mycobacterial infection. *Disease models & mechanisms.* 2015;8(3):253-69.
37. Lundvig DM, Scharstuhl A, Cremers NA, Pennings SW, Te Paske J, van Rheden R, et al. Delayed cutaneous wound closure in HO-2 deficient mice despite normal HO-1 expression. *Journal of cellular and molecular medicine.* 2014;18(12):2488-98.
38. Bellner L, Marrazzo G, van Rooijen N, Dunn MW, Abraham NG, Schwartzman ML. Heme oxygenase-2 deletion impairs macrophage function: implication in wound healing. *FASEB journal : official publication of the Federation of American Societies for Experimental Biology.* 2015;29(1):105-15.
39. Kaplan AP. Chemokines, chemokine receptors and allergy. *International archives of allergy and immunology.* 2001;124(4):423-31.
40. Van Raemdonck K, Van den Steen PE, Liekens S, Van Damme J, Struyf S. CXCR3 ligands in disease and therapy. *Cytokine & growth factor reviews.* 2015;26(3):311-27.
41. Balaji S, Watson CL, Ranjan R, King A, Bollyky PL, Keswani SG. Chemokine Involvement in Fetal and Adult Wound Healing. *Adv Wound Care (New Rochelle).* 2015;4(11):660-72.
42. Poss KD, Thomas MJ, Ebralidze AK, O'Dell TJ, Tonegawa S. Hippocampal long-term potentiation is normal in heme oxygenase-2 mutant mice. *Neuron.* 1995;15(4):867-73.
43. Behringer R, Gertszenstein M, Nagy KV, Nagy A. Selecting Female Mice in Estrus and Checking Plugs. *Cold Spring Harb Protoc.* 2016;2016(8):pdb prot092387.
44. Dudas M, Li WY, Kim J, Yang A, Kaartinen V. Palatal fusion - where do the midline cells go? A review on cleft palate, a major human birth defect. *Acta histochemica.* 2007;109(1):1-14.
45. Livak KJ, Schmittgen TD. Analysis of relative gene expression data using real-time quantitative PCR and the 2⁻(Delta Delta C(T)) Method. *Methods.* 2001;25(4):402-8.
46. Tan SD, Xie R, Klein-Nulend J, van Rheden RE, Bronckers AL, Kijpers-Jagtman AM, et al. Orthodontic force stimulates eNOS and iNOS in rat osteocytes. *J Dent Res.* 2009;88(3):255-60.
47. Siemieniuch MJ. Apoptotic changes in the epithelium germinativum of the cat (*Felis catus* s. *domestica*, L. 1758) at different ages and breeding seasons. *Reproduction in domestic animals = Zuchthygiene.* 2008;43(4):473-6.

48. Lin HH, Faunce DE, Stacey M, Terajewicz A, Nakamura T, Zhang-Hoover J, et al. The macrophage F4/80 receptor is required for the induction of antigen-specific efferent regulatory T cells in peripheral tolerance. *J Exp Med*. 2005;201(10):1615-25.
49. Shibahara S, Yoshida T, Kikuchi G. Mechanism of increase of heme oxygenase activity induced by hemin in cultured pig alveolar macrophages. *Archives of biochemistry and biophysics*. 1979;197(2):607-17.
50. Okinaga S, Takahashi K, Takeda K, Yoshizawa M, Fujita H, Sasaki H, et al. Regulation of human heme oxygenase-1 gene expression under thermal stress. *Blood*. 1996;87(12):5074-84.
51. Elliott MR, Chekeni FB, Trampont PC, Lazarowski ER, Kadl A, Walk SF, et al. Nucleotides released by apoptotic cells act as a find-me signal to promote phagocytic clearance. *Nature*. 2009;461(7261):282-6.
52. Seta F, Bellner L, Rezzani R, Regan RF, Dunn MW, Abraham NG, et al. Heme oxygenase-2 is a critical determinant for execution of an acute inflammatory and reparative response. *The American journal of pathology*. 2006;169(5):1612-23.
53. Bellner L, Wolstein J, Patil KA, Dunn MW, Laniado-Schwartzman M. Biliverdin Rescues the HO-2 Null Mouse Phenotype of Unresolved Chronic Inflammation Following Corneal Epithelial Injury. *Investigative ophthalmology & visual science*. 2011;52(6):3246-53.
54. Burgess AP, Vanella L, Bellner L, Gotlinger K, Falck JR, Abraham NG, et al. Heme oxygenase (HO-1) rescue of adipocyte dysfunction in HO-2 deficient mice via recruitment of epoxyeicosatrienoic acids (EETs) and adiponectin. *Cellular physiology and biochemistry : international journal of experimental cellular physiology, biochemistry, and pharmacology*. 2012;29(1-2):99-110.
55. He JZ, Ho JJ, Gingerich S, Courtman DW, Marsden PA, Ward ME. Enhanced translation of heme oxygenase-2 preserves human endothelial cell viability during hypoxia. *The Journal of biological chemistry*. 2010;285(13):9452-61.
56. Huen AC, Wells A. The Beginning of the End: CXCR3 Signaling in Late-Stage Wound Healing. *Adv Wound Care (New Rochelle)*. 2012;1(6):244-8.
57. Kroeze KL, Boink MA, Sampat-Sardjoeppersad SC, Waaijman T, Scheper RJ, Gibbs S. Autocrine regulation of re-epithelialization after wounding by chemokine receptors CCR1, CCR10, CXCR1, CXCR2, and CXCR3. *The Journal of investigative dermatology*. 2012;132(1):216-25.
58. Yates CC, Whaley D, A YC, Kulesekaran P, Hebda PA, Wells A. ELR-negative CXC chemokine CXCL11 (IP-9/I-TAC) facilitates dermal and epidermal maturation during wound repair. *The American journal of pathology*. 2008;173(3):643-52.
59. Ma B, Khazali A, Wells A. CXCR3 in carcinoma progression. *Histology and histopathology*. 2015;30(7):781-92.
60. Fulton AM. The chemokine receptors CXCR4 and CXCR3 in cancer. *Current oncology reports*. 2009;11(2):125-31.
61. Cuervo R, Covarrubias L. Death is the major fate of medial edge epithelial cells and the cause of basal lamina degradation during palatogenesis. *Development*. 2004;131(1):15-24.

Chapter 4

Mechanical stress changes the complex interplay between heme oxygenase-1, inflammation and fibrosis during excisional wound repair.

Cremers NA, Suttorp M, Gerritsen MM, Wong RJ, van Run-van Breda C, van Dam GM, Brouwer KM, Kuijpers-Jagtman AM, Carels CE, Lundvig DM, Wagener FA.

Front Med (Lausanne). 2015 Dec 15;2:86.

Abstract

Mechanical stress following surgery or injury can promote pathological wound healing and fibrosis, and lead to functional loss and esthetic problems. Splinted excisional wounds can be used as model for inducing mechanical stress. The cytoprotective enzyme heme oxygenase-1 (HO-1) is thought to orchestrate the defense against inflammatory and oxidative insults that drive fibrosis. Here, we investigated the activation of the HO-1 system in a splinted and non-splinted full thickness excisional wound model using HO-1-*luc* transgenic mice. Effects of splinting on wound closure, HO-1 promoter activity, and markers of inflammation and fibrosis were assessed. After seven days, splinted wounds were more than 3 times larger than non-splinted wounds, demonstrating a delay in wound closure. HO-1 promoter activity rapidly decreased following removal of the (epi)dermis, but was induced in both splinted and non-splinted wounds during skin repair. Splinting induced more HO-1 gene expression in 7-day wounds; however, HO-1 protein expression remained lower in the epidermis, likely due to lower number of keratinocytes in the re-epithelialization tissue. Higher numbers of F4/80-positive macrophages, α SMA-positive myofibroblasts, and increased levels of the inflammatory genes IL-1 β , TNF- α , and COX-2 were present in 7-day splinted wounds. Surprisingly, mRNA expression of newly-formed collagen (type III) was lower in 7-day wounds after splinting; whereas, VEGF and MMP-9 were increased. Summarizing, these data demonstrate that splinting delays cutaneous wound closure and HO-1 protein induction. The pro-inflammatory environment following splinting, may facilitate higher myofibroblast numbers and increases the risk of fibrosis and scar formation. Therefore, inducing HO-1 activity against mechanical stress-induced inflammation and fibrosis may be an interesting strategy to prevent negative effects of surgery on growth and function in patients with orofacial clefts or in burns patients.

Keywords: cleft palate, burns, mechanical stress, wound healing, heme oxygenase-1, inflammation, fibrosis.

Abbreviations

ABC	Avidin-biotin-peroxidase complex
ANOVA	Analysis of variance
α SMA	Alpha smooth muscle actin
AU	Arbitrary units
CL/P	Cleft lip with or without cleft palate
CO	Carbon monoxide
COX-2	Cyclooxygenase-2
CXCL1	Chemokine (C-X-C) ligand 1
DAB	Diaminobenzidine-peroxidase
DPX	Distyrene plasticizer xylene
ECM	Extracellular matrix
HO-1	Heme oxygenase-1
ICAM-1	Intercellular adhesion molecule-1
IL-1 β	Interleukin-1 beta
MCP-1	Monocyte chemotactic protein-1
MMP-9	Matrix metalloproteinase-9
NDS	Normal donkey serum
PBS-G	Phosphate buffered saline with glycin
ROI	Regions of interest
TNF- α	Tumor necrosis factor-alpha
VEGF	Vascular endothelial growth factor

Introduction

Cleft lip with or without cleft palate (CL/P) is a developmental craniofacial disorder that is characterized by an opening in the upper lip and/ or palate and alveolar bone (1). Patients with CL/P need multiple surgeries that inevitably result in scar formation (Figure 4.1A) (2, 3). Especially, the scars on the palate may disrupt normal midfacial growth and impair dento-alveolar development (4, 5). Also, patients with severe burns can exhibit excessive scar formation (Figure 4.1B) (6). Scarring can be exaggerated by mechanical tension, such as due to the growth of the child and by tension of the wound during wound repair (7). Overall, pathological wound healing following mechanical stress can result in hypertrophic scars and subsequently lead to functional, psychosocial, and esthetical problems for patients (8, 9).

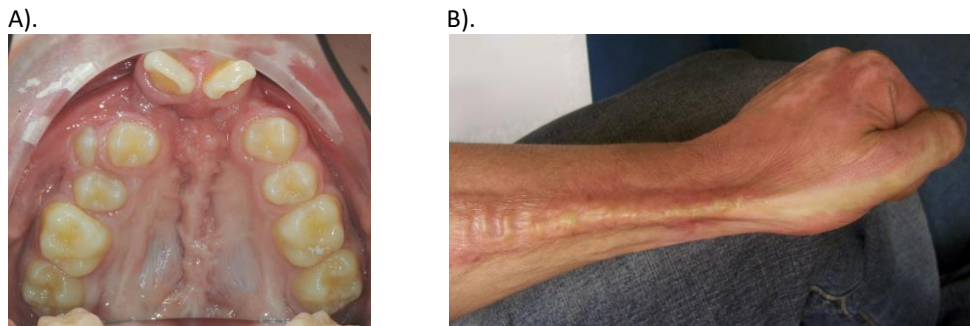


Figure 4.1. Mechanical stress may promote excessive scar formation following injury

(A) An intra-oral photo of the maxillary arch of a patient of our clinic with an operated complete bilateral cleft lip and palate is shown. Mechanical stress-induced scar formation impairs development of the upper jaw and the dentition. (B) Also, burns can result in excessive scar formation leading to cosmetic and functional problems as exemplified by scar formation near the wrist.

Mechanical load, together with cytokine expression and the composition of the extracellular matrix (ECM), promote the differentiation of fibroblasts into myofibroblasts (10-12). During wound repair, myofibroblasts play a key role in the deposition of ECM and in wound contraction, thereby reducing wound size and preventing invasion by pathogens (10, 12). When a wound closes, myofibroblasts normally disappear by apoptosis. However, during pathologic wound healing, extended presence of myofibroblasts may result in excessive wound contracture and ECM deposition, leading to excessive scar formation and functional problems (5, 13). Mechanical stress during wound repair can trigger a continued expression of the myofibroblast marker alpha smooth muscle actin (α -SMA), and a prolonged survival of myofibroblasts (5, 14-17). Prolonged inflammatory and oxidative stress may also increase myofibroblast survival (18). A better understanding of the effects of mechanical stress during the wound healing process is warranted to develop novel adjuvant therapies.

Rodents, in contrast to humans, possess a subcutaneous muscle layer (*m. panniculus carnosus*), which can cause wound contraction (19). In these animals, the use of splinting can induce static mechanical stress to healing wounds (5, 14, 20), interfere with this muscle contraction, and thus better simulate human wound healing that is mainly dependent on granulation and re-epithelialization of tissues (19). The effects of static mechanical stress, caused by splinting, on the different phases of wound healing remains to

be unraveled. In addition, the involvement of cytoprotective mechanisms needs further exploration. Activation of the cytoprotective heme oxygenase (HO) system has shown protective effects in both inflammatory and fibrotic models (6, 18, 21).

HO is an enzyme that catabolizes heme, yielding the gasotransmitter carbon monoxide (CO), free iron, which is scavenged by co-induced ferritin, and biliverdin that is rapidly converted into the antioxidant bilirubin by biliverdin reductase (22). The HO system possesses antioxidative, anti-inflammatory, anti-fibrotic, and anti-apoptotic properties (18, 23) and can influence cell proliferation, differentiation, and migration. When these processes are disrupted, wound repair may be hampered (24). There are two isoforms of HO, the inducible HO-1 and the constitutively-expressed HO-2. It has been shown that HO-1 is rapidly induced in wounded tissues (25, 26). Decreased HO-1 or HO-2 expression and enzyme activity in mice results in slower cutaneous wound closure; whereas, induction of HO-1 expression or administration of the HO effector molecule bilirubin attenuates the inflammatory response and accelerates wound healing in HO-1-deficient mice (27-29).

In this study, we investigated the expression of HO-1 during wound repair in both non-splinted and splinted wounds using transgenic HO-1-*luc* mice. Because mechanical stress has been shown to induce HO-1 expression in different experimental settings in a time- and force-dependent manner (30-32), we therefore postulated that mechanical stress by splinting would induce HO-1 expression during wound healing. In addition, we investigated the effects of mechanical stress on markers of inflammation, ECM remodeling, and fibrosis.

Material and Methods

Animals

The Committee for Animal Experiments of Radboud University Nijmegen approved all procedures involving mice (RU-DEC 2010-248). Twelve mice (strain: HO-1-*luc* FVB/ N-Tg background), 4 to 5 months of age and weighing 30 ± 5 g, were provided with food and water *ad libitum*. Mice were maintained on a 12h light/dark cycle and specific pathogen-free housing conditions at the Central Animal Facility Nijmegen. More details on the housing conditions have been previously described (33). Mice were originally derived from Xenogen Corporation (Alameda, CA, USA) and generated as previously described (34).

The mice were euthanized with a standard CO₂/O₂ protocol seven days after wounding, after which control skin, and wounded skin were isolated. Half of the tissue was fixed for 24h in 4% paraformaldehyde and then embedded in paraffin following regular histosafe procedures and the other half was snap-frozen in liquid nitrogen and stored at -80°C until isolation of mRNA.

Excisional non-splinted and splinted wound model

Splinted (n=6) and non-splinted (n=6) full-thickness excisional wounds 4 mm in diameter were created on the dorsum of the mice after shaving as previously described (35). In brief, excisional wounds were created using a sterile disposable 4-mm skin biopsy punch (Kai Medical, Seki City, Japan) on the dorsum to either side of the midline, and halfway between the shoulders and pelvis. Circular silicone splints of 6-mm inner- and 12-mm outer-diameter made from silicone sheets (3M, Saint Paul, Minnesota, USA) were glued to the skin around the wound. Mice receiving splinted excisional wounds were wrapped with semi-permeable

dressing (Petflex; Andover, Salisbury, MA, USA) around their torso, to cover the wound. One mouse in the splinted group died due to pulmonary failure as a result of respiratory obstruction by the bandage during the recovery from anaesthesia.

Photographs of the wounds were taken immediately after wounding and then 1h and 1, 3, 5 and 7 days thereafter with a reference placed perpendicular next to the wounds for wound size normalization. The area of the wounds was blindly measured in triplicates using ImageJ (NIH) v1.44p software.

HO-1 promoter activity measurements

HO-1 promoter activity was determined at baseline, immediately after wounding and 1h and 1, 3, and 7 days thereafter in the HO-1-*luc*-Tg mice by *in vivo* bioluminescence imaging using the IVIS Lumina system (Caliper Life Sciences, Hopkinton, MA, USA) as previously described (36). Images were quantified using Living Image 3.0 software (Caliper Life Sciences) by selecting regions of interest (ROI). The amount of emitted photons per second (total flux) per ROI was measured, and then calculated as fold change from baseline levels.

Immunohistochemical staining

Immunohistochemical staining for HO-1, macrophages (F4/80), and myofibroblasts (α -SMA) were performed on paraffin sections of the wounds as previously described (35). In short, paraffin-embedded tissues were cut into 5- μ m sections, which were then de-paraffinized, quenched for endogenous peroxidase activity with 3% H₂O₂ in methanol for 20 min, and rehydrated. Sections were post-fixed with 4% formalin, and washed with PBS containing 0.075 μ g/ mL glycine (PBSG). Antigens were retrieved with citrate buffer (0.01 M, pH 6.0) at 70°C for 10 min, followed by incubation in 0.075 g/mL trypsin in PBS at 37°C for 7 min. Next, the sections were pre-incubated with 10% normal donkey serum (NDS) in PBS-G. First antibodies (HO-1 from Stressgen #SPA-895 1:600 dilution, α -SMA from Sigma-Aldrich #A2547 1:600 dilution, and F4/80 from AbD Serotec #MCA497R 1:200 dilution) were diluted in 2% NDS in PBSG and incubated overnight at 4°C. After washing with PBSG, sections were incubated for 60 min with a biotin-labeled secondary antibody against host species (1:5000 dilution). Next, the sections were washed with PBSG and treated with avidin-biotin-peroxidase complex (ABC) for 45 min in the dark. After extensive washing with PBSG, diaminobenzidine-peroxidase (DAB) staining was performed for 10 min. After rinsing with water, staining was intensified with Cu₂SO₄ in 0.9% NaCl and rinsed with water again. Finally, the nuclei were stained with hematoxylin for 10 s and sections were rinsed for 10 min in water, dehydrated and embedded in distyrene plasticizer xylene (DPX).

Immunoreactivity was evaluated by blindly scoring the wounds. For the HO-1 staining, we scored both the epidermal and dermal region of the wounds separately, since there were two different positively-stained populations. A single section per wound was semi-quantitatively scored, by two assessors independently of each other, as previously described according to the following scale: 0 (minimal), 1 (mild), 2 (moderate), and 3 (marked) (35).

RNA isolation and quantitative-RT-PCR

Non-wounded control skin and wounds were pulverized in TRIzol (Invitrogen) using a micro-dismembrator (Sartorius BBI Systems GmbH, Melsungen, Germany) and RNA was further extracted as previously described (37). Quantitative-Real-Time-PCR was performed.

mRNA expression levels were calculated as minus delta delta Ct ($-\Delta\Delta Ct$) values, normalized to the reference gene GAPDH, and corrected for non-wounded control skin. Fold change were calculated by $2^{(-\Delta\Delta Ct)}$. The sequences of the mouse-specific primers are shown in Table 4.1.

Table 4.1. Mouse primers

Marker	Gene name	Forward primer (5'-3')	Reverse primer (5'-3')
Reference gene	GAPDH	GGCAAATTC AACGGCACA	GTTAGTGGGGTCTCGTCCTG
Inflammation	IL-1 β	TGCAGCTGGAGAGTGTGG	TCCACTTTGCTCTTGACTTCTATC
	TNF- α	CTCTTCTCATTCTGCTTGTG	GGGAACCTTCTATCCCTTTG
	COX-2	CCAGCACTTCAACCCATCAGTT	ACCCAGGTCTCGCTTATGA
Cytoprotection	MCP-1	ACTGAAGCCAGCTCTCTCTTCTC	TTCCTTCTGGGGTCAGCACAGAC
	HO-1	CAACATTGAGCTGTTTGAGG	TGGTCTTTGTGTTCTCTGTGTC
	HO-2	AAGGAAGGGACCAAGGAAG	AGTGGTGGCCAGCTTAAATAG
Angiogenesis	VEGF	GGAGATCCTTCGAGGAGCACTT	GGCGATTTAGCAGCAGATATAAGAA
Fibrosis	α -SMA (acta2)	CAGGCATGGATGGCATCAATCAC	ACTCTAGCTGTGAAGTCAGTGTCC
	MMP-9	TGCCATTTTCGACGACGAC	GTGCAGGCCGAATAGGAGC
	Collagen 3a1	ATCCCATTTGGAGAATGTTG	AAGCACAGGAGCAGGTGTAG
Keratinocytes	Krt-6	GACGACCTACGCAACACC	AGTTGGCACACTGCTTC

Statistics

Data were analyzed using GraphPad Prism 5.01 software (San Diego, CA, US). No outliers were detected using the Grubbs' test. Data was analyzed by a paired t-test for comparisons of two groups and a one- or two-way analysis of variance (ANOVA) for the comparison of multiple groups with a *post-hoc* Bonferroni correction for multiple comparisons. The non-parametrical one-tailed Mann-Whitney U-test was used to compare the arbitrary scored immunohistological sections. Results were considered significant different when $p < 0.05$ (* $p < 0.05$, ** $p < 0.01$, *** $p < 0.001$).

Results

Static mechanical stress induced by splinting delays excisional wound closure

Because mechanical stress can lead to excessive scar formation (Figure 4.1AB), we used both splinted and non-splinted excisional wound healing to assess the effects of static mechanical stress on wound closure. Wound sizes of non-splinted and splinted wounds were monitored over time and representative photos are shown in Figure 4.2A. After quantification of the wound area the wound closure time in relation to $t = 0h$ was displayed (Figure 4.2B). All wounds closed gradually, but there were differences in wound closure between splinted and non-splinted wounds. After three days, significant differences between the groups were found. Non-splinted wounds were already closed for 45%; whereas, splinted wounds had only closed for 10%. After seven days, closure of non-splinted wounds was 75% of the wound area, while that for splinted wounds was only 23%. This corresponds to a 3.3 times faster wound closure when no mechanical stress was applied. This demonstrates that splinting effectively delays wound closure.

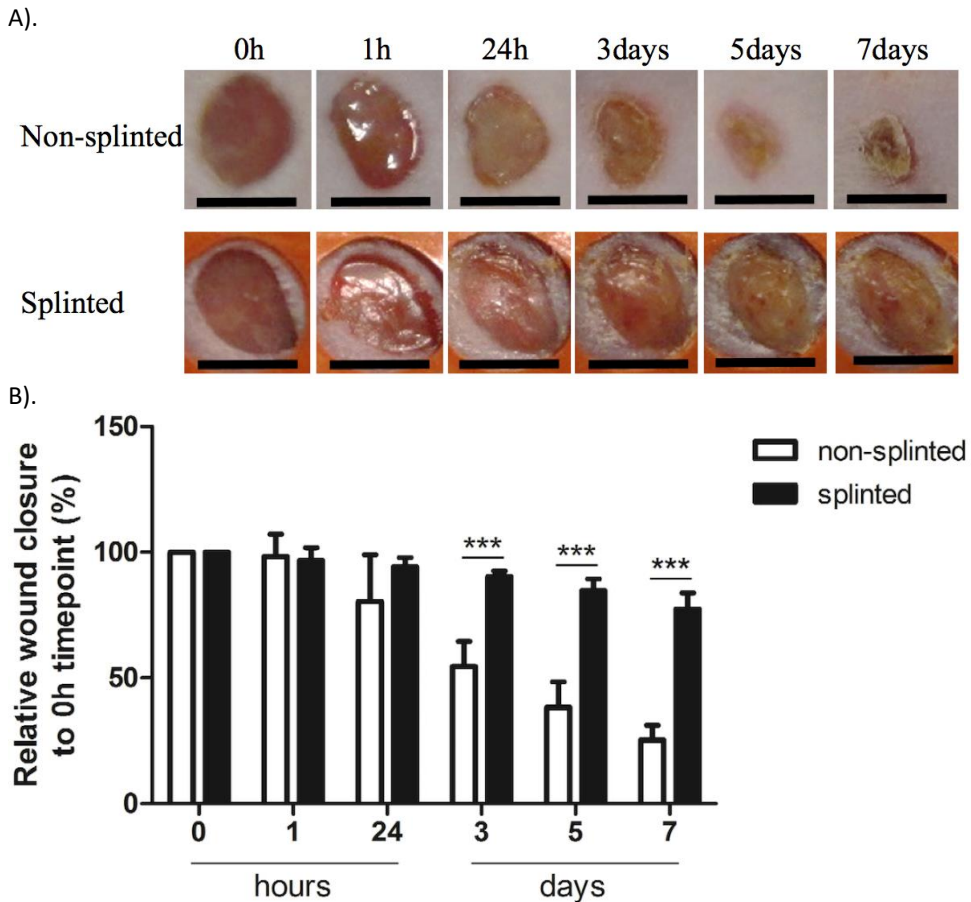


Figure 4.2: Splinted and non-splinted excisional wound closure over time

(A) Representative pictures of non-splinted and splinted wounds immediately following injury, and 1h, and 1, 3, 5 and 7 days after wounding (black bars = 4 mm). (B) Quantification of closures of non-splinted (n=6) and splinted (n=5) wounds over time (0-7 days). Each mouse had two wounds. Time point 0h was used as 100%. Data represent mean±SD. * is significantly different between non-splinted and splinted wounds (**p<0.001).

The HO system is affected by mechanical stress during excisional wound healing

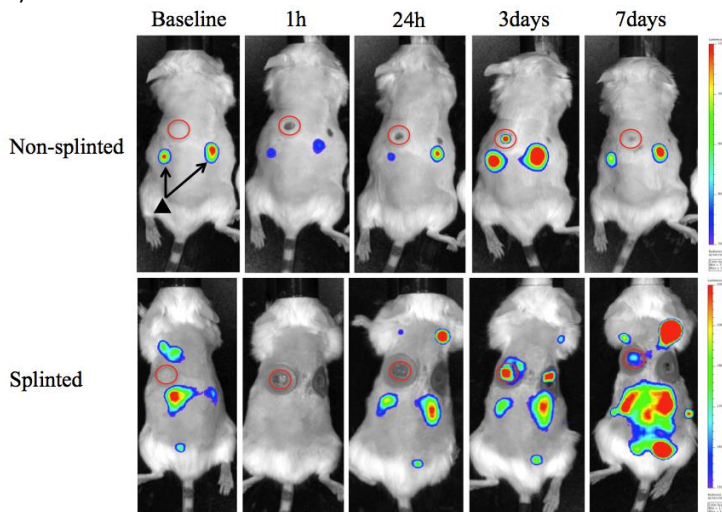
HO-1 is thought to be a critical regulator and expressed in distinct cell types during the different phases of wound repair. In order to investigate the role of HO-1 following mechanical stress (splinting) during excisional wound healing, we used HO-1-*luc* mice to monitor HO-1 promoter activity (Figure 4.3A). HO-1 promoter activity was already present in the kidneys in non-injured HO-1-*luc* mice. In the wound area, HO-1 promoter activity was evident especially at days 3 and 7 after splinting.

Surprisingly, we found that following wounding, there was an initial significant decrease in HO-1 promoter activity after 1h in both splinted as well as non-splinted wounds (Figure 4.3B). This decrease of HO-1 promoter activity returned to basal levels at day 1 and further increased at days 3 to 7, independent of splinting. Three days following wounding, the splinted wounds showed a significant increase of HO-1 promoter activity compared to basal levels.

To further elucidate the role of splinting on HO-1 expression during wound repair, we measured both HO-1 mRNA and protein expression in day-7 wounds. Using RT-PCR, HO-1 mRNA expression was assessed in the wounds and corrected for expression in non-wounded control skin (Figure 4.4A). Here, we found significantly higher (2.6 times) HO-1 mRNA expression in splinted wounds compared to non-splinted wounds. As expected, the constitutively-expressed HO-2 levels were not significantly different after induction of mechanical stress.

Immunohistochemical staining demonstrated that HO-1 levels were severely affected by wounding when compared to non-wounded skin. The number of HO-1-positive cells 7 days after wounding was increased in the dermal region of the wounds; also, more HO-1-positive cells were present in the epidermal region when compared to non-wounded skin.

A).



B).

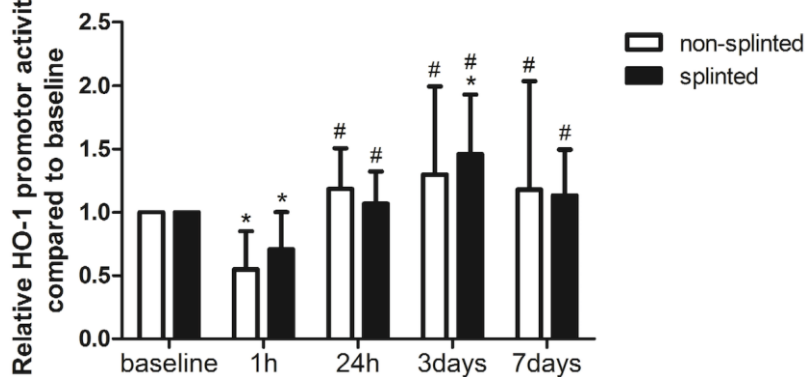


Figure 4.3: HO-1 promoter activity in splinted and non-splinted wounds

(A) Representative images of HO-1 promoter activity of non-splinted and splinted wounds over time using the IVIS system to measure *in vivo* bioluminescence in HO-1-*Luc* mice. The rainbow colored bar at the right side indicates the amount of luciferase signal represented in each group with a high signal in red and low signal in blue. The red

circles surround the wounds in the mice and indicate the measured region of interest (ROI). Note: black triangle (▲) with black arrows shows that there is basal HO-1 promoter activity around the kidneys. (B) Quantification of HO-1 promoter activity during non-splinted (n=6) and splinted (n=5) wound healing. Each mouse had two wounds. Data represent mean±SD. * is significantly different within the non-splinted or splinted group when compared to the baseline at the start of the experiment (*p<0.05). # is significantly different within the non-splinted or splinted group when compared to 1h after wounding (#p<0.05).

HO-1 protein was particularly evident in the epithelial cells at the leading edge of the wound in the epidermis and in recruited inflammatory leukocytes in the dermis (Figure 4.4B). Since, we observed two different populations of HO-1-positive cells depending on their region, the wounds were scored for the level of HO-1 protein expression in both the epidermal and dermal regions, which were compared between the different treatment groups (Figure 4.4C). Importantly, non-splinted wounds showed significantly higher HO-1 protein expression in the epidermal region compared to splinted wounds. In the dermal region, HO-1 was slightly higher after mechanical stress compared to the non-splinted wounds; however, this did not reach statistical significance (p=0.21). Variation in HO-1 protein expression was found between animals, but was independent of the wound model.

Thus, wounding initially decreased HO-1 promoter activity in the wound, after which HO-1 levels were restored and further induced by recruitment of inflammatory cells and keratinocytes. Surprisingly, although splinted wounds delay HO-1 expression, as shown by an increased HO-1 promoter activity and HO-1 mRNA expression, HO-1 protein expression was, in contrast to in the dermis, lower in the epidermis when compared to non-splinted wounds.

Interplay between HO-1 and inflammation in non-splinted and splinted wound healing

Since there was a clear delay in wound closure and HO-1 protein expression in splinted wounds, we investigated whether this delay correlated with altered levels of inflammatory gene expression. Because HO-1 has anti-inflammatory and antioxidative properties, we expected that the delayed HO-activity in the skin would result in increased levels of inflammation. Therefore, we quantitated the number of F4/80-positive macrophages using immunohistochemical staining in sections of non-splinted and splinted wounds (Figure 4.5A).

We found that there were indeed significantly more macrophages present in 7-day splinted wounds compared to non-splinted wounds (Figure 4.5B). Next, we investigated whether mRNA expression of monocyte chemoattractant protein 1 (MCP-1), the main chemokine to attract monocytes/ macrophages, was altered by mechanical stress. We observed that MCP-1 was elevated 1.8 fold in splinted wounds compared to non-splinted wounds, however, this difference did not reach statistical significance (p=0.10).

Finally, when we examined the gene expression of several other inflammatory markers, we found that mRNA expression levels of the pro-inflammatory cytokines IL-1 β , TNF- α , and COX-2 in splinted wounds were significantly higher when compared to non-splinted wounds (36.9-, 24.4-, 8.8-fold, respectively) (Figure 4.5C).

In summary, we showed that delayed wound closure and reduced HO-1 protein expression following mechanical stress was clearly associated with elevated levels of macrophages and several other inflammatory genes.

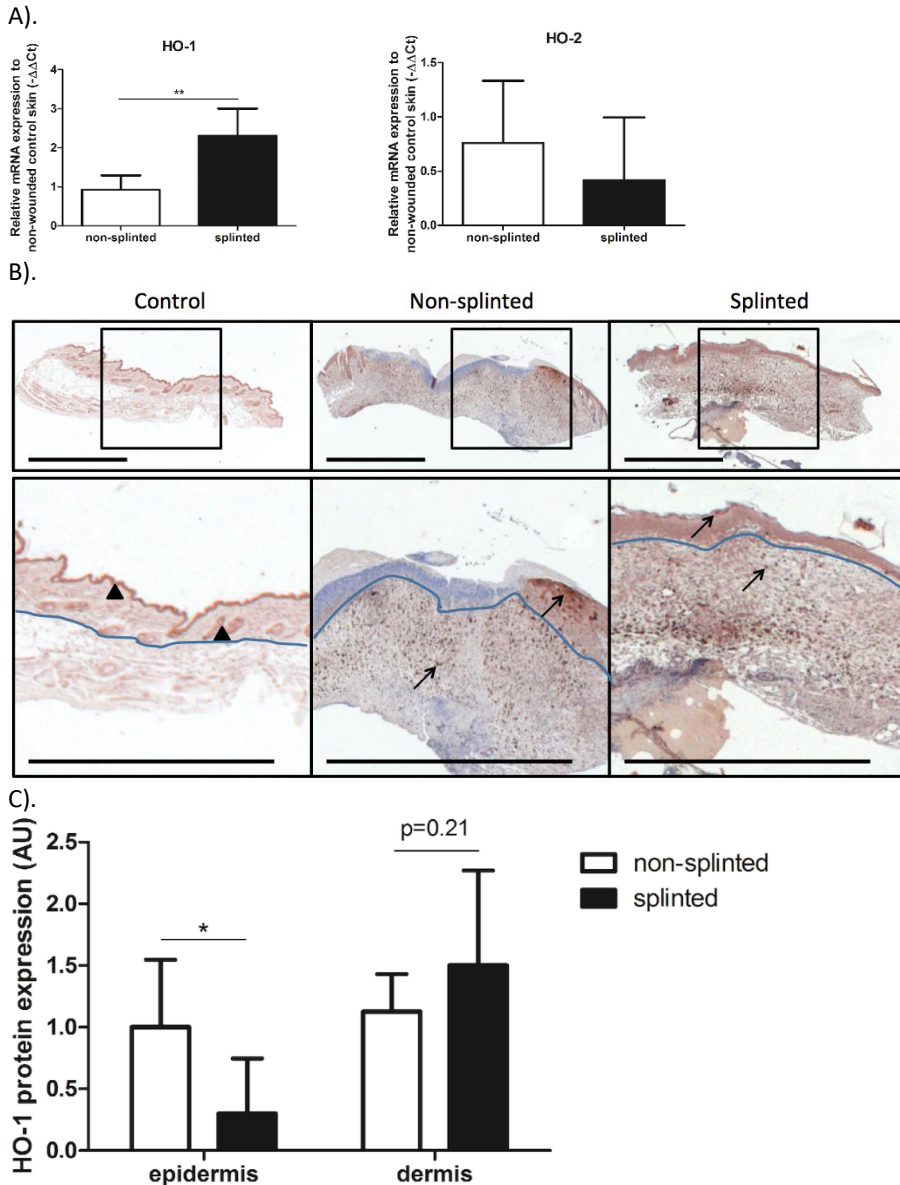
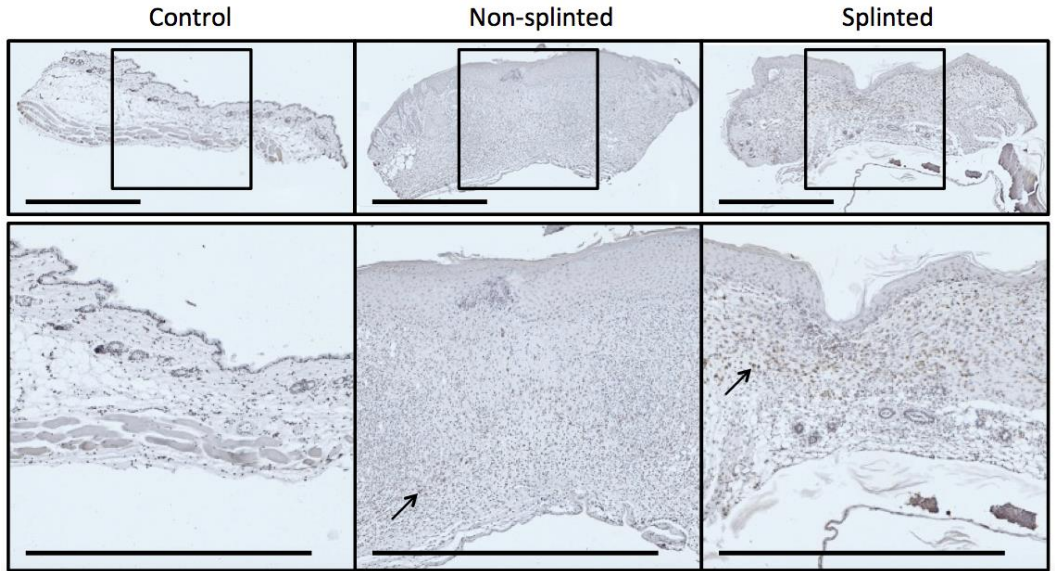


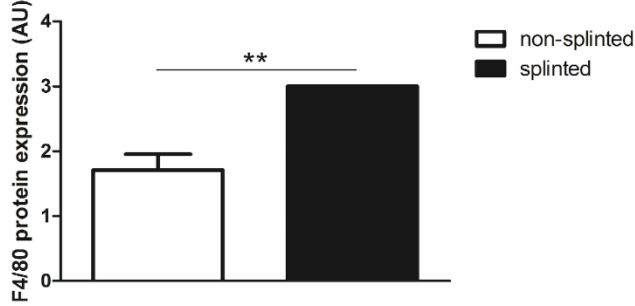
Figure 4.4: HO expression in wounds

(A) HO-1 and HO-2 mRNA expression levels in non-splinted and splinted wounds were determined in 7-day wounds and compared to control unwounded skin. Data represent mean±SD. * is significantly different between non-splinted and splinted wounds (**p<0.01). (B) HO-1 protein expression in control and non-splinted and splinted wounds after 7 days of healing. Region above the marked blue line is the epidermis and underneath the line is the dermal layer (bars = 1 mm). Note: black triangle (▲) in the non-wounded control skin shows HO-1-positive keratinocytes at the front of the epithelial layer, and HO-1 positive hair follicles. Black arrows (→) shows HO-1-positive cells in the epidermis and dermis of non-splinted and splinted wounds. (C) Quantification of scored HO-1 protein staining in epidermis and dermis of the wounds after 7 days in arbitrary units (AU). Data represent mean±SD. * is significantly different between non-splinted and splinted wounds (*p<0.05).

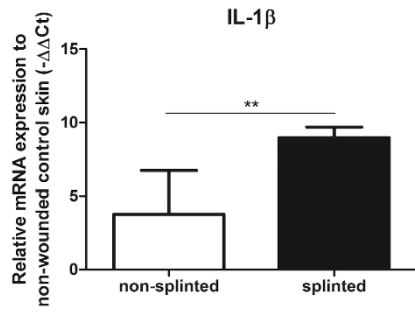
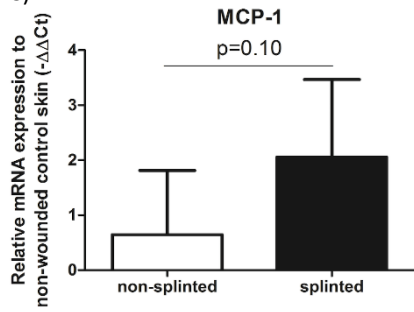
A).



B).



C).



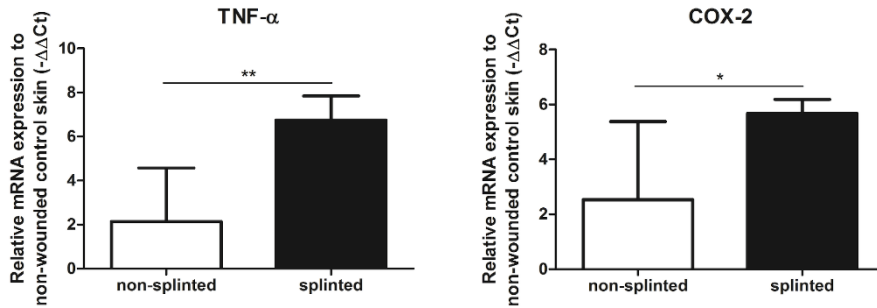


Figure 4.5: Effects of splinting on markers of inflammation

(A) Immunohistological staining of macrophages (F4/80) in control skin and non-splinted and splinted 7-day wounds (bars = 1 mm). Black arrow (\rightarrow) shows F4/80-positive macrophages in non-splinted and splinted wounds. (B) Quantification of scored F4/80 protein staining of the wounds after 7 days in arbitrary units (AU). Data represent mean \pm SD. * is significantly different between non-splinted and splinted wounds (** p <0.01). (C) mRNA expression levels of inflammatory markers in 7-day non-splinted and splinted wounds normalized to levels in control unwounded skin (MCP-1, IL-1 β , TNF- α , and COX-2). Data represent mean \pm SD. * is significantly different between non-splinted and splinted wounds (* p <0.05, ** p <0.01).

Effects of mechanical stress on remodeling and fibrotic genes

Because increased levels of inflammation by mechanical stress during wound repair may also affect markers of fibrosis, we investigated the effects of splinting on markers of ECM remodeling and fibrosis.

During wound healing, fibroblasts can transform into myofibroblasts. These myofibroblasts cause wound contraction and produce ECM. Normally, these myofibroblasts go into apoptosis after wound repair has finished. When these myofibroblasts fail to become apoptotic, ECM production continues, and pathologic wound healing with excessive scarring follows. The presence of myofibroblasts is dependent on the phase of wound healing. To investigate the role of splinting on myofibroblasts, we stained 7-day wound sections with the myofibroblast marker α -SMA. In non-wounded skin, α -SMA staining was already evident in the muscles of the vascular wall and the arrector pili muscles of the hair follicles (Figure 4.6A). Following injury, myofibroblasts were present both in non-splinted as well as splinted wounds. However, quantification of arbitrarily scored α -SMA-positive myofibroblasts showed significantly increased levels in splinted wounds when compared to non-splinted wounds (Figure 4.6B).

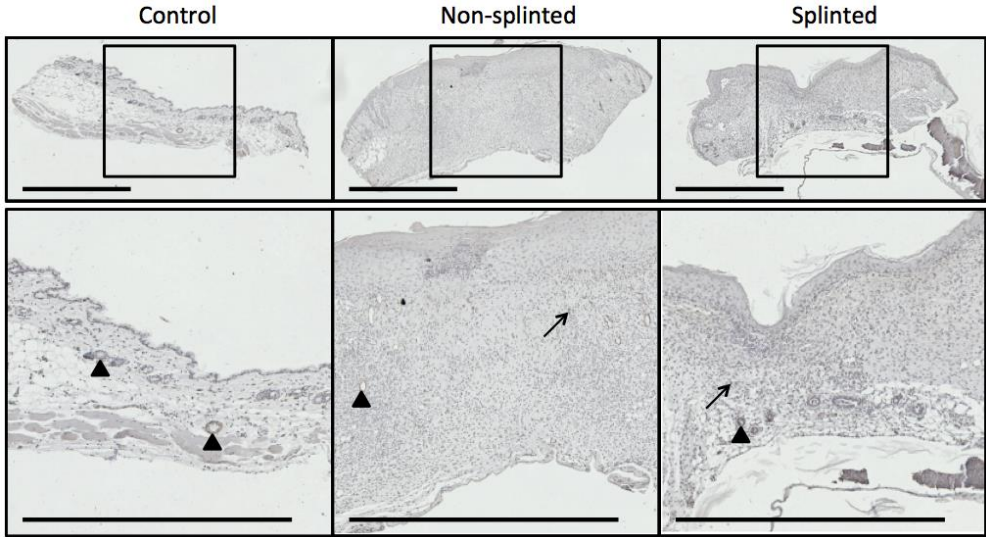
Next, we measured mRNA expression levels of genes involved in remodeling and fibrosis (Figure 4.6C). Vascular endothelial growth factor (VEGF) is an important regulator of angiogenesis, and was 2.9 times higher in splinted wounds compared to non-splinted wounds. Also matrix metalloproteinase (MMP)-9, an important enzyme that helps remodel the provisional ECM following wounding, was increased (4-fold).

Surprisingly, collagen type 3 gene expression, which is produced by (myo)fibroblasts, and forms the major collagen type expressed in granulation tissue, was almost 3 times lower in splinted wounds compared to non-splinted wounds (p =0.0544).

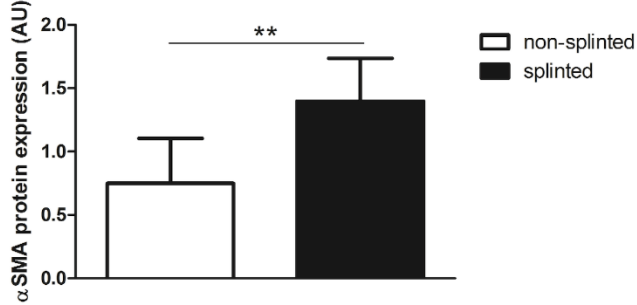
Interestingly, we found significantly more (5.8-fold) gene expression of keratinocyte marker *krt-6* in non-splinted wounds compared to splinted wounds.

Thus, there were more myofibroblasts and higher expression of VEGF and MMP-9 in day-7 wounds following mechanical stress.

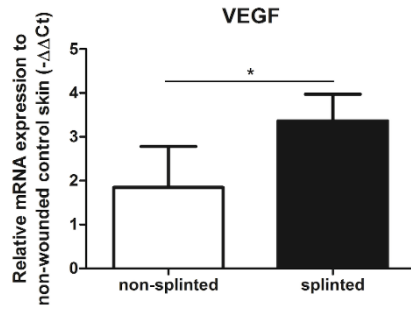
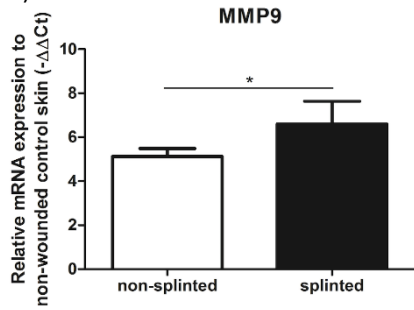
A).



B).



C).



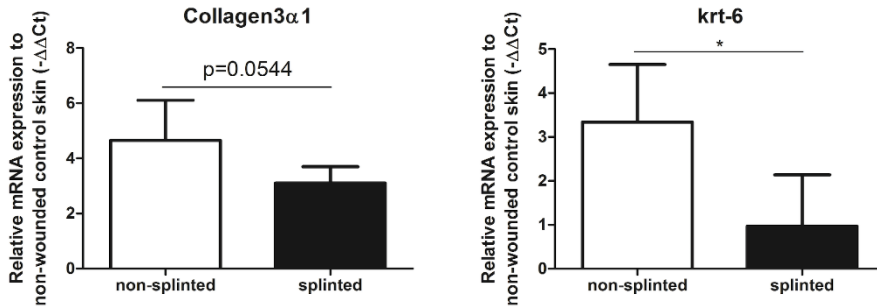


Figure 4.6: Effects of splinting on markers of fibrosis

(A) Immunohistological staining of α -SMA-positive myofibroblasts in control skin and non-splinted and splinted 7-day wounds (bars = 1 mm). Note: black triangle (\blacktriangle) in the non-wounded control skin shows α -SMA-positive muscles in the vascular wall and the arrector pili muscles of the hair follicles. Black arrow (\rightarrow) shows α -SMA-positive myofibroblasts. (B) Quantification of scored α -SMA protein staining of wounds after 7 days in arbitrary units (AU). Data represent mean \pm SD. * is significantly different between non-splinted and splinted wounds (** $p < 0.01$). (C) mRNA expression levels of VEGF, MMP-9, collagen type 3, and krt-6 in 7-day non-splinted and splinted wounds normalized to levels in control unwounded skin. Data represent mean \pm SD. * is significantly different between non-splinted and splinted wounds (* $p < 0.05$).

Discussion

We found that splinting effectively delayed wound closure. Interestingly, HO-1 promoter activity initially decreased upon wounding, but was followed by induction of HO-1 mRNA and protein. However, HO-1 protein expression was delayed in the splinted wounds. Since HO activity attenuates inflammatory and oxidative stress and is thought to reduce fibrosis, we postulated that the splinting-mediated delay in HO-1 protein expression could result in a reduced defense against inflammatory and fibrotic processes. Indeed, more F4/80-positive macrophages, α -SMA-positive myofibroblasts, and pro-inflammatory cytokines were present in splinted wounds at day 7 when compared to non-splinted wounds. Normally, the wound healing cascade is characterized by three distinct phases: inflammation, proliferation and remodeling (9, 38, 39). This suggests that mechanical stress causes delayed wound closure, a prolongation of the inflammatory phase, and an altered remodeling phase, and may promote fibrosis.

Mechanical stress and HO-1

We found that mechanical stress by splinting delays wound closure 3.3 times in comparison to non-splinted wounds after 7 days. This was likely largely mediated by inhibiting the contraction of the subcutaneous muscle layer in mice; however, it may also be caused by interfering with other processes involved in wound healing, such as inflammation, proliferation or remodeling.

Previously, it was shown that *in vitro* administration of mechanical stress with a Flex-cell strain unit induces HO-1 mRNA and protein expression in periodontal ligament cells in a time- and force-dependent manner (30). HO-1 mRNA levels are also upregulated *in vitro* after mechanical stress in human aortic endothelial cells (40) and human dental pulp cells (41). Aortic smooth muscle cells also respond to mechanical stress, and induce HO-1 expression in a time-dependent response to laminar shear stress (32). In an *in vivo* model with inflammatory, oxidative and mechanical stress, HO-1 mRNA was induced after 6 and

12h as a result of unilateral urethral obstruction (31). We therefore postulated that splinting would induce HO-1 as a protective response.

We have shown that within the first hour of wounding, HO-1 promoter activity at the place of the wound decreases. This may be related to the removal of the HO-1-positive skin layer. This suggests that there is basal HO-1 promoter activity present in normal skin, which we previously validated in the epithelium of the skin (6). More precisely, keratinocytes in the hyperproliferative epithelium express high levels of HO-1 as normal physiology (25, 26). After the initial decrease in HO-1 promoter activity in both groups, HO-1 promoter activity significantly increased within one day, which may be due to the attraction of HO-1-positive macrophages during the inflammatory phase, and the influx of HO-1-positive epithelial cells during the re-epithelialization of the wounds (22, 26, 42). This rapid HO-1 induction is in line with a previous study in mouse excisional wounds, showing increased HO-1 mRNA and protein at day 1 after wounding (24). Additionally, the constitutively-expressed HO-2 was also not affected by wounding in this previous study, which was similar to our current results. We found that effects on HO-1 promoter activity were independent of the wound model, since both splinted and non-splinted wounds showed similar activity. However, at day 3, there was only a significant increase in the splinted model compared to the baseline level. Increased HO-1 expression was also found for both models in 7-day wounds at the mRNA level when compared to non-wounded skin. This increase was significantly higher after mechanical stress.

On the protein level, we saw contradictory results with significantly more HO-1 protein staining in the epidermis of non-splinted wounds and a slight, non-statistically significant, increase of HO-1 protein in the dermis in splinted wounds after 7 days. Thus, although HO-1 induction was shown in diverse models of mechanical stress, we found only HO-1 promoter activation and HO-1 mRNA induction. HO-1 protein expression was, in fact, reduced by the static mechanical stress of the splint in the epidermal region.

When comparing protein levels in the epidermis, HO-1-positive cells were clustered in re-epithelialized tissue underneath the wound crust and were likely newly-formed keratinocytes (25, 26). It is likely that the highly increased keratinocyte gene expression in non-splinted wounds account for the observed increase in HO-1 protein expression.

In the dermis, HO-1-positive cells in inflamed tissues were individually spread, and based on their location and morphology, appeared to be macrophages (25, 42). We and others demonstrated previously that HO-1-positive macrophages can be recruited during the wound repair process (6, 25, 26).

It is, however, striking that splinted wounds exhibited similar levels of HO-1-positive cells in the dermis when compared to non-splinted wounds, while there were higher levels of F4/80-positive macrophages in splinted wounds.

Mechanical stress by splinting enhances inflammation; the role of HO-1

Macrophages promote strong inflammatory responses through secretion of cytokines, such as IL-1 β and TNF- α (43). It is thought that during the wound repair process, first pro-inflammatory M1 macrophages enter the wound site to clear cellular debris and destroy invading pathogens. Besides pro-inflammatory M1 macrophages, there are other macrophage subsets, including the anti-inflammatory M2 macrophages and the Mhem, Mox, and M4 macrophages (44-46). To enter the proliferation phase, resolution of

inflammation is necessary. Under the right conditions, M1 macrophages may therefore skew into other anti-inflammatory macrophage subsets (45, 46). The presence of large numbers of macrophages in the splinted wounds and the increased levels of pro-inflammatory mediators IL-1 β , TNF- α and COX-2 suggests that in the splinted wounds there were mainly M1 macrophages present. Prolonged inflammation and high levels of oxidative stress may result in excessive deposition of ECM, leading to fibrosis and excessive/hypertrophic scarring (18, 47). Cytokines that mediate inflammation, such as IL-1 β and TNF- α , are well known to be involved in mechanical stretch-induced inflammation. For example, *in vitro* administration of mechanical stress induces both IL-1 β and COX-2 in fibroblast-like synovioyte cells (48), epithelial cells (49), chondrocytes (50), and cardiac muscle cells (51) in a time- and force-dependent manner. This increased expression of inflammatory markers corresponded to our findings. Moreover, we found a trend in MCP-1 mRNA induction ($p=0.10$) after mechanical stress, matching the enhanced protein staining for macrophages after mechanical stress.

HO-1-positive macrophages are thought to protect the wound environment against oxidative stress (25, 52). Following injury, the HO substrate heme is abundantly released at the edges of the wound site and can stimulate recruitment of leukocytes (6, 25, 53). In contrast, HO activity inhibits leukocyte recruitment via down-regulation of vascular adhesion molecules (6). Moreover, HO-1 activity inhibits production of various pro-inflammatory cytokines, including IL-1 β and TNF- α (54, 55). In 7-day wounds, the inflammation levels were high in both non-splinted and splinted wounds, but however were much higher after mechanical stress in the splinted wounds.

The expression of HO-1 may facilitate resolution of inflammatory and oxidative stress at the wound site. When mechanical stress delays HO-1 protein expression, this may also delay resolution of inflammation, and lead to fibrogenesis.

Mechanical stress results in more fibrosis by a prolonged survival of myofibroblasts; the relation between inflammation, remodeling and HO-1

Mechanical stress, which is present in CL/P patients following palatal surgery and in patients with wounds in the vicinity of joints, increases the risk of excessive scar formation. In our splinting model, we demonstrated the increased presence of pro-inflammatory and pro-fibrotic cells and markers, suggesting that mechanical stress interferes with resolution of inflammation, which may ultimately lead to hampered wound repair and excessive scar formation. Application of mechanical loading to healing wounds in mice can cause hypertrophic scarring, through decreased apoptosis of myofibroblasts (56). It is tempting to speculate that the delayed HO-1 protein expression in the splinted model contributes to the delay in resolution of inflammation and allows the pro-inflammatory environment and the myofibroblast survival that we observed in the wound area at day 7.

When myofibroblasts fail to go into apoptosis, this leads to continuation of contraction and production of ECM, and ultimately to fibrosis (5, 13, 17, 18). We found an increased presence of myofibroblasts after splinting, suggesting that either more myofibroblasts are formed upon mechanical stress, less myofibroblasts die, or splinting causes a delay in the myofibroblast formation when compared to non-splinted wounds. This corresponds to other reports, which showed that mechanical tension induces myofibroblast differentiation in wound granulation tissue in 6-day splinted wounds compared to non-

splinted wounds (14, 20). These processes may be fine-tuned by HO-1 and its effector molecules as is shown *in vitro* by regulating the apoptosis of fibroblasts (18, 57).

Pathological cutaneous wound healing resulting in excessive scarring and fibrosis is the consequence of an imbalance between ECM synthesis by myofibroblasts and degradation and remodeling by MMPs (13). We found that remodeling marker MMP-9 was increased after mechanical stress, which was also observed by other groups (58-60). VEGF is an important promoter of angiogenesis and therefore microvessel density might be increased by mechanical tension. Chemokine and cytokine processing by MMPs affects the progression of inflammatory responses and leukocyte migration (61). For example, MMP-9 can inactivate/ degrade CXCL1, CXCL4, CXCL9, and CXCL10, resulting in anti-inflammatory effects (62, 63). Increased MMP-9 may be indicative of inflammation and poor wound healing (64). The interplay between VEGF and HO-1 is complex and it was demonstrated that they can both inhibit or induce each other (65-68). Induction of HO-1 in a rat excisional wound model enhanced wound healing by increased cellular proliferation and collagen synthesis (28). HO-1 induction also reduced the inflammatory response by inhibition of pro-inflammatory molecules TNF- α , and ICAM-1 and an induction of the anti-inflammatory cytokine IL-10 (28).

In summary, mechanical stress leads to delayed wound closure, increased inflammation, and altered remodeling during the wound healing process. Since more myofibroblasts are present after splinting, mechanical stress may result in more scar formation. This was associated with a delayed anti-inflammatory and anti-fibrotic HO-1 protein expression in splinted wounds compared to non-splinted wounds. Since HO-1 attacks multiple targets that play an important role during fibrogenesis, pharmacologic induction of HO-1 may facilitate resolution of inflammation and attenuate fibrosis.

Conclusion

We demonstrated that splinting significantly delays wound closure and potentiates the influx of pro-inflammatory leukocytes and myofibroblasts in day-7 wounds, which may promote fibrosis. The cytoprotective HO-1 gene is increased upon wounding, but HO-1 protein was lower in the epidermis after mechanical stress, probably as a result of the increased number of HO-1-positive keratinocytes in the re-epithelialization tissue of non-splinted wounds. Therefore, targeted pharmacologic induction of cytoprotective mechanisms, including HO-1, as preventive therapy against mechanical stress-induced inflammation and fibrosis must be considered.

References

1. Bartzela TN, Carels CE, Bronkhorst EM, Ronning E, Rizell S, Kuijpers-Jagtman AM. Tooth agenesis patterns in bilateral cleft lip and palate. *Eur J Oral Sci.* 2010;118(1):47-52.
2. Nollet PJ, Katsaros C, Van't Hof MA, Kuijpers-Jagtman AM. Treatment outcome in unilateral cleft lip and palate evaluated with the GOSLON yardstick: a meta-analysis of 1236 patients. *Plastic and reconstructive surgery.* 2005;116(5):1255-62.
3. Biggs LC, Goudy SL, Dunnwald M. Palatogenesis and cutaneous repair: A two-headed coin. *Dev Dyn.* 2015;244(3):289-310.
4. Li J, Johnson CA, Smith AA, Salmon B, Shi B, Brunski J, et al. Disrupting the intrinsic growth potential of a suture contributes to midfacial hypoplasia. *Bone.* 2014;81:186-95.
5. Brouwer KM, Lundvig DM, Middelkoop E, Wagener FA, Von den Hoff JW. Mechanical cues in orofacial tissue engineering and regenerative medicine. *Wound Repair Regen.* 2015;23(3):302-11.
6. Wagener FA, van Beurden HE, von den Hoff JW, Adema GJ, Figdor CG. The heme-heme oxygenase system: a molecular switch in wound healing. *Blood.* 2003;102(2):521-8.
7. van Beurden HE, Von den Hoff JW, Torensma R, Maltha JC, Kuijpers-Jagtman AM. Myofibroblasts in palatal wound healing: prospects for the reduction of wound contraction after cleft palate repair. *Journal of dental research.* 2005;84(10):871-80.
8. Eming SA, Martin P, Tomic-Canic M. Wound repair and regeneration: mechanisms, signaling, and translation. *Science translational medicine.* 2014;6(265):265sr6.
9. Gurtner GC, Werner S, Barrandon Y, Longaker MT. Wound repair and regeneration. *Nature.* 2008;453(7193):314-21.
10. Hinz B, Gabbiani G. Mechanisms of force generation and transmission by myofibroblasts. *Current opinion in biotechnology.* 2003;14(5):538-46.
11. Eckes B, Zweers MC, Zhang ZG, Hallinger R, Mauch C, Aumailley M, et al. Mechanical tension and integrin alpha 2 beta 1 regulate fibroblast functions. *The journal of investigative dermatology Symposium proceedings / the Society for Investigative Dermatology, Inc [and] European Society for Dermatological Research.* 2006;11(1):66-72.
12. Desmouliere A, Chaponnier C, Gabbiani G. Tissue repair, contraction, and the myofibroblast. *Wound Repair Regen.* 2005;13(1):7-12.
13. Micallef L, Vedrenne N, Billet F, Coulomb B, Darby IA, Desmouliere A. The myofibroblast, multiple origins for major roles in normal and pathological tissue repair. *Fibrogenesis & tissue repair.* 2012;5(Suppl 1):S5.
14. Hinz B, Mastrangelo D, Iselin CE, Chaponnier C, Gabbiani G. Mechanical tension controls granulation tissue contractile activity and myofibroblast differentiation. *The American journal of pathology.* 2001;159(3):1009-20.
15. van der Veer WM, Bloemen MC, Ulrich MM, Molema G, van Zuijlen PP, Middelkoop E, et al. Potential cellular and molecular causes of hypertrophic scar formation. *Burns.* 2009;35(1):15-29.
16. Darby IA, Laverdet B, Bonte F, Desmouliere A. Fibroblasts and myofibroblasts in wound healing. *Clinical, cosmetic and investigational dermatology.* 2014;7:301-11.
17. Van De Water L, Varney S, Tomasek JJ. Mechanoregulation of the Myofibroblast in Wound Contraction, Scarring, and Fibrosis: Opportunities for New Therapeutic Intervention. *Advances in wound care.* 2013;2(4):122-41.
18. Lundvig DM, Immenschuh S, Wagener FA. Heme oxygenase, inflammation, and fibrosis: the good, the bad, and the ugly? *Front Pharmacol.* 2012;3:81.
19. Galiano RD, Michaels Jt, Dobryansky M, Levine JP, Gurtner GC. Quantitative and reproducible murine model of excisional wound healing. *Wound Repair Regen.* 2004;12(4):485-92.
20. Tomasek JJ, Gabbiani G, Hinz B, Chaponnier C, Brown RA. Myofibroblasts and mechano-regulation of connective tissue remodelling. *Nature reviews Molecular cell biology.* 2002;3(5):349-63.
21. Gozzelino R, Jeney V, Soares MP. Mechanisms of cell protection by heme oxygenase-1. *Annual review of pharmacology and toxicology.* 2010;50:323-54.
22. Wagener FA, Volk HD, Willis D, Abraham NG, Soares MP, Adema GJ, et al. Different faces of the heme-heme oxygenase system in inflammation. *Pharmacol Rev.* 2003;55(3):551-71.
23. Wagener FA, Dankers AC, van Summeren F, Scharstuhl A, van den Heuvel JJ, Koenderink JB, et al. Heme Oxygenase-1 and breast cancer resistance protein protect against heme-induced toxicity. *Curr Pharm Des.* 2013;19(15):2698-707.
24. Schafer M, Werner S. Oxidative stress in normal and impaired wound repair. *Pharmacological research.* 2008;58(2):165-71.

25. Hanselmann C, Mauch C, Werner S. Haem oxygenase-1: a novel player in cutaneous wound repair and psoriasis? *The Biochemical journal*. 2001;353(Pt 3):459-66.
26. Kampfner H, Kolb N, Manderscheid M, Wetzler C, Pfeilschifter J, Frank S. Macrophage-derived heme-oxygenase-1: expression, regulation, and possible functions in skin repair. *Molecular medicine*. 2001;7(7):488-98.
27. Grochot-Przeczek A, Lach R, Mis J, Skrzypek K, Gozdecka M, Sroczyńska P, et al. Heme oxygenase-1 accelerates cutaneous wound healing in mice. *PLoS One*. 2009;4(6):e5803.
28. Ahanger AA, Prawez S, Leo MD, Kathirvel K, Kumar D, Tandan SK, et al. Pro-healing potential of hemin: an inducer of heme oxygenase-1. *European journal of pharmacology*. 2010;645(1-3):165-70.
29. Wagener FA, Scharstuhl A, Tyrrell RM, Von den Hoff JW, Jozkowicz A, Dulak J, et al. The heme-heme oxygenase system in wound healing; implications for scar formation. *Current drug targets*. 2010;11(12):1571-85.
30. Cho JH, Lee SK, Lee JW, Kim EC. The role of heme oxygenase-1 in mechanical stress- and lipopolysaccharide-induced osteogenic differentiation in human periodontal ligament cells. *The Angle orthodontist*. 2010;80(4):552-9.
31. Carlsen I, Nilsson L, Frokiaer J, Norregaard R. Changes in phosphorylated heat-shock protein 27 in response to acute ureteral obstruction in rats. *Acta physiologica*. 2013;209(2):167-78.
32. Wagner CT, Durante W, Christodoulides N, Hellums JD, Schafer AI. Hemodynamic forces induce the expression of heme oxygenase in cultured vascular smooth muscle cells. *The Journal of clinical investigation*. 1997;100(3):589-96.
33. Wever KE, Wagener FA, Frielink C, Boerman OC, Scheffer GJ, Allison A, et al. Diannexin protects against renal ischemia reperfusion injury and targets phosphatidylserines in ischemic tissue. *PLoS One*. 2011;6(8):e24276.
34. Su H, van Dam GM, Buis CI, Visser DS, Hesselink JW, Schuur TA, et al. Spatiotemporal expression of heme oxygenase-1 detected by in vivo bioluminescence after hepatic ischemia in HO-1/Luc mice. *Liver transplantation*. 2006;12(11):1634-9.
35. Lundvig DM, Scharstuhl A, Cremers NA, Pennings SW, Te Paske J, van Rheden R, et al. Delayed cutaneous wound closure in HO-2 deficient mice despite normal HO-1 expression. *Journal of cellular and molecular medicine*. 2014;18(12):2488-98.
36. van den Brand BT, Vermeij EA, Waterborg CE, Arntz OJ, Kracht M, Bennink MB, et al. Intravenous delivery of HIV-based lentiviral vectors preferentially transduces F4/80+ and Ly-6C+ cells in spleen, important target cells in autoimmune arthritis. *PLoS One*. 2013;8(2):e55356.
37. Cremers NA, Lundvig DM, van Dalen SC, Schelbergen RF, van Lent PL, Szarek WA, et al. Curcumin-induced heme oxygenase-1 expression prevents H2O2-induced cell death in wild type and heme oxygenase-2 knockout adipose-derived mesenchymal stem cells. *Int J Mol Sci*. 2014;15(10):17974-99.
38. Baum CL, Arpey CJ. Normal cutaneous wound healing: clinical correlation with cellular and molecular events. *Dermatologic surgery : official publication for American Society for Dermatologic Surgery [et al]*. 2005;31(6):674-86; discussion 86.
39. Singer AJ, Clark RA. Cutaneous wound healing. *The New England journal of medicine*. 1999;341(10):738-46.
40. Liu XM, Peyton KJ, Durante W. Physiological cyclic strain promotes endothelial cell survival via the induction of heme oxygenase-1. *American journal of physiology Heart and circulatory physiology*. 2013;304(12):H1634-43.
41. Lee SK, Lee CY, Kook YA, Lee SK, Kim EC. Mechanical stress promotes odontoblastic differentiation via the heme oxygenase-1 pathway in human dental pulp cell line. *Life sciences*. 2010;86(3-4):107-14.
42. Schurmann C, Seitz O, Klein C, Sader R, Pfeilschifter J, Muhl H, et al. Tight spatial and temporal control in dynamic basal to distal migration of epithelial inflammatory responses and infiltration of cytoprotective macrophages determine healing skin flap transplants in mice. *Annals of surgery*. 2009;249(3):519-34.
43. Rees P, Greaves N, Bayat A. Chemokines in wound healing and as potential therapeutic targets for reducing cutaneous scarring. *Advances in wound care*. 2015:1-17.
44. Hull TD, Agarwal A, George JF. The mononuclear phagocyte system in homeostasis and disease: a role for heme oxygenase-1. *Antioxidants & redox signaling*. 2014;20(11):1770-88.
45. Chistiakov DA, Bobryshev YV, Orekhov AN. Changes in transcriptome of macrophages in atherosclerosis. *Journal of cellular and molecular medicine*. 2015;19(6):1163-73.
46. Medbury HJ, Williams H, Fletcher JP. Clinical significance of macrophage phenotypes in cardiovascular disease. *Clinical and translational medicine*. 2014;3(1):63.

47. Sidgwick GP, Bayat A. Extracellular matrix molecules implicated in hypertrophic and keloid scarring. *Journal of the European Academy of Dermatology and Venereology* : JEADV. 2012;26(2):141-52.
48. Takao M, Okinaga T, Ariyoshi W, Iwanaga K, Nakamichi I, Yoshioka I, et al. Role of heme oxygenase-1 in inflammatory response induced by mechanical stretch in synovial cells. *Inflammation research*. 2011;60(9):861-7.
49. Toshinaga A, Hosokawa R, Okinaga T, Masaki C. Inflammatory response in epithelial cells induced by mechanical stress is suppressed by hyaluronic acid. *The Japanese Society of Inflammation and Regeneration* 2010 30(2):120-17.
50. Huang J, Ballou LR, Hasty KA. Cyclic equibiaxial tensile strain induces both anabolic and catabolic responses in articular chondrocytes. *Gene*. 2007;404(1-2):101-9.
51. Vandenberg HH, Shansky J, Solerssi R, Chromiak J. Mechanical stimulation of skeletal muscle increases prostaglandin F2 alpha production, cyclooxygenase activity, and cell growth by a pertussis toxin sensitive mechanism. *Journal of cellular physiology*. 1995;163(2):285-94.
52. Ishii T, Itoh K, Sato H, Bannai S. Oxidative stress-inducible proteins in macrophages. *Free radical research*. 1999;31(4):351-5.
53. auf dem Keller U, Kumin A, Braun S, Werner S. Reactive oxygen species and their detoxification in healing skin wounds. *The journal of investigative dermatology Symposium proceedings / the Society for Investigative Dermatology, Inc [and] European Society for Dermatological Research*. 2006;11(1):106-11.
54. Morse D, Pischke SE, Zhou Z, Davis RJ, Flavell RA, Loop T, et al. Suppression of inflammatory cytokine production by carbon monoxide involves the JNK pathway and AP-1. *The Journal of biological chemistry*. 2003;278(39):36993-8.
55. Lee TS, Tsai HL, Chau LY. Induction of heme oxygenase-1 expression in murine macrophages is essential for the anti-inflammatory effect of low dose 15-deoxy-Delta 12,14-prostaglandin J2. *The Journal of biological chemistry*. 2003;278(21):19325-30.
56. Aarabi S, Bhatt KA, Shi Y, Paterno J, Chang EI, Loh SA, et al. Mechanical load initiates hypertrophic scar formation through decreased cellular apoptosis. *FASEB journal : official publication of the Federation of American Societies for Experimental Biology*. 2007;21(12):3250-61.
57. Scharstuhl A, Mutsaers HA, Pennings SW, Szarek WA, Russel FG, Wagener FA. Curcumin-induced fibroblast apoptosis and in vitro wound contraction are regulated by antioxidants and heme oxygenase: implications for scar formation. *Journal of cellular and molecular medicine*. 2009;13(4):712-25.
58. Beckmann R, Houben A, Tohidnezhad M, Kweider N, Fragoulis A, Wruck CJ, et al. Mechanical forces induce changes in VEGF and VEGFR-1/sFlt-1 expression in human chondrocytes. *Int J Mol Sci*. 2014;15(9):15456-74.
59. Kawata T, Kohno S, Kaku M, Fujita T, Ohtani J, Motokawa M, et al. Expression of vascular endothelial growth factor on neovascularization during experimental tooth movement by magnets. *Biomed Res-India*. 2011;22(2):249-54.
60. Huang D, Liu Y, Huang Y, Xie Y, Shen K, Zhang D, et al. Mechanical compression upregulates MMP9 through SMAD3 but not SMAD2 modulation in hypertrophic scar fibroblasts. *Connective tissue research*. 2014;55(5-6):391-6.
61. Van Lint P, Libert C. Chemokine and cytokine processing by matrix metalloproteinases and its effect on leukocyte migration and inflammation. *Journal of leukocyte biology*. 2007;82(6):1375-81.
62. Van den Steen PE, Proost P, Wuyts A, Van Damme J, Opdenakker G. Neutrophil gelatinase B potentiates interleukin-8 tenfold by aminoterminal processing, whereas it degrades CTAP-III, PF-4, and GRO-alpha and leaves RANTES and MCP-2 intact. *Blood*. 2000;96(8):2673-81.
63. Van den Steen PE, Husson SJ, Proost P, Van Damme J, Opdenakker G. Carboxyterminal cleavage of the chemokines MIG and IP-10 by gelatinase B and neutrophil collagenase. *Biochemical and biophysical research communications*. 2003;310(3):889-96.
64. Liu Y, Min D, Bolton T, Nube V, Twigg SM, Yue DK, et al. Increased matrix metalloproteinase-9 predicts poor wound healing in diabetic foot ulcers. *Diabetes care*. 2009;32(1):117-9.
65. Bussolati B, Ahmed A, Pemberton H, Landis RC, Di Carlo F, Haskard DO, et al. Bifunctional role for VEGF-induced heme oxygenase-1 in vivo: induction of angiogenesis and inhibition of leukocytic infiltration. *Blood*. 2004;103(3):761-6.
66. Jozkowicz A, Huk I, Nigisch A, Weigel G, Weidinger F, Dulak J. Effect of prostaglandin-J(2) on VEGF synthesis depends on the induction of heme oxygenase-1. *Antioxidants & redox signaling*. 2002;4(4):577-85.
67. Chao HM, Chuang MJ, Liu JH, Liu XQ, Ho LK, Pan WH, et al. Baicalein protects against retinal ischemia by antioxidation, antiapoptosis, downregulation of HIF-1alpha, VEGF, and MMP-9 and upregulation of

- HO-1. *Journal of ocular pharmacology and therapeutics : the official journal of the Association for Ocular Pharmacology and Therapeutics*. 2013;29(6):539-49.
68. Jayasooriya RG, Park SR, Choi YH, Hyun JW, Chang WY, Kim GY. Camptothecin suppresses expression of matrix metalloproteinase-9 and vascular endothelial growth factor in DU145 cells through PI3K/Akt-mediated inhibition of NF-kappaB activity and Nrf2-dependent induction of HO-1 expression. *Environmental toxicology and pharmacology*. 2015;39(3):1189-98.

PART II:

ACTIVATION OF PROTECTIVE MECHANISMS TO ENHANCE TISSUE REGENERATION

Chapter 5

Curcumin-induced heme oxygenase-1 expression prevents H₂O₂-induced cell death in wild type and heme oxygenase-2 knockout adipose-derived mesenchymal stem cells.

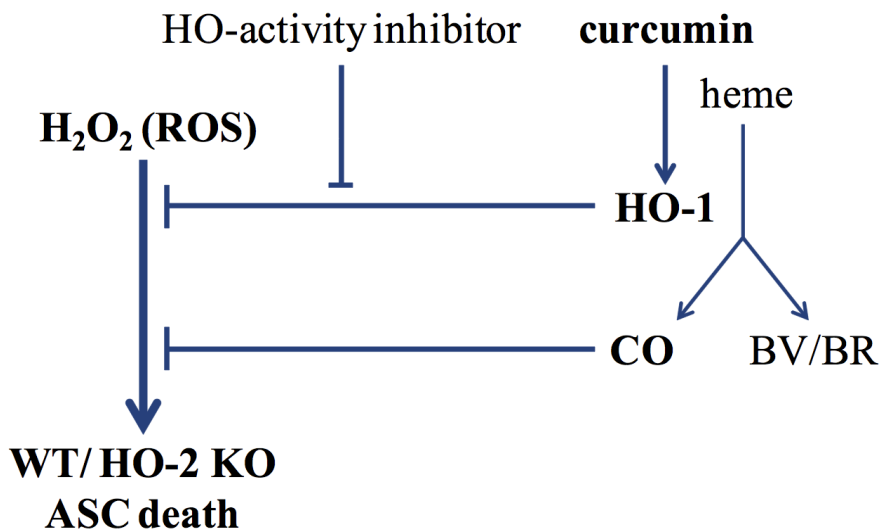
Cremers NA, Lundvig DM, van Dalen SC, Schelbergen RF, van Lent PL, Szarek WA, Regan RF, Carels CE, Wagener FA.

Int J Mol Sci. 2014 Oct 8;15(10):17974-99.

Abstract

Mesenchymal stem cell (MSC) administration is a promising adjuvant therapy to treat tissue injury. However, MSC survival after administration is often hampered by oxidative stress at the site of injury. Heme oxygenase (HO) generates the cytoprotective effector molecules biliverdin/bilirubin, carbon monoxide (CO) and iron/ferritin by breaking down heme. Since HO-activity mediates anti-apoptotic, anti-inflammatory, and anti-oxidative effects, we hypothesized that modulation of the HO-system affects MSC survival. Adipose-derived MSCs (ASCs) from wild-type (WT) and HO-2 knockout (KO) mice were isolated and characterized with respect to ASC marker expression. In order to analyze potential modulatory effects of the HO-system on ASC survival, WT and HO-2 KO ASCs were pre-treated with HO-activity modulators, or downstream effector molecules biliverdin, bilirubin, and CO before co-exposure of ASCs to a toxic dose of H₂O₂. Surprisingly, sensitivity to H₂O₂-mediated cell death was similar in WT and HO-2 KO ASCs. However, pre-induction of HO-1 expression using curcumin increased ASC survival after H₂O₂ exposure in both WT and HO-2 KO ASCs. Simultaneous inhibition of HO-activity resulted in loss of curcumin-mediated protection. Co-treatment with glutathione precursor N-Acetylcysteine promoted ASC survival. However, co-incubation with HO-effector molecules bilirubin and biliverdin did not rescue from H₂O₂-mediated cell death, whereas co-exposure to CO-releasing molecules-2 (CORM-2) significantly increased cell survival, independently from HO-2 expression. Summarizing, our results show that curcumin protects via an HO-1 dependent mechanism against H₂O₂-mediated apoptosis, and likely through the generation of CO. HO-1 pre-induction or administration of CORMs may thus form an attractive strategy to improve MSC therapy.

Keywords: adipose-derived mesenchymal stem cells, oxidative stress, apoptosis, heme oxygenase, carbon monoxide.



Graphical abstract

Abbreviations

ASC	Adipose-derived MSCs
BM	Bone marrow
BR	Bilirubin
BV	Biliverdin
CO	Carbon monoxide
CORM-2	CO Releasing molecule-2
GPX	Glutathione peroxidase
GSH	Glutathione
H ₂ O ₂	Hydrogen peroxide
HO	Heme oxygenase
IL	Interleukin
iPSC	Induced pluripotent stem cells
KO	Knockout
MAPK	Mitogen-activated protein kinase
MSC	Mesenchymal stem cell
MEF	Murine embryonic fibroblasts
NAC	N-acetyl-L-cysteine
nrf2	Nuclear factor-erythroid 2-related factor 2
PI	Propidium iodide
qPCR	Quantitative Reverse-Transcriptase PCR
SDF-1	Stromal cell-derived factor-1
WT	Wild-type

Introduction

Administration of mesenchymal stem cells (MSCs) forms a promising novel adjuvant treatment to improve tissue repair (1-4). MSCs have been shown to accelerate dermal wound healing and can regenerate diverse injured organs, such as kidney, lung and heart (5-9). MSCs are a heterogeneous population of fibroblast-like, multipotent stem cells characterized by their ability to differentiate into mature cells of the mesodermal lineage, like osteoblasts, chondrocytes, adipocytes, endothelial cells, and myocytes, and into cells outside the mesodermal lineage, such as keratinocytes, and fibroblasts (3, 10-12). Adipose tissue forms an easy accessible source for isolating MSCs for the use in (autologous) regenerative medicine and may therefore be a better alternative than MSCs isolated from other sources, such as bone marrow (BM) (13-16). These adipose-derived MSCs (ASCs) are abundantly present in adipose tissue, easy to isolate, and highly proliferative. In addition, they secrete extensively regenerative factors, such as hepatocyte growth factor, vascular endothelial growth factor, basic fibroblast growth factor, interleukin (IL)-6, -7, -8, and -11, and stromal cell-derived factor-1 (SDF-1) (14-16).

Despite the promising utilization of MSCs in regenerative medicine, the low survival after administration and the limited migration of MSCs to the site of injury limits their therapeutic efficacy (17, 18). Local administration to the site of injury may attenuate the problems with MSC migration. However, MSC administration in vicinity to the injured tissue may also affect MSC survival, as the wound microenvironment harbors excessive levels of inflammatory and oxidative mediators, hypoxia, and limited blood flow (19). Oxidative and inflammatory stresses are known causes of MSC death (17, 18, 20). Cells have several mechanisms to protect themselves against inflammatory and oxidative insults, including cytoprotective enzyme systems (e.g., glutathione S-transferase, dismutases, catalases, and peroxidases) or anti-oxidants (vitamin A, C, and E, urate, glutathione, and bilirubin) (21). In addition, MSCs may upregulate anti-apoptotic and anti-oxidative genes (16, 19). Pre-induction of cytoprotective pathways in the ASCs may improve their therapeutic potential by protecting them against the harsh microenvironment (22, 23).

The cytoprotective enzyme heme oxygenase (HO) is important for (stem) cell survival and functioning (17, 18, 24, 25). HO breaks down heme into biliverdin, free iron (Fe^{2+}) and carbon monoxide (CO). Biliverdin (BV) is rapidly converted into bilirubin (BR) by biliverdin reductase (26, 27). The iron scavenger ferritin is co-induced by HO-derived iron and is important for protection against iron-mediated reactive oxygen species (ROS) formation (28). Two distinct isoforms (HO-1 and HO-2) exist. HO-2 is mainly constitutively expressed whereas HO-1 is highly inducible by a variety of patho-physiological stimuli, such as free heme, cytokines, hypoxia, and oxidative stress (29). HO-2 is responsible for maintaining normal metabolic cellular functions, and regulating physiological levels of ROS (30-32).

Induction of HO-1 has been demonstrated to improve MSC therapy *in vivo* by improving tissue functioning of the damaged organ, whereas inhibition of HO-activity worsened MSC therapy outcome in diverse pathologic conditions, such as ischemia-reperfusion injury of the heart, pulmonary arterial hypertension, diabetes, and dermal wound healing (31, 33-40). It has been shown *in vitro* that HO-1 overexpression increases BM-derived MSC survival against oxidative stress, but the exact mechanism remains unknown (17, 34). By contrast, induced pluripotent stem cells (iPSCs) and murine embryonic fibroblasts (MEFs) derived from HO-1 knockout mice accumulate higher levels of

intracellular ROS after exposure to oxidative stress (41, 42). Moreover, HO-1 KO iPSCs and MEFs are more sensitive to hydrogen peroxide (H₂O₂)-induced cell death (41, 42). Since, the effects of HO-1 are extensively studied in stem cells, we investigate here the role of the HO-2 isoform in protection against oxidative stress. HO-2 has been shown to act protective against inflammatory and oxidative injury and cell apoptosis in diverse cell types (43-51).

In the present study we postulated that HO-2 WT ASCs would be better protected against oxidative stress when compared to HO-2 deficient ASCs. Additionally, we aimed to investigate the role of HO-activity and HO-effector molecules BR/BV and CO on ASC survival after H₂O₂-induced oxidative stress.

Experimental Section

Reagents

Biliverdin and bilirubin were purchased from Frontier Scientific, Carnforth, UK. Curcumin, N-acetyl-L-cysteine (NAC), tricarbonyldichlororuthenium(II)dimer (CO releasing molecule: CORM-2), and Ruthenium(III)chloride (CORM-2 control) were purchased from Sigma-Aldrich, Zwijndrecht, the Netherlands. Biliverdin, and bilirubin were prepared by dissolving this together with Trizma base in 2 mL 0.1M NaOH and 5 mL H₂O. The pH was adjusted to pH 8 with HCl, and further diluted till 10 mL with H₂O. An end concentration of 1 µM was used in the experiments (52). Curcumin was dissolved in 99.5% ethanol at a concentration of 2 mM. The stock solutions were filter-sterilized (0.2 µm filter), protected from light and directly used at a final concentration of 5- 15 µM. NAC was dissolved in PBS and used at a final concentration of 6 mM (52). CORM-2, and CORM-2 control were both dissolved in DMSO, and diluted 1000x in work solution to 50 µM. QC15 was produced by Dr. Szarek; Department of Chemistry, Queen's University, Kingston, Ontario, Canada (53, 54), and used at an end concentration of 50 µM. Hydrogen peroxide (H₂O₂) (30%) was purchased from Merck, Hohenbrunn, Germany.

Mice

The Committee for Animal Experiments of the Radboud University Nijmegen approved all procedures involving animals. Mice (HO-2 KO and WT with a mixed C57BL/6_129/Sv background (55)) of 6-12 weeks in age were housed under standard specific pathogen-free housing conditions.

Isolation and culture of ASCs

Adipose-derived mesenchymal stem cells (ASCs) were routinely isolated from WT and HO-2 KO mice as described previously (56). In brief, adipose tissue surrounding the mouse inguinal lymph nodes were isolated and cut up using scalpels, followed by 30 min of incubation at 37 °C with digestion buffer [30 wt/v%, fat/digestion buffer]. Digestion buffer consisted of complete ASC culture media: DMEM/F12 (Gibco, New York, USA) supplemented with 2 % Penicillin/Streptomycin (Pen/Strep) (Invitrogen, Carlsbad, CA, USA), 0.5% Amphotericin B (Invitrogen, Carlsbad, CA, USA), 16 µM Biotin (Sigma Aldrich, St. Louis, USA), 18 µM Panthotenic Acid (Sigma Aldrich, St. Louis, USA), 100 µM Ascorbic Acid (Sigma Aldrich, St. Louis, USA), and 10% Newborn Calf Serum (Sigma Aldrich, St Louis, USA, ref. N4762), with additionally 2 mg/ml collagenase A (Roche, ref. 10103586001) and 2 wt/v % Bovine Serum Albumin (Sigma Aldrich). Digested adipose tissue was filtered over a 25 µm

filter and the filtrate was centrifuged 10 min at 500g. Pellet was resuspended in 1 mL culture media and red blood cells were lysed with 7 mL ammonium chloride solution (Stem Cell technologies, ref. 07850). Next, the cells were counted (Beckman coulter Z2: >4 μm <25 μm) and seeded at a concentration of 8.000 cells/cm² in complete culture media.

Genotypes were confirmed using qPCR showing that HO-2 KO ASCs were in contrast to WT ASCs, negative for HO-2 mRNA expression (data not shown). In order to phenotypically analyze the ASC population we further used a panel of specific ASC markers and exclusion markers expressed on macrophages, endothelial cells, and hematopoietic cells to exclude non-ASCs. Cells (passage 3) isolated from WT and HO-2 KO mice were tested for six different stem cell markers using flow cytometry. The adipose-derived cells were stained with the MSC markers Sca-1, CD44 and CD105 (BD Bioscience, Breda, the Netherlands; Biolegend, San Diego, CA, USA and eBioscience, San Diego, CA, USA, respectively) and exclusion markers CD11b, cKit and CD34 (Biolegend, San Diego, CA, USA; BD Bioscience, Breda, the Netherlands and eBioscience, San Diego, CA, USA, respectively). In addition, we chose a subset of cell markers for Quantitative Reverse-Transcriptase PCR (qPCR), analysis (Table 5.1). ASCs up to passage number 5 were used for the different experiments.

Table 5.1. Primer sequences of mouse ASC cell surface markers and cytoprotective enzymes.

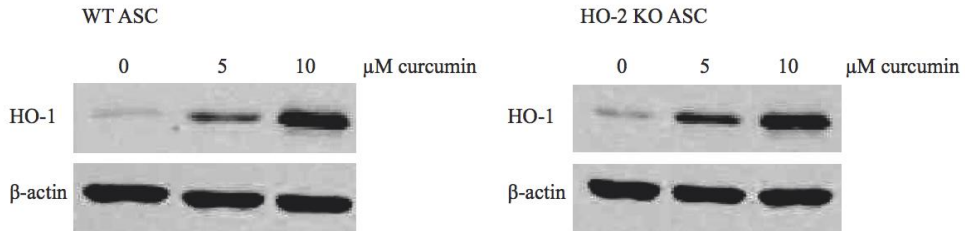
	Sense	Antisense
Cell surface marker		
CD45	5'-GACAGAGTGCAAAGGAGACC-3'	5'-ATCACTGGGTGTAGGTGTTG-3'
Sca1	5'-AGCAGTTATTGTGGATTCTC-3'	5'-TAGTACCCAGGATCTCCATAC-3'
CD105	5'-TTGTACCACAACAGGTCTC-3'	5'-GGTGGTAAACGTCACCTCAC-3'
CD29	5'-AAATTGAGATCAGGAGAACCAC-3'	5'-GGTAATCTTCAGCCCTCTG-3'
CD11b	5'-CTGGTCACAGCCCTAGCC-3'	5'-TTTGATTCTCTTGGAAAGGTC-3'
CD31	5'-CTGGTGCTCTATGCAAGC-3'	5'-GCTGTTGATGGTGAAGGAG-3'
CD34	5'-TGAGTCTGCTGCATCTAAATAAC-3'	5'-CTCATTGGTAGGAAGTATGG-3'
CD117	5'-GCCAGACAGCCACGTCTC-3'	5'-CTGATTGTGCTGGATGGATG-3'
CD106	5'-CGTGAGCATCTACTTTCC-3'	5'-TGTAAGTGGGTAATGTCTGG-3'
CD86	5'-GTCAGTGATCGCAACTTC-3'	5'-TCTTCTAGGTTTCGGGTGAC-3'
Housekeeping gene		
Gapdh	5'-GGCAAATCAACGGCACA-3'	5'-GTTAGTGGGGTCTCGCTCCTG-3'
Cytoprotective enzymes		
HO-1	5'-CAACATTGAGCTGTTTGAGG-3'	5'-TGGTCTTTGTGTTCTCTGTC-3'
HO-2	5'-AAGGAAGGGACCAAGGAAG-3'	5'-AGTGGTGCCAGCTTAATAG-3'

Heme oxygenase protein expression by In-Cell Western

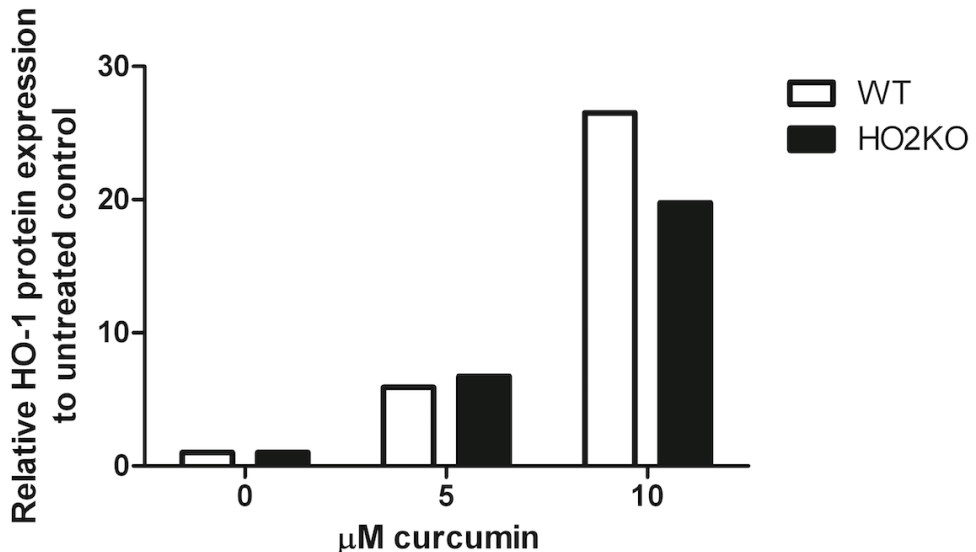
ASCs were cultured in a 96-well plate, fixed with 4% PFA for 15 minutes, and permeabilized with 0.1% Triton X-100 in PBS for 30 minutes. The cells were blocked with 5% ELK (Campina skimmed milk powder) in PBS for 90 minutes. First antibody (rabbit-anti-HO-1 polyclonal antibody; Stressgen Biotechnologies, Victoria, BC, Canada; cat# SPA895: 6,7 $\mu\text{g}/\text{mL}$ in 2.5% ELK and mouse-anti- β -actin monoclonal antibody; Sigma-Aldrich, St. Louis, MO, US, cat# A5441: 5 $\mu\text{g}/\text{mL}$ in 2.5% ELK) treatment was performed overnight at 4 °C. Secondary antibody treatment (goat-anti rabbit Alexa fluor 680; Invitrogen: Molecular Probes, Eugene, US, cat# A21109: 2.5 $\mu\text{g}/\text{mL}$ in 2.5% ELK, and goat-anti-mouse InfraRedDye 800; Rockland, US, cat# 610-132-121: 1.25 $\mu\text{g}/\text{mL}$ in 2.5% ELK) was performed for one hour. The plate was measured using the Odyssey Imager with detection in both 700 nm and 800 nm channels at an intensity of 5 and 7.5, respectively, and was analyzed using Odyssey software (LI-COR Biosciences; version 2.1.12). The amount of HO-1 protein expression was

quantified in relation to the expression of β -actin protein. Since the Western blot shows only one single band following induction with curcumin, the SPA895 antibody specifically recognizes HO-1 (see supplemental figure 5.1). Therefore, we used this antibody for immuno-fluorescent and In-Cell Western techniques.

A).



B).



Supplemental figure 5.1. HO-1 protein expression was induced with [0-10 μ M] curcumin after 24 hour treatment in isolated WT and HO-2 KO ASCs.

(A). WT and HO-2 KO ASCs were treated with curcumin for 24 hours and HO-1 protein expression was analyzed using Western blot, and housekeeping protein β -actin was used to correct for the amount of cells. Experiment was performed once. (B). Quantification of the HO-1 protein expression of the Western blot, corrected for the amount of cells with β -actin and related to untreated control.

Heme oxygenase protein expression by Western blot

ASCs were cultured in a 6-well plate in the presence of 0, 5, and 10 μ M of curcumin for 24 hours. After treatment, cells were harvested using trypsin-EDTA, pelleted by centrifugation and protein was extracted by resuspending the cell pellet for 30 minutes on ice in lysis buffer consisting of 1 mM EDTA, 0.5% triton-X-100, 100 μ M phenylmethylsulfonyl fluoride (PMSF) in ethanol, and 1:100 complete mini protease inhibitor (Roche complete mini: 11 836 153 001). Cell lysates were centrifuged for 2 minutes at 13000 rpm at 4°C and 7.5 μ g total protein was separated by SDS/PAGE using a 10% gel. Subsequently, proteins were blotted

onto a nitrocellulose membrane using the iBlot system (Invitrogen). The membrane was blocked for 30 minutes in 5% ELK in PBS and overnight incubated with first antibodies (rabbit-anti-HO-1 polyclonal antibody; Stressgen Biotechnologies, Victoria, BC, Canada; cat# SPA895: 1:5000 and mouse-anti- β -actin monoclonal antibody; Sigma-Aldrich, St. Louis, MO, US, cat# A5441: 1:100000) in 2.5% ELK containing 0.1% Tween-20. Afterwards, the membrane was briefly washed three times with PBS and twice with PBS containing 0.1% Tween-20 for 10 minutes. The secondary antibodies (goat-anti rabbit Alexa fluor 680; Invitrogen: Molecular Probes, Eugene, US, cat# A21109: 1:10000, and goat-anti-mouse InfraRedDye 800; Rockland, US, cat# 610-132-121: 1:10000) dissolved in 2.5% ELK containing 0.1% Tween-20 and 0.01% SDS were incubated for 45 minutes at room temperature. After thorough washing, the membrane was measured using the Odyssey Imager with detection in both 700 nm and 800 nm channels at an intensity of 3.5 and 7.5, respectively. The intensity of the bands of the Western blot was analyzed using Odyssey software (LI-COR Biosciences; version 2.1.12). The amount of HO-1 protein expression was quantified in relation to the expression of β -actin protein.

Heme oxygenase protein expression by immuno-fluorescent staining

HO-1 protein expression was also evaluated by immuno-fluorescent staining of ASCs treated with curcumin on plastic chamberslides (Nunc, Lab-Tek: permanox 8-well chamberslides: Thermo scientific, Rochester, NY, US). In the chambers, cells were fixated with 4% PFA for 15 minutes, permeabilized with 0.5% Triton X-100 in PBS for 20 minutes, and washed with 0.05% Tween in PBS (PBS-T). Next, the cells were incubated with blocking buffer consisting of 2% bovine serum albumin, 2% normal goat serum, 0.1% Triton X-100, 0.05% Tween, and 100 mM glycine in PBS for 30 minutes. First antibody (Rb-a-HO-1; Stressgen Biotechnologies, Victoria, BC, Canada; CAT#SPA895) was diluted 1:600 in blocking buffer without glycine and incubated on cells for 60 minutes. After washing with PBS-T, cells were incubated with secondary antibody goat-anti-rabbit alexa 594 (Life Technologies, cat# A-11037 diluted 1:200 in blocking buffer without glycine) for 60 minutes. Next, the cells were washed with PBS-T, followed by washing with PBS, and nuclei were stained with DAPI for 10 minutes. Finally, cells were washed with PBS, 1:1 PBS:MQ, and MQ and sealed with DABCO. The Zeiss Imager Z1 microscope was used to make fluorescent pictures of the cells using Axiovision software version 4.8.

mRNA isolation and Quantitative-Reverse-Transcriptase-PCR

Cells were lysed and homogenized in TRIzol (Invitrogen) and RNA was further extracted with the RNeasy mini kit (Qiagen, Venlo, The Netherlands). DNase treatment (Qiagen: RNase-Free DNase Set) was performed between the first washing steps with RW1 buffer. RNA concentration was determined using the nanodrop 2000 spectrophotometer (Thermo Scientific). For the reverse transcriptase treatment 1 μ g sample RNA together with total RT mix (iScript cDNA Synthesis kit from Bio-Rad Laboratories) in a total volume of 20 μ L was incubated for 5 minutes at 25 °C, 30 minutes at 42 °C and 5 minutes at 85 °C. Hereafter the cDNA was diluted 10x and used for Quantitative Reverse-Transcriptase PCR (qPCR), using CFX96 Real-Time System (Bio-Rad Laboratories). The reaction was performed in 25 μ L containing 5 μ L cDNA, 0.6 μ M primers, 12.5 μ L iQ SYBR Green Supermix (Bio-Rad Laboratories). After incubation of 3 minutes, amplification was carried out for 40 cycles of 15 s at 95°C and 30 s at 60°C. The melting temperature of the products was defined to

indicate amplification specificity. All values were normalized to the housekeeping gene Gapdh. Data of the ASC characterization were presented as $2^{-\Delta Ct}$. HO-1 mRNA expression was evaluated after treatment with curcumin for 24 hours and related to untreated control ($2^{-\Delta\Delta Ct}$). All used primers are summarized in table 5.1.

Determination of cell viability

Cells were seeded into a 96 wells plate at 2000 cells/ well and after overnight culturing of the cells were pre-treated with HO-activity modulators or HO-system related molecules for 24 hours, followed by a co-treatment with 350 μ M hydrogen peroxide (selected from a 100-500 μ M H₂O₂ dose range) for 24 hours in 100 μ L media. Hereafter, media was removed and replaced by media containing 10% AlamarBlue® Cell Viability Reagent (Invitrogen) and further incubated at 37°C for three hours. The oxidized form of this Alamar blue (resazurin) enters the cytosol where it is converted into the reduced form (resorufin) by mitochondrial enzyme activity. The amount of resorufin is directly proportional to the amount of proliferating viable cells and was measured fluorescently at 530/ 590 nm using the Universal Microplate reader FL600 (Bio-TEK instruments Inc., Winooski, VT, USA). Viability was calculated as percent of the difference in reduction of Alamar blue in treated versus non-treated cells, corrected for background signal of Alamar blue: Viability = (Ex-Eblanc)/ (Ec-Eblanc)*100; where Ex = extinction treatment, Ec = Extinction untreated control, and Eblanc= extinction Alamar blue background.

Detection of Apoptosis by Flowcytometric Analysis

Flowcytometry was used to study the effects of H₂O₂ on apoptotic signals, by double staining with fluorescein isothiocyanate (FITC) labeled – Annexin V and propidium iodide (PI). Untreated and H₂O₂-treated ASCs were resuspended in binding buffer and stained with Annexin V-FITC and PI for 15 minutes at RT in the dark, according to manufacturer's protocol (BioVision Inc, ITK Diagnostics, Uithoorn, the Netherlands). Cells treated with 4% paraformaldehyde containing 0.1% saponine and stained with Annexin V and PI were used as positive control. Detection of Annexin V-FITC and PI binding was performed by a FACSCalibur (Becton Dickinson Biosciences, San Jose, CA, USA) using channels FL-1 (Annexin V-FITC) and FL-3 (PI). Viable cells (Annexin V -/ PI-), early apoptotic cells (Annexin V+/ PI-), late apoptotic cells (Annexin V+/ PI+), and necrotic cells (Annexin V-/ PI+) were quantified as a percentage of the gated population, using FlowJO software (version 7.6.5 for windows, Tree Star, Inc.).

Determination of cell amount

The influence of pre- and co-treatment with HO-modulators and effector molecules on cell loss after H₂O₂-treatment was determined using PicoGreen dsDNA Quantification reagent (Molecular Probes Inc, Eugene, OR, USA). The amount of double stranded DNA can be quantified using this assay and this correlates to the amount of cells. After measuring the Alamar plate, the media was removed and the plate was washed twice with PBS. Cells were lysated by adding 0.1% Triton X-100 and frozen (-80°C) and thawed (37°C) for three consecutive times. The assay was performed according to the protocol of the manufacturer. The fluorescent signal was measured in a FL600 Microplate Fluorescence Reader (Bio-Tek Instruments Inc., Winooski, VT, USA) at excitation 485 nm, emission 520 nm. DNA standards

ranging from 0 to 2000 ng DNA /mL were used. The total amount of DNA after treatment was calculated using the standard curve.

Statistical analysis

Data were analyzed using GraphPad Prism 5.01 software (San Diego, CA, US). Outliers were tested using the Grubbs' test. In Alamar blue experiments, one outlier was detected in a control untreated group of WT ASCs in two experiments. In picogreen experiments, one outlier was found in a control treated group of WT ASCs and one outlier was found in NAC treated group of HO-2 KO ASCs, in single experiments. Data was analyzed by one- or two way analysis of variance (ANOVA) with Bonferroni's multiple comparison post test. One-way ANOVA was used in survival studies and picogreen studies and two-way ANOVA was used in other experiments. Results were considered significant different when $p < 0.05$ (* $p < 0.05$, ** $p < 0.01$, and *** $p < 0.001$).

Results and Discussion

Isolation and characterization of adipose-derived MSCs (ASCs)

ASCs were isolated from mouse (WT and HO-2 KO) adipose tissue around the inguinal lymph nodes and cultured in defined media as described in the materials and methods section. The cells adhered to plastic and had, as expected for ASCs, a fibroblast-like morphology. Passage three of the isolated cell populations were characterized for the expression of mesenchymal, endothelial, and hematopoietic markers by immunophenotyping (Figure 5.1A) and qPCR (Figure 5.1B). Surface antigen expression of the isolated cells, using flow cytometry, was consistent with literature data and our previous results (56). The cells expressed ASC surface markers Sca-1, CD44, and CD105 and were negative for the exclusion markers CD117 (hematopoietic stem cells), CD11b (macrophages) (Figure 5.1A), and showed low expression of CD34 (endothelial/ hematopoietic progenitor cells)(16, 57-62). No significant differences in ASC marker expression was detected between WT and HO-2 KO ASCs. These phenotypic observations at the protein level were further corroborated at the mRNA level using common MSC markers (Figure 5.1B). The isolated cells expressed high mRNA levels of ASC markers Sca-1, CD29 (16, 58-60, 62), CD105, and CD106 (16, 58), whereas cells were negative for exclusion markers CD11b, CD31 (16, 57-61), CD34, hematopoietic marker CD45 (16, 57-62), antigen-presenting cell marker CD86 (62), and CD117 showing low levels of mRNA expression, compared to housekeeping gene GAPDH. No significant difference in marker expression was found between WT and HO-2 KO ASCs. We conclude that the isolated cells are ASCs, since the marker expression profile corresponded well with literature data of earlier reported isolated murine ASCs.

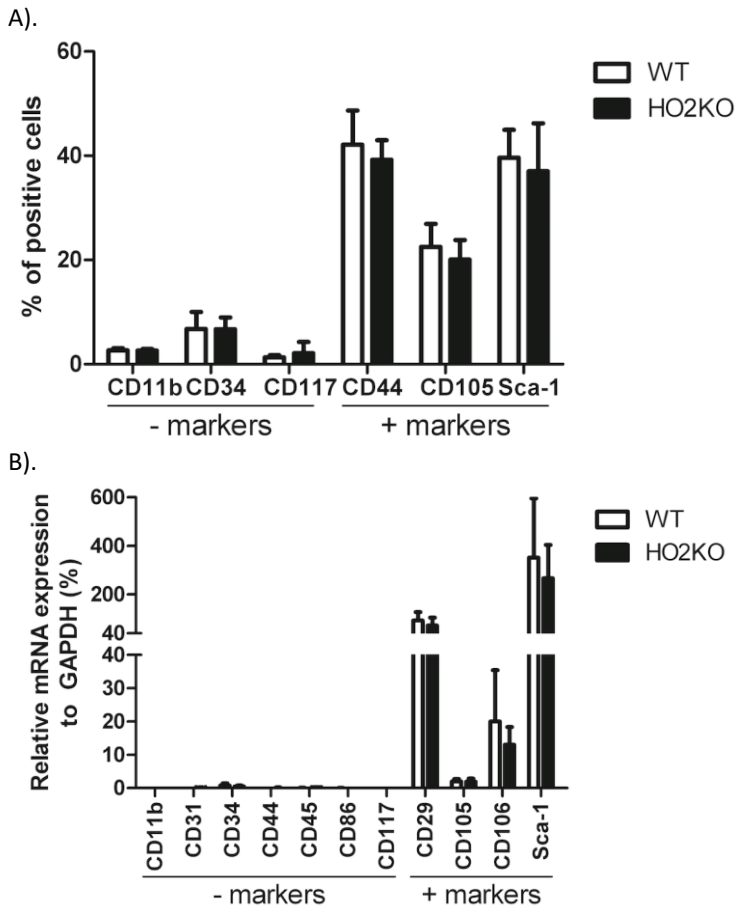


Figure 5.1. Phenotypic analysis of isolated WT and HO-2 KO ASCs.

(A). Percentage of positive cells for ASC exclusion markers (negative) and ASC cell surface markers (positive) of isolated WT and HO-2 KO ASCs, measured using flow cytometry. **(B).** mRNA levels of negative and positive ASC markers of isolated WT and HO-2 KO ASCs, analyzed by qPCR and presented as $2^{-\Delta Ct}$. No significant differences were observed between in the expression of selected markers between WT and HO-2 KO ASCs using both flow cytometry and qPCR. Data represent mean \pm SD of three independent experiments.

H₂O₂ induces cell death in ASCs in a dose-dependent manner independently from HO-2 expression

ASCs were exposed to increasing concentrations of H₂O₂ (0 - 500 μ M) to investigate the effect of oxidative stress on ASC survival. H₂O₂ is a strong oxidant that can cause cell death and apoptosis. Compared to other ROS, H₂O₂ is a relatively long-lived molecule commonly used in models of oxidative stress (63). Exposing cells to H₂O₂ results in deleterious effects of hydroxyl and peroxy radicals on membrane lipids and proteins, resulting in loss of mitochondrial membrane potential, mitochondrial dysfunction, and eventually apoptosis (64, 65).

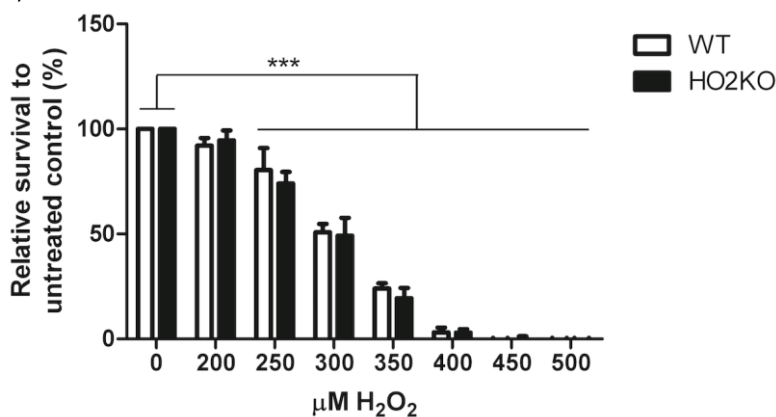
ASCs were exposed for 24 hours to increasing concentrations of H₂O₂ and cell viability was assessed using the Alamar blue assay. This assay is based on the ability of

metabolically active cells to convert the Alamar blue reagent into a fluorescent signal, which is directly proportional to the cellular viability. Damaged and non-viable cells have lower innate metabolic activity, and generate thus a proportionally lower signal.

ASC viability decreased gradually after exposure to increasing concentrations of 200-500 μM H_2O_2 for 24 hours (Figure 5.2A). Exposure to doses of 250 μM H_2O_2 and higher had a significant cytotoxic effect for both WT and HO-2 KO ASCs compared to controls (all $p < 0.001$). No ASCs survived at concentrations of 450 μM H_2O_2 and higher. In parallel, the amount of cells after 24 hours treatment with H_2O_2 were analyzed using the picogreen assay. This assay quantifies the amount of double stranded DNA and is directly proportional to the amount of cells. These results were similar and corroborated our findings with the Alamar blue assay. The amount of cells decreased significantly at H_2O_2 concentrations of 250 μM and higher in a dose-dependent fashion for both WT and HO-2 KO ASCs (Figure 5.2B). After treatment with 350 μM H_2O_2 24% \pm 2.5% of WT and 19.5% \pm 4.9% of HO-2 KO ASCs survived. At this concentration, we found increased apoptotic signals in WT and HO-2 KO ASCs as measured by the increased levels of phosphatidylserine flip-flops and membrane disruption, using AnnexinV-FITC and propidium iodide (PI) staining (see Supplemental figure 5.2). Surprisingly, no significant difference could be observed between WT and HO-2 KO ASCs in sensitivity towards H_2O_2 -induced cell death at any measured concentration. This suggests that HO-2 does not protect against H_2O_2 -induced ASC death. Probably, the HO-2-activity level in naïve ASCs is too low. Although HO-2 has been demonstrated to protect against a wide range of oxidative insults in diverse cells, the role of HO-2 may be cell and stressor dependent (43, 44, 46, 49). HO-2 can either protect or augment apoptosis (45, 50). In this setting, ASCs were not dependent on HO-2 for their protection against H_2O_2 -induced cell death.

Based on the above data, 350 μM H_2O_2 was chosen as cytotoxic dose since it offers an analytical window to assess whether the HO-system could mediate protection against oxidative stress-induced cell death in ASCs.

A).



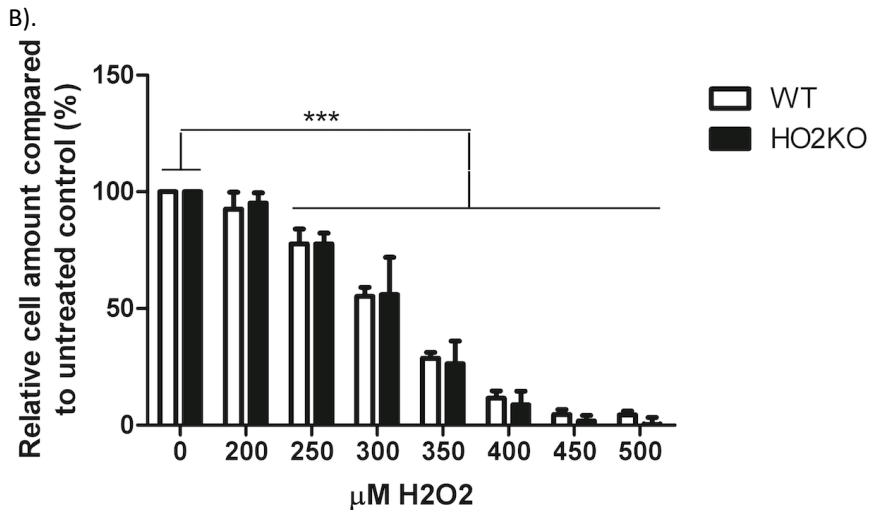
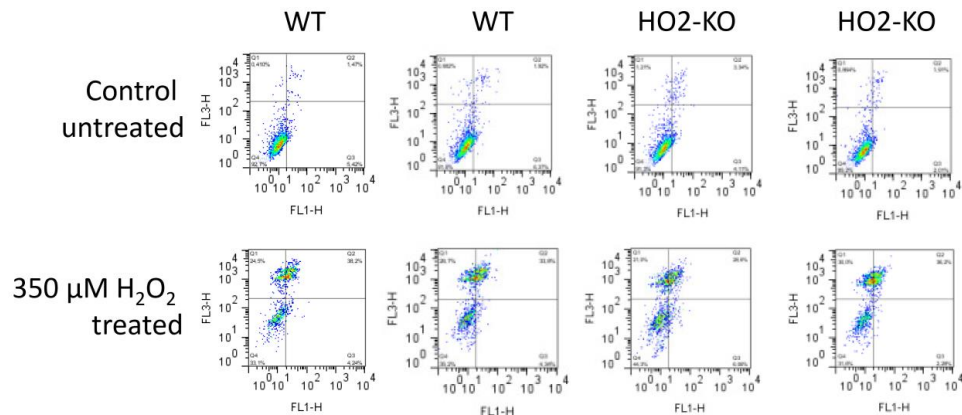


Figure 5.2. Survival and cell amount of isolated WT and HO-2 KO ASCs after exposure to increasing doses of H₂O₂ [0-500 μM] for 24 hours.

(A) WT and HO-2 KO ASC survival and (B) amount of ASCs after H₂O₂-treatment were analyzed using the Alamar blue assay and picogreen assay, respectively.

Doses of 250 μM H₂O₂ and higher resulted in a significant decreased survival and, subsequently, lower cell amounts (all p<0.001) compared to untreated control. No significant differences were observed between WT and HO-2 KO ASCs at any concentration. A dose of 350 μM H₂O₂ was chosen in further experiments to induce ASC death.

Data represent mean ± SD of three independent experiments with four samples per condition.



Supplemental figure 5.2. Apoptosis of WT and HO-2 KO ASCs after treatment with 350 μM H₂O₂ or control for 24 hours using AnnexinV-FITC (FL-1) and PI (FL-3) labeling. It was found that both WT and HO-2 KO ASCs showed similar induction of apoptosis following H₂O₂ treatment.

Can curcumin induce HO-1 expression in ASCs?

Next, we studied if we could induce the expression of HO-1 in ASCs to provide protection against oxidative damage. Therefore, ASCs were treated with increasing curcumin concentrations for 24 hours and HO-1 gene transcription was subsequently assessed by qPCR (Figure 5.3A).

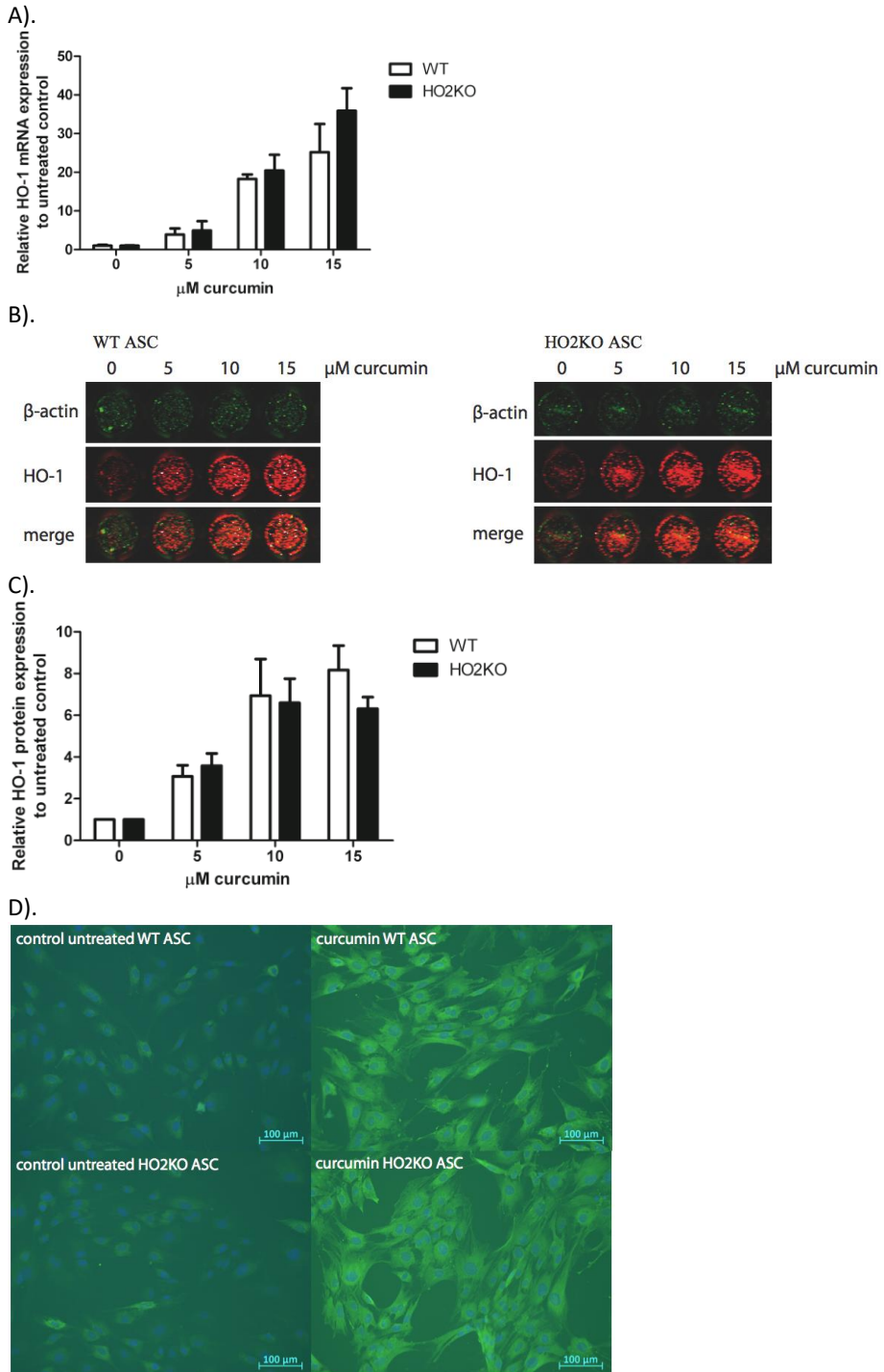


Figure 5.3. HO-1 mRNA and protein expression was induced with increasing doses of curcumin [0 - 25 μM] for 24 hours in isolated WT and HO-2 KO ASCs.

(A). WT and HO-2 KO ASCs were treated with curcumin for 24 hours and HO-1 mRNA expression was evaluated with QPCR, corrected for the housekeeping gene GAPDH and normalized to untreated control. HO-1 mRNA expression was significantly ($p < 0.05$) induced at every concentration in comparison to untreated control. Data represent mean \pm SD of three independent experiments. No significant differences between WT and HO-2 KO ASCs were found. (B). WT and HO-2 KO ASCs were treated with curcumin for 24 hours and HO-1 protein expression was evaluated with In-Cell Western (green: β -actin, and red: HO-1). (C). Quantification of the In-Cell Western signal, corrected for the amount of cells with β -actin and related to untreated control. HO-1 protein expression was significantly ($p < 0.05$) induced at every concentration in comparison to untreated control. Data represent mean \pm SD of three independent experiments. Four samples were analyzed per condition. No significant differences between WT and HO-2 KO ASCs were found. (D). WT and HO-2 KO ASCs were untreated or treated with 10 μ M curcumin for 24 hours and HO-1 protein expression was evaluated using immuno-fluorescent staining of chamberslides (green is HO-1, blue is nuclear staining with DAPI). Representative of three independent experiments.

Exposure to curcumin for 24 hours induced HO-1 mRNA levels dose-dependently in WT and HO-2 KO ASCs compared to untreated control. No significant differences in HO-1 induction were found between the two genotypes.

Next, the HO-1 protein expression after treatment with different concentrations of curcumin was assessed using In-Cell Western (Figure 5.3B). HO-1 protein expression was quantified in relation to β -actin protein expression (Figure 5.3C). We observed that HO-1 protein expression was significantly and dose-dependently induced after 24 hours treatment with increasing doses of curcumin compared to untreated control in both WT and HO-2 KO ASCs. HO-1 protein expression after induction with curcumin was not significantly different between WT and HO-2 KO ASCs at any of the used concentrations. Furthermore, a plateau in expression was reached as we did not detect any difference in HO-1 expression levels at concentrations of 10 and 15 μ M. For our next experiments we used 10 μ M curcumin, since high concentrations of curcumin (25 μ M) may cause cell death *in vitro* (54). Treatment with 10 μ M curcumin did not result in cytotoxic effects and induced HO-1 mRNA expression 20-fold and HO-1 protein levels roughly 7-fold compared to untreated cells.

The HO-1 protein induction in WT and HO-2 KO ASCs was also measured using immuno-fluorescent staining (Figure 5.3D). In accordance with the mRNA and In-Cell Western expression data we demonstrated that HO-1 protein expression was highly upregulated in ASCs from both genotypes after treatment with 10 μ M curcumin in comparison with untreated control.

There were no significant differences observed in HO-1 induction at either mRNA or protein level between WT and HO-2 KO ASCs after treatment with 10 μ M curcumin. We demonstrated that curcumin acts as a potent inducer of HO-1 in both WT and HO-2 KO ASCs after treatment for 24 hours.

HO-1 inducer curcumin protects against H₂O₂-mediated ASC death in a HO-2 independent manner

Pre-conditioning of MSCs with cytoprotective factors can improve MSC survival against several injurious stressors *in vitro*, such as serum-free conditions, hypoxia and oxidative stress (14, 66). It has been shown that pre-conditioning of MSCs with melatonin (65), NO-donor SNAP (67), or overexpression of transcription factor nuclear factor-erythroid 2-related factor 2 (nrf2) (18) can prevent MSC death caused by H₂O₂. Interestingly, these preconditioning factors are also potent inducers of HO-1 (68-70). Since HO-1 can protect

against oxidative stress in diverse models (17, 34), we investigated if HO-1 induction can also protect against oxidative stress-induced ASC death. Since HO-1 transfection is difficult to introduce safely into the clinic, we investigated the use of the safe pharmaceutical HO-1 inducer curcumin. Curcumin is a natural product that is already used in daily life as a spice in the Indian kitchen (71, 72), acts as an anti-oxidant (73), and provides protection against a wide variety of diseases and conditions (74-76). Moreover, a protective role for polyphenols, including curcumin, on BM-derived MSC survival against oxidative stress was recently demonstrated (21). However, any relation to the HO-system was not investigated, and the survival was thought to relate to the induction of ROS-reducing enzymes glutathione peroxidase (GPX) and catalase (21).

In order to investigate the role of curcumin on H₂O₂-induced cell death in more detail, ASCs were pre-treated for 24 hours with 10 μM of curcumin followed by co-treatment with 350 μM H₂O₂ for 24 hours after which the cell viability was assessed using the Alamar blue assay. Pre-conditioning with curcumin significantly improved ASC survival during oxidative stress (Figure 5.4). Pre-treatment with 10 μM curcumin increased ASC survival 2.7 and 3.6 fold in WT (Figure 5.4A) and HO-2 KO ASCs (Figure 5.4B), respectively, compared to cells exposed to solely 350 μM H₂O₂. This is further supported by picogreen data that showed significant more WT and HO-2 KO ASCs when pre-treated with curcumin (Figure 5.5). Vehicle control ethanol did not increase ASC survival and cell amount compared to H₂O₂-treated control cells. Since we found that curcumin acts as a strong inducer of HO-1 this suggests a possible role for HO-1 in ASC survival from oxidative stress.

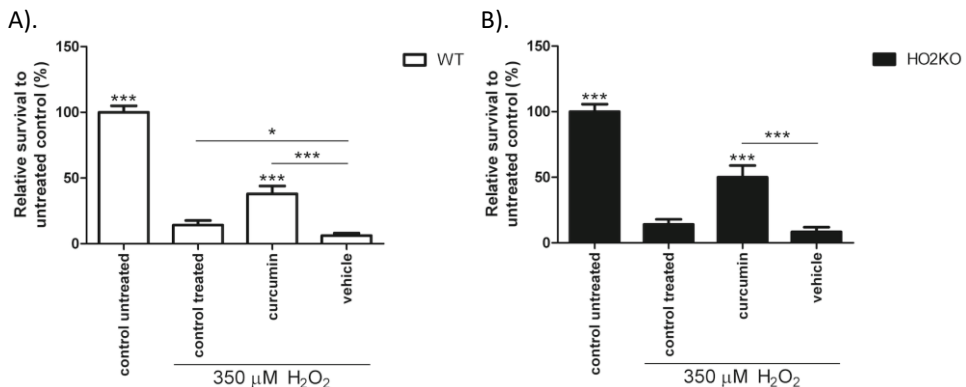


Figure 5.4. Curcumin treatment rescues WT and HO-2 KO ASCs against H₂O₂-induced cell death.

(A) WT ASC and **(B)** HO-2 KO ASC survival after 24 hour pre-treatment with curcumin, vehicle control, or untreated (control) and 24 hour co-treatment together with 350 μM H₂O₂ following an Alamar blue assay and fluorimetric quantification, related to untreated control.

Vehicle consisted of 0.5% ethanol (curcumin solvent) in culture media. * is significant different from H₂O₂-treated control. (*p<0.05, ***p<0.001). Data represent a representative of three independent experiments and present mean ± SD. For each condition six samples were analyzed.

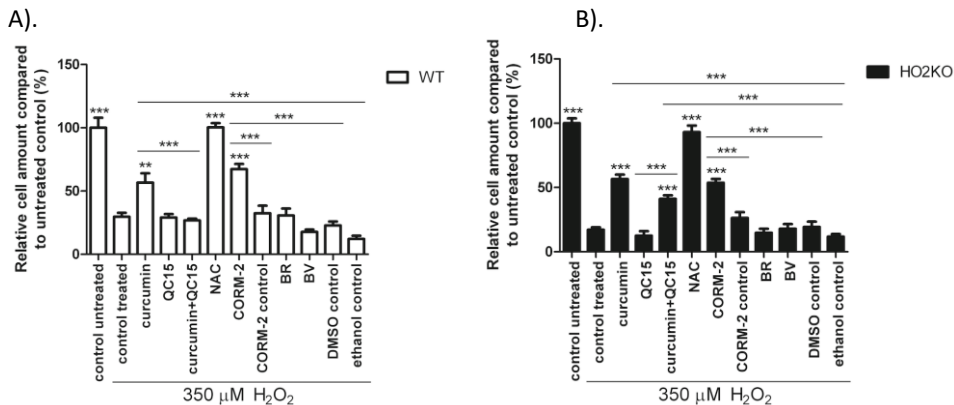


Figure 5.5. Cell amount of WT and HO-2 KO ASCs after treatment with HO-system related molecules and H₂O₂-induced cell death.

(A) WT ASC and **(B)** HO-2 KO ASC after 24 hour pre-treatment with several substances, and 24 hour co-treatment together with 350 μM H₂O₂ following a picogreen assay and fluorimetric quantification, related to untreated control.

DMSO control represents the vehicle for CORM-2 and CORM-2 control consisted of 0.1% DMSO in culture media. Ethanol control is the vehicle for curcumin and consisted of 0.5% ethanol in culture media. * is significant different from treated control (**p<0.01, and ***p<0.001). Experiments are performed in triplicate with samples in sextet. Representative graph is shown. Data are presented as mean ± SD.

NAC: N-acetylcysteine; CORM-2: CO-releasing molecule-2; BR: Bilirubin; BV: Biliverdin.

Interestingly, transient overexpression of the human HO-1 gene in BM-derived MSCs has been shown to protect against oxidative stress-induced cell death (17, 34). HO-1 transfected BM-derived MSCs were more resistant to cell death than non-transfected MSCs after exposure to H₂O₂ (34). Survival at 500 μM H₂O₂ for two hours was higher after HO-1 transfection and HO-1 induction could thus protect BM-MSCs to a short exposure of high concentrations H₂O₂. At a lower concentration of H₂O₂ but longer treatment time with H₂O₂ we showed also protection for ASC following curcumin exposure, suggesting that HO-1 induction plays a role. We further investigated the downstream mechanism of protection after pre-conditioning with the clinically more relevant curcumin towards an exposure of H₂O₂ for 24 hours.

In summary, curcumin provides similar protection against H₂O₂-induced cell death both in WT and HO-2 KO ASCs. A possible involvement of HO-activity will be further evaluated.

Is rescue from H₂O₂-induced ASC death by curcumin mediated by HO-activity?

We have shown that curcumin can prevent from ASC death caused by oxidative stress. Since we demonstrated that curcumin induces HO-1 expression in ASCs, we next examined whether the protective mechanism of curcumin is HO-dependent using a specific HO-activity inhibitor. We used the synthetic isozyme-selective non-porphyrin HO-activity inhibitor QC-15 to test its effect on ASC survival. QC-15 is an imidazole-dioxolane compound that binds to the distal side of the heme-binding place in the HO protein and is a highly selective HO-1 activity inhibitor and has less potency to inhibit HO-2 activity (52, 77-79).

Specifically, we investigated whether HO-1 activity inhibition would reduce ASC survival, and in addition, if the protecting effect of curcumin could be attenuated by co-

treatment with QC-15. ASCs were therefore pre-incubated for 24 hours with HO-activity modulators followed by a co-treatment with 350 μM H_2O_2 for 24 hours, after which the ASC-survival was assessed using the Alamar blue assay.

Surprisingly, we found that co-exposure of 50 μM QC15 together with H_2O_2 did not influence cell survival when compared to cells treated with only H_2O_2 in both WT and HO-2 KO ASCs (Figure 5.6). This suggests that the basal levels of both HO-1 and HO-2 are not sufficient for protection. However, the increased survival of ASCs after 10 μM curcumin treatment, and subsequent induced HO-1 expression, against H_2O_2 was completely abrogated ($p < 0.001$) following co-treatment with 50 μM QC15 in both WT as HO-2 KO ASCs. These results clearly demonstrate the protective potential of pre-induction of HO-1-activity in preventing oxidative stress-induced ASC death. Surprisingly, this is likely independent from HO-2, since no differences in survival were found between WT and HO-2 KO ASCs. In addition, picogreen data also showed a decline in cell amount after co-treating curcumin with QC15 (Figure 5.5). However, this decrease in cell amount was not always significant for both WT and HO-2 KO ASCs in replicate experiments. Similar protective effects of HO-activity from injurious insults have also been demonstrated in other cell lines (80, 81). Induction of HO-activity by flavonoid baicalcin and HO-1 transfection protected raw 264.7 macrophages and vascular smooth muscle cells against H_2O_2 -induced cell death. Also here, inhibition of HO-activity attenuated this protection (80, 81).

Thus, curcumin-induced protection against H_2O_2 -induced ASC death acts via induction of HO-1, whereas inhibition of HO-activity abrogates this protective effect.

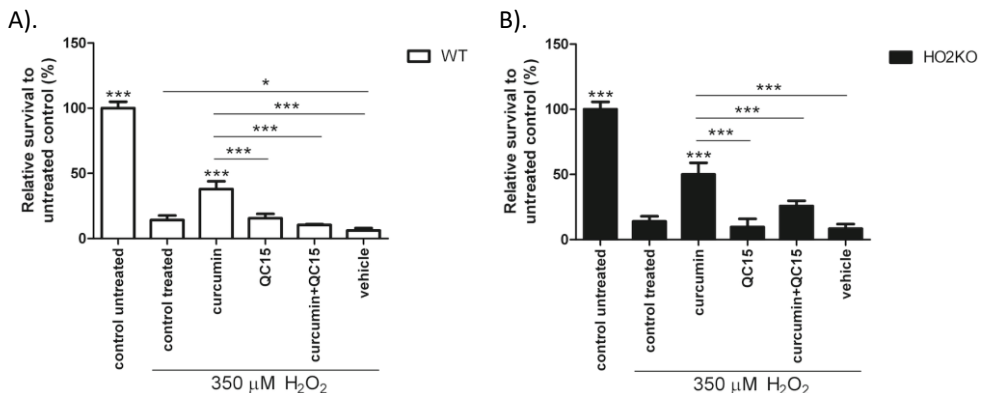


Figure 5.6. Inhibition of HO-activity abrogated the protective effect of curcumin against H_2O_2 -induced cell death in isolated WT and HO-2 KO ASCs.

(A) WT ASC and (B) HO-2 KO ASC survival after 24 hours pre-treatment with HO-modulators or untreated (control) and 24 hours co-treatment together with 350 μM H_2O_2 as measured by Alamar blue assay and fluorimetric quantification, related to untreated control.

Vehicle consisted of 0.5% ethanol (curcumin solvent) in culture media. * is significant different from treated control. (* $p < 0.05$, and *** $p < 0.001$).

Data represent a representative of three independent experiments and present mean \pm SD. For each condition six samples were analyzed.

Do anti-oxidants bilirubin, biliverdin, and NAC rescue from H_2O_2 -induced ASC death?

Since HO-activity protects against H_2O_2 -mediated cell death, we investigated whether the anti-oxidative properties of HO-effector molecules BR and BV, or anti-oxidant N-acetyl

cysteine (NAC) could mediate a protective effect. It has previously been reported that NAC; a precursor of glutathione (GSH) synthesis, and BR and BV can protect cells from ROS-induced cell death (54, 82, 83). GSH serves as electron donor for glutathione peroxidase to catalyze the reduction of H_2O_2 into H_2O , and is together with catalase the only defense available to metabolize H_2O_2 (84, 85). GSH and BR are both prominent endogenous anti-oxidant molecules, protecting against oxidative stress on a complementary basis and have a distinct antioxidant mechanism (86). Therefore, we investigated the possible contribution of the different anti-oxidants NAC, BR, and BV on ASC survival. Pre-treatment for 24 hours with 10 μM BR, 10 μM BV, and 6 mM NAC and co-exposure for another 24 hours with 350 μM H_2O_2 was performed to investigate the effects on ASC survival. This was assessed using the Alamar blue assay. Anti-oxidant NAC significantly increased cell survival compared to H_2O_2 -treated control in WT and HO-2 KO ASCs 6.3- and 7.1- fold, respectively (Figure 5.7). NAC may also influence mitochondrial biogenesis (87), and thus might cause bias in the Alamar blue assay, since this assay is a measure of mitochondrial activity. However, NAC significantly increased the cell amount compared to H_2O_2 -treated control as confirmed by the picogreen assay, suggesting that NAC does not only promote mitochondrial biogenesis but also cell survival (Figure 5.5). Since NAC can interfere with several cell viability test methods (88), we corroborated that cell-free NAC containing media did not influence the Alamar blue signal (data not shown). Increasing GSH formation results in a more reduced intracellular environment, and promotes cell proliferation and survival (89). NAC has been demonstrated to promote the proliferation of different cell types, including adipose derived stem cells and BM stromal cells (90, 91). Surprisingly, the anti-oxidants BR and BV did not improve ASC survival in both WT and HO-2 KO ASCs (Fig. 6.5 and 6.7). Treatment with BR and BV in the absence of H_2O_2 did not result in increased cell death, as measured by the Alamar blue assay (data not shown). The observed differences between NAC and BR/BV may be related to the different targets that these anti-oxidants have (86). GSH is hydrophilic and protects mainly water-soluble proteins in the cytosol, while BR and BV are more lipophilic and protect against lipid peroxidation of cell membranes (86). The microenvironment largely determines which mechanism is needed to sustain redox homeostasis (89). H_2O_2 can easily penetrate the cell membrane, and form hydroxyl radicals with intracellular metal ions. Treatment with H_2O_2 results in cytosolic release of cytochrome c as well as activating caspase-9 and caspase-3 and works through the intrinsic/mitochondrial apoptotic pathway in several cell types, including MSCs (92-97). And hence, H_2O_2 scavenging is likely more dependent on GSH, rather than BR and BV.

Our results show that H_2O_2 -induced cytotoxicity can be prevented by NAC, but not BR and BV. This suggests that HO-1-mediated ASC survival following H_2O_2 -treatment is independent from HO-effector molecules BR and BV and independent of intrinsic HO-2 expression.

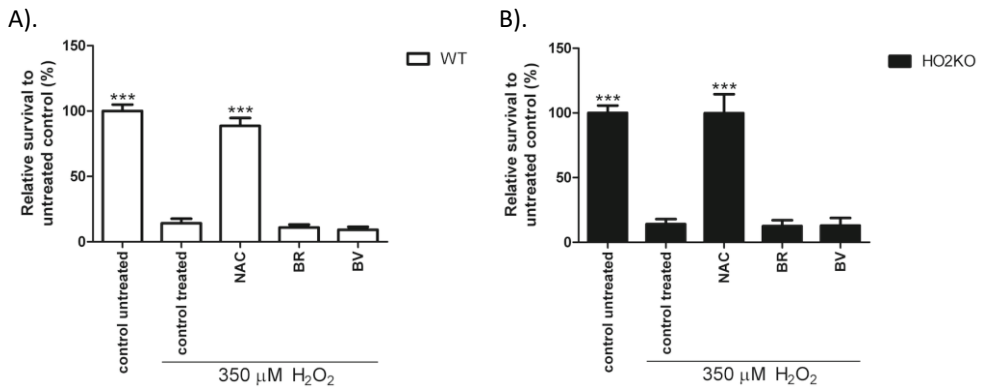


Figure 5.7. Survival of WT and HO-2 KO ASC against H₂O₂-induced cell death after treatment with anti-oxidants. (A) WT ASC and (B) HO-2 KO ASC survival after 24 hour pre-treatment with anti-oxidant NAC or HO-effector molecules BR and BV, and 24 hour co-treatment together with 350 μM H₂O₂ following an Alamar blue assay and fluorimetric quantification, related to untreated control.

* is significant different from treated control. (***)*p*<0.001). Data represent a representative of three independent experiments and present mean ± SD. For each condition six samples were analyzed.

NAC: N-acetylcysteine; BR: Bilirubin; BV: Biliverdin.

Does HO-effector molecule carbon monoxide influence H₂O₂-induced ASC death?

Since we have shown that HO-activity is responsible for ASC survival, and is independent from the effector molecules BR and BV, we next investigated the effects of the HO-effector molecule CO. The HO-effector molecules also provide protection through different mechanisms; BR and BV are anti-oxidants, whereas CO is thought to work on regulating downstream signaling pathways. Furthermore, CO may produce mitochondrial ROS initiating intracellular protective signaling pathways and maintain cells in homeostasis (98-100).

In order to determine whether CO could mediate the HO-induced protection against H₂O₂-induced ASC death, we treated the cells with CO releasing molecules-2 (CORM-2), and found that this resulted in significantly higher ASC survival in WT and HO-2 KO ASCs compared to H₂O₂-exposed ASCs (Figure 5.8). The absence of HO-2 expression in the ASCs in our experimental setup did not have any significant influence on its survival against H₂O₂-induced cell death. In addition, CORM-2 control and solvent control (DMSO) treated cells showed no protection and survival were comparable to cells treated with H₂O₂. Thus, the HO-mediated protection mechanism is likely dependent on the effects of CO-release. This was partly confirmed by our picogreen data (Figure 5.5). Here, we found that more cells were present after CORM-2 treatment in WT ASCs (*p*<0.001) exposed to H₂O₂. However, in HO-2 KO ASCs this protective effect of CORM-2 on cell amount was not always significant in replicate experiments. A decrease in viability may therefore not always mean a decrease in cell amount. In line with our results, Lin *et al.* also demonstrated that CO, but not BR and BV administration inhibited H₂O₂-induced cytotoxicity in macrophages (80), suggesting that CO is responsible for the protective effect caused by HO-1 overexpression in both macrophages and ASCs. Furthermore, the ruthenium-based CORM-2 and CORM-2 control have been demonstrated to be potent inducers of HO-1, which could have further boosted the protective effects of CORM-2 via a positive feedback loop (101, 102). Preliminary experiments show indeed induction of HO-1 following exposure to CORM-2 and to a lower

extent for CORM-2 control. This positive feedback between HO-1 and CO (and nrf2) has previously been demonstrated in hepatocytes (103) and vascular endothelium cells (104).

The down-stream protective effects of CO can be mediated by several protective signaling pathways. Pre-treatment with CORM-2 increases mitochondrial ROS signaling, which leads to pre-conditioning of the cells, making them more resistant to secondary stresses with H₂O₂ (105, 106). In addition, CO may activate diverse other downstream signaling pathways, including nrf2, guanylate cyclase, p38 mitogen-activated protein kinase (MAPK), PI3K-Akt, and iNOS (104, 106, 107). Finally, CO can reduce the production of ROS in cells treated with H₂O₂, probably by preventing the formation of hydroxyl radicals by binding to ionized iron (108).

More research is warranted to unravel the exact mechanism by which CORM-2 exerts its protective effects. These results suggest that CO is responsible for the observed HO-mediated ASC survival from oxidative stress.

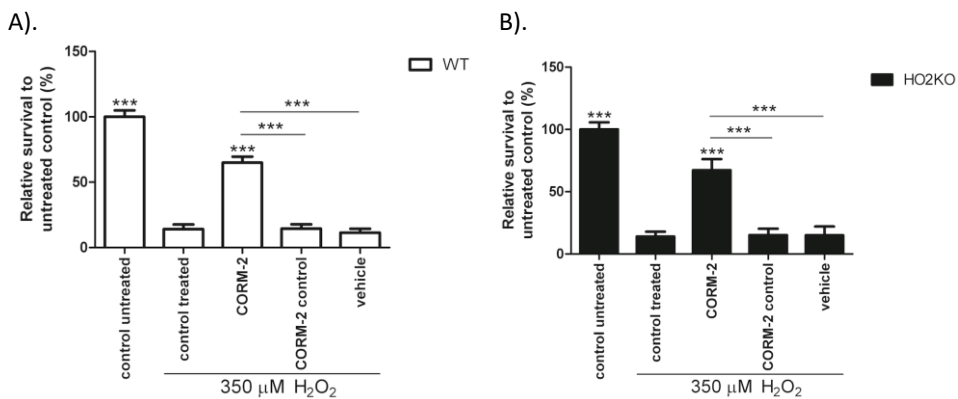


Figure 5.8. CORM-2 increases WT and HO-2 KO ASC survival against H₂O₂-induced cell death.

(A) WT ASC and **(B)** HO-2 KO ASC survival after 24 hour pre-treatment with CORM-2, or its controls, and 24 hour co-treatment together with 350 μM H₂O₂ following an Alamar blue assay and fluorimetric quantification, related to untreated control.

Vehicle consisted of 0.1% DMSO (CORM-2 and CORM-2 control solvent) in culture media. * is significant different from treated control. (***)p<0.001. Experiments are performed in triplicate with samples in sextet. Representative graph is shown. Data are presented as mean ± SD.

CORM-2: CO-releasing molecule-2.

In summary,

Administering MSCs forms a promising therapy following pathologic tissue injury. However, the poor survival of MSCs following administration limits their therapeutic efficacy. In this study, we demonstrated that exposure of adipose-derived MSCs (ASCs) to oxidative stress results in ASC death and that induction of the HO-system by curcumin can attenuate this. Simultaneous inhibition of HO-activity could abrogate the protective effects of curcumin, demonstrating an essential role for HO-1. We found that also NAC improved ASC survival, whereas BR or BV did not demonstrate a protective effect, and thus suggest differential anti-oxidative protective mechanisms. Since administration of the HO-effector molecule CO also attenuated H₂O₂-induced ASC death, it is likely that CO mediates in part the protective effects of HO-1 induction. All these effects were independent from HO-2 expression, as the results for WT and HO-2 KO ASCs were similar.

Clinical Relevance

Increased levels of ASCs at the site of injury may ameliorate tissue repair by their differentiation capacity and the excretion of paracrine factors into the tissue environment further promoting wound repair (109-112). The clinical relevance of HO-1 induction in MSCs is further supported by *in vivo* models of tissue injury, improving MSC survival and tissue function (33-35, 112-115).

Our results further emphasize on the important role of HO-1 and CO as target for improved ASC survival and therapy in tissue repair. We also show that HO-2 expression is less important in mediating protection against oxidative insults in ASCs.

Conclusions

Survival from H₂O₂-induced apoptosis was similar for WT and HO-2 KO ASCs, suggesting that the HO-2 isoform is not able to provide protection in this specific setting. ASC survival was ameliorated following pre-induction of HO-1 using the cytoprotective flavonoid curcumin. This protection by curcumin was mediated by HO-1 activity since simultaneous inhibition of HO-activity abrogated this curcumin-mediated protection. HO-effector molecules BR/ BV did not provide protection, whereas CO protected against H₂O₂-induced cell death, suggesting involvement of CO in HO-1 mediated protection. HO-1 pre-induction by curcumin or CO exposure could therefore form a novel promising adjuvant strategy to promote stem cell survival during therapy.

References

1. Leung A, Crombleholme TM, Keswani SG. Fetal wound healing: implications for minimal scar formation. *Current opinion in pediatrics*. 2012;24(3):371-8.
2. Meyer M, Muller AK, Yang J, Sulcova J, Werner S. The role of chronic inflammation in cutaneous fibrosis: fibroblast growth factor receptor deficiency in keratinocytes as an example. *The journal of investigative dermatology Symposium proceedings / the Society for Investigative Dermatology, Inc [and] European Society for Dermatological Research*. 2011;15(1):48-52.
3. Butler KL, Goverman J, Ma H, Fischman A, Yu YM, Bilodeau M, et al. Stem cells and burns: review and therapeutic implications. *Journal of burn care & research : official publication of the American Burn Association*. 2010;31(6):874-81.
4. Chen FM, Wu LA, Zhang M, Zhang R, Sun HH. Homing of endogenous stem/progenitor cells for in situ tissue regeneration: Promises, strategies, and translational perspectives. *Biomaterials*. 2011;32(12):3189-209.
5. Chen JS, Wong VW, Gurtner GC. Therapeutic potential of bone marrow-derived mesenchymal stem cells for cutaneous wound healing. *Frontiers in immunology*. 2012;3:192.
6. Maxson S, Lopez EA, Yoo D, Danilkovitch-Miagkova A, Leroux MA. Concise review: role of mesenchymal stem cells in wound repair. *Stem cells translational medicine*. 2012;1(2):142-9.
7. Aggarwal S, Moggio A, Bussolati B. Concise review: stem/progenitor cells for renal tissue repair: current knowledge and perspectives. *Stem cells translational medicine*. 2013;2(12):1011-9.
8. Bernstein HS, Srivastava D. Stem cell therapy for cardiac disease. *Pediatric research*. 2012;71(4 Pt 2):491-9.
9. Sinclair K, Yerkovich ST, Chambers DC. Mesenchymal stem cells and the lung. *Respirology*. 2013;18(3):397-411.
10. Sasaki M, Abe R, Fujita Y, Ando S, Inokuma D, Shimizu H. Mesenchymal stem cells are recruited into wounded skin and contribute to wound repair by transdifferentiation into multiple skin cell type. *Journal of immunology*. 2008;180(4):2581-7.
11. Fu X, Fang L, Li X, Cheng B, Sheng Z. Enhanced wound-healing quality with bone marrow mesenchymal stem cells autografting after skin injury. *Wound Repair Regen*. 2006;14(3):325-35.
12. Liu ZJ, Zhuge Y, Velazquez OC. Trafficking and differentiation of mesenchymal stem cells. *Journal of cellular biochemistry*. 2009;106(6):984-91.
13. Marconi S, Bonaconsa M, Scambi I, Squintani GM, Rui W, Turano E, et al. Systemic treatment with adipose-derived mesenchymal stem cells ameliorates clinical and pathological features in the amyotrophic lateral sclerosis murine model. *Neuroscience*. 2013;248C:333-43.
14. Jiang XY, Lu DB, Jiang YZ, Zhou LN, Cheng LQ, Chen B. PGC-1alpha prevents apoptosis in adipose-derived stem cells by reducing reactive oxygen species production in a diabetic microenvironment. *Diabetes research and clinical practice*. 2013;100(3):368-75.
15. Zuk PA. The adipose-derived stem cell: looking back and looking ahead. *Molecular biology of the cell*. 2010;21(11):1783-7.
16. Mizuno H, Tobita M, Uysal AC. Concise review: Adipose-derived stem cells as a novel tool for future regenerative medicine. *Stem cells*. 2012;30(5):804-10.
17. Hamed-Asl P, Halabian R, Bahmani P, Mohammadipour M, Mohammadzadeh M, Roushandeh AM, et al. Adenovirus-mediated expression of the HO-1 protein within MSCs decreased cytotoxicity and inhibited apoptosis induced by oxidative stresses. *Cell stress & chaperones*. 2012;17(2):181-90.
18. Mohammadzadeh M, Halabian R, Gharehbaghian A, Amirzadeh N, Jahanian-Najafabadi A, Roushandeh AM, et al. Nrf-2 overexpression in mesenchymal stem cells reduces oxidative stress-induced apoptosis and cytotoxicity. *Cell stress & chaperones*. 2012;17(5):553-65.
19. Halabian R, Tehrani HA, Jahanian-Najafabadi A, Habibi Roudkenar M. Lipocalin-2-mediated upregulation of various antioxidants and growth factors protects bone marrow-derived mesenchymal stem cells against unfavorable microenvironments. *Cell stress & chaperones*. 2013;18(6):785-800.
20. Zhu W, Chen J, Cong X, Hu S, Chen X. Hypoxia and serum deprivation-induced apoptosis in mesenchymal stem cells. *Stem cells*. 2006;24(2):416-25.
21. Yagi H, Tan J, Tuan RS. Polyphenols suppress hydrogen peroxide-induced oxidative stress in human bone-marrow derived mesenchymal stem cells. *Journal of cellular biochemistry*. 2013;114(5):1163-73.
22. McGinley L, McMahon J, Strappe P, Barry F, Murphy M, O'Toole D, et al. Lentiviral vector mediated modification of mesenchymal stem cells & enhanced survival in an in vitro model of ischaemia. *Stem cell research & therapy*. 2011;2(2):12.

23. Xie X, Sun A, Zhu W, Huang Z, Hu X, Jia J, et al. Transplantation of mesenchymal stem cells preconditioned with hydrogen sulfide enhances repair of myocardial infarction in rats. *The Tohoku journal of experimental medicine*. 2012;226(1):29-36.
24. Kongpetch S, Kukongviriyapan V, Prawan A, Senggunprai L, Kukongviriyapan U, Buranrat B. Crucial role of heme oxygenase-1 on the sensitivity of cholangiocarcinoma cells to chemotherapeutic agents. *PLoS one*. 2012;7(4):e34994.
25. Wagener FA, Dankers AC, van Summeren F, Scharstuhl A, van den Heuvel JJ, Koenderink JB, et al. Heme Oxygenase-1 and breast cancer resistance protein protect against heme-induced toxicity. *Curr Pharm Des*. 2013;19(15):2698-707.
26. Gozzelino R, Jeney V, Soares MP. Mechanisms of cell protection by heme oxygenase-1. *Annual review of pharmacology and toxicology*. 2010;50:323-54.
27. Morse D, Choi AM. Heme oxygenase-1: from bench to bedside. *Am J Respir Crit Care Med*. 2005;172(6):660-70.
28. Gozzelino R, Soares MP. Coupling Heme and Iron Metabolism via Ferritin H Chain. *Antioxidants & redox signaling*. 2013.
29. Wagener FA, Scharstuhl A, Tyrrell RM, Von den Hoff JW, Jozkowicz A, Dulak J, et al. The heme-heme oxygenase system in wound healing; implications for scar formation. *Current drug targets*. 2010;11(12):1571-85.
30. Burgess AP, Vanella L, Bellner L, Gotlinger K, Falck JR, Abraham NG, et al. Heme oxygenase (HO-1) rescue of adipocyte dysfunction in HO-2 deficient mice via recruitment of epoxyeicosatrienoic acids (EETs) and adiponectin. *Cellular physiology and biochemistry : international journal of experimental cellular physiology, biochemistry, and pharmacology*. 2012;29(1-2):99-110.
31. Abraham NG, Kappas A. Pharmacological and clinical aspects of heme oxygenase. *Pharmacological reviews*. 2008;60(1):79-127.
32. Sodhi K, Inoue K, Gotlinger KH, Canestraro M, Vanella L, Kim DH, et al. Epoxyeicosatrienoic acid agonist rescues the metabolic syndrome phenotype of HO-2-null mice. *The Journal of pharmacology and experimental therapeutics*. 2009;331(3):906-16.
33. Hou C, Shen L, Huang Q, Mi J, Wu Y, Yang M, et al. The effect of heme oxygenase-1 complexed with collagen on MSC performance in the treatment of diabetic ischemic ulcer. *Biomaterials*. 2013;34(1):112-20.
34. Tsubokawa T, Yagi K, Nakanishi C, Zuka M, Nohara A, Ino H, et al. Impact of anti-apoptotic and anti-oxidative effects of bone marrow mesenchymal stem cells with transient overexpression of heme oxygenase-1 on myocardial ischemia. *Am J Physiol Heart Circ Physiol*. 2010;298(5):H1320-9.
35. Jiang Y, Chen L, Tang Y, Ma G, Shen C, Qi C, et al. HO-1 gene overexpression enhances the beneficial effects of superparamagnetic iron oxide labeled bone marrow stromal cells transplantation in swine hearts underwent ischemia/reperfusion: an MRI study. *Basic research in cardiology*. 2010;105(3):431-42.
36. Yang JJ, Yang X, Liu ZQ, Hu SY, Du ZY, Feng LL, et al. Transplantation of adipose tissue-derived stem cells overexpressing heme oxygenase-1 improves functions and remodeling of infarcted myocardium in rabbits. *The Tohoku journal of experimental medicine*. 2012;226(3):231-41.
37. Wojakowski W, Tendera M, Cybulski W, Zuba-Surma EK, Szade K, Florkczyk U, et al. Effects of intracoronary delivery of allogenic bone marrow-derived stem cells expressing heme oxygenase-1 on myocardial reperfusion injury. *Thrombosis and haemostasis*. 2012;108(3):464-75.
38. Liang OD, Mitsialis SA, Chang MS, Vergadi E, Lee C, Aslam M, et al. Mesenchymal stromal cells expressing heme oxygenase-1 reverse pulmonary hypertension. *Stem cells*. 2011;29(1):99-107.
39. Zeng B, Chen H, Zhu C, Ren X, Lin G, Cao F. Effects of combined mesenchymal stem cells and heme oxygenase-1 therapy on cardiac performance. *European journal of cardio-thoracic surgery : official journal of the European Association for Cardio-thoracic Surgery*. 2008;34(4):850-6.
40. Zeng B, Lin G, Ren X, Zhang Y, Chen H. Over-expression of HO-1 on mesenchymal stem cells promotes angiogenesis and improves myocardial function in infarcted myocardium. *Journal of biomedical science*. 2010;17:80.
41. Poss KD, Tonegawa S. Reduced stress defense in heme oxygenase 1-deficient cells. *Proceedings of the National Academy of Sciences of the United States of America*. 1997;94(20):10925-30.
42. Sinno H, Tahiri Y, Thibaudeau S, Izadpanah A, Christodoulou G, Lin SJ, et al. Cleft lip and palate: an objective measure outcome study. *Plastic and reconstructive surgery*. 2012;130(2):408-14.
43. Basuroy S, Bhattacharya S, Tcheranova D, Qu Y, Regan RF, Leffler CW, et al. HO-2 provides endogenous protection against oxidative stress and apoptosis caused by TNF-alpha in cerebral vascular endothelial cells. *American journal of physiology Cell physiology*. 2006;291(5):C897-908.

44. Chen J, Regan RF. Heme oxygenase-2 gene deletion increases astrocyte vulnerability to hemin. *Biochemical and biophysical research communications*. 2004;318(1):88-94.
45. Rogers B, Yakopov V, Teng ZP, Guo Y, Regan RF. Heme oxygenase-2 knockout neurons are less vulnerable to hemoglobin toxicity. *Free radical biology & medicine*. 2003;35(8):872-81.
46. Chen J, Tu Y, Connolly EC, Ronnett GV. Heme oxygenase-2 protects against glutathione depletion-induced neuronal apoptosis mediated by bilirubin and cyclic GMP. *Current neurovascular research*. 2005;2(2):121-31.
47. Chen J, Tu Y, Moon C, Nagata E, Ronnett GV. Heme oxygenase-1 and heme oxygenase-2 have distinct roles in the proliferation and survival of olfactory receptor neurons mediated by cGMP and bilirubin, respectively. *Journal of neurochemistry*. 2003;85(5):1247-61.
48. Kim YM, Choi BM, Kim YS, Kwon YG, Kibbe MR, Billiar TR, et al. Protective effect of p53 in vascular smooth muscle cells against nitric oxide-induced apoptosis is mediated by up-regulation of heme oxygenase-2. *BMB reports*. 2008;41(2):164-9.
49. Parfenova H, Basuroy S, Bhattacharya S, Tcheranova D, Qu Y, Regan RF, et al. Glutamate induces oxidative stress and apoptosis in cerebral vascular endothelial cells: contributions of HO-1 and HO-2 to cytoprotection. *American journal of physiology Cell physiology*. 2006;290(5):C1399-410.
50. Dore S, Takahashi M, Ferris CD, Zakhary R, Hester LD, Guastella D, et al. Bilirubin, formed by activation of heme oxygenase-2, protects neurons against oxidative stress injury. *Proceedings of the National Academy of Sciences of the United States of America*. 1999;96(5):2445-50.
51. Dore S, Goto S, Sampei K, Blackshaw S, Hester LD, Ingi T, et al. Heme oxygenase-2 acts to prevent neuronal death in brain cultures and following transient cerebral ischemia. *Neuroscience*. 2000;99(4):587-92.
52. Rahman MN, Vlahakis JZ, Szarek WA, Nakatsu K, Jia Z. X-ray crystal structure of human heme oxygenase-1 in complex with 1-(adamantan-1-yl)-2-(1H-imidazol-1-yl)ethanone: a common binding mode for imidazole-based heme oxygenase-1 inhibitors. *Journal of medicinal chemistry*. 2008;51(19):5943-52.
53. Di Francesco L, Totani L, Dovizio M, Piccoli A, Di Francesco A, Salvatore T, et al. Induction of prostacyclin by steady laminar shear stress suppresses tumor necrosis factor-alpha biosynthesis via heme oxygenase-1 in human endothelial cells. *Circulation research*. 2009;104(4):506-13.
54. Scharstuhl A, Mutsaers HA, Pennings SW, Szarek WA, Russel FG, Wagener FA. Curcumin-induced fibroblast apoptosis and in vitro wound contraction are regulated by antioxidants and heme oxygenase: implications for scar formation. *Journal of cellular and molecular medicine*. 2009;13(4):712-25.
55. Bellner L, Martinelli L, Halilovic A, Patil K, Puri N, Dunn MW, et al. Heme oxygenase-2 deletion causes endothelial cell activation marked by oxidative stress, inflammation, and angiogenesis. *The Journal of pharmacology and experimental therapeutics*. 2009;331(3):925-32.
56. ter Huurde M, Schelbergen R, Blattes R, Blom A, de Munter W, Grevers LC, et al. Antiinflammatory and chondroprotective effects of intraarticular injection of adipose-derived stem cells in experimental osteoarthritis. *Arthritis and rheumatism*. 2012;64(11):3604-13.
57. Zheng B, Cao B, Li G, Huard J. Mouse adipose-derived stem cells undergo multilineage differentiation in vitro but primarily osteogenic and chondrogenic differentiation in vivo. *Tissue engineering*. 2006;12(7):1891-901.
58. Kolf CM, Cho E, Tuan RS. Mesenchymal stromal cells. *Biology of adult mesenchymal stem cells: regulation of niche, self-renewal and differentiation*. *Arthritis research & therapy*. 2007;9(1):204.
59. Cawthorn WP, Scheller EL, MacDougald OA. Adipose tissue stem cells meet preadipocyte commitment: going back to the future. *Journal of lipid research*. 2012;53(2):227-46.
60. Yamamoto N, Akamatsu H, Hasegawa S, Yamada T, Nakata S, Ohkuma M, et al. Isolation of multipotent stem cells from mouse adipose tissue. *Journal of dermatological science*. 2007;48(1):43-52.
61. Nakagami H, Maeda K, Morishita R, Iguchi S, Nishikawa T, Takami Y, et al. Novel autologous cell therapy in ischemic limb disease through growth factor secretion by cultured adipose tissue-derived stromal cells. *Arteriosclerosis, thrombosis, and vascular biology*. 2005;25(12):2542-7.
62. Sung JH, Yang HM, Park JB, Choi GS, Joh JW, Kwon CH, et al. Isolation and characterization of mouse mesenchymal stem cells. *Transplantation proceedings*. 2008;40(8):2649-54.
63. Wang L, Huang H, Fan Y, Kong B, Hu H, Hu K, et al. Effects of Downregulation of MicroRNA-181a on H₂O₂-Induced H9c2 Cell Apoptosis via the Mitochondrial Apoptotic Pathway. *Oxidative medicine and cellular longevity*. 2014;2014:960362.
64. Kou X, Shen K, An Y, Qi S, Dai WX, Yin Z. Ampelopsin inhibits H₂O₂-induced apoptosis by ERK and Akt signaling pathways and up-regulation of heme oxygenase-1. *Phytotherapy research : PTR*. 2012;26(7):988-94.

65. Wang FW, Wang Z, Zhang YM, Du ZX, Zhang XL, Liu Q, et al. Protective effect of melatonin on bone marrow mesenchymal stem cells against hydrogen peroxide-induced apoptosis in vitro. *Journal of cellular biochemistry*. 2013;114(10):2346-55.
66. Zeng B, Ren X, Lin G, Zhu C, Chen H, Yin J, et al. Paracrine action of HO-1-modified mesenchymal stem cells mediates cardiac protection and functional improvement. *Cell Biol Int*. 2008;32(10):1256-64.
67. Masoud MS, Anwar SS, Afzal MZ, Mehmood A, Khan SN, Riazuddin S. Pre-conditioned mesenchymal stem cells ameliorate renal ischemic injury in rats by augmented survival and engraftment. *Journal of translational medicine*. 2012;10:243.
68. Loboda A, Was H, Jozkowicz A, Dulak J. Janus face of Nrf2-HO-1 axis in cancer--friend in chemoprevention, foe in anticancer therapy. *Lung cancer*. 2008;60(1):1-3.
69. Alcaraz MJ, Habib A, Lebreton M, Creminon C, Levy-Toledano S, Maclouf J. Enhanced expression of haem oxygenase-1 by nitric oxide and anti-inflammatory drugs in NIH 3T3 fibroblasts. *British journal of pharmacology*. 2000;130(1):57-64.
70. Zhang QH, Zhou ZS, Lu GS, Song B, Guo JX. Melatonin improves bladder symptoms and may ameliorate bladder damage via increasing HO-1 in rats. *Inflammation*. 2013;36(3):651-7.
71. Hatcher H, Planalp R, Cho J, Torti FM, Torti SV. Curcumin: from ancient medicine to current clinical trials. *Cellular and molecular life sciences : CMLS*. 2008;65(11):1631-52.
72. Epstein J, Sanderson IR, Macdonald TT. Curcumin as a therapeutic agent: the evidence from in vitro, animal and human studies. *The British journal of nutrition*. 2010;103(11):1545-57.
73. Motterlini R, Foresti R, Bassi R, Green CJ. Curcumin, an antioxidant and anti-inflammatory agent, induces heme oxygenase-1 and protects endothelial cells against oxidative stress. *Free radical biology & medicine*. 2000;28(8):1303-12.
74. Aggarwal BB, Sundaram C, Malani N, Ichikawa H. Curcumin: the Indian solid gold. *Advances in experimental medicine and biology*. 2007;595:1-75.
75. Prasad S, Gupta SC, Tyagi AK, Aggarwal BB. Curcumin, a component of golden spice: From bedside to bench and back. *Biotechnology advances*. 2014.
76. Zhou H, Beevers CS, Huang S. The targets of curcumin. *Current drug targets*. 2011;12(3):332-47.
77. Sugishima M, Higashimoto Y, Oishi T, Takahashi H, Sakamoto H, Noguchi M, et al. X-ray crystallographic and biochemical characterization of the inhibitory action of an imidazole-dioxolane compound on heme oxygenase. *Biochemistry*. 2007;46(7):1860-7.
78. Kinobe RT, Vlahakis JZ, Vreman HJ, Stevenson DK, Brien JF, Szarek WA, et al. Selectivity of imidazole-dioxolane compounds for in vitro inhibition of microsomal haem oxygenase isoforms. *British journal of pharmacology*. 2006;147(3):307-15.
79. Vlahakis JZ, Kinobe RT, Bowers RJ, Brien JF, Nakatsu K, Szarek WA. Synthesis and evaluation of azalanstat analogues as heme oxygenase inhibitors. *Bioorganic & medicinal chemistry letters*. 2005;15(5):1457-61.
80. Lin HY, Shen SC, Lin CW, Yang LY, Chen YC. Baicalein inhibition of hydrogen peroxide-induced apoptosis via ROS-dependent heme oxygenase 1 gene expression. *Biochimica et biophysica acta*. 2007;1773(7):1073-86.
81. Zhang M, Zhang BH, Chen L, An W. Overexpression of heme oxygenase-1 protects smooth muscle cells against oxidative injury and inhibits cell proliferation. *Cell research*. 2002;12(2):123-32.
82. Fu YQ, Fang F, Lu ZY, Kuang FW, Xu F. N-acetylcysteine protects alveolar epithelial cells from hydrogen peroxide-induced apoptosis through scavenging reactive oxygen species and suppressing c-Jun N-terminal kinase. *Experimental lung research*. 2010;36(6):352-61.
83. Samuni Y, Goldstein S, Dean OM, Berk M. The chemistry and biological activities of N-acetylcysteine. *Biochimica et biophysica acta*. 2013;1830(8):4117-29.
84. Fernandez-Checa JC, Garcia-Ruiz C, Colell A, Morales A, Mari M, Miranda M, et al. Oxidative stress: role of mitochondria and protection by glutathione. *Biofactors*. 1998;8(1-2):7-11.
85. Fernandez-Checa JC, Kaplowitz N, Garcia-Ruiz C, Colell A, Miranda M, Mari M, et al. GSH transport in mitochondria: defense against TNF-induced oxidative stress and alcohol-induced defect. *The American journal of physiology*. 1997;273(1 Pt 1):G7-17.
86. Sedlak TW, Saleh M, Higginson DS, Paul BD, Juluri KR, Snyder SH. Bilirubin and glutathione have complementary antioxidant and cytoprotective roles. *Proceedings of the National Academy of Sciences of the United States of America*. 2009;106(13):5171-6.
87. Aronis A, Aharoni-Simon M, Madar Z, Tirosh O. Triacylglycerol-induced impairment in mitochondrial biogenesis and function in J774.2 and mouse peritoneal macrophage foam cells. *Archives of biochemistry and biophysics*. 2009;492(1-2):74-81.

88. Bruggisser R, von Daeniken K, Jundt G, Schaffner W, Tullberg-Reinert H. Interference of plant extracts, phytoestrogens and antioxidants with the MTT tetrazolium assay. *Planta medica*. 2002;68(5):445-8.
89. Krifka S, Hiller KA, Spagnuolo G, Jewett A, Schmalz G, Schweikl H. The influence of glutathione on redox regulation by antioxidant proteins and apoptosis in macrophages exposed to 2-hydroxyethyl methacrylate (HEMA). *Biomaterials*. 2012;33(21):5177-86.
90. Xiong L, Sun J, Hirche C, Yang J, Yang Y, Xia Y, et al. In vitro N-acetyl-L-cysteine promotes proliferation and suppresses interleukin-8 expression in adipose-derived stem cells. *Aesthetic plastic surgery*. 2012;36(5):1260-5.
91. Ji H, Liu Y, Zhao X, Zhang M. N-acetyl-L-cysteine enhances the osteogenic differentiation and inhibits the adipogenic differentiation through up regulation of Wnt 5a and down regulation of PPARG in bone marrow stromal cells. *Biomedicine & pharmacotherapy = Biomedecine & pharmacotherapie*. 2011;65(5):369-74.
92. Park C, So HS, Shin CH, Baek SH, Moon BS, Shin SH, et al. Quercetin protects the hydrogen peroxide-induced apoptosis via inhibition of mitochondrial dysfunction in H9c2 cardiomyoblast cells. *Biochemical pharmacology*. 2003;66(7):1287-95.
93. Singh M, Sharma H, Singh N. Hydrogen peroxide induces apoptosis in HeLa cells through mitochondrial pathway. *Mitochondrion*. 2007;7(6):367-73.
94. Qian Y, Du YH, Tang YB, Lv XF, Liu J, Zhou JG, et al. CIC-3 chloride channel prevents apoptosis induced by hydrogen peroxide in basilar artery smooth muscle cells through mitochondria dependent pathway. *Apoptosis : an international journal on programmed cell death*. 2011;16(5):468-77.
95. Liu NS, Du X, Lu J, He BP. Diva reduces cell death in response to oxidative stress and cytotoxicity. *PLoS one*. 2012;7(8):e43180.
96. Chen HY, Zhang X, Chen SF, Zhang YX, Liu YH, Ma LL, et al. The protective effect of 17beta-estradiol against hydrogen peroxide-induced apoptosis on mesenchymal stem cell. *Biomedicine & pharmacotherapy = Biomedecine & pharmacotherapie*. 2012;66(1):57-63.
97. Wei H, Li Z, Hu S, Chen X, Cong X. Apoptosis of mesenchymal stem cells induced by hydrogen peroxide concerns both endoplasmic reticulum stress and mitochondrial death pathway through regulation of caspases, p38 and JNK. *Journal of cellular biochemistry*. 2010;111(4):967-78.
98. Lee SJ, Ryter SW, Xu JF, Nakahira K, Kim HP, Choi AMK, et al. Carbon Monoxide Activates Autophagy via Mitochondrial Reactive Oxygen Species Formation. *Am J Resp Cell Mol*. 2011;45(4):867-73.
99. Choi YK, Por ED, Kwon YG, Kim YM. Regulation of ROS Production and Vascular Function by Carbon Monoxide. *Oxidative medicine and cellular longevity*. 2012.
100. Piantadosi CA. Carbon monoxide, reactive oxygen signaling, and oxidative stress. *Free Radical Bio Med*. 2008;45(5):562-9.
101. Chi PL, Liu CJ, Lee IT, Chen YW, Hsiao LD, Yang CM. HO-1 induction by CO-RM2 attenuates TNF-alpha-induced cytosolic phospholipase A2 expression via inhibition of PKCalpha-dependent NADPH oxidase/ROS and NF-kappaB. *Mediators of inflammation*. 2014;2014:279171.
102. Kim HJ, Zheng M, Kim SK, Cho JJ, Shin CH, Joe Y, et al. CO/HO-1 Induces NQO-1 Expression via Nrf2 Activation. *Immune network*. 2011;11(6):376-82.
103. Lee BS, Heo J, Kim YM, Shim SM, Pae HO, Kim YM, et al. Carbon monoxide mediates heme oxygenase 1 induction via Nrf2 activation in hepatoma cells. *Biochemical and biophysical research communications*. 2006;343(3):965-72.
104. Kim HP, Choi AM. A new road to induce heme oxygenase-1 expression by carbon monoxide. *Circulation research*. 2007;101(9):862-4.
105. Ozaki KS, Kimura S, Murase N. Use of carbon monoxide in minimizing ischemia/reperfusion injury in transplantation. *Transplant Rev-Orlan*. 2012;26(2):125-39.
106. Bilban M, Haschemi A, Wegiel B, Chin BY, Wagner O, Otterbein LE. Heme oxygenase and carbon monoxide initiate homeostatic signaling. *Journal of molecular medicine*. 2008;86(3):267-79.
107. Piantadosi CA. Carbon monoxide, reactive oxygen signaling, and oxidative stress. *Free radical biology & medicine*. 2008;45(5):562-9.
108. Heo JM, Kim HJ, Ha YM, Park MK, Kang YJ, Lee YS, et al. YS 51, 1-(beta-naphthylmethyl)-6,7-dihydroxy-1,2,3,4-tetrahydroisoquinoline, protects endothelial cells against hydrogen peroxide-induced injury via carbon monoxide derived from heme oxygenase-1. *Biochemical pharmacology*. 2007;74(9):1361-70.
109. Wei L, Fraser JL, Lu ZY, Hu X, Yu SP. Transplantation of hypoxia preconditioned bone marrow mesenchymal stem cells enhances angiogenesis and neurogenesis after cerebral ischemia in rats. *Neurobiology of disease*. 2012;46(3):635-45.

110. Malgieri A, Kantzari E, Patrizi MP, Gambardella S. Bone marrow and umbilical cord blood human mesenchymal stem cells: state of the art. *International journal of clinical and experimental medicine*. 2010;3(4):248-69.
111. Tse WT, Pendleton JD, Beyer WM, Egalka MC, Guinan EC. Suppression of allogeneic T-cell proliferation by human marrow stromal cells: implications in transplantation. *Transplantation*. 2003;75(3):389-97.
112. Shin L, Peterson DA. Human mesenchymal stem cell grafts enhance normal and impaired wound healing by recruiting existing endogenous tissue stem/progenitor cells. *Stem cells translational medicine*. 2013;2(1):33-42.
113. Tang YL, Tang Y, Zhang YC, Qian K, Shen L, Phillips MI. Improved graft mesenchymal stem cell survival in ischemic heart with a hypoxia-regulated heme oxygenase-1 vector. *Journal of the American College of Cardiology*. 2005;46(7):1339-50.
114. Caplan AI, Correa D. The MSC: an injury drugstore. *Cell stem cell*. 2011;9(1):11-5.
115. Herrmann JL, Abarbanell AM, Weil BR, Manukyan MC, Poynter JA, Brewster BJ, et al. Optimizing stem cell function for the treatment of ischemic heart disease. *The Journal of surgical research*. 2011;166(1):138-45.

Chapter 6

Effects of remote ischemic preconditioning on heme oxygenase-1 expression and cutaneous wound repair.

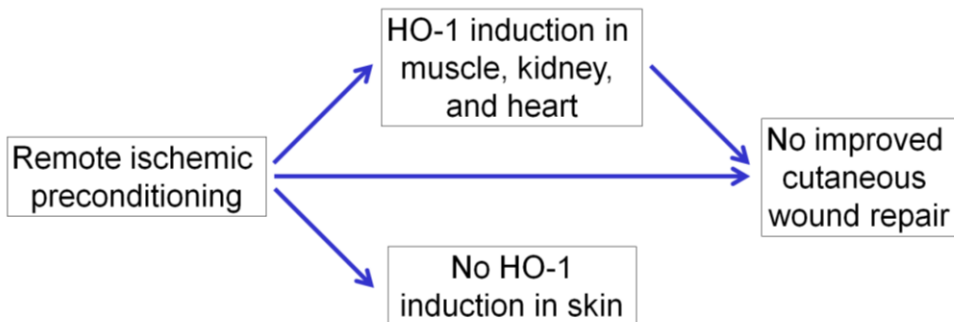
Cremers NA, Wever KE, Wong RJ, van Rheden RE, Vermeij EA, van Dam GM, Carels CE, Lundvig DM, Wagener FA.

Int J Mol Sci. 2017 Feb 17;18(2):438.

Abstract

Skin wounds may lead to scar formation and impaired functionality. Remote ischemic preconditioning (RIPC) can induce the anti-inflammatory enzyme heme oxygenase-1 (HO-1) and protect against tissue injury. We aim to improve cutaneous wound repair by RIPC treatment via induction of HO-1. RIPC was applied to HO-1-*luc* transgenic mice and HO-1 promoter activity and mRNA expression in skin and several other organs were determined in real-time. In parallel, RIPC was applied directly or 24h prior to excisional wounding in mice to investigate the early and late protective effects of RIPC on cutaneous wound repair, respectively. HO-1 promoter activity was significantly induced on the dorsal side and locally in the kidneys following RIPC treatment. Next, we investigated the origin of this RIPC-induced HO-1 promoter activity and demonstrated increased mRNA in the ligated muscle, heart and kidneys, but not in the skin. RIPC did not change HO-1 mRNA and protein levels in the wound 7 days after cutaneous injury. Both early and late RIPC did not accelerate wound closure nor affect collagen deposition. RIPC induces HO-1 expression in several organs, but not the skin, and did not improve excisional wound repair, suggesting that the skin is insensitive to RIPC-mediated protection.

Keywords: remote ischemic preconditioning, heme oxygenase-1, tissue injury, wound repair.



Graphical abstract

Abbreviations

H&E	Hematoxylin and eosin
HO-1	Heme oxygenase-1
HO-1- <i>luc</i> Tg	HO-1- <i>luciferase</i> transgenic
I/R	Ischemia/Reperfusion
IPC	Ischemic preconditioning
IRI	Ischemia/Reperfusion injury
RIPC	Remote ischemic preconditioning
ROS	Reactive oxygen species
RPCT	Remote preconditioning by trauma

Introduction

Severe skin wounds following burns, trauma, or surgery often lead to scar formation and impaired functionality (1). Cutaneous wound repair is a dynamic and highly regulated process, involving several overlapping phases: inflammation, proliferation, and remodelling (2). Aberrant wound repair and scarring occurs following prolongation of the inflammatory phase that together with oxidative stress fuels (myo)fibroblast proliferation and interferes with myofibroblast apoptosis (2). This leads to excessive deposition of extracellular matrix proteins, subsequently promoting excessive scar formation (3, 4). Unfortunately, conventional therapies to accelerate wound repair and to prevent scarring are insufficient (5-7). Therefore, adjuvant therapies aimed at resolving inflammation are warranted. Pharmacological preconditioning has been shown to improve wound repair, as exemplified by heme and curcumin that also induce the cytoprotective protein heme oxygenase-1 (HO-1) (8-14). HO-1 is one of the most important enzymes protecting against oxidative and inflammatory insults (15). HO catabolizes heme to biliverdin, free iron, and carbon monoxide (CO). Biliverdin is then rapidly converted to the antioxidant bilirubin by biliverdin reductase (16, 17). The iron scavenger ferritin is co-induced by HO-1 and renders iron inactive (18). Recent studies have shown that induction of HO-1 expression attenuates the inflammatory response and accelerates wound healing in HO-1-deficient mice; whereas, decreased HO activity in mice results in slower cutaneous wound closure (9, 19). In addition, intraperitoneal administration of the HO-effector molecule bilirubin accelerates wound repair (20). Since increased HO-1 expression improves wound repair, its induction may be a good candidate for preventing aberrant cutaneous wound repair.

A promising novel preconditioning strategy is ischemic preconditioning (IPC), hereby, short cycles of ischemia/reperfusion to an organ protects against subsequent more harmful insults to the same organ. In remote ischemic preconditioning (RIPC), the target organ is not subjected to the initial stress, but a remote organ, e.g., the hind limb, is exposed (21, 22). Interestingly, RIPC protects against injury in the liver (23-26), lung (27), intestines (28), heart (29, 30), and kidneys (31, 32) often via the induction of HO-1, since inhibition of HO-activity abrogates the protective effects of RIPC (23, 26, 33). Following RIPC, there exists both a rapid phase of protection initiated within 1h after preconditioning, and a later phase after one to several days (21, 34). In addition, different modes of action have been reported between single and repeated RIPC procedures, as demonstrated by differential expression of genes involved in autophagy, endoplasmic reticulum stress, mitochondrial oxidative metabolism, and cell survival (35, 36).

Successful translation towards its clinical use was recently established by inducing temporary occlusion and restoration of blood flow in arm or thigh of patients (29, 30, 37). Patient outcome after myocardial surgery was significantly improved when RIPC was applied before surgery (27). However, recently conflicting results have been reported showing that RIPC does not always mediate protection (38-41). Data from animal and human studies demonstrated the need for careful interpretation because of translational differences (38-43). RIPC improves microcirculation by an increase in tissue oxygenation and capillary blood flow in the skin (44) and skin flaps (45), and forms a novel target for skin flap transplantation (46) and the healing of diabetic foot ulcers (47, 48). Although RIPC has been shown to protect in several models of tissue injury, its role in cutaneous excisional wound

healing is still unclear. We postulated that RIPC induces HO-1 expression and improves skin repair following excisional skin injury.

Materials and Methods

Animals

The Committee for Animal Experiments of the Radboud University Nijmegen approved all procedures involving animals (RU-DEC 2010-248) on 1 February 2011. Fifty mice (strain: HO-1-*luc* FVB/N-Tg background; see Table 6.1) of 4–5 months in age, and weighing 21–35 g were provided with food and water ad libitum and maintained on a 12 h light/dark cycle and specific pathogen-free housing conditions at the Central Animal Facility Nijmegen. The transgene consists of the full-length mouse HO-1 promoter fused to the reporter gene luciferase (*luc*). More details on the housing conditions are previously described (49). Mice were originally derived from Stanford University (Stanford, CA, USA) as previously described (50). An overview of the animals used for the different experiments can be found in Table 6.1. No animals died during the experiments and no animals were excluded during the experiments or data analyses. All mice were randomly divided over the experiments, and split evenly over their sex and age. All outcomes were measured by an observer who was blinded for the allocation of the animals to the experimental groups, when possible.

Table 6.1. Overview animal experiments.

Aim Experiment	Read Out	Animals (n: ♂/♀)
Investigate the effects of RIPC on HO-1 promoter activity	HO-1 promoter activity at 1, 6 and 24 h after RIPC treatment	6: 0/6
Investigate the effects of RIPC on HO-1 gene expression in different organs during time	HO-1 mRNA levels at 0, 1, 6, and 24 h after RIPC treatment	24: 0/24 (6 per time point)
Investigate the effects of RIPC on dermal wound healing	Early (5 min before wounding) and late (24 h before wounding) effects of RIPC on wound healing compared to controls without receiving RIPC treatment (endpoint: day 7)	6: 4/2 (early RIPC) 6: 4/2 (late RIPC) 8: 4/4 (controls)

RIPC Treatment

RIPC by brief hind limb ischemia was induced by applying elastic latex-free O-rings (Miltex Integra: 28–155) using a hemorrhoidal ligator (Miltex McGivney: 26–154B) bilaterally around the most upper position of the proximal thigh (Supplemental figure S6.1). Reperfusion was accomplished by cutting the elastic rings with scissors, confirmed by the disappearance of blue color to the limbs (Supplemental figure S6.1) as described previously (51–53). The mice were anesthetized with isoflurane in O₂/N₂O (5% isoflurane for induction and 2%–3% to maintain anesthesia) during RIPC treatment and treatment consisted of three cycles of 4-min ischemia interspersed with 4-min reperfusion. This RIPC regime is based on a previous study in which we found that bilateral repetitive (3 times 4 min) ischemia/reperfusion gave the most potent protection in a kidney injury model (32).



Supplemental figure S6.1. Hind limb ischemia by ligation using elastic ring (**red arrow**). Note the difference in the color of the legs after obstruction of the blood flow, confirming RIPC treatment was successful.

Measuring of HO-1 Promoter Activity

In order to monitor HO-1 promoter activity after RIPC treatment in time, HO-1-*luc* Tg mice underwent RIPC treatment as described above. HO-1-*luc* expression was measured in vivo and the mice were sacrificed at 24 h. In vivo bioluminescence imaging was performed as described before on the IVIS Lumina System (Caliper Life Sciences, Hopkinton, MA, USA) (54). Images taken were quantified using Living Image 3.0 software (Caliper Life Sciences) by selecting the regions of interest (ROI). ROIs included both the dorsal images encompassing the back region below the head and above the tail to cover the area where the wounds would be made and the renal area. Emitted photons per second (or total flux) per region of interest (ROI) was measured, and then calculated as fold change from baseline levels and related to 1 h after RIPC.

Excisional Wound Model

Wounds were made 24 h or 5 min after RIPC. Control mice did not receive RIPC, but underwent the same anesthetic procedure 1h before wounding. Two full-thickness excisional wounds of 4 mm in diameter were made on the shaved dorsal side of anesthetized mice using a sterile disposable biopsy punch (Kai Medical, Seki City, Japan), as previously described by our group (55). The wounds were created on the dorsum to either side of the midline, with approximately 1cm between the wounds, and just below the shoulders and pelvis. Skin biopsies taken to create the 4-mm wounds served as control skin. Wounds were photographically documented immediately, and 1, 3 and 7 days after wounding with a ruler placed perpendicular to the wounds for wound size normalization. The area of the wounds was blindly measured twice using ImageJ v1.44p software (<http://imagej.nih.gov/ij>; NIH, Bethesda, MD, USA).

Sample Collection

At day 7, the mice were anesthetized with 5% isoflurane in O₂/N₂O and sacrificed by exsanguination, followed by cervical dislocation. Kidney and muscle (*m. quadriceps femoris*) were dissected, and wound tissue was collected using a 4-mm biopsy punch. Half of the tissue was fixated with 4% paraformaldehyde and processed for paraffin embedding and (immuno-)histochemistry, and the other half was snap frozen in liquid nitrogen and stored at -80 °C until use for RT-PCR.

(Immuno-)histochemical Staining and Analyses

Standard H&E, Weigert-AZAN staining (azo carmine and aniline blue), and immunohistochemical HO-1 staining were performed on paraffin sections of the wounds as previously described (55). Stained sections were analyzed and photographed using the Zeiss Imager Z1 microscope (Zeiss, Sliedrecht, The Netherlands) and Axiovision software version 4.8 (Zeiss).

Analysis of collagen deposition in AZAN stained wound sections was performed by image analysis using a macro built in Image J (56). The wound area was manually defined using the edges of the *m. panniculus carnosus* and epithelium as boundaries before running the macro. Measurements were averaged per mouse and mean intensity/mm² was used for further analysis.

HO-1 immunoreactivity was evaluated by blindly scoring the epidermal zone and the dermal region of the wounds. A single section per wound of each animal was semi-quantitatively scored as previously described using the following scale: 0 (minimal), 1 (mild), 2 (moderate), and 3 (marked).

RNA Isolation and Quantitative-RT-PCR

Tissue was pulverized in TRIzol (Invitrogen, Carlsbad, CA, USA) using a micro-dismembrator (Sartorius BBI Systems GmbH, Melsungen, Germany) and RNA was further extracted as previously described (13). All values were normalized to the household gene *gapdh*, which is often used in RIPC experiments (57, 58) according to the comparative method ($2^{-\Delta\Delta Ct}$). *Gapdh* mRNA expression levels were stable and were not affected by RIPC treatment. The sequences of the mouse-specific primers for *gapdh* are forward 5'GGCAAATTC AACGGCACA3', and reverse 5'GTTAGTGGGGTCTCGC TCCTG3', and for *Hmox1* (*HO-1*) forward 5'CAACATTGAGCTGTTTGAGG3', and reverse 5'TGGTCTTTGTTCCTCTGTC3'.

Statistics

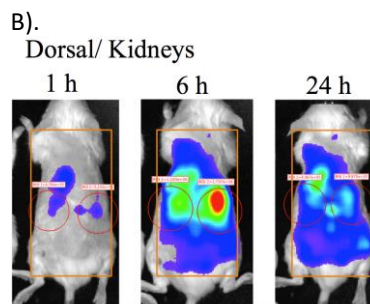
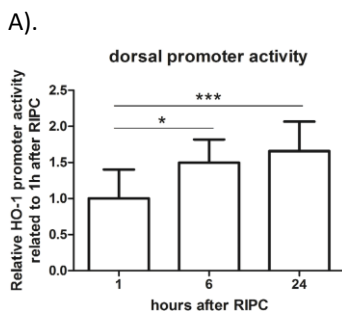
Data were analyzed using GraphPad Prism 5.01 software (San Diego, CA, USA). Outliers were tested using the Grubbs' test, but no outliers were found (except for the data in supplemental figure S6.3 where one outlier was found in the skin and one in the kidney group). Data were analyzed using two-sided *t*-tests to compare two variables or a one-way analysis of variance when comparing multiple variables. Bonferroni's multiple comparison *post hoc* test was applied as correction for multiple comparisons when investigating multiple dependent research questions. Results were considered significantly different at $p < 0.05$ (* $p < 0.05$, ** $p < 0.01$, and *** $p < 0.001$).

Results

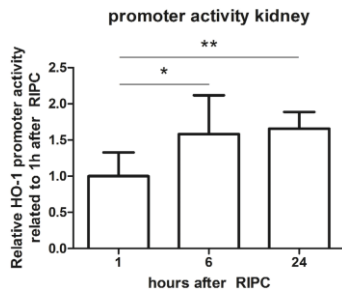
Effects of RIPC on HO-1 Promoter Activity and HO-1 mRNA Expression in Mice

RIPC can induce HO-1 expression in different organs. In order to evaluate if RIPC can induce HO-1 expression, we used a combination of HO-1 promoter activity and HO-1 mRNA analyses in HO-1-*luc* transgenic (Tg) mice. We previously demonstrated that treatment with cadmium chloride (CdCl₂) potentially induced HO-1 promoter activity in the liver and kidney using the HO-1-*luc* Tg model (59). To validate the RIPC model, we corroborated that blood flow was indeed hampered after applying elastic rings (Supplemental figure S6.1). After RIPC treatment, HO-1 promoter activity was measured using the In Vivo Imaging System at 1, 6, and 24 h. Measurements of HO-1 promoter activity were acquired at the dorsal aspect of each mouse (Figure 6.1A). Because of variations in HO-1 promoter activity, each mouse served as its own control. Relative HO-1 promoter activity of the dorsal side of the mice after RIPC treatment is shown over time (Figure 6.1B). We found a significant increase in HO-1 promoter activity after 6 and 24 h of RIPC treatment compared to 1 h after RIPC. HO-1 promoter activity was strongly observed in the renal area, suggesting RIPC induced HO-1 promoter activity in an organ-specific manner 6 and 24 h after RIPC treatment when compared to 1 h after RIPC treatment (Figure 6.1C).

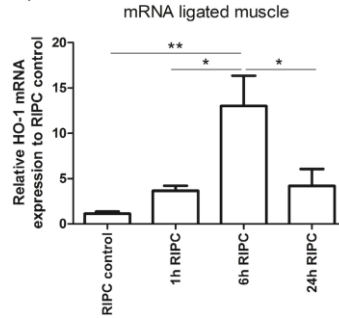
To discriminate whether the skin or underlying organs were responsible for the increase in HO-1 promoter activity, and to test whether RIPC induced HO-1 expression in a tissue-specific manner, we measured HO-1 mRNA expression levels in the skin and several organs 1, 6 and 24 h after RIPC using RT-PCR and then compared these results to untreated controls. First, HO-1 mRNA expression in the hind limb muscles that had been exposed to repeated ischemia/ reperfusion cycles were measured and significantly increased 6 h after RIPC treatment when compared to untreated controls and other time points after RIPC (Figure 6.1D). We then analyzed the effects of RIPC on HO-1 mRNA levels in remote organs like kidney, heart, and skin. We also observed a significant increase in HO-1 mRNA expression in the kidney 6h after RIPC treatment when compared to untreated controls and other time points after RIPC (Figure 6.1E). Similarly, in the heart, HO-1 mRNA levels significantly increased 6h after RIPC treatment when compared to untreated controls (Figure 6.1F). No significant induction was found at other time points compared to untreated controls. After 24 h, HO-1 mRNA levels returned to control levels. However, no significant induction in HO-1 mRNA expression was detected in the skin at any time point (Figure 6.1G). In conclusion, we demonstrated a tissue- and time-specific induction of HO-1 promoter activity and HO-1 mRNA expression after RIPC treatment.



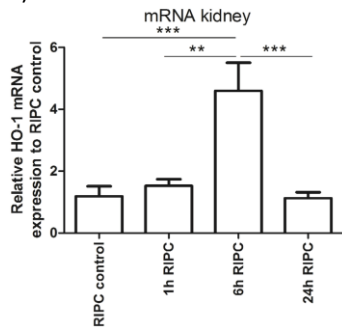
C).



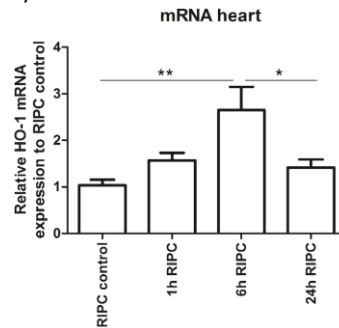
D).



E).



F).



G).

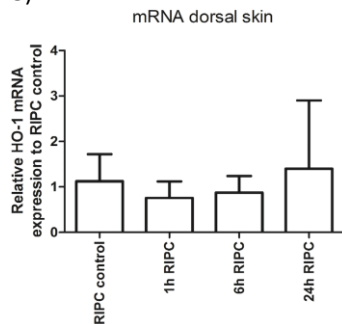


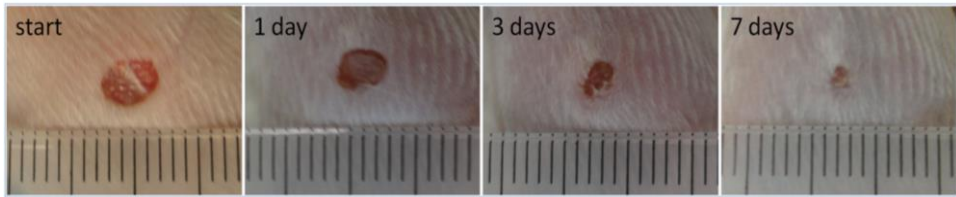
Figure 6.1. Heme oxygenase-1 (HO-1) promoter activity (A–C) and mRNA expression (D–G) after remote ischemic preconditioning (RIPC) treatment. (A) Representative dorsal images of HO-1 promoter activity after RIPC over time. Both the overall dorsal side (inserted orange rectangles) and the specific regions of the kidneys (inserted red circles) were analyzed and the total flux of emitted photons per second was quantified. Quantification of HO-1 promoter activity in the overall dorsal area after RIPC treatment (B); and locally in the regions of the kidneys (C), and HO-1 mRNA expression in muscle at the place of ligation (D); kidney (E); heart (F); and dorsal skin (G), 1, 6 and 24 h after RIPC treatment compared to untreated controls ($n = 6$ animals per group). Data are expressed as mean \pm SD of six individual mice. * $p < 0.05$, ** $p < 0.01$, *** $p < 0.001$.

Effects of Early or Late RIPC on Excisional Cutaneous Wound Closure in Mice

Since RIPC was observed to improve the cutaneous microcirculation (44), we next investigated whether RIPC could also modulate cutaneous wound repair. RIPC induced HO-1 expression in several organs, but not in the skin. Interestingly, HO-1 can also promote regeneration in a paracrine fashion via its versatile effector molecules biliverdin/bilirubin,

CO, and ferritin (20, 60-64), which are increased following (R)IPC (65-68). Moreover, RIPC-mediated protection can act via various alternative signaling pathways, including humoral, neuronal, and systemic mechanisms (22, 69). Since there are early and late protective effects of RIPC, we evaluated whether early (5 min) and/or late (24 h) RIPC treatment before wounding improved full-thickness excisional wound closure. Examples of untreated excisional wounds are shown in Figure 6.2A. Wound sizes were normalized to the wound size at day 0 (Figure 6.2B). As expected, after quantification of the wound surface area, we found a reduction in the wound size over time. However, no significant differences were observed in wound closures between early or late RIPC treatment mice and controls.

A).



B).



Figure 6.2. Excisional wound closure in time after RIPC treatment 24 h and directly after wounding compared to the control group. Representative images of the wounds of a single mouse receiving no RIPC treatment at day 0, and at 1, 3, and 7 days after wounding (ruler is incorporated in the pictures and each bar represent 1 mm) (A) and their relative wound sizes after different treatments in time, compared to control group at day 0 (B). Data are expressed as mean \pm SD. No significant differences were observed between the different groups: no RIPC ($n = 8$), RIPC 5 min ($n = 6$) and RIPC 24 h ($n = 6$).

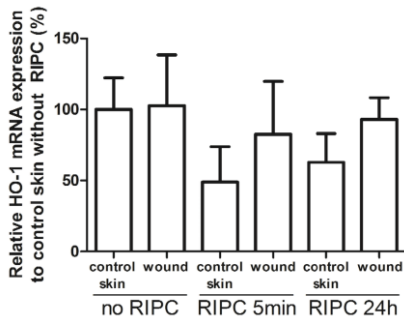
HO-1 mRNA and Protein Expression in Wounds After RIPC

To further elucidate the role of RIPC-induced HO-1 expression during wound repair, we investigated whether RIPC modulates HO-1 mRNA and protein expression in day-7 wounds. Using RT-PCR, HO-1 mRNA expression was assessed in the wounds and compared to non-wounded day-0 skin (Figure 6.3A). Here, we found no significant differences between the wounds and their corresponding control skins for both RIPC-treated and control groups as well as between the different treatment groups.

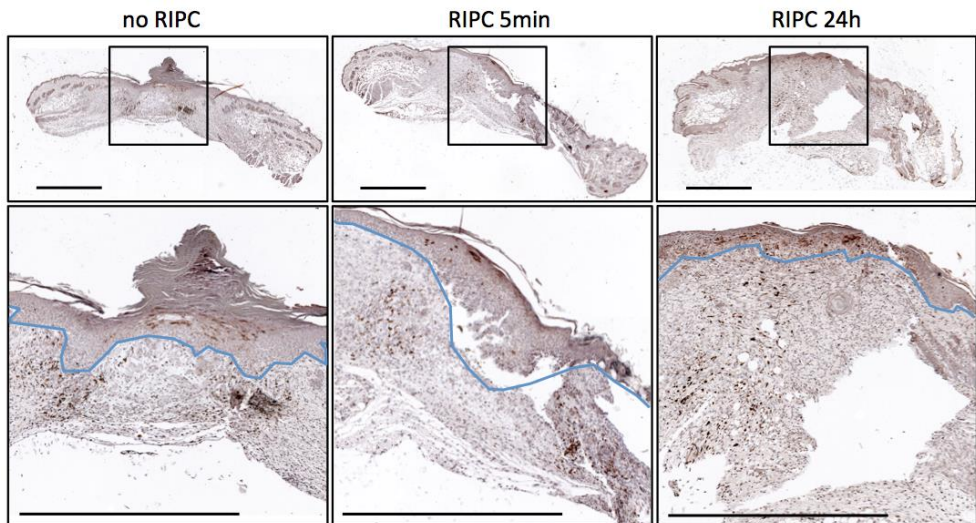
HO-1 protein was found in the epithelial cells of the epidermis and in recruited leukocytes in the dermis (Figure 6.3B). In the epidermis, HO-1-positive cells were clustered in the re-epithelialized tissue underneath the wound crust and were likely newly-formed keratinocytes (70, 71). In the dermis, HO-1-positive cells in inflamed tissues were individually spread, and based on their location and morphology, they appear to be macrophages (70-73). Moreover, in unpublished data from a previous experiment on excisional wound healing in C57Bl/6 mice at day-2 post-wounding, fluorescent staining for HO-1 (red) and F4/80 (green) clearly showed co-localization (orange) of HO-1 and macrophages in a majority of cells (Supplemental figure S6.2).

The wounds were scored for the levels of HO-1 expression in the epidermal and dermal regions, and compared between the different treatment groups (Figure 6.3C). RIPC treatment did not modulate HO-1 protein expression in either region of day-7 wounds when compared to controls. Variations in HO-1 expression was found between animals, but was independent of RIPC treatment. In summary, RIPC treatment does not appear to alter HO-1 mRNA and protein expression in day-7 wounds.

A).



B).



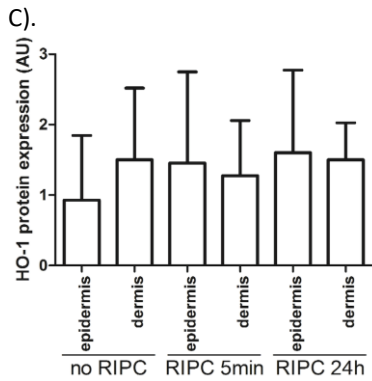
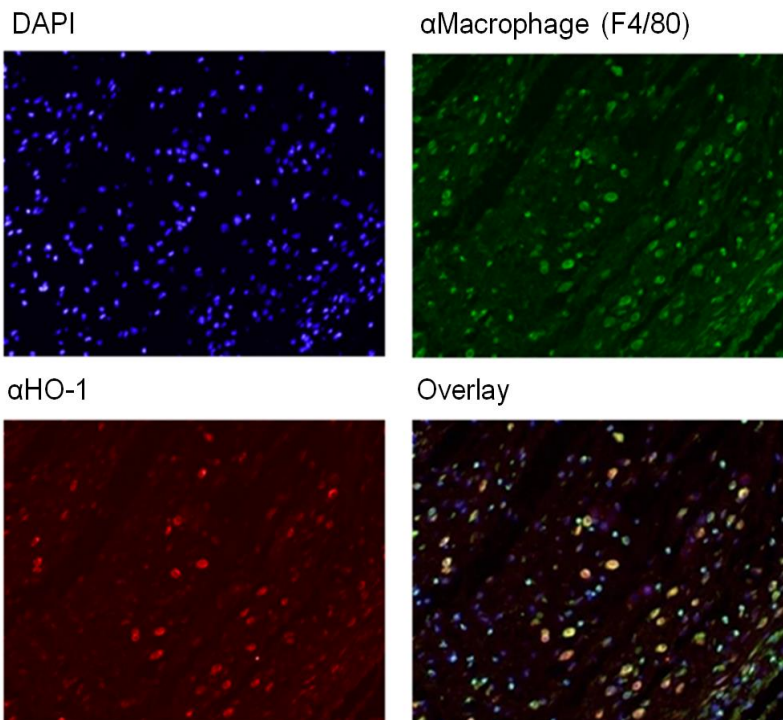


Figure 6.3. HO-1 expression in wounds. (A). HO-1 mRNA expression in unwounded (control) skin at day 0 and wounds after 7 days for the different treatments compared to control skin; (B) HO-1 protein expression in control, and early and late RIPC-treated wounds after 7 days of healing. Region above the marked blue line is the epidermis and underneath the blue line is the dermal layer (bars represent 1 mm); (C) Scored HO-1 protein staining in epidermis and dermis of the wounds after 7 days in arbitrary units (AU). Data are expressed as mean \pm SD. No significant differences were observed between the different groups: no RIPC ($n = 8$), RIPC 5 min ($n = 6$) and RIPC 24 h ($n = 6$).



Supplemental figure S6.2. Co-localization of HO-1 and macrophages during excisional wound healing. Fluorescent staining from a previous experiment on excisional wound healing in C57Bl/6 mice at day 2 post wounding, showing cell nuclei stained with DAPI (blue), HO-1 (red), macrophages stained for F4/80 (green), and an overlay. The overlay picture clearly shows co-localization (orange) of HO-1 and macrophages.

Effects of RIPC on Wound Morphology and Collagen Deposition

To determine if RIPC modulates other processes during wound repair, we performed H&E staining to examine wound morphology, and AZAN staining to investigate the effects on collagen deposition.

H&E staining revealed that the wound area could be easily distinguished from non-injured skin by a disruption of the epidermis, subcutaneous fat, and muscle layers. Figure 6.4A shows H&E staining of day-7 wounds from mice treated with early and late RIPC, and control mice (left). At the surface of the wound, the re-epithelialized tissue had marked epithelial hyperplasia under the crust of the wound. More distally, the highly cellularized granulation tissue was less organized, and consisted of inflammatory cells, such as macrophages, granulocytes, and (myo)fibroblasts. Variations in the thickness and size of the wounds were observed between the tissue sections of the animals. When comparing the different treatment groups, no differences were found in morphology and in the presence of different cell types in day-7 wounds.

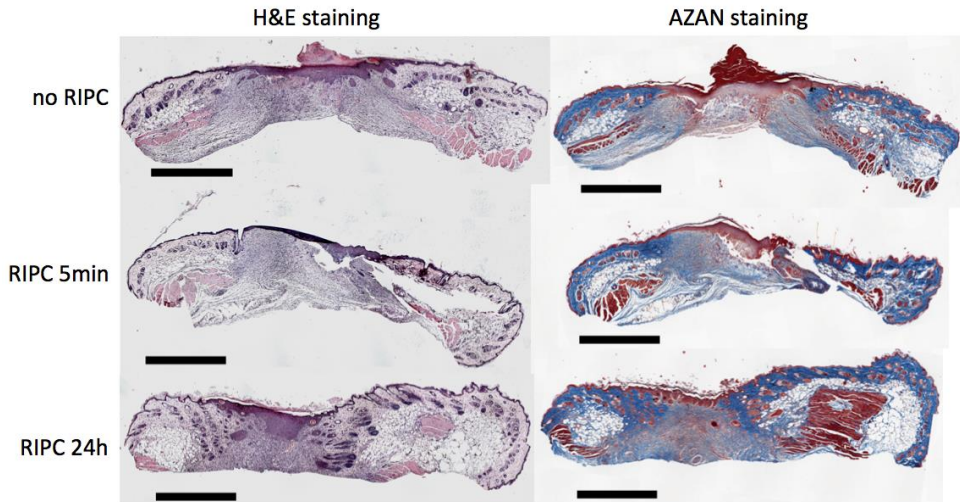
Figure 6.4A (right) shows collagen deposition by AZAN staining. The wound regions were marked after which the level of collagen deposition in the wounds were measured and corrected for the total wound area (Figure 6.4B). No significant differences were observed between the different groups. Summarizing, RIPC did not affect wound morphology and collagen deposition of day-7 wounds.

Discussion

We postulated that RIPC increases HO-1 induction and improves cutaneous wound repair. RIPC induced HO-1 in kidney, heart, and skeletal muscles, but not in the skin. Although RIPC had previously been shown to target the skin (44-46, 48), both early and late RIPC did not affect cutaneous wound closure. In addition, skin morphology and collagen deposition at day-7 wounds did not change after early or late RIPC.

RIPC-mediated protection to organs seems therefore tissue-specific and/or dependent on the insult. Organ- and time-specific protective effects of RIPC have also previously been demonstrated. For example, RIPC does not improve wound healing in small bowel anastomoses (74, 75). Although late RIPC (24 h) attenuates ischemia/reperfusion injury (IRI) in muscle flaps, it is ineffective in adipocutaneous flaps (76). In contrast, early RIPC (30 min) enhances adipocutaneous flap survival (77). IPC improves the survival of myocutaneous and skin flaps subjected to secondary ischemia of 1h in rats (78, 79). Since these RIPC protocols vary from ours, and IPC and RIPC are different procedures, these studies cannot be directly extrapolated to our study. The protective actions of RIPC are thus dependent on the targeted organ and the type of RIPC treatment (80). Remote preconditioning by trauma (RPCT) by abdominal incision, has previously been reported to improve cardiac outcome following induced heart infarcts by coronary artery occlusion in murine and canine models (81-83). Similarly, the inflicted injuries in our study could have led to the induction of overlapping cytoprotective pathways. When these RPCT-induced protective pathways were stronger than the effects by RIPC or used similar pathways, this could explain in part the observed lack of protective effects by RIPC on cutaneous wound repair. Similar protective pathways of RIPC and RPCT include the activation of protein kinase C, mitogen-activated protein kinases and mitochondrial potassium ATP channels, bradykinin and adenosine (81, 83, 84).

A).



B).

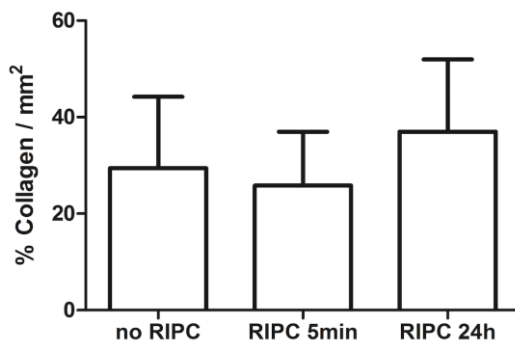
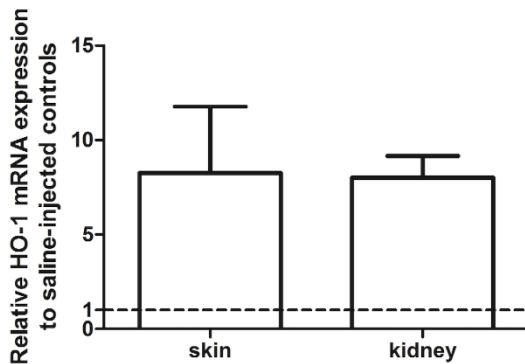


Figure 6.4. Effects of early and late RIPC on morphology of 7-day-old excisional wounds. **(A)** H&E and AZAN staining were performed to evaluate wound morphology (bars represent 1 mm); **(B)** Quantification of collagen deposition to assess the level of wound remodeling using AZAN staining. Data are expressed as mean \pm SD. No significant differences were observed between the different groups: no RIPC ($n = 8$), RIPC 5 min ($n = 6$) and RIPC 24 h ($n = 6$).

Previously, the stress enzyme HO-1 was found to be important in wound repair and is generally expressed at wound sites (70, 85, 86). HO-1 and HO-2 knockout mice showed a delayed wound repair; whereas, induction of HO-1 or administration of its effector molecule bilirubin accelerated wound repair (19, 20, 55). Since some of the protective effects of RIPC were shown to be dependent on HO-1 expression in IRI of diverse organs, like the liver (23, 24, 26), lungs (33), and intestines (28), we further evaluated the role of RIPC on HO-1 in excisional wound healing. HO-1-*luc* Tg mice allowed monitoring the effects of RIPC on HO-1 promoter activity levels in different organs in real-time. 6 and 24 h after RIPC treatment, HO-1 promoter activity was significantly induced compared to 1h after RIPC. This correlates well with our RT-PCR data showing significantly increased endogenous HO-1 mRNA levels in muscle, heart, and kidney 6h after RIPC treatment. However, despite RIPC improving cutaneous microcirculation (44), no HO-1 mRNA induction was found in the skin, and may

thus not affect the skin directly. HO-1 induction in the skin is possible using pharmacological preconditioning since we previously observed that i.p. administration of the HO-1 inducer cobalt protoporphyrin at a concentration of 25 mg/kg body weight in HO-1 *luc* Tg mice induced HO-1 mRNA specifically in the skin after 24 h (Supplemental figure S6.3). This underscores the tissue- and time-dependent effects of RIPC, which is probably due to the structural and physiological differences between different organs. Since organs that have induce HO-1 expression upon RIPC treatment correlate with the organs that are protected by RIPC, it is tempting to speculate that HO-1 facilitates these protective effects.



Supplemental figure S6.3. Pharmacological preconditioning with cobalt protoporphyrin (25 mg/kg body weight) in HO-1 *luc* Tg mice ($n = 6$) induced HO-1 mRNA expression in both the skin and kidney 24 h after treatment when compared to saline-injected control mice ($n = 6$). Dashed line represents the mRNA expression levels in the corresponding control organs after saline injection, which are set at 1. Data represents the relative mean \pm SD. One significant outlier was found in both skin and kidney group and therefore excluded in the graph.

Also the long-term protective effects of RIPC via activation of HO-1 were absent in the skin. Both HO-1 mRNA and protein expression levels were observed to be independent of RIPC treatment in the epidermal and dermal regions of day-7 wounds. Like others, we found HO-1-positive keratinocytes in the hyperproliferative epithelia of the wound margins covering the wound (70, 71, 87). In the dermis, we also observed HO-1-positive infiltrating leukocytes that are likely macrophages (70, 72, 88). HO-1-positive macrophages are thought to protect the wound environment against oxidative stress (70, 89). The pro-inflammatory HO substrate heme is abundantly released at the edges of the wound site and stimulates recruitment of leukocytes (70, 73, 87). HO-1 is thought to attenuate these inflammatory and oxidative triggers at the wound site.

The effect of both early and late RIPC on wound closure was monitored regularly. However, the (immuno-)histochemical and PCR analysis was only performed on day 7 wounds, which limits our insight in wound repair processes, like inflammatory signaling, during the first days. Using the HO-1-*luc* Tg mice we previously found that HO-1 promoter activity was indeed significantly induced on day 3 post-wounding, however the level of HO-1 promoter activity did not decline significantly at day 7 compared to day 3 (88). Although no effects in wound closure, collagen deposition, or HO-1 expression in the skin were observed, we cannot exclude that paracrine effects of HO-1 or other protective signaling pathways may have been triggered by RIPC. HO-effector molecules biliverdin, bilirubin, CO, and ferritin, have all shown to improve wound repair (20, 61-64), suggesting that RIPC-

induced HO-1 induction in various organs stimulate wound repair in a paracrine fashion. Interestingly, increased systemic levels of bilirubin augment vascular function (90, 91) and may contribute to the reported RIPC induced improvement of cutaneous microcirculation. In a previous study, no adverse effects of HO inhibition following RIPC were observed in a kidney injury model, suggesting that other mediators may have been protective (31). Alternative protective pathways triggered by RIPC include humoral, neural, or systemic anti-inflammatory, anti-apoptotic responses (22, 69). In addition, RIPC may have more effects in more stringent wound repair models where there is a shortage of cytoprotective molecules, such as in diabetic wound repair models and pressure ulcers (47). Although our method has shown to be effective in diverse animal models (32), other RIPC regimens may enhance these protective effects such as combinations with remote ischemic postconditioning (35, 36, 47). Recently, it was found that the sex of the animal may play a role in the efficacy of RIPC treatment, and was observed to be lower in experimental groups of mixed sexes, which we also used in our wound repair study (92).

Conclusions

RIPC treatment induced HO-1 mRNA expression in kidney, heart, and ligated muscle, and may therefore directly contribute to enhanced protection to injurious stressors and/or microcirculation in these tissues. However, RIPC did not alter HO-1 in the skin and was not modulated in day-7 skin wounds, demonstrating organ- and time-specific effects. Both early and late RIPC treatment did not affect dermal wound closure time, collagen deposition, or wound morphology. A better understanding of the mechanistic insight by which RIPC mediates organ protection is needed.

References

1. Rabello FB, Souza CD, Farina Junior JA. Update on hypertrophic scar treatment. *Clinics (Sao Paulo)*. 2014;69(8):565-73.
2. Eming SA, Martin P, Tomic-Canic M. Wound repair and regeneration: mechanisms, signaling, and translation. *Sci Transl Med*. 2014;6(265):265sr6.
3. Sidgwick GP, Bayat A. Extracellular matrix molecules implicated in hypertrophic and keloid scarring. *J Eur Acad Dermatol Venereol*. 2012;26(2):141-52.
4. Grice EA, Segre JA. Interaction of the microbiome with the innate immune response in chronic wounds. *Adv Exp Med Biol*. 2012;946:55-68.
5. Pereira RF, Bartolo PJ. Traditional Therapies for Skin Wound Healing. *Adv Wound Care (New Rochelle)*. 2016;5(5):208-29.
6. Aarabi S, Longaker MT, Gurtner GC. Hypertrophic scar formation following burns and trauma: new approaches to treatment. *PLoS Med*. 2007;4(9):e234.
7. Tziotzios C, Profyris C, Sterling J. Cutaneous scarring: Pathophysiology, molecular mechanisms, and scar reduction therapeutics Part II. Strategies to reduce scar formation after dermatologic procedures. *J Am Acad Dermatol*. 2012;66(1):13-24; quiz 5-6.
8. Chen QY, Wang GG, Li W, Jiang YX, Lu XH, Zhou PP. Heme Oxygenase-1 Promotes Delayed Wound Healing in Diabetic Rats. *J Diabetes Res*. 2016;2016:9726503.
9. Ahanger AA, Prawez S, Leo MD, Kathirvel K, Kumar D, Tandan SK, et al. Pro-healing potential of hemin: an inducer of heme oxygenase-1. *Eur J Pharmacol*. 2010;645(1-3):165-70.
10. Panchatcharam M, Miriyala S, Gayathri VS, Suguna L. Curcumin improves wound healing by modulating collagen and decreasing reactive oxygen species. *Mol Cell Biochem*. 2006;290(1-2):87-96.
11. Tejada S, Manayi A, Daglia M, Nabavi SF, Sureda A, Hajheydari Z, et al. Wound Healing Effects of Curcumin: A Short Review. *Curr Pharm Biotechnol*. 2016;17(11):1002-7.
12. Kant V, Gopal A, Kumar D, Pathak NN, Ram M, Jangir BL, et al. Curcumin-induced angiogenesis hastens wound healing in diabetic rats. *J Surg Res*. 2015;193(2):978-88.
13. Cremers NA, Lundvig DM, van Dalen SC, Schelbergen RF, van Lent PL, Szarek WA, et al. Curcumin-induced heme oxygenase-1 expression prevents H₂O₂-induced cell death in wild type and heme oxygenase-2 knockout adipose-derived mesenchymal stem cells. *Int J Mol Sci*. 2014;15(10):17974-99.
14. Akbik D, Ghadirri M, Chrzanowski W, Rohanzadeh R. Curcumin as a wound healing agent. *Life Sci*. 2014;116(1):1-7.
15. Wagener FA, Volk HD, Willis D, Abraham NG, Soares MP, Adema GJ, et al. Different faces of the heme-heme oxygenase system in inflammation. *Pharmacol Rev*. 2003;55(3):551-71.
16. Gozzelino R, Jeney V, Soares MP. Mechanisms of cell protection by heme oxygenase-1. *Annu Rev Pharmacol Toxicol*. 2010;50:323-54.
17. Morse D, Choi AM. Heme oxygenase-1: from bench to bedside. *Am J Respir Crit Care Med*. 2005;172(6):660-70.
18. Gozzelino R, Soares MP. Coupling heme and iron metabolism via ferritin H chain. *Antioxid Redox Signal*. 2014;20(11):1754-69.
19. Grochot-Przeczek A, Lach R, Mis J, Skrzypek K, Gozdecka M, Sroczyńska P, et al. Heme oxygenase-1 accelerates cutaneous wound healing in mice. *PLoS One*. 2009;4(6):e5803.
20. Ahanger AA, Leo MD, Gopal A, Kant V, Tandan SK, Kumar D. Pro-healing effects of bilirubin in open excision wound model in rats. *Int Wound J*. 2016;13(3):398-402.
21. Souza Filho MV, Loiola RT, Rocha EL, Simao AF, Gomes AS, Souza MH, et al. Hind limb ischemic preconditioning induces an anti-inflammatory response by remote organs in rats. *Braz J Med Biol Res*. 2009;42(10):921-9.
22. Hausenloy DJ, Yellon DM. Remote ischaemic preconditioning: underlying mechanisms and clinical application. *Cardiovasc Res*. 2008;79(3):377-86.
23. Lai IR, Chang KJ, Chen CF, Tsai HW. Transient limb ischemia induces remote preconditioning in liver among rats: the protective role of heme oxygenase-1. *Transplantation*. 2006;81(9):1311-7.
24. Tapuria N, Junnarkar SP, Dutt N, Abu-Amara M, Fuller B, Seifalian AM, et al. Effect of remote ischemic preconditioning on hepatic microcirculation and function in a rat model of hepatic ischemia reperfusion injury. *HPB (Oxford)*. 2009;11(2):108-17.
25. Kageyama S, Hata K, Tanaka H, Hirao H, Kubota T, Okamura Y, et al. Intestinal ischemic preconditioning ameliorates hepatic ischemia/reperfusion injury in rats: role of heme oxygenase 1 in the second window of protection. *Liver Transpl*. 2015;21(1):112-22.

26. Wang Y, Shen J, Xiong X, Xu Y, Zhang H, Huang C, et al. Remote ischemic preconditioning protects against liver ischemia-reperfusion injury via heme oxygenase-1-induced autophagy. *PLoS One*. 2014;9(6):e98834.
27. Thielmann M, Kottenberg E, Kleinbongard P, Wendt D, Gedik N, Pasa S, et al. Cardioprotective and prognostic effects of remote ischaemic preconditioning in patients undergoing coronary artery bypass surgery: a single-centre randomised, double-blind, controlled trial. *Lancet*. 2013;382(9892):597-604.
28. Saeki I, Matsuura T, Hayashida M, Taguchi T. Ischemic preconditioning and remote ischemic preconditioning have protective effect against cold ischemia-reperfusion injury of rat small intestine. *Pediatr Surg Int*. 2011;27(8):857-62.
29. Kharbanda RK, Mortensen UM, White PA, Kristiansen SB, Schmidt MR, Hoschtitzky JA, et al. Transient limb ischemia induces remote ischemic preconditioning in vivo. *Circulation*. 2002;106(23):2881-3.
30. Lim SY, Hausenloy DJ. Remote ischemic conditioning: from bench to bedside. *Front Physiol*. 2012;3:27.
31. Wever KE, Masereeuw R, Wagener FA, Verweij VG, Peters JG, Pertijs JC, et al. Humoral signalling compounds in remote ischaemic preconditioning of the kidney, a role for the opioid receptor. *Nephrol Dial Transplant*. 2013;28(7):1721-32.
32. Wever KE, Warle MC, Wagener FA, van der Hoorn JW, Masereeuw R, van der Vliet JA, et al. Remote ischaemic preconditioning by brief hind limb ischaemia protects against renal ischaemia-reperfusion injury: the role of adenosine. *Nephrol Dial Transplant*. 2011;26(10):3108-17.
33. Jan WC, Chen CH, Tsai PS, Huang CJ. Limb ischemic preconditioning mitigates lung injury induced by haemorrhagic shock/resuscitation in rats. *Resuscitation*. 2011;82(6):760-6.
34. Narayanan SV, Dave KR, Perez-Pinzon MA. Ischemic preconditioning and clinical scenarios. *Curr Opin Neurol*. 2013;26(1):1-7.
35. Depre C, Park JY, Shen YT, Zhao X, Qiu H, Yan L, et al. Molecular mechanisms mediating preconditioning following chronic ischemia differ from those in classical second window. *Am J Physiol Heart Circ Physiol*. 2010;299(3):H752-62.
36. Shen YT, Depre C, Yan L, Park JY, Tian B, Jain K, et al. Repetitive ischemia by coronary stenosis induces a novel window of ischemic preconditioning. *Circulation*. 2008;118(19):1961-9.
37. Hausenloy DJ, Boston-Griffiths E, Yellon DM. Cardioprotection during cardiac surgery. *Cardiovasc Res*. 2012;94(2):253-65.
38. Hausenloy DJ, Candilio L, Evans R, Ariti C, Jenkins DP, Kolvekar S, et al. Remote Ischemic Preconditioning and Outcomes of Cardiac Surgery. *N Engl J Med*. 2015;373(15):1408-17.
39. Sukkar L, Hong D, Wong MG, Badve SV, Rogers K, Perkovic V, et al. Effects of ischaemic conditioning on major clinical outcomes in people undergoing invasive procedures: systematic review and meta-analysis. *BMJ*. 2016;355:i5599.
40. Garratt KN, Whittaker P, Przyklenk K. Remote Ischemic Conditioning and the Long Road to Clinical Translation: Lessons Learned From ERICCA and RIPHeart. *Circ Res*. 2016;118(7):1052-4.
41. King N, Dieberg G, Smart NA. Remote ischaemic pre-conditioning does not affect clinical outcomes following coronary Artery bypass grafting. A systematic review and meta-analysis. *Clinical Trials and Regulatory Science in Cardiology*. 2016;17:1-8.
42. Przyklenk K. Ischaemic conditioning: pitfalls on the path to clinical translation. *Br J Pharmacol*. 2015;172(8):1961-73.
43. Dorresteyn MJ, Paine A, Zilian E, Fenten MG, Frenzel E, Janciauskiene S, et al. Cell-type-specific downregulation of heme oxygenase-1 by lipopolysaccharide via Bach1 in primary human mononuclear cells. *Free Radic Biol Med*. 2015;78:224-32.
44. Kraemer R, Lorenzen J, Kabani M, Herold C, Busche M, Vogt PM, et al. Acute effects of remote ischemic preconditioning on cutaneous microcirculation--a controlled prospective cohort study. *BMC Surg*. 2011;11:32.
45. Kolbenschlag J, Sogorski A, Kapalschinski N, Harati K, Lehnhardt M, Daigeler A, et al. Remote Ischemic Conditioning Improves Blood Flow and Oxygen Saturation in Pedicled and Free Surgical Flaps. *Plast Reconstr Surg*. 2016;138(5):1089-97.
46. Masaoka K, Asato H, Umekawa K, Imanishi M, Suzuki A. Value of remote ischaemic preconditioning in rat dorsal skin flaps and clamping time. *J Plast Surg Hand Surg*. 2016;50(2):107-10.
47. Shaked G, Czeiger D, Abu Arar A, Katz T, Harman-Boehm I, Sebbag G. Intermittent cycles of remote ischemic preconditioning augment diabetic foot ulcer healing. *Wound Repair Regen*. 2015;23(2):191-6.
48. Epps JA, Smart NA. Remote ischaemic conditioning in the context of type 2 diabetes and neuropathy: the case for repeat application as a novel therapy for lower extremity ulceration. *Cardiovasc Diabetol*. 2016;15(1):130.

49. Wever KE, Wagener FA, Frielink C, Boerman OC, Scheffer GJ, Allison A, et al. Diannexin protects against renal ischemia reperfusion injury and targets phosphatidylserines in ischemic tissue. *PLoS One*. 2011;6(8):e24276.
50. Su H, van Dam GM, Buis CI, Visser DS, Hesselink JW, Schuurs TA, et al. Spatiotemporal expression of heme oxygenase-1 detected by in vivo bioluminescence after hepatic ischemia in HO-1/Luc mice. *Liver Transpl*. 2006;12(11):1634-9.
51. Shin HJ, Won NH, Lee HW. Remote ischemic preconditioning prevents lipopolysaccharide-induced liver injury through inhibition of NF-kappaB activation in mice. *J Anesth*. 2014;28(6):898-905.
52. Abu-Amara M, Yang SY, Quaglia A, Rowley P, Tapuria N, Seifalian AM, et al. Effect of remote ischemic preconditioning on liver ischemia/reperfusion injury using a new mouse model. *Liver Transpl*. 2011;17(1):70-82.
53. Cai ZP, Parajuli N, Zheng X, Becker L. Remote ischemic preconditioning confers late protection against myocardial ischemia-reperfusion injury in mice by upregulating interleukin-10. *Basic Res Cardiol*. 2012;107(4):277.
54. van den Brand BT, Vermeij EA, Waterborg CE, Arntz OJ, Kracht M, Bennink MB, et al. Intravenous delivery of HIV-based lentiviral vectors preferentially transduces F4/80+ and Ly-6C+ cells in spleen, important target cells in autoimmune arthritis. *PLoS One*. 2013;8(2):e55356.
55. Lundvig DM, Scharstuhl A, Cremers NA, Pennings SW, te Paske J, van Rheden R, et al. Delayed cutaneous wound closure in HO-2 deficient mice despite normal HO-1 expression. *J Cell Mol Med*. 2014;18(12):2488-98.
56. Hadi AM, Mouchaers KT, Schaliij I, Grunberg K, Meijer GA, Vonk-Noordegraaf A, et al. Rapid quantification of myocardial fibrosis: a new macro-based automated analysis. *Cell Oncol (Dordr)*. 2011;34(4):343-54.
57. Bjornsson B, Winblad A, Bojmar L, Sundqvist T, Gullstrand P, Sandstrom P. Conventional, but not remote ischemic preconditioning, reduces iNOS transcription in liver ischemia/reperfusion. *World J Gastroenterol*. 2014;20(28):9506-12.
58. He X, Zhao M, Bi XY, Yu XJ, Zang WJ. Delayed preconditioning prevents ischemia/reperfusion-induced endothelial injury in rats: role of ROS and eNOS. *Lab Invest*. 2013;93(2):168-80.
59. Zhang W, Contag PR, Hardy J, Zhao H, Vreman HJ, Hajdena-Dawson M, et al. Selection of potential therapeutics based on in vivo spatiotemporal transcription patterns of heme oxygenase-1. *J Mol Med (Berl)*. 2002;80(10):655-64.
60. Zarjou A, Kim J, Traylor AM, Sanders PW, Balla J, Agarwal A, et al. Paracrine effects of mesenchymal stem cells in cisplatin-induced renal injury require heme oxygenase-1. *Am J Physiol Renal Physiol*. 2011;300(1):F254-62.
61. Halilovic A, Patil KA, Bellner L, Marrazzo G, Castellano K, Cullara G, et al. Knockdown of heme oxygenase-2 impairs corneal epithelial cell wound healing. *J Cell Physiol*. 2011;226(7):1732-40.
62. Dulak J, Deshane J, Jozkowicz A, Agarwal A. Heme oxygenase-1 and carbon monoxide in vascular pathobiology: focus on angiogenesis. *Circulation*. 2008;117(2):231-41.
63. Ahanger AA, Prawez S, Kumar D, Prasad R, Amarpal, Tandan SK, et al. Wound healing activity of carbon monoxide liberated from CO-releasing molecule (CO-RM). *Naunyn Schmiedebergs Arch Pharmacol*. 2011;384(1):93-102.
64. Coffman LG, Parsonage D, D'Agostino R, Jr., Torti FM, Torti SV. Regulatory effects of ferritin on angiogenesis. *Proc Natl Acad Sci U S A*. 2009;106(2):570-5.
65. Penna C, Granata R, Tocchetti CG, Gallo MP, Alloati G, Pagliaro P. Endogenous Cardioprotective Agents: Role in Pre and Postconditioning. *Curr Drug Targets*. 2015;16(8):843-67.
66. Guimaraes Filho MA, Cortez E, Garcia-Souza EP, Soares Vde M, Moura AS, Carvalho L, et al. Effect of remote ischemic preconditioning in the expression of IL-6 and IL-10 in a rat model of liver ischemia-reperfusion injury. *Acta Cir Bras*. 2015;30(7):452-60.
67. Chevion M, Leibowitz S, Aye NN, Novogrodsky O, Singer A, Avizemer O, et al. Heart protection by ischemic preconditioning: a novel pathway initiated by iron and mediated by ferritin. *J Mol Cell Cardiol*. 2008;45(6):839-45.
68. Andreadou I, Iliodromitis EK, Rassaf T, Schulz R, Papapetropoulos A, Ferdinandy P. The role of gasotransmitters NO, H2S and CO in myocardial ischaemia/reperfusion injury and cardioprotection by preconditioning, postconditioning and remote conditioning. *Br J Pharmacol*. 2015;172(6):1587-606.
69. Tapuria N, Kumar Y, Habib MM, Abu Amara M, Seifalian AM, Davidson BR. Remote ischemic preconditioning: a novel protective method from ischemia reperfusion injury--a review. *J Surg Res*. 2008;150(2):304-30.

70. Hanselmann C, Mauch C, Werner S. Haem oxygenase-1: a novel player in cutaneous wound repair and psoriasis? *Biochem J.* 2001;353(Pt 3):459-66.
71. Kampfer H, Kolb N, Manderscheid M, Wetzler C, Pfeilschifter J, Frank S. Macrophage-derived heme-oxygenase-1: expression, regulation, and possible functions in skin repair. *Mol Med.* 2001;7(7):488-98.
72. Schurmann C, Seitz O, Klein C, Sader R, Pfeilschifter J, Muhl H, et al. Tight spatial and temporal control in dynamic basal to distal migration of epithelial inflammatory responses and infiltration of cytoprotective macrophages determine healing skin flap transplants in mice. *Ann Surg.* 2009;249(3):519-34.
73. Wagener FA, van Beurden HE, von den Hoff JW, Adema GJ, Figdor CG. The heme-heme oxygenase system: a molecular switch in wound healing. *Blood.* 2003;102(2):521-8.
74. Holzner PA, Kulemann B, Kuesters S, Timme S, Hoepfner J, Hopt UT, et al. Impact of remote ischemic preconditioning on wound healing in small bowel anastomoses. *World J Gastroenterol.* 2011;17(10):1308-16.
75. Colak T, Turkmenoglu O, Dag A, Polat A, Comelekoglu U, Bagdatoglu O, et al. The effect of remote ischemic preconditioning on healing of colonic anastomoses. *J Surg Res.* 2007;143(2):200-5.
76. Kuntscher MV, Kastell T, Engel H, Gebhard MM, Heitmann C, Germann G. Late remote ischemic preconditioning in rat muscle and adipocutaneous flap models. *Ann Plast Surg.* 2003;51(1):84-90.
77. Kuntscher MV, Schirmbeck EU, Menke H, Klar E, Gebhard MM, Germann G. Ischemic preconditioning by brief extremity ischemia before flap ischemia in a rat model. *Plast Reconstr Surg.* 2002;109(7):2398-404.
78. Shah AA, Arias JE, Thomson JG. The effect of ischemic preconditioning on secondary ischemia in myocutaneous flaps. *J Reconstr Microsurg.* 2009;25(9):527-31.
79. Zahir KS, Syed SA, Zink JR, Restifo RJ, Thomson JG. Ischemic preconditioning improves the survival of skin and myocutaneous flaps in a rat model. *Plast Reconstr Surg.* 1998;102(1):140-50; discussion 51-2.
80. Kolh P. Remote ischaemic pre-conditioning in cardiac surgery: benefit or not? *Eur Heart J.* 2014;35(3):141-3.
81. Gross GJ, Baker JE, Moore J, Falck JR, Nithipatikom K. Abdominal surgical incision induces remote preconditioning of trauma (RPCT) via activation of bradykinin receptors (BK2R) and the cytochrome P450 epoxygenase pathway in canine hearts. *Cardiovasc Drugs Ther.* 2011;25(6):517-22.
82. Gross GJ, Hsu A, Gross ER, Falck JR, Nithipatikom K. Factors mediating remote preconditioning of trauma in the rat heart: central role of the cytochrome p450 epoxygenase pathway in mediating infarct size reduction. *J Cardiovasc Pharmacol Ther.* 2013;18(1):38-45.
83. Jones WK, Fan GC, Liao S, Zhang JM, Wang Y, Weintraub NL, et al. Peripheral nociception associated with surgical incision elicits remote nonischemic cardioprotection via neurogenic activation of protein kinase C signaling. *Circulation.* 2009;120(11 Suppl):S1-9.
84. Chai Q, Liu J, Hu Y. Cardioprotective effect of remote preconditioning of trauma and remote ischemia preconditioning in a rat model of myocardial ischemia/reperfusion injury. *Exp Ther Med.* 2015;9(5):1745-50.
85. Wagener FA, Scharstuhl A, Tyrrell RM, Von den Hoff JW, Jozkowicz A, Dulak J, et al. The heme-heme oxygenase system in wound healing; implications for scar formation. *Curr Drug Targets.* 2010;11(12):1571-85.
86. Lundvig DM, Immenschuh S, Wagener FA. Heme oxygenase, inflammation, and fibrosis: the good, the bad, and the ugly? *Front Pharmacol.* 2012;3:81.
87. auf dem Keller U, Kumin A, Braun S, Werner S. Reactive oxygen species and their detoxification in healing skin wounds. *J Investig Dermatol Symp Proc.* 2006;11(1):106-11.
88. Cremers NA, Suttorp M, Gerritsen MM, Wong RJ, van Run-van Breda C, van Dam GM, et al. Mechanical Stress Changes the Complex Interplay Between HO-1, Inflammation and Fibrosis, During Excisional Wound Repair. *Front Med (Lausanne).* 2015;2:86.
89. Ishii T, Itoh K, Sato H, Bannai S. Oxidative stress-inducible proteins in macrophages. *Free Radic Res.* 1999;31(4):351-5.
90. Dekker D, Dorresteyn MJ, Pijnenburg M, Heemskerk S, Rasing-Hoogveld A, Burger DM, et al. The bilirubin-increasing drug atazanavir improves endothelial function in patients with type 2 diabetes mellitus. *Arterioscler Thromb Vasc Biol.* 2011;31(2):458-63.
91. Maruhashi T, Soga J, Fujimura N, Idei N, Mikami S, Iwamoto Y, et al. Hyperbilirubinemia, augmentation of endothelial function, and decrease in oxidative stress in Gilbert syndrome. *Circulation.* 2012;126(5):598-603.

92. Wever KE, Hooijmans CR, Riksen NP, Sterenborg TB, Sena ES, Ritskes-Hoitinga M, et al. Determinants of the Efficacy of Cardiac Ischemic Preconditioning: A Systematic Review and Meta-Analysis of Animal Studies. *PLoS One*. 2015;10(11):e0142021.

Chapter 7

Heme scavenging discriminates between tissue survival and immune activation.

Cremers NAJ, Wong RJ, Helmich P, Bilos A, Brouwer KM, van Dam GM, Carels CEL, Kuijpers-Jagtman AM, Immenschuh S, Matzinger P, Wagener FADTG.

To be submitted.

Abstract

Following injury, the immune system gets activated by released danger signals, including heme, to eliminate injurious stressors. However, how the surrounding tissue is protected from collateral damage remains still unclear. Better understanding the protective mechanisms following remote ischemic preconditioning (RIPC) may give us clues. When a small local injury is inflicted to a remote tissue as the leg, organs as the heart and kidney get protected from subsequent injuries. High amounts of danger signals activate immune cells, whereas low levels may promote tissue protection. Since low levels of heme are directly scavenged by hemopexin (hpx), we postulate that RIPC-mediated protection acts via the formation of heme-hpx complexes, activating cytoprotective genes including heme oxygenase 1 (HO-1). Serum heme levels, HO-1 promoter activity, and HO-1 expression were measured following RIPC in HO-1-*luc* transgenic mice. After RIPC, free heme levels increase rapidly but mildly. HO-1 expression gets induced both locally in the ligated skeletal muscle and remotely in the kidney and heart. The majority of HO-1-positive cells also expressed LRP-1, the only known receptor for heme-hpx complexes. Systemic protection may be mediated by the formation of tissue survival factors (TSFs). Heme-hpx complexes bind to LRP-1, subsequently activating nrf2-responsive cytoprotective genes, including HO-1. We propose therefore a “tissue survival model” next to the “danger model” where TSFs as the heme-hpx complex prepares the tissue for injurious insults by inducing cytoprotective genes. When the tissue is warned, hpx is depleted and free heme can no longer form TSFs, but acts as danger signal by binding to TLR4 and alerting the immune system.

Keywords: RIPC, heme, heme oxygenase-1, hemopexin, LRP-1, tissue survival factor, danger signals.

Abbreviations

CoPP	Cobalt protoporphyrin
DAMP	Damage-associated molecular patterns
Hb	Hemoglobin
Hp	Haptoglobin
hpx	Hemopexin
HO-1	Heme oxygenase-1
iNOS	Inducible nitric oxide synthase
IRI	Ischemia-reperfusion-injury
LRP-1	LDL receptor-related protein-1
nrf2	Nuclear factor erythroid 2-related factor 2
RIPC	Remote ischemic preconditioning
ROS	Reactive oxygen species
SnPP	Tin protoporphyrin
TLR	Toll-like receptors
TSF	Tissue survival factor

Introduction

Following injury, endogenous alarm signals (1) activate the immune system to eliminate possible pathogenic invaders. Unfortunately, the resulting immune response can also cause considerable collateral damage (1, 2), both locally and distally (via the elaboration of soluble cytokines, chemokines and other signaling entities) that can result in tissue injury, organ failure and fatality (3-5). Therefore, harnessing tissue damage is as important for survival as activating immunity (3, 6, 7), and a powerful, but little known, aspect of physiology is the bodily response that protects distant organs from such damage. This can be seen in studies on remote ischemic preconditioning (RIPC), where short ischemic insults are induced in remote non-vital tissues (e.g., skeletal muscle of the legs) leading to enhanced tolerance against a subsequent stress in vital organs (e.g. heart, brain, kidney) (8). RIPC protects different organs and tissues in pre-clinical models. For example, RIPC has been shown to reduce myocardial injury after ischemia-reperfusion injury (IRI) in models of surgery and organ transplantation (9). Although the potential for clinical use is obvious, the responsible molecular mechanisms remain elusive (10). If the underlying mechanisms could be found, it might be possible to mimic them, rather than do the damage that elicits them.

One intriguing possibility arises from the “Danger model” (1). Given that high local concentrations of alarm signals act as immune stimulators, we postulated that lower concentrations of some of those same molecules might act distally to elicit tissue-protective mechanisms. In effect, they might act as “Tissue Survival Factors” (TSFs) to trigger tissue protection. This is commonly accepted for exogenous alarm signals, such as LPS, where pretreatment with low doses is well known to protect against the effects of subsequent higher doses (11). We postulated that this may also be true of endogenous alarm signals. To test this idea, we studied the alarm properties of heme.

Heme is the prosthetic group of various hemoproteins and indispensable for many cellular processes. However, heme is also involved in the pathology of many different pathologies, including sickle cell disease, malaria, sepsis and kidney failure. Excess of free heme can be detrimental to tissues by mediating oxidative injury (by catalyzing the formation of reactive oxygen species (ROS) via the Fenton reaction). Previously, we and others have shown that heme is released following injury (12) and acts as an alarm signal to induce inflammatory responses (13-16). We also demonstrated that heme induces ICAM-1 expression in vascular endothelial cells and causes recruitment of granulocytes and macrophages (12, 15, 16). Based on these findings, we were the first to postulate that heme could act as a danger molecule and promote inflammation (12). Later it was found that heme can indeed activate TLR-4 (17), and induce NLRP3 inflammasome formation, thus promoting pro-inflammatory signaling (18, 19). Heme has also been described to be part of the damage-associated molecular patterns (DAMP)-family and alarmins (18, 20). Thus, in high local concentrations, heme can act as a danger signal and alert the immune system.

In lower concentrations, heme has also been shown to mediate protective effects. For example, several *in vitro* and *in vivo* pre-clinical studies showed that administration of low doses of heme resulted in protection against diabetes, human immunodeficiency virus replication, and heart injury (21-26). In addition, administration of hemoglobin before provoking rhabdomyolysis in rats prevented kidney failure and drastically reduced mortality, and was dependent on HO activity. Induction of HO-activity may be generally beneficial for oxidative and inflammatory diseases and immuno-suppressed states (27, 28).

To test whether heme can also act as a TSF, and to elucidate the mechanisms involved, we assessed whether heme gets released following RIPC treatment and whether this was associated with induction of cytoprotective pathways.

Several protective pathways of RIPC have been proposed, including the release or induction of erythropoietin, bradykinin, adenosin, glucagon, endogenous opioids, IL-10, nitrates, CXCL12, HIF-1 α , or heme oxygenase (HO)-1 (29). When cardiac infarction was induced in rabbits, RIPC was found to attenuate the cardiac infarction size compared to naive rabbits. Most likely, RIPC-mediated protective factors are released into the serum, as transfer of serum from RIPC-treated rabbits to naive rabbits still protected induced cardiac infarct size in the recipient naive rabbits (30).

Pharmacological preconditioning with low levels of heme may lead to tissue protection. Interestingly, in IRI models of the heart, liver, and lung, RIPC-mediated protection was dependent on the expression of the cytoprotective enzyme HO-1, emphasized by abrogated protection when HO activity was inhibited (31-34). HO is one of the most important cytoprotective enzymes involved in the protection against oxidative stress and resolution of inflammation (35, 36). HO degrades heme into biliverdin/bilirubin, free iron, and carbon monoxide (CO). Ferritin is co-induced by HO-derived iron and is important for protection against iron-induced ROS formation (37). How HO-1 mediates this protection is not yet completely understood, but it may be related to its antioxidant activities and attenuation of vascular adhesion molecule expression (16, 38-40). The HO-1 isoform can be induced by a variety of stimuli (41), among which heme, and pharmacological induction can be used as preconditioning strategy against subsequent stresses (28), such as IRI in the lung, liver, intestine, pancreas, and kidney (42-47).

Since RIPC protects against heart failure, we aimed to investigate the role of HO-1 in regulating RIPC-mediated protective effects. Although HO-1 has been demonstrated to be important in RIPC-mediated protection in diverse organs, it is not yet clear how this protective mechanism is triggered. LRP-1 is ubiquitously expressed in many cell types, including fibroblasts, macrophages, and endothelial cells in diverse organs, where it activates protective signaling pathways.

A dual role for heme is proposed with heme in complex with hpx promoting protective TSF signaling, whereas free heme acts as danger signal, alerts the immune system and promotes inflammation. We postulate that heme gets released following RIPC and acts, by binding to hemopexin (hpx), as a TSF signal. This heme-hpx-complex binds to its only receptor LRP-1 that next activates tissue protective pathways via nrf2-responsive HO-1 signaling.

Materials and methods

Animals

30 female mice (strain: HO-1-*luc* FVB/ N-Tg background) of 4-5 months in age and weighing 22-31 g (25.9 \pm 2.3 g) were provided with food and water *ad libitum* and maintained on a 12h light/dark cycle and specific pathogen-free housing conditions at the Central Animal Facility in Nijmegen. Details on the housing conditions have been previously described (48). In these mice, the transgene consists of the full-length mouse HO-1 promoter fused to the reporter gene luciferase (*luc*). Mice were originally derived from Stanford University (Stanford, CA) (49). An overview of our experimental design is shown in Table 7.1. All mice were randomly

assigned to treatment or control groups. All outcomes were measured by an observer who was blinded for the allocation of the animals to the experimental groups, when possible. No animals died during the experiments, nor were excluded in our data analyses.

Table 7.1. Overview animal experiments.

Aim	Measurement	Animals (n)
Investigate the effects of RIPC on HO-1 promoter activity	HO-1 promoter activity at 1, 6 and 24h after RIPC treatment	6
Investigate the effects of RIPC on gene and protein expression during time	HO-1 mRNA levels at 0, 1, 6, and 24h after RIPC treatment	24 (6 per time point)

The Committee for Animal Experiments of the Radboud University Nijmegen approved all procedures involving animals (RU-DEC 2010-248).

RIPC treatment

As previously demonstrated, RIPC was performed by applying brief hindlimb ischemia using a hemorrhoidal ligator (Miltex McGivney: 26-154B) to place elastic latex-free O-rings (Miltex Integra: 28-155) placed bilaterally around the most upper portion of the proximal thigh (Figure 7.1, reproduced with permission) (50). Reperfusion was accomplished by cutting the elastic rings and confirmed by the disappearance of blue color to the limbs. During the entire RIPC procedure, mice were anesthetized with isoflurane in O₂/N₂O (5% for induction and 2%3% as maintenance) and consisted of three cycles of 4-min ischemia interspersed with 4-min reperfusion. This regime is based on a previous study in which we found that bilateral repetitive (3x4 min) ischemia/reperfusion resulted in the most potent protection in a kidney injury model (8).



Figure 7.1: Hind limb ischemia by ligation using the black elastic ring (red arrow). Note the difference in the color of the legs after obstruction of the blood flow with the elastic ring.

Measuring of HO-1 promoter activity

In order to monitor HO-1 promoter activity after RIPC treatment in real time, HO-1-luc Tg mice underwent RIPC treatment as described above. HO-1-luc expression was measured in vivo by bioluminescence imaging (BLI) using the IVIS Lumina System (Caliper Life Sciences, Hopkinton, MA, USA) as previously described (51). HO-1 promoter activity in the heart were quantified using LivingImage 3.0 software (Caliper Life Sciences), calculated as emitted photons per second (or total flux), and then expressed as fold change from baseline levels and then compared with levels measured at 1h after RIPC.

Sample collection

Mice were anesthetized with 5% isoflurane in O₂/N₂O and sacrificed by exsanguination, followed by cervical dislocation. Plasma samples were stored at -80°C until further use. The ligated muscle (m. quadriceps femoris), kidneys, and heart were dissected. Half of the tissue was fixated with 4% paraformaldehyde and processed for paraffin embedding and immunohistochemistry, and the other half was snap frozen in liquid nitrogen and stored at -80°C for later RNA isolation and RT-PCR.

Measurement of free heme levels in the circulation using HPLC

A stock solution of heme (2 mM; 13.4 mg/10 mL pure DMSO) was freshly prepared and serially diluted to 2.0, 4.0, 6.0, 8.0 and 10.0 μM heme as standards. An aliquot of 20 μL of serum or standards was mixed with 160-μL HCl/acetone (1:40 ratio), and after 2 min cooling and centrifugation at 13,400 rpm for 3 min, the upper organic layer was collected and used for HPLC analysis. The chromatographic system consisted of a Thermo Separations Products (TSP) binary pump (P2000), autosampler (AS3000) and a single wavelength UV detector (UV1000). The autosampler was programmed to inject 50 μL of sample. Pump flow-rate was 1.0 mL/min with mobile phase comprised of degassed 44% methanol, 56% 0.1 M ammonium phosphate buffer pH 3.4, v/v (Solvent A) and the sample/ standard (solvent B) using the following gradient: Solvent B, 0% at t₀ to 100% at 14 min; then isocratic to 15 min; down to 0% at 16 min and isocratic to 21 min. The UV detector was set at a wavelength of 400 nm. Gradient separation of heme was performed on a GraceSmart RP18 column, 150x4.6 mm i.d., 5-μm particle size at a column temperature of 60°C.

Immunohistochemical staining and analyses

Immunohistochemical staining was performed on paraffin sections of heart tissues as previously described (52). Double stainings were performed to characterize HO-1-positive cells as follows: first, fields of HO-1-positive cells were located on stained tissue sections using the Zeiss Imager Z1 microscope and Axiovision software version 4.8; and the second staining of cell-specific markers was performed on the same tissue section using the “mark and find” option to locate the stained HO-1-positive cells. For the co-localization studies of HO-1 and LRP-1 expression, we performed immunohistochemical stainings on subsequent tissue sections of 5 μm in thickness and scanned the complete sections using the automatic slide scanner Panoramic scan II (3DHISTECH), in which co-localization can be studied based on tissue morphology. HO-1-positive cells were easily located and matched to cells stained with LRP-1. HO-1 immunoreactivity was semi-quantitatively evaluated blindly by two independent trained observers for a single section of the whole heart tissue from each

animal using the following scoring scale: 0 (minimal), 1 (mild), 2 (moderate), and 3 (marked) as previously described (52).

RNA isolation and quantitative-RT-PCR

Tissue was pulverized in TRIzol (Invitrogen) using a micro-dismembrator (Sartorius BBI Systems GmbH, Melsungen, Germany) and RNA was further extracted as previously described (35). All values were normalized to the household gene *gapdh* according to the comparative method ($2^{-\Delta\Delta Ct}$). The sequences of the mouse-specific primers for *gapdh* are forward 5'GGCAAATTCAACGGCACAA3', and reverse 5'GTTAGTGGGGTCTCGCTCCTG3', and for *Hmox1* (HO-1) forward 5'CAACATTGAGCTGTTTGAGG3', and reverse 5'TGGTCTTTGTTCCTCTGTC3'.

Statistical analyses

Data were analyzed using GraphPad Prism 5.01 software (San Diego, CA, US). Outliers were tested using the Grubbs' test, but no outliers were found. Data were analyzed using two-sided t-tests to compare two variables or a one-way analysis of variance when comparing multiple variables. Bonferroni's multiple comparison *post hoc* test was applied as a correction for multiple comparisons when investigating multiple dependent research questions. The non-parametrical one-tailed Mann-Whitney U-test was used to compare the arbitrary scored immunohistological sections. Results were considered significantly different at $p < 0.05$ (* $p < 0.05$, ** $p < 0.01$, and *** $p < 0.001$).

Results

Low amounts of heme are released following RIPIC

RIPIC has been reported to protect the tissue; however, the mechanism by which this occurs is not yet completely understood. In order to investigate the possible involvement of heme, we postulated that during RIPIC, local mild damage leads to the release of small amounts of heme into the circulation, which could then act protectively. To this end, we measured plasma levels of free heme after RIPIC treatment over time using HPLC analysis (Figure 7.2). We observed a significant increase in free heme levels within 1h after RIPIC treatment. No significant effects were found 6 or 24h after RIPIC treatment. This release of low levels of heme into the circulation early after RIPIC treatment could possibly lead to induction of the cytoprotective enzyme HO-1.

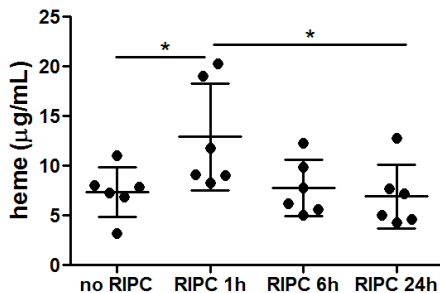


Figure 7.2: Free heme levels in the plasma are elevated early in mice after RIPIC treatment
Data are expressed as mean \pm SD of six individual mice. * $p < 0.05$

RIPC treatment induces HO-1 mRNA and protein expression locally in the ligated muscle

Induction of HO-1 expression has been observed previously after RIPC treatment (31-34). To determine whether HO-1 is also induced in our model, we isolated total RNA from ligated muscles of the hind limbs and performed quantitative RT-PCR (Figure 7.3A). RIPC significantly ($p < 0.05$) induced HO-1 mRNA expression a 3.5- and 10.8-fold at 1 and 6h, respectively, and non-significantly a 2.4-fold ($p = 0.11$) at 24h, following RIPC compared with the no RIPC-treated control group. In addition, HO-1 protein expression was strongly enhanced in individual cells in the ligated hind limb muscle; whereas, HO-1-positive cells were not found in the muscle of the no RIPC-treated control group. After quantification, HO-1 protein expression was significantly elevated at 6 and 24h after RIPC when compared with the no RIPC-treated control group (Figure 7.3B). Thus, local HO-1 induction is observed after RIPC treatment of the ligated skeletal muscle.

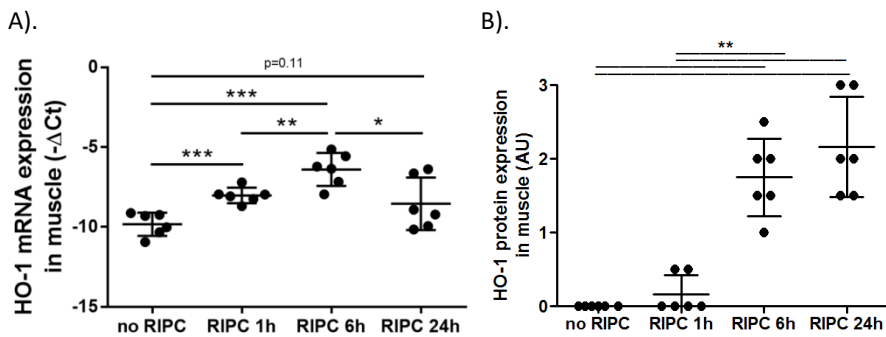


Figure 7.3: HO-1 is induced locally in the skeletal muscle upon RIPC treatment

Time course of HO-1 mRNA level (A) and protein (B) levels in ligated skeletal muscles of the hind limbs of mice after RIPC treatment. Data are expressed as mean \pm SD of six individual mice. AU, arbitrary units. * $p < 0.05$, ** $p < 0.01$, *** $p < 0.001$

HO-1 expression is induced in kidney and heart after RIPC treatment

To assess whether HO-1 is also induced in remote organs, we analyzed the HO-1 mRNA expression levels of the kidney and heart after RIPC. HO-1 mRNA expression in the kidney was significantly elevated (4.2-fold) 6h after RIPC treatment (Figure 7.4A). Next, HO-1 promoter activity in the heart region of HO-1-*luc* tg mice after RIPC treatment was investigated. We observed that there were significant increases 6h and 24h after RIPC treatment in HO-1 promoter activity compared to 1h after RIPC treatment (Figure 7.4B). Since measured HO-1 promoter activity may be affected by HO-1 promoter activity in other organs that lay near to the heart, we next investigated HO-1 induction in the heart also on mRNA and protein level as confirmation. Indeed, also on mRNA level, there was a significant induction of HO-1 expression at 1 and 6h after RIPC treatment (a 1.5-fold and 2.4-fold, respectively) when compared to no RIPC-treated control. However, significance disappeared after 24h ($p = 0.094$) (Figure 7.4C). When we subsequently analyzed HO-1 protein expression in the heart, we could only find a significant induction 6h after RIPC treatment (Figure 4D). Taken together, we show that HO-1 is induced in multiple remote organs following RIPC treatment.

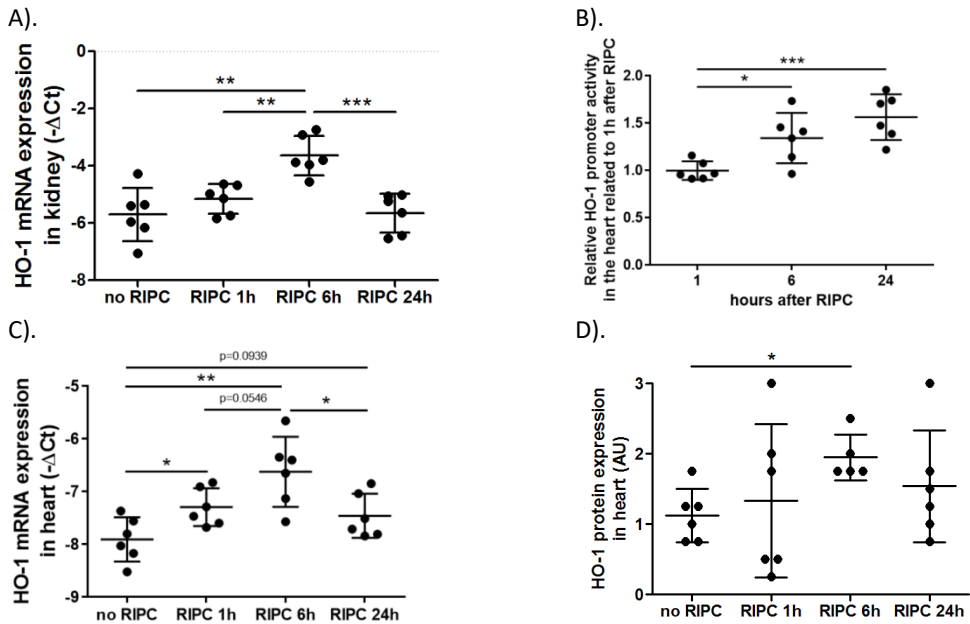


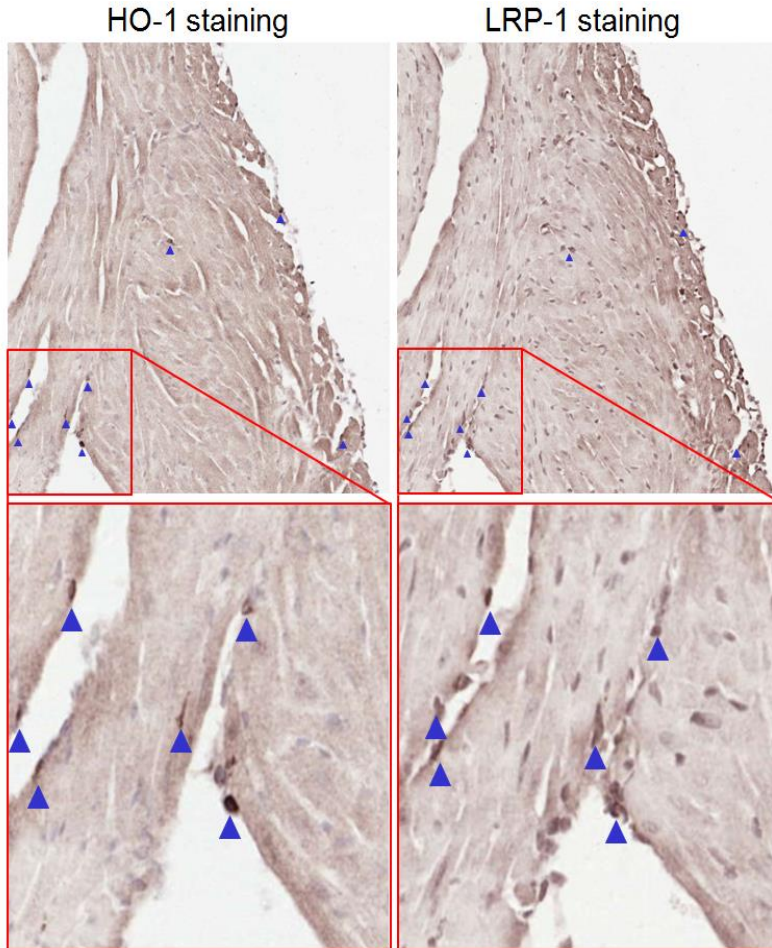
Figure 7.4: HO-1 is induced in remote organs after RIPIC treatment

A). HO-1 mRNA expression levels in the kidney after RIPIC treatment in time compared with those of no RIPIC-treated controls. B). Time course of HO-1 promoter activity in the heart after RIPIC treatment compared with the 1h RIPIC time point. Time course of HO-1 mRNA level (C) and protein (D) levels expression levels after RIPIC treatment compared with that of no RIPIC-treated controls. Data are expressed as mean±SD of six individual mice. AU, arbitrary units. * $p < 0.05$, ** $p < 0.01$, *** $p < 0.001$

HO-1 induction is mediated via LRP-1 activation

In large amounts, free heme has been demonstrated to bind to TLR-4 and act as danger signal activating inflammatory responses. However, shortly following RIPIC treatment only small amounts of free heme were observed in the circulation. It has been demonstrated that free heme in the circulation gets directly scavenged by hpx (53). Since hpx can completely scavenge low levels of free heme, we aimed to investigate whether this heme-hpx complex could induce HO-1 in cells via activation of LRP-1 signaling. To test this, we performed HO-1 and LRP-1 immunohistological staining on subsequent tissue sections to show that HO-1 and LRP-1 proteins co-localize in the cells of the heart. In Figure 7.5A, a representative example of the HO-1 and LRP-1 stainings of the heart, 6h after RIPIC treatment are depicted, clearly showing HO-1 and LRP-1 double positive cells. After quantification of the number of HO-1-positive cells in multiple fields (at least 5) of the heart, the number of double positive cells was determined. An average of at least 86% of the HO-1 positive cells were positive for and LRP-1 in the 6h time-point group (Figure 7.5B) showing that HO-1 induction is likely mediated via LRP-1.

A).



B).

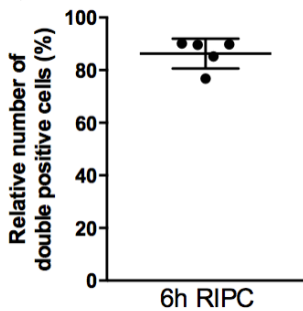


Figure 7.5: Most of the cells expressing HO-1 protein also express LRP-1 protein

A). Representative example of double-positive staining of HO-1 and LRP-1 on consecutive stained sections of a heart 6h after RIPc treatment. B). Number of HO-1 and LRP-1 double-positive cells in immunohistological sections of the heart. Quantification was performed on at least five regions where HO-1-positive cells were present. On subsequent tissue sections stained for LRP-1 protein, HO-1-positive cells were identified based on location and tissue morphology, and LRP-1 double-positive cells were determined.

Discussion

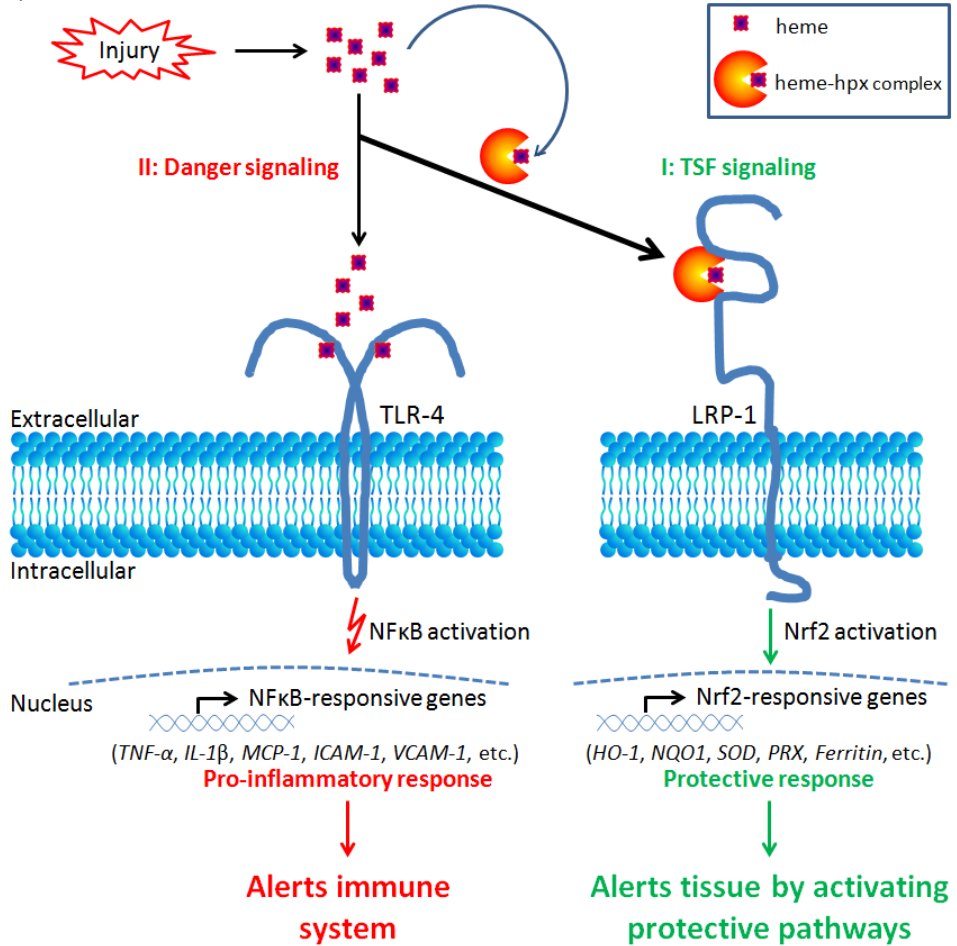
With the “danger theory” we better understand how the immune system is activated following injury. Here, we propose to extend this theory with a “tissue survival theory” and explain how first the tissue gets warned by TSF-signaling for both injurious stressors and for an immune response that may cause collateral damage. The tissue will prepare itself by inducing cytoprotective pathways.

RIPC protects against various forms of tissue injuries (54-56). We postulated that RIPC leads to the release of heme that upon binding to hpx activates tissue protective pathways via LRP-1 and nrf2-responsive HO-1 signaling. We demonstrated that RIPC induced the cytoprotective enzyme HO-1 locally in the ligated muscle, and remotely in the kidney and heart. Since serum heme levels are mildly but significantly elevated early following RIPC treatment, it is likely that HO-1 is induced via LRP-1 activation by heme-hpx complexes (57), which is supported by massive co-localization of HO-1-positive cells with LRP-1. Based on these RIPC data, we propose a novel model to explain tissue protective effects following injury by the formation of TSFs that can activate cytoprotective genes (Figure 7.6A). Following alerting the tissue by TSFs (e.g., heme-hpx complexes), danger signals may take over and activate the immune system (Figure 7.6B).

The heme-hpx complex acts as TSF by binding to LRP-1 and inducing protective signaling

The heme that gets released upon small injuries is directly scavenged by hpx. The only receptor described to recognize the heme-hpx complex to date is LRP-1 (CD91) (58), which can recognize a wide range of different ligands (59). LRP-1 is ubiquitously expressed throughout the body in many cell types, including fibroblasts, macrophages, vascular smooth muscle cells, endothelial cells, adipocytes, neurons, and foam cells (60-62), and has physiological functions for endocytosis and regulation of signaling pathways (63). LRP-1 is an important switch in protective/inflammatory responses, as LRP-1 expression reduces NF- κ B activation of pro-inflammatory genes; whereas, deletion of LRP-1 enhances pro-inflammatory signals (64, 65). LRP-1 has an atheroprotective effect on the vascular wall (59). Interestingly, LRP-1 induction makes the tissue more susceptible to heme-hpx-mediated protective signaling as more receptors can be activated. LRP-1 expression is increased in several pathologies; hypoxia and IRI as exemplified by the observation that during myocardial infarction LRP-1 expression gets induced (66). However, LRP-1 is involved in phagocytosis and removal of apoptotic cells, which is critical for development, tissue homeostasis, and resolution of inflammation (63, 67-69). LRP-1 and their signaling cascades may serve as new target for the treatment of different diseases, such as cardiovascular and neuronal disorders (63). LRP-1 overexpression probably makes the tissue more prone to hpx-mediated protective signaling as more LRP-1 receptors are available for activation by heme-hpx complexes.

A).



B).

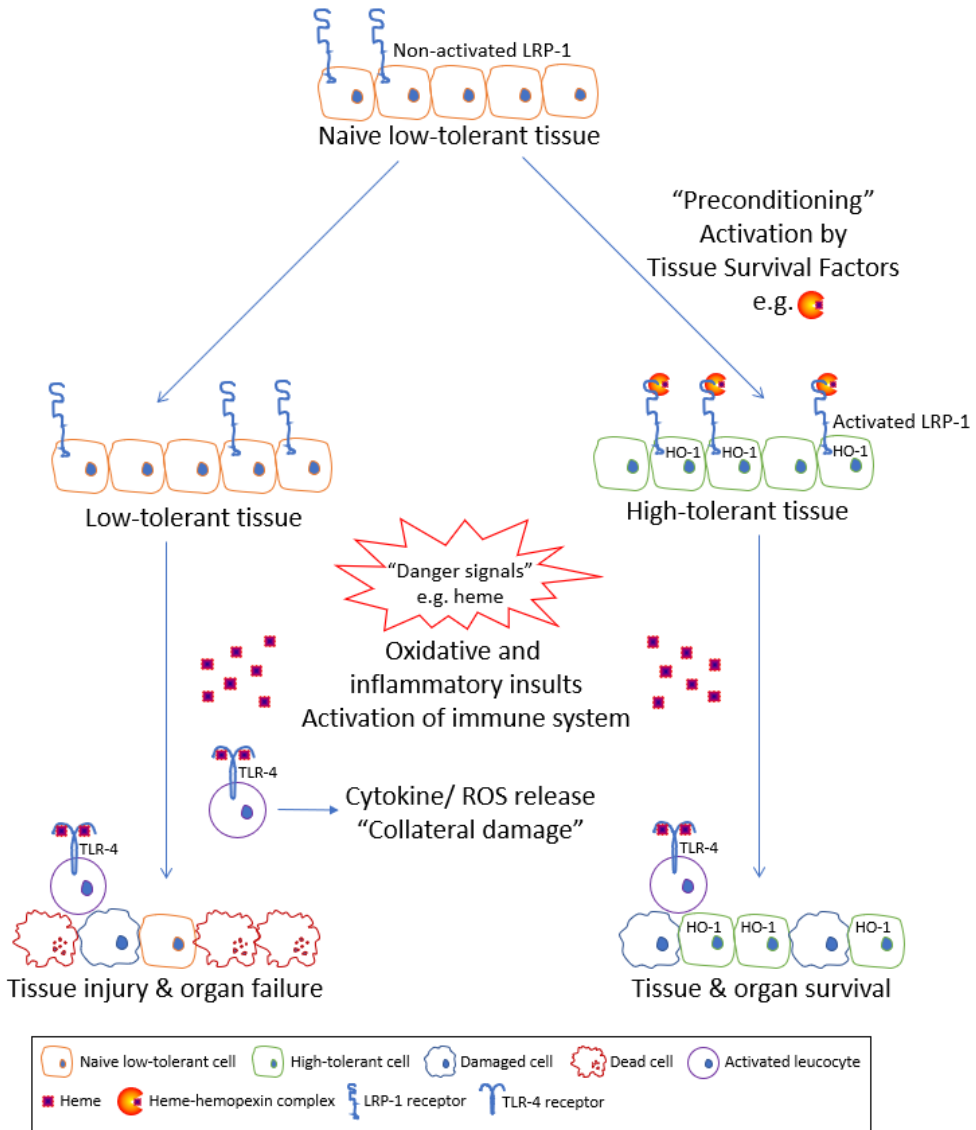


Figure 7.6: Proposed mechanisms of tissue protection by TSFs and immune cell activation by danger signals

A). Low amounts of heme get scavenged by hpx and bind in complex to LRP-1, which activates cytoprotective nrf2-responsive pathways, such as HO-1, to promote tissue protection. Excess free heme molecules can bind TLR-4 and induce pro-inflammatory pathways (e.g. TNF- α , ICAM-1) and activate immune cells; B). Preconditioning of naive cells with RIPc or hpx administration may increase tissue tolerance towards oxidative and inflammatory stress, e.g., as experienced during heme overload. Heme overload activates the immune response resulting in cytokine and ROS release, and collateral damage. High-tolerant tissue is better protected against injurious insults resulting in organ survival, while not protected low-tolerant tissue gets injured and lead to organ dysfunction.

TLR-4: Toll-like Receptor-4, LRP-1: LDL Receptor-Related Protein-1, TNF- α : Tumor Necrosis Factor- α , IL-1 β : Interleukin-1 β , MCP-1: Monocyte Chemoattractant Protein-1, ICAM-1: Intercellular Adhesion Molecule-1, VCAM-1: Vascular Cell Adhesion Molecule-1, HO-1: Heme Oxygenase-1, NQO1: NAD(P)H Quinone Oxidoreductase-1, SOD: Superoxide Dismutase, PRX: Peroxiredoxin, ROS: Reactive Oxygen Species.

Heme-hpx mediated activation of LRP-1 leads to the induction of the nrf2-responsive gene HO-1 and tissue protection

After oxidative and inflammatory stress, nrf2 balances redox levels by inducing the expression of cytoprotective proteins (70, 71). A major nrf2 target is the inducible protective enzyme HO-1 (72). Decreased levels of the HO-1 effector molecules bilirubin and CO are implicated in ischemic heart disease; whereas, enhanced expression of HO-1 or administration of its effector molecules prevents cardiac injury and transplant rejection (73). In cultured monocytes, uptake of heme-hpx complexes elevates LRP-1-dependent HO-1 induction (60).

The importance of the nrf2/HO-1 axis in cardiac protection is shown by the association of RIPC with elevated levels of nrf2 expression in a porcine model of deep hypothermic circulatory arrest, which improved cardiac outcome (74). In addition, lack of nrf2 leads to rapid development of heart failure after ischemic injury (75). Also, administration of cobalt protoporphyrin (CoPP) improved heart function following myocardial ischemia via the induction of HO-1 by reducing oxidative stress and apoptosis, and preserving mitochondrial membrane potential in cardiomyocytes (76). The protective role of nrf2/HO-1 is further supported by studies reporting that preconditioning of cardiac stem cells with CoPP induces several cytokines, such as EGF, FGFs, colony-stimulating factors, and chemokine ligand, and pro-survival genes that protect against apoptosis via a nrf2 and HO-1-dependent manner, as blocking these pathways abrogated the protective effects of CoPP (77, 78).

High levels of free hemoglobin and heme can activate the immune system when haptoglobin and hemopexin are depleted

In pathological conditions and tissue injuries, such as sickle cell disease, malaria, IRI and severe sepsis, large amounts of hemoproteins, such as hemoglobin and myoglobin are released into the circulation (53, 79-82). After exhausting the hemoglobin (Hb) scavenger protein haptoglobin (hp), "labile" free heme is released from methemoglobin (53). Free heme is subsequently scavenged by hpx and can then warn the tissue for upcoming stress. However, when also the binding capacity of hpx is overwhelmed, free heme accumulates in the plasma where it can promote oxidative and inflammatory stress and act as danger signal (79). After binding of heme to TLR-4, NF- κ B-responsive genes are activated resulting in the induction of pro-inflammatory cytokines and activation of the immune system (79).

Protective mechanisms against free heme are therefore pivotal for cellular survival. When the release of heme is massive, the tissue will have only few time left to prepare its defense by TSF signaling, because of the limited amount of haptoglobin and hemopexin.

Hpx skews away from danger molecule signaling by promoting tissue survival via TSF signaling

The scavenger hpx binds to free heme and directly prevents oxidative and inflammatory insults. Hemopexin is not recycled after the clearance of heme-hpx complexes; and under pathologic conditions, e.g., during cardiovascular surgery or hemolysis, hpx levels are rapidly exhausted (83). Additional administration of hpx to cell cultures containing high levels of free heme prevents heme-induced toxicity (84). This may be possibly due to direct scavenging of heme by hpx, but may also likely be the result of induction of HO-1 via LRP-1. The latter is supported by reduced protection in the presence of HO-1 inhibitors (85). Also,

in diverse pre-clinical models, the protective role of hpx has been demonstrated. Administration of hpx protected against heme-induced inflammation in sepsis (86). Studies using hpx knockout animals further confirmed the protective role of hpx against heme-induced toxicity (84, 87, 88). In a model of heme overload using hpx knockout mice, the excess accumulation of free heme in the plasma produced ROS, induced adhesion molecules, reduced nitric oxide availability (89), and caused severe systolic dysfunction in the heart (84). Supplementation of hpx in hpx knockout mice after heme overload in models of hemolytic diseases (sickle cell disease and β -thalassemia) resulted in the preservation of cardiac function, limited oxidative stress and promoted recovery and hepatic detoxification, mainly via the induction of HO-1 (84, 89, 90). The levels of heme and hpx appear to determine also disease severity and adverse clinical outcomes in malaria, sepsis, and sickle cell disease (91-93). Normally, hpx concentrations in mice range from 0.55–1.25 mg ml⁻¹ (94). This level is sufficient to scavenge all the heme we observed after RIPC treatment. Excess levels of heme contribute to pathogenesis; whereas, increased levels of the heme-hpx complex has a protective role (86, 95-97). And hence, we propose that heme binding to hpx can be considered a systemic protective response complex (TSF).

Sickle cell disease models strongly support a “tissue survival theory” next to a “danger theory”

We previously postulated that heme could play a decisive role in the stasis observed in sickle cell disease (93). It was indeed shown that in transgenic sickle cell mice heme can provoke vascular adhesion molecule expression and contribute to vascular occlusion via TLR4-signaling (98-100). Interestingly, the nrf2 inducer dimethyl fumarate was shown to protect against oxidative stress and inflammation in sickle cell disease in an HO-1-dependent manner (101).

The hemoglobin scavenger haptoglobin and the heme scavenger hpx get swiftly depleted during hemolytic episodes in sickle cell disease (102), abrogating protective TSF signaling (Figure 7.6A). Hpx gene transfer in transgenic sickle mice significantly increased plasma and hepatic hpx levels compared to controls, and ameliorates heme-induced vascular inflammation and occlusion, suggesting that it is possible to abrogate danger molecule signaling by promoting TSF formation (61, 90, 103). Administration of hpx increased HO-1 in the liver, kidney and skin within 1h, and decreased nuclear NF κ B -p65, and vaso-occlusion for 48h after infusion. Hpx-induced protection was abrogated when HO-activity was inhibited with tin protoporphyrin (SnPP) (103).

In addition, hpx overexpression increased hepatic nuclear nrf2 expression, HO-activity and HO-1 protein and LRP-1, while decreasing NF κ B activation and down-stream pro-inflammatory signaling (61). The heme-hpx/LRP-1/nrf2/HO-1 axis was elegantly proven by the use of mutant hpx proteins. A hpx missense construct that did not bind heme could not prevent heme-induced vascular occlusion, and another hpx missense construct that was not able to bind LRP-1 did not prevent heme-induced vascular occlusion, showing that hpx can only provide protection when in complex with heme and only when it can activate protective LRP-1 signaling (61).

Free heme was demonstrated to mediate pro-inflammatory effects also in renal epithelial cells via TLR-4 signaling; whereas, blocking of TLR-4 did not result in less nrf2 and HO-1 activation, indicating that anti-inflammatory effects of heme are not TLR-4 mediated,

and thus likely mediated via LRP-1 signaling (104). Heme-hpx binding to the LRP-1 receptor may thus activate protective nrf2-responsive pathways.

Summarizing, these data support our model that heme in the presence of hpx is skewed towards the protective TSF-pathway via LRP-1/nrf2/HO-1, whereas in the absence of hpx, heme activates TLR4-mediated induction of NFκB responsive inflammatory genes is enhanced (see Figure 7.6A).

Clinical relevance of the described RIPC-mediated protective concept

Patients have an individual predisposition towards oxidative and inflammatory stress. For example, patients with sickle cell disease, diabetes, older age or infectious diseases will have more depleted antioxidant and anti-inflammatory defenses and be less tolerant to subsequent exposure to injurious stressors. The tolerance of tissue may be increased by applying preconditioning strategies, e.g., RIPC or hpx administration, which both can activate tissue survival factors (Figure 7.6B). Interestingly, it was found that in contrast to preconditioning with heme that caused attenuation of inflammatory stress, post-conditioning with heme exacerbated inflicted kidney injury (105), showing that heme only acts protective in the presence of hpx. When hpx is depleted, administration of heme aggravates inflammatory conditions. There is a differential response between high and low tolerant tissues towards oxidative and inflammatory stressors. For example, heme overload cannot be completely scavenged by hpx and will then bind to TLR-4. Next, TLR-4 signaling activates an immune response and extensive release of cytokines resulting in collateral damage by recruited immune cells. While high tolerant tissue is better protected against such damage and results in organ survival, low tolerant tissue is not equipped to deal with this stress and may develop towards organ dysfunction.

However, heme shows dose-dependent effects and can act as a double-edged sword. Therefore, quantification of the amount of plasma heme, hpx, hemoglobin-hp, heme-hpx, and heme-albumin levels in various disease states may aid the diagnosis and treatment of several pathologic conditions (86). High levels of heme often lead to oxidative stress and inflammation-induced damage, whereas low levels of heme are essential for physiological processes, but can also protect individuals in several diseases (106, 107). Pharmacological preconditioning with low levels of heme-hpx or RIPC treatment forms an interesting strategy. However, heme is unstable and heme arginate forms a better alternative as it is also less toxic (53, 108, 109).

In addition, the induction of TSFs may not be restricted to the heme-hpx complex alone, but may also apply to other factors, such as e.g., the hemoglobin-haptoglobin complex by binding to CD163 and activate anti-inflammatory pathways (60). This is supported by a study showing that haptoglobin supplementation induces cytoprotective cellular responses via a HO-1 dependent mechanism in a murine model of sickle cell diseases, as protection is blocked by HO-activity inhibitor SnPP (103).

With our “tissue survival model” in mind, we may now develop novel strategies to skew either towards a pro-inflammatory or anti-inflammatory microenvironment. Hemopexin harnesses the pro-inflammatory and oxidative properties of heme, and the heme-hpx complex initiates protective pathways. This concept may be beneficial for the development of therapeutic strategies in a plethora of conditions, including tissue injury, diabetes, transplantations and graft failure, fibrosis, IRI, cardiac diseases, aging, pathological pregnancies and heme-mediated pathologies such as sickle cell disease,

malaria, hemolytic-uremic syndrome, and thrombotic thrombocytopenic purpura (101). Also, patients receiving blood transfusion have elevated levels of free hemoglobin and heme, and often suffer from a certain disease. We propose to administer hpx to patients suffering from the aforementioned diseases. Also, the induction of nrf2 or HO signaling or administration of HO-effector molecules forms an interesting strategy to skew towards protection (109, 110).

Summarizing, the amount of the heme scavenger hpx plays a decisive role in discriminating between heme acting as a danger signal or heme-hpx acting as TSF. However, the exact role of hpx in the protection against heme-mediated toxicity needs to be further confirmed in clinical settings (86). Thus, besides the direct protective effects of hpx in shielding the bioreactive and pro-inflammatory heme, the heme-hpx complex can also act as secondary messenger (TSF) and activate tissue protective signaling pathways.

References

1. Nathan C. Points of control in inflammation. *Nature*. 2002;420(6917):846-52.
2. Goldszmid RS, Trinchieri G. The price of immunity. *Nat Immunol*. 2012;13(10):932-8.
3. Wagener FA, Immenschuh S. Editorial: Molecular Mechanisms Protecting against Tissue Injury. *Front Pharmacol*. 2016;7:272.
4. Nathan C, Ding A. Nonresolving inflammation. *Cell*. 2010;140(6):871-82.
5. Reuter S, Gupta SC, Chaturvedi MM, Aggarwal BB. Oxidative stress, inflammation, and cancer: how are they linked? *Free Radic Biol Med*. 2010;49(11):1603-16.
6. Soares MP, Gozzelino R, Weis S. Tissue damage control in disease tolerance. *Trends Immunol*. 2014;35(10):483-94.
7. Soares MP. "Nuts and bolts" of disease tolerance. *Immunity*. 2014;41(2):176-8.
8. Wever KE, Warle MC, Wagener FA, van der Hoorn JW, Masereeuw R, van der Vliet JA, et al. Remote ischaemic preconditioning by brief hind limb ischaemia protects against renal ischaemia-reperfusion injury: the role of adenosine. *Nephrology, dialysis, transplantation*. 2011;26(10):3108-17.
9. Anttila V, Haapanen H, Yannopoulos F, Herajarvi J, Anttila T, Juvonen T. Review of remote ischemic preconditioning: from laboratory studies to clinical trials. *Scand Cardiovasc J*. 2016;50(5-6):355-61.
10. Garcia-Dorado D, Rodriguez-Sinovas A, Ruiz-Meana M, Inerte J. Protection against myocardial ischemia-reperfusion injury in clinical practice. *Rev Esp Cardiol (Engl Ed)*. 2014;67(5):394-404.
11. Medvedev AE, Kopydlowski KM, Vogel SN. Inhibition of lipopolysaccharide-induced signal transduction in endotoxin-tolerized mouse macrophages: dysregulation of cytokine, chemokine, and toll-like receptor 2 and 4 gene expression. *J Immunol*. 2000;164(11):5564-74.
12. Wagener FA, van Beurden HE, von den Hoff JW, Adema GJ, Figdor CG. The heme-heme oxygenase system: a molecular switch in wound healing. *Blood*. 2003;102(2):521-8.
13. Vercellotti GM, Balla G, Balla J, Nath K, Eaton JW, Jacob HS. Heme and the vasculature: an oxidative hazard that induces antioxidant defenses in the endothelium. *Artif Cells Blood Substit Immobil Biotechnol*. 1994;22(2):207-13.
14. Nath KA, Vercellotti GM, Grande JP, Miyoshi H, Paya CV, Manivel JC, et al. Heme protein-induced chronic renal inflammation: suppressive effect of induced heme oxygenase-1. *Kidney Int*. 2001;59(1):106-17.
15. Wagener FA, Feldman E, de Witte T, Abraham NG. Heme induces the expression of adhesion molecules ICAM-1, VCAM-1, and E selectin in vascular endothelial cells. *Proc Soc Exp Biol Med*. 1997;216(3):456-63.
16. Wagener FA, Eggert A, Boerman OC, Oyen WJ, Verhofstad A, Abraham NG, et al. Heme is a potent inducer of inflammation in mice and is counteracted by heme oxygenase. *Blood*. 2001;98(6):1802-11.
17. Figueiredo RT, Fernandez PL, Mourao-Sa DS, Porto BN, Dutra FF, Alves LS, et al. Characterization of heme as activator of Toll-like receptor 4. *J Biol Chem*. 2007;282(28):20221-9.
18. Soares MP, Bozza MT. Red alert: labile heme is an alarmin. *Curr Opin Immunol*. 2016;38:94-100.
19. Li Q, Fu W, Yao J, Ji Z, Wang Y, Zhou Z, et al. Heme induces IL-1beta secretion through activating NLRP3 in kidney inflammation. *Cell Biochem Biophys*. 2014;69(3):495-502.
20. Wegiel B, Hauser CJ, Otterbein LE. Heme as a danger molecule in pathogen recognition. *Free Radic Biol Med*. 2015;89:651-61.
21. Lu X, Chen-Roetling J, Regan RF. Systemic hemin therapy attenuates blood-brain barrier disruption after intracerebral hemorrhage. *Neurobiol Dis*. 2014;70:245-51.
22. Gupta I, Goyal A, Singh NK, Yadav HN, Sharma PL. Hemin, a heme oxygenase-1 inducer, restores the attenuated cardioprotective effect of ischemic preconditioning in isolated diabetic rat heart. *Hum Exp Toxicol*. 2017;36(8):867-75.
23. Ben-Mordechai T, Kain D, Holbova R, Landa N, Levin LP, Elron-Gross I, et al. Targeting and modulating infarct macrophages with hemin formulated in designed lipid-based particles improves cardiac remodeling and function. *J Control Release*. 2017;257:21-31.
24. Levere RD, Gong YF, Kappas A, Bucher DJ, Wormser GP, Abraham NG. Heme inhibits human immunodeficiency virus 1 replication in cell cultures and enhances the antiviral effect of zidovudine. *Proc Natl Acad Sci U S A*. 1991;88(5):1756-9.
25. Devadas K, Dhawan S. Hemin activation ameliorates HIV-1 infection via heme oxygenase-1 induction. *J Immunol*. 2006;176(7):4252-7.
26. Ndisang JF, Lane N, Jadhav A. The heme oxygenase system abates hyperglycemia in Zucker diabetic fatty rats by potentiating insulin-sensitizing pathways. *Endocrinology*. 2009;150(5):2098-108.
27. Willis D, Moore AR, Frederick R, Willoughby DA. Heme oxygenase: a novel target for the modulation of the inflammatory response. *Nat Med*. 1996;2(1):87-90.

28. Keyse SM, Tyrrell RM. Heme oxygenase is the major 32-kDa stress protein induced in human skin fibroblasts by UVA radiation, hydrogen peroxide, and sodium arsenite. *Proc Natl Acad Sci U S A*. 1989;86(1):99-103.
29. Gleadle JM, Mazzone A. Remote ischaemic preconditioning: closer to the mechanism? *F1000Res*. 2016;5:2846.
30. Dickson EW, Lorbar M, Porcaro WA, Fenton RA, Reinhardt CP, Gysembergh A, et al. Rabbit heart can be "preconditioned" via transfer of coronary effluent. *Am J Physiol*. 1999;277(6 Pt 2):H2451-7.
31. Zhou C, Li L, Li H, Gong J, Fang N. Delayed remote preconditioning induces cardioprotection: role of heme oxygenase-1. *J Surg Res*. 2014;191(1):51-7.
32. Lai IR, Chang KJ, Chen CF, Tsai HW. Transient limb ischemia induces remote preconditioning in liver among rats: the protective role of heme oxygenase-1. *Transplantation*. 2006;81(9):1311-7.
33. Wang Y, Shen J, Xiong X, Xu Y, Zhang H, Huang C, et al. Remote ischemic preconditioning protects against liver ischemia-reperfusion injury via heme oxygenase-1-induced autophagy. *PLoS One*. 2014;9(6):e98834.
34. Jan WC, Chen CH, Tsai PS, Huang CJ. Limb ischemic preconditioning mitigates lung injury induced by haemorrhagic shock/resuscitation in rats. *Resuscitation*. 2011;82(6):760-6.
35. Cremers NA, Lundvig DM, van Dalen SC, Schelbergen RF, van Lent PL, Szarek WA, et al. Curcumin-induced heme oxygenase-1 expression prevents H2O2-induced cell death in wild type and heme oxygenase-2 knockout adipose-derived mesenchymal stem cells. *Int J Mol Sci*. 2014;15(10):17974-99.
36. Wagener FA, Volk HD, Willis D, Abraham NG, Soares MP, Adema GJ, et al. Different faces of the heme-heme oxygenase system in inflammation. *Pharmacological reviews*. 2003;55(3):551-71.
37. Gozzelino R, Soares MP. Coupling heme and iron metabolism via ferritin H chain. *Antioxidants & redox signaling*. 2014;20(11):1754-69.
38. Dekker D, Dorresteyn MJ, Pijnenburg M, Heemskerk S, Rasing-Hoogveld A, Burger DM, et al. The bilirubin-increasing drug atazanavir improves endothelial function in patients with type 2 diabetes mellitus. *Arterioscler Thromb Vasc Biol*. 2011;31(2):458-63.
39. Wagener FA, da Silva JL, Farley T, de Witte T, Kappas A, Abraham NG. Differential effects of heme oxygenase isoforms on heme mediation of endothelial intracellular adhesion molecule 1 expression. *J Pharmacol Exp Ther*. 1999;291(1):416-23.
40. Durante W. Targeting heme oxygenase-1 in vascular disease. *Curr Drug Targets*. 2010;11(12):1504-16.
41. Wagener FA, Scharstuhl A, Tyrrell RM, Von den Hoff JW, Jozkowicz A, Dulak J, et al. The heme-heme oxygenase system in wound healing; implications for scar formation. *Curr Drug Targets*. 2010;11(12):1571-85.
42. Xia ZY, Gao J, Ancharaz AK. Protective effect of ischemic postconditioning on lung ischemia-reperfusion injury in rats and the role of heme oxygenase-1. *Chinese journal of traumatology = Zhonghua chuang shang za zhi / Chinese Medical Association*. 2009;12(3):162-6.
43. Attuwaybi BO, Kozar RA, Moore-Olufemi SD, Sato N, Hassoun HT, Weisbrodt NW, et al. Heme oxygenase-1 induction by hemin protects against gut ischemia/reperfusion injury. *J Surg Res*. 2004;118(1):53-7.
44. Holzen JP, August C, Bahde R, Minin E, Lang D, Heidenreich S, et al. Influence of heme oxygenase-1 on microcirculation after kidney transplantation. *J Surg Res*. 2008;148(2):126-35.
45. Kato Y, Shimazu M, Kondo M, Uchida K, Kumamoto Y, Wakabayashi G, et al. Bilirubin rinse: A simple protectant against the rat liver graft injury mimicking heme oxygenase-1 preconditioning. *Hepatology*. 2003;38(2):364-73.
46. Lai IR, Chang KJ, Tsai HW, Chen CF. Pharmacological preconditioning with simvastatin protects liver from ischemia-reperfusion injury by heme oxygenase-1 induction. *Transplantation*. 2008;85(5):732-8.
47. von Dobschuetz E, Schmidt R, Scholtes M, Thomsch O, Schwer CI, Geiger KK, et al. Protective role of heme oxygenase-1 in pancreatic microcirculatory dysfunction after ischemia/reperfusion in rats. *Pancreas*. 2008;36(4):377-84.
48. Wever KE, Wagener FA, Frielink C, Boerman OC, Scheffer GJ, Allison A, et al. Diannexin protects against renal ischemia reperfusion injury and targets phosphatidylserines in ischemic tissue. *PLoS One*. 2011;6(8):e24276.
49. Su H, van Dam GM, Buis CI, Visser DS, Hesselink JW, Schuur TA, et al. Spatiotemporal expression of heme oxygenase-1 detected by in vivo bioluminescence after hepatic ischemia in HO-1/Luc mice. *Liver transplantation*. 2006;12(11):1634-9.
50. Cremers NA, Wever KE, Wong RJ, van Rheden RE, Vermeij EA, van Dam GM, et al. Effects of Remote Ischemic Preconditioning on Heme Oxygenase-1 Expression and Cutaneous Wound Repair. *Int J Mol Sci*. 2017;18(2).

51. van den Brand BT, Vermeij EA, Waterborg CE, Arntz OJ, Kracht M, Bennink MB, et al. Intravenous delivery of HIV-based lentiviral vectors preferentially transduces F4/80+ and Ly-6C+ cells in spleen, important target cells in autoimmune arthritis. *PLoS One*. 2013;8(2):e55356.
52. Lundvig DM, Scharstuhl A, Cremers NA, Pennings SW, Te Paske J, van Rheden R, et al. Delayed cutaneous wound closure in HO-2 deficient mice despite normal HO-1 expression. *Journal of cellular and molecular medicine*. 2014;18(12):2488-98.
53. Immenschuh S, Vijayan V, Janciauskiene S, Gueler F. Heme as a Target for Therapeutic Interventions. *Front Pharmacol*. 2017;8:146.
54. Wang X, Kong N, Zhou C, Mungun D, Iyan Z, Guo Y, et al. Effect of Remote Ischemic Preconditioning on Perioperative Cardiac Events in Patients Undergoing Elective Percutaneous Coronary Intervention: A Meta-Analysis of 16 Randomized Trials. *Cardiol Res Pract*. 2017;2017:6907167.
55. Ravingerova T, Farkasova V, Griecsova L, Carnicka S, Murarikova M, Barlaka E, et al. Remote preconditioning as a novel "conditioning" approach to repair the broken heart: potential mechanisms and clinical applications. *Physiol Res*. 2016;65 Suppl 1:S55-64.
56. Stokfisz K, Ledakowicz-Polak A, Zagorski M, Zielinska M. Ischaemic preconditioning - Current knowledge and potential future applications after 30 years of experience. *Adv Med Sci*. 2017;62(2):307-16.
57. Nielsen MJ, Moller HJ, Moestrup SK. Hemoglobin and heme scavenger receptors. *Antioxidants & redox signaling*. 2010;12(2):261-73.
58. Schaefer DJ, Vinchi F, Ingoglia G, Tolosano E, Buehler PW. Haptoglobin, hemopexin, and related defense pathways-basic science, clinical perspectives, and drug development. *Front Physiol*. 2014;5:415.
59. May P. The low-density lipoprotein receptor-related protein 1 in inflammation. *Curr Opin Lipidol*. 2013;24(2):134-7.
60. Hvidberg V, Maniecki MB, Jacobsen C, Hojrup P, Moller HJ, Moestrup SK. Identification of the receptor scavenging hemopexin-heme complexes. *Blood*. 2005;106(7):2572-9.
61. Vercellotti GM, Zhang P, Nguyen J, Abdulla F, Chen C, Nguyen P, et al. Hepatic Overexpression of Hemopexin Inhibits Inflammation and Vascular Stasis in Murine Models of Sickle Cell Disease. *Mol Med*. 2016;22.
62. Llorente-Cortes V, Badimon L. LDL receptor-related protein and the vascular wall: implications for atherothrombosis. *Arterioscler Thromb Vasc Biol*. 2005;25(3):497-504.
63. May P, Woldt E, Matz RL, Boucher P. The LDL receptor-related protein (LRP) family: an old family of proteins with new physiological functions. *Ann Med*. 2007;39(3):219-28.
64. Yancey PG, Ding Y, Fan D, Blakemore JL, Zhang Y, Ding L, et al. Low-density lipoprotein receptor-related protein 1 prevents early atherosclerosis by limiting lesion apoptosis and inflammatory Ly-6Chigh monocytes: evidence that the effects are not apolipoprotein E dependent. *Circulation*. 2011;124(4):454-64.
65. Mantuano E, Brifault C, Lam MS, Azmoon P, Gilder AS, Gonias SL. LDL receptor-related protein-1 regulates NFkappaB and microRNA-155 in macrophages to control the inflammatory response. *Proc Natl Acad Sci U S A*. 2016;113(5):1369-74.
66. Revuelta-Lopez E, Soler-Botija C, Nasarre L, Benitez-Amaro A, de Gonzalo-Calvo D, Bayes-Genis A, et al. Relationship among LRP1 expression, Pyk2 phosphorylation and MMP-9 activation in left ventricular remodelling after myocardial infarction. *Journal of cellular and molecular medicine*. 2017;21(9):1915-28.
67. Gardai SJ, Xiao YQ, Dickinson M, Nick JA, Voelker DR, Greene KE, et al. By binding SIRPalpha or calreticulin/CD91, lung collectins act as dual function surveillance molecules to suppress or enhance inflammation. *Cell*. 2003;115(1):13-23.
68. Patel M, Morrow J, Maxfield FR, Strickland DK, Greenberg S, Tabas I. The cytoplasmic domain of the low density lipoprotein (LDL) receptor-related protein, but not that of the LDL receptor, triggers phagocytosis. *J Biol Chem*. 2003;278(45):44799-807.
69. Gardai SJ, McPhillips KA, Frasch SC, Janssen WJ, Starefeldt A, Murphy-Ullrich JE, et al. Cell-surface calreticulin initiates clearance of viable or apoptotic cells through trans-activation of LRP on the phagocyte. *Cell*. 2005;123(2):321-34.
70. Bryan HK, Olayanju A, Goldring CE, Park BK. The Nrf2 cell defence pathway: Keap1-dependent and -independent mechanisms of regulation. *Biochem Pharmacol*. 2013;85(6):705-17.
71. Barancik M, Gresova L, Bartekova M, Dovinova I. Nrf2 as a key player of redox regulation in cardiovascular diseases. *Physiol Res*. 2016;65 Suppl 1:S1-S10.
72. Gomperts E, Belcher JD, Otterbein LE, Coates TD, Wood J, Skolnick BE, et al. The role of carbon monoxide and heme oxygenase in the prevention of sickle cell disease vaso-occlusive crises. *Am J Hematol*. 2017;92(6):569-82.

73. Morse D, Choi AM. Heme oxygenase-1: the "emerging molecule" has arrived. *Am J Respir Cell Mol Biol.* 2002;27(1):8-16.
74. Herajarvi J, Anttila T, Dimova EY, Laukka T, Myllymaki M, Haapanen H, et al. Exploring effects of remote ischemic preconditioning in a pig model of hypothermic circulatory arrest. *Scand Cardiovasc J.* 2017;51(4):233-41.
75. Strom J, Chen QM. Loss of Nrf2 promotes rapid progression to heart failure following myocardial infarction. *Toxicol Appl Pharmacol.* 2017;327:52-8.
76. Issan Y, Kornowski R, Aravot D, Shainberg A, Laniado-Schwartzman M, Sodhi K, et al. Heme oxygenase-1 induction improves cardiac function following myocardial ischemia by reducing oxidative stress. *PLoS One.* 2014;9(3):e92246.
77. Cai C, Teng L, Vu D, He JQ, Guo Y, Li Q, et al. The heme oxygenase 1 inducer (CoPP) protects human cardiac stem cells against apoptosis through activation of the extracellular signal-regulated kinase (ERK)/NRF2 signaling pathway and cytokine release. *J Biol Chem.* 2012;287(40):33720-32.
78. Luo J, Weaver MS, Cao B, Dennis JE, Van Biber B, Laflamme MA, et al. Cobalt protoporphyrin pretreatment protects human embryonic stem cell-derived cardiomyocytes from hypoxia/reoxygenation injury in vitro and increases graft size and vascularization in vivo. *Stem Cells Transl Med.* 2014;3(6):734-44.
79. Dutra FF, Bozza MT. Heme on innate immunity and inflammation. *Front Pharmacol.* 2014;5:115.
80. Sawicki KT, Chang HC, Ardehali H. Role of heme in cardiovascular physiology and disease. *J Am Heart Assoc.* 2015;4(1):e001138.
81. Haque A, Engwerda CR. An antioxidant link between sickle cell disease and severe malaria. *Cell.* 2011;145(3):335-6.
82. Wagener FA, Dankers AC, van Summeren F, Scharstuhl A, van den Heuvel JJ, Koenderink JB, et al. Heme Oxygenase-1 and breast cancer resistance protein protect against heme-induced toxicity. *Curr Pharm Des.* 2013;19(15):2698-707.
83. Vermeulen Windsant IC, Hanssen SJ, Buurman WA, Jacobs MJ. Cardiovascular surgery and organ damage: time to reconsider the role of hemolysis. *J Thorac Cardiovasc Surg.* 2011;142(1):1-11.
84. Ingoglia G, Sag CM, Rex N, De Franceschi L, Vinchi F, Cimino J, et al. Hemopexin counteracts systolic dysfunction induced by heme-driven oxidative stress. *Free Radic Biol Med.* 2017;108:452-64.
85. Li RC, Saleem S, Zhen G, Cao W, Zhuang H, Lee J, et al. Heme-hemopexin complex attenuates neuronal cell death and stroke damage. *J Cereb Blood Flow Metab.* 2009;29(5):953-64.
86. Smith A, McCulloh RJ. Hemopexin and haptoglobin: allies against heme toxicity from hemoglobin not contenders. *Front Physiol.* 2015;6:187.
87. Tolosano E, Hirsch E, Patrucco E, Camaschella C, Navone R, Silengo L, et al. Defective recovery and severe renal damage after acute hemolysis in hemopexin-deficient mice. *Blood.* 1999;94(11):3906-14.
88. Tolosano E, Fagoonee S, Hirsch E, Berger FG, Baumann H, Silengo L, et al. Enhanced splenomegaly and severe liver inflammation in haptoglobin/hemopexin double-null mice after acute hemolysis. *Blood.* 2002;100(12):4201-8.
89. Vinchi F, De Franceschi L, Ghigo A, Townes T, Cimino J, Silengo L, et al. Hemopexin therapy improves cardiovascular function by preventing heme-induced endothelial toxicity in mouse models of hemolytic diseases. *Circulation.* 2013;127(12):1317-29.
90. Vinchi F, Costa da Silva M, Ingoglia G, Petrillo S, Brinkman N, Zuercher A, et al. Hemopexin therapy reverts heme-induced proinflammatory phenotypic switching of macrophages in a mouse model of sickle cell disease. *Blood.* 2016;127(4):473-86.
91. Larsen R, Gozzelino R, Jeney V, Tokaji L, Bozza FA, Japiassu AM, et al. A central role for free heme in the pathogenesis of severe sepsis. *Sci Transl Med.* 2010;2(51):51ra71.
92. Ferreira A, Balla J, Jeney V, Balla G, Soares MP. A central role for free heme in the pathogenesis of severe malaria: the missing link? *J Mol Med (Berl).* 2008;86(10):1097-111.
93. Wagener FA, Abraham NG, van Kooyk Y, de Witte T, Figdor CG. Heme-induced cell adhesion in the pathogenesis of sickle-cell disease and inflammation. *Trends Pharmacol Sci.* 2001;22(2):52-4.
94. Ishiguro T, Imanishi K, Suzuki I. Hemopexin levels in mice. *Int J Immunopharmacol.* 1984;6(3):241-4.
95. Elphinstone RE, Conroy AL, Hawkes M, Hermann L, Namasopo S, Warren HS, et al. Alterations in Systemic Extracellular Heme and Hemopexin Are Associated With Adverse Clinical Outcomes in Ugandan Children With Severe Malaria. *J Infect Dis.* 2016;214(8):1268-75.
96. Elphinstone RE, Riley F, Lin T, Higgins S, Dhabangi A, Musoke C, et al. Dysregulation of the haem-haemopexin axis is associated with severe malaria in a case-control study of Ugandan children. *Malar J.* 2015;14:511.

97. Janz DR, Bastarache JA, Sills G, Wickersham N, May AK, Bernard GR, et al. Association between haptoglobin, hemopexin and mortality in adults with sepsis. *Crit Care*. 2013;17(6):R272.
98. Guarda CCD, Santiago RP, Fiuza LM, Aleluia MM, Ferreira JRD, Figueiredo CVB, et al. Heme-mediated cell activation: the inflammatory puzzle of sickle cell anemia. *Expert Rev Hematol*. 2017;10(6):533-41.
99. Belcher JD, Mahaseth H, Welch TE, Otterbein LE, Hebbel RP, Vercellotti GM. Heme oxygenase-1 is a modulator of inflammation and vaso-occlusion in transgenic sickle mice. *J Clin Invest*. 2006;116(3):808-16.
100. Belcher JD, Chen C, Nguyen J, Milbauer L, Abdulla F, Alayash AI, et al. Heme triggers TLR4 signaling leading to endothelial cell activation and vaso-occlusion in murine sickle cell disease. *Blood*. 2014;123(3):377-90.
101. Belcher JD, Chen C, Nguyen J, Zhang P, Abdulla F, Nguyen P, et al. Control of Oxidative Stress and Inflammation in Sickle Cell Disease with the Nrf2 Activator Dimethyl Fumarate. *Antioxidants & redox signaling*. 2017;26(14):748-62.
102. Muller-Eberhard U, Javid J, Liem HH, Hanstein A, Hanna M. Plasma concentrations of hemopexin, haptoglobin and heme in patients with various hemolytic diseases. *Blood*. 1968;32(5):811-5.
103. Belcher JD, Chen C, Nguyen J, Abdulla F, Zhang P, Nguyen H, et al. Haptoglobin and hemopexin inhibit vaso-occlusion and inflammation in murine sickle cell disease: Role of heme oxygenase-1 induction. *PLoS One*. 2018;13(4):e0196455.
104. Nath KA, Belcher JD, Nath MC, Grande JP, Croatt AJ, Ackerman AW, et al. The Role of TLR4 Signaling in the Nephrotoxicity of Heme and Heme Proteins. *Am J Physiol Renal Physiol*. 2017:ajprenal.00432.2017.
105. Rossi M, Delbaue S, Wespes E, Roumeguere T, Leo O, Flamand V, et al. Dual effect of hemin on renal ischemia-reperfusion injury. *Biochem Biophys Res Commun*. 2018.
106. Balla G, Jacob HS, Balla J, Rosenberg M, Nath K, Apple F, et al. Ferritin: a cytoprotective antioxidant strategem of endothelium. *J Biol Chem*. 1992;267(25):18148-53.
107. Ferreira A, Marguti I, Bechmann I, Jeney V, Chora A, Palha NR, et al. Sickle hemoglobin confers tolerance to Plasmodium infection. *Cell*. 2011;145(3):398-409.
108. Thomas RA, Czopek A, Bellamy CO, McNally SJ, Kluth DC, Marson LP. Hemin Preconditioning Upregulates Heme Oxygenase-1 in Deceased Donor Renal Transplant Recipients: A Randomized, Controlled, Phase IIB Trial. *Transplantation*. 2016;100(1):176-83.
109. Vijayan V, Wagener F, Immenschuh S. The macrophage heme-heme oxygenase-1 system and its role in inflammation. *Biochem Pharmacol*. 2018;153:159-67.
110. Vermeulen Windsant IC, de Wit NC, Sertorio JT, Beckers EA, Tanus-Santos JE, Jacobs MJ, et al. Blood transfusions increase circulating plasma free hemoglobin levels and plasma nitric oxide consumption: a prospective observational pilot study. *Crit Care*. 2012;16(3):R95.

PART III:

GENERAL DISCUSSION AND SUMMARY

Chapter 8

General discussion and future perspectives

Abbreviations

CL/P	Cleft lip and/ or palate
CO	Carbon monoxide
CORM	CO-releasing molecules
CXCL11	C-X-C motif chemokine 11
CXCR3	C-X-C motif chemokine receptor 3
DAMPs	Damage-associated molecular patterns
ECM	Extracellular matrix
HO	Heme oxygenase
hpx	Hemopexin
ICAM-1	Intercellular adhesion molecule-1
IRI	Ischemia-reperfusion injury
KO	Knockout
LRP-1	LDL receptor-related protein-1
MES	Midline epithelial seam
MSC	Mesenchymal stem cells
NF- κ B	Nuclear factor kappa-light-chain-enhancer of activated B cells
nrf2	Nuclear-related factor-2
PAMPs	Pathogen-associated molecular patterns
PRDX1	Peroxiredoxin 1
RIPC	Remote ischemic preconditioning
TGF- β	Transforming growth factor-beta
TLR	Toll-like receptors
TNF- α	Tumor necrosis factor alpha
TSF	Tissue survival factor
VEGF	Vascular endothelial growth factor
WT	Wild-type

Synopsis of the problem

In the Western world, an orofacial cleft is surgically treated at an early age which leads to scar formation (1). Unfortunately, exposure of healing wounds to oxidative and inflammatory stimuli together with mechanical stress in a growing child may exacerbate scar formation (1, 2). Scar formation after CL/P repair may lead to functional problems, including hampered growth of the maxilla and velopharyngeal dysfunction resulting in speech difficulties (3, 4). Similar biological processes that are important during palatogenesis and development of CL/P also play a crucial role in cutaneous wound repair (5). Therefore, this thesis aimed to better understand the molecular and cellular mechanisms that discriminate between tissue repair and tissue regeneration.

We postulated that decreased activity of protective pathways impairs wound repair and palatogenesis, whereas induction of protective signaling cascades, provides a regenerative microenvironment that improves wound repair and regeneration.

In this thesis, several protective strategies were explored to find the decisive factors that determine the outcome of tissue repair by studying developmental, inflammatory, preconditioning and wound repair processes. More specifically, in part I, the effects of decreased protective mechanisms on wound repair and palatogenesis were studied. In part II, the role of inducing protective mechanisms on stem cell survival and wound repair was investigated, aiming at new therapeutic strategies towards tissue regeneration and developing a novel “tissue survival theory”.

Next, the main findings of this thesis are discussed, elaborating on the consequences for future research and possible therapeutic strategies.

Similarities between processes taking place during wound repair and palatogenesis

Accumulating evidence shows that palatogenesis and the wound healing process encompass many overlapping biological processes (5).

CL/P occurs, as the palatal shelves and/ or lip do not entirely fuse during embryogenesis. Processes that orchestrate palatal fusion include the mobilization of (stem) cells, cell proliferation and differentiation, migration of cells towards the fusion edge, and disintegration of the midline epithelial seam (MES) by epithelial-to-mesenchymal transition, migration or apoptosis of the epithelial cells, followed by remodeling of the extracellular matrix (ECM) (6-9). During cutaneous wound repair, leukocytes, mesenchymal cells (e.g., fibroblasts), and stem cells are recruited into the wound area, and keratinocytes migrate and re-epithelialize the damaged tissue (10). Fibroblasts can proliferate and differentiate into myofibroblasts, and subsequently, synthesize and remodel the ECM and eventually go into apoptosis. And hence, similar processes that are crucial for palatogenesis also control cutaneous wound repair (5). Epithelial-mesenchymal crosstalk and chemokine signaling play an important role herein. In both palatogenesis and wound repair, the final aim is to (re)generate the tissue. Not surprisingly, many genes associated with CL/P development are also essential during wound repair and scar formation (e.g., IRF6, PDGF-C, TGF- β 3, RhoGTPase activating protein 29, and Sonic hedgehog) (5).

Inflammatory and oxidative stress both promote CL/P and scar formation (11-16). The importance of suppressing inflammatory and oxidative stress for both preventing CL/P and improving wound repair is further strengthened by observations that embryos heal

wounds with reduced scar formation by an attenuated inflammatory response (17-19). Controlling the inflammatory and oxidative components may therefore be crucial during hampered palatogenesis and wound repair (1). Likely, the importance of this control will not be limited to these indications, but probably also plays a role in patients with higher levels of oxidative stress and inflammation, such as diabetes, infections, obesity, or elderly people (20-22). We postulated that decreased activity of protective pathways exacerbates wound repair and developmental problems, whereas induction of protective signaling pathways, with a focus on the resolution of oxidative and inflammatory stress, will provide a regenerative environment leading to improved wound repair.

Notably, there are environmental differences between skin and oral tissue, e.g., temperature, moisture environment, and microflora. Although both the oral mucosa and skin consist of stratified epithelium, anatomical differences exist with the oral mucosa covering bony tissue (hard palate) and muscle (soft palate) and the presence of taste buds, whereas the skin epithelium holds sweat glands and hair follicles (19, 23). Despite these differences, inflammation and oxidative stress remain important in the healing process of both tissues. However, the inflammation phase is less pronounced in oral wound repair with less influx of neutrophils, macrophages, and T-cells and differential expression of cytokines such as TGF- β and VEGF (24, 25). Interestingly, oral wounds heal more rapidly than skin wounds and with less scar formation (19, 24-29). Additional factors that could explain this include the moisture microenvironment in the oral tissue with saliva, accompanied by the presence of pro-healing factors such as histatin and growth factors, or enhanced cellular proliferation resulting in a quicker re-epithelialization in oral tissue, supporting a more regenerative environment (19, 24-29).

Part I: Decreased protective pathways during natural wound repair and palatogenesis

HO during excisional wound repair

The important role of HO-1 has been demonstrated in models of tissue injury and HO improves tissue repair by its anti-oxidative and anti-inflammatory effects (30-32). Inducing HO-1 expression accelerates cutaneous wound repair, whereas absence or inhibition of HO-1 attenuates wound repair (33, 34). Although the role of HO-2 has been much less investigated than HO-1, it was shown that the absence of HO-2 leads to slower corneal wound repair (35-38).

The role of HO-2 in excisional skin wound repair was not yet investigated and is discussed in **Chapter 2** of this thesis.

We reported that excisional skin wound repair was delayed in HO-2 knockout mice, despite the absence of differences in inflammation, and independent of HO-1 expression. Reduced collagen deposition and angiogenesis was found in HO-2 KO mice, and may be associated with the delay in CXCL11 expression in these mice compared to WT mice. Decreased expression of CXCL11 and its receptor CXCR3 has been demonstrated to result in delayed wound healing and disturbed angiogenesis (39-43). Our study is the first describing basal HO-2 expression to be important for cutaneous wound repair and provides critical insight into the wound healing mechanism. Analyzing genetic polymorphisms of HO-2 or whether the expression is down-regulated in patients suffering from impeded wound repair may give insight into what is going wrong. Since HO-2 is hardly pharmacologically

inducible, the inducible HO-1 isoform or HO-effector molecules can be used as an alternative for therapeutic application (44). To translate our findings to embryogenesis, we next studied the role of HO and CXCL11/CXCR3 in craniofacial and palatal development.

Palatogenesis

To gain more insight into the etiology of CL/P, we need to understand the biological mechanisms during palatogenesis better.

In **Chapter 3**, the molecular process of palatogenesis was studied in more detail using WT and HO-2 KO mice. Since the palate normally develops between day 10-15 of intrauterine gestation in mice, we investigated the development and palatogenesis at day 15 and 16 of the embryos since the palates then usually should have been fused.

We showed that the offspring of HO-2 KO mice had more malformations compared to WT mice and are behind in growth at day 15 of embryological development. In both WT and HO-2 KO mice, multiple apoptotic fragments were found within the MES, which were taken up by macrophages, indicating that apoptosis plays a principal role in the disintegration of the MES. CXCL11 was strongly expressed in the MES, suggesting that this caused the recruitment of CXCR3-positive macrophages. Since macrophages in HO-2 KO mice located around the MES have increased expression of HO-1 compared to those in WT mice, a compensatory mechanism is suggested, dealing with the oxidative stress as a result of the absence of HO-2.

The lack of effect in the absence of HO-2 on palatogenesis may be related to the absence of an inflammatory trigger. There is no need for the fire brigade when there is no fire. It would be interesting to follow this up with research in a more stringent model (e.g., following the induction of diabetes), since this may lead to a more substantial effect on palatogenesis. Taken together, HO and the CXCL11/CXCR3 axis play an important role in embryogenesis and facilitating palatal fusion. Previously, it was demonstrated that HO-2 is down-regulated in murine and human pathological pregnancies and may lead to enhanced levels of free heme that subsequently elevates an inflammatory response (45, 46). HO was proposed as a putative therapeutic target in immunological pregnancy complications (47). Whether the induction of HO-1 can be used as a therapeutic approach to prevent CL/P formation is under active investigation. Currently, our research group evaluates whether administration of different doses of heme during pregnancy in mice leads to craniofacial malformations and whether this can either be worsened by inhibition of HO-activity or be rescued by HO-1 induction. When successful, this could give new therapeutic strategies preventing CL/P formation.

Mechanical stress during excisional wound repair

Understanding the wound healing process is important for different patient groups with tissue injuries, such as those with diabetes, obesity, trauma injuries, burn wounds, cancer, and CL/P after cleft surgery (48). Experimental wound healing studies in humans are limited due to ethical and practical obstacles, such as scarcity of wound biopsies due to the painful procedure and risk of infection and scarring (49). Wound repair models in animals are therefore often used to investigate the molecular mechanisms behind wound repair.

There are several *in vivo* models that can be used to study the different aspects of wound repair. Although the skin characteristics of humans are more related to the pig (48, 50), murine models have many advantages. Rodents are small, easy to handle, and relatively cheap, but most importantly their genome is similar to the human genome and transgenic rodents are widely available and relatively easy to develop due to the short reproduction time (50, 51). Using knockout or transgenic rodents, e.g., *HO-2* KO mice and *HO-1 luc tg* mice, makes it possible to investigate molecular mechanisms in more detail. A difference between murine and human wound healing is that wound contraction in mice is primarily mediated by the *musculus panniculus carnosus* underneath the murine skin which is lacking in humans (50, 52, 53). Wound healing in humans is mainly based on granulation tissue formation and re-epithelialization (50, 52, 53).

In **Chapter 4** of this thesis, we described a splinted excisional wound model in mice, which is more closely related to human wound repair. In this model wound contraction by the *musculus panniculus carnosus* is inhibited by a splint, which leads to static mechanical stress on the healing wound by the difference in force between the muscle and the splint. Similarly, mechanical stress is also experienced on the healing palate in surgically operated CL/P patients and wound repair, which is exacerbated during growth and results in scar formation. The basal expression of the protective HO-1 enzyme in this mechanical stress-induced splinted wound repair was investigated using HO-1 luciferase mice.

In brief, splinting delayed excisional wound repair. Splinting-induced mechanical stress induced more HO-1 gene expression in 7-day wounds; however, HO-1 protein expression remained lower in the epidermis, likely due to a lower number of keratinocytes in the re-epithelialization tissue. Higher numbers of macrophages, myofibroblasts, and increased levels of inflammatory genes in 7-day splinted wounds, indicate an elevated or extended pro-inflammatory microenvironment. Mechanical stress because of splinting delays wound repair and induces a pro-inflammatory environment that may explain the higher number of myofibroblasts and subsequently increases the risk of fibrosis. This splinted wound model simulates surgically-treated cleft palate wound repair. Although HO-1 was expressed in both splinted and non-splinted wounds, the lower HO-1 protein expression in splinted wounds suggests that inducing HO-1 activity may form an interesting strategy for attenuating inflammatory and fibrotic processes caused by mechanical stress. Also, administration of HO effector molecules may form a possible therapeutic option, as both CO and bilirubin can enhance wound repair (54-56).

Part II: Activation of protective mechanisms to enhance tissue regeneration

Part II was divided into three chapters. Chapter 5 showed that pharmacological preconditioning can improve mesenchymal stem cell survival. In Chapter 6, we investigated the effects of remote ischemic preconditioning (RIPC) on wound repair. Lastly, Chapter 7 describes the possible molecular mechanism that discriminates between tissue survival and activation of the immune system.

Mesenchymal stem cells in tissue repair

A novel therapeutic approach in a plethora of disease settings is the administration of stem cells. Administration of mesenchymal stem cells (MSC) forms a promising adjuvant

treatment to improve wound repair and to prevent scarring (12, 57-60). Stem cells can differentiate into different cell types and are crucial during embryogenesis, palatogenesis, and repair of injured tissue. In addition to their pluripotency, stem cells excrete paracrine factors that improve wound repair (61-63). Many studies are showing that MSC administration during wound healing is effective and contributes to an enhanced wound repair and proper skin restoration during all phases of wound healing in both pre-clinical and clinical settings (64-67). The exact mechanism is unknown, but paracrine effects are likely more important than cell replacement and differentiation for the therapeutic effects (68, 69). Injection of solely the conditioned media derived from MSCs can already improve wound repair, suggesting that the paracrine factors exert the principal protective mechanism of action (70-72). Since the administration of MSCs to one side of a two-sided excisional wound model, improved wound repair to both sides, this suggests a systemic effect, which could not be explained by cell differentiation (73). Protective paracrine factors of MSCs improve wound repair by enhancing cell viability and proliferation, attenuating oxidative and inflammatory signals, improving angiogenesis, and improving mobilization/attraction of reparative cells (69, 70, 74, 75).

Unfortunately, administered MSCs die quickly upon administration and are only limited incorporated into the injured tissue due to the hostile wound environment consisting of oxidative and inflammatory mediators (66, 67).

Improving MSC survival at the place of injury may further enhance the protective effects as these cells can continue to produce paracrine factors for prolonged periods and create a pro-healing regenerative wound microenvironment.

HO-1 is a promising target to improve MSC therapy in tissue repair

Systemic administration of MSCs may reduce the direct lethal effects of the hostile wound environment on the cells and chemokines from the injury site may direct the cells by cell migration (66, 76, 77). However, less than 1% of systemically administered MSCs may persist at the injury site after seven days (59, 78), maybe because access from the circulation to the wound site may be hampered by damaged blood vessels and disorganized tissue and inhibit MSC therapy efficacy (66). The limited migration of stem cells to the site of injury after systemic administration, together with the low MSC survival, constitute the main complications of systemic MSC therapy (59, 78).

We postulated that the outcome of stem cell therapy can potentially be further improved by inducing cytoprotective mechanisms. HO has anti-apoptotic, anti-oxidative, and anti-inflammatory effects and forms a promising candidate. It was found that HO-1 has a prominent role in MSC therapy (79-82). MSC secrete a variety of paracrine factors, of which HO-1 critically determines the outcome. Paracrine factors excreted by MSCs from WT mice protected against kidney injury after intraperitoneal administration of MSC-derived conditioned media, whereas conditioned media of MSCs derived from HO-1 KO mice did not provide protection (81). Furthermore, modulating MSC by transfection or chemical inducers or inhibitors of HO affect the therapeutic paracrine effects of the MSC (79-82).

Interestingly, it was shown that HO-1 is upregulated in various tissues after MSC therapy, which had a beneficial effect on the function of the different injured organs (83-87). In addition, induction of HO activity during MSC therapy in the stem cell and systemically in the organism further increased the anti-apoptotic, anti-inflammatory and

anti-oxidative effects of MSC therapy, and this was significantly attenuated when HO-activity was inhibited (79, 82, 83, 88, 89). Moreover, angiogenesis and cell migration are increased after HO-induction in several animal models (83, 90, 91). All these processes are intricately involved in wound healing and create a more friendly wound microenvironment and stimulate wound repair. Thus, HO improves the power of MSC therapy by addressing the problems that are causative for pathologic wound repair, which ultimately leads to better tissue regeneration.

Curcumin induces HO-1 and MSC survival and can be used for wound repair

Since ancient Egyptian times, vegetable substances have been applied to skin wounds, and substances such as curcumin are still used to investigate the effects on wound repair (92). Curcumin has shown to be beneficial in skin diseases, such as scleroderma, psoriasis, and skin cancer, but also enhances normal and impaired wound repair by improving collagen deposition, and increasing fibroblast and vascular density in wounds (93, 94). These effects are orchestrated by the activation of cytoprotective genes (nrf2, HO-1), and its downstream anti-inflammatory and anti-oxidative effects (95, 96).

In **Chapter 5** of this thesis, we report the results of investigations on the effects of curcumin on MSC survival. Curcumin is found to be a potent inducer of HO-1 and provide protection against oxidative stress mediated by hydrogen peroxide as shown by the increased survival of curcumin pre-treated MSCs when exposed to hydrogen peroxide. This protection was prevented when HO-activity was specifically inhibited, pointing to a direct protective effect of curcumin via HO-1. Pre-treatment with CO-releasing molecules (CORMs) showed that the HO-effector molecule CO could also protect against oxidative-stress-induced cell death. Altogether, this study demonstrated that preconditioning of MSCs improves cell survival and suggests that pre-treatment of MSCs before administration may improve MSC therapy outcome.

Administration of stem cells or its secreted protective paracrine factors forms an attractive therapy to improve wound and tissue repair and regeneration. Induction of HO-1, e.g., by curcumin, or exposure to HO-effector molecules, such as CO, may enhance the production of beneficial paracrine factors and may enhance stem cell survival. Preconditioning techniques may further improve the beneficial effects of MSC therapy by creating a microenvironment that harnesses inflammatory and oxidative stress and increases the survival of locally present and administered MSCs. More research is needed to investigate whether MSC therapy can be used therapeutically for CL/P patients.

Remote ischemic preconditioning (RIPC)

Effects of RIPC on wound repair

In contrast to most medicinal drugs, RIPC is a non-invasive, inexpensive and safe approach, and hence, clinical trials are performed in diverse disease settings. Although the exact mechanism of action still has to be further elucidated, RIPC shows promising pre-clinical and clinical results in the field of organ transplantation and cardiovascular diseases by inhibition of oxidative and inflammatory insults (97, 98).

Since oxidative and inflammatory stress plays an important role in CL/P formation and wound repair and can be inhibited by RIPC, we next investigated if RIPC could improve

wound repair following excisional skin injury. In parallel, we assessed whether HO-1 is induced upon RIPC treatment. These studies are described in **Chapter 6** of this thesis.

Unfortunately, both early and late RIPC did not affect excisional wound repair in mice. Interestingly, we observed that RIPC induced HO-1 expression in several organs, including skeletal muscle, kidney, and heart, but not in the skin. This suggested that the protection mediated by RIPC may act via HO-1, as organs that were previously shown to be protected by RIPC (heart, muscle, and kidney), upregulated HO-1 expression, in contrast to the skin where no protection was observed. Interestingly, survival of transplanted skin flaps was increased when RIPC treatment was applied (99), indicating that RIPC can have protective effects in the skin as well. Also, other studies showed that RIPC improves microcirculation by an increase in tissue oxygenation and capillary blood flow in the skin (100) and skin flaps (101). Other RIPC regimens than the ones we used may be more efficient, and other molecular pathways may be involved or may be affected at different time-points. RIPC may have therapeutic effects in other wound models. For example, it was found that RIPC significantly improves the healing of diabetic foot ulcers (102, 103). In addition, there is an ongoing clinical trial where the protective effects of RIPC on the microcirculation and pathological wound repair, including burns, non-healing wounds, and skin grafts are investigated in more details (clinicaltrials.gov identifier: NCT02417805).

Implications of RIPC to prevent CL/P

RIPC has shown protective effects in several oxidative and inflammatory stress models. Since these same conditions increase the risk of CL/P, application of RIPC may act protectively against CL/P development. Hereto, RIPC should be applied at the moment or before the crucial phases of palatogenesis; e.g., day 10-15 of pregnancy in mice, or week 8-10 during human embryonic development. In this way, the incidence of CL/P may be decreased in women with imminent risk (e.g., having diabetes, obesity, infections, or older age) (13-16).

Moreover, in CL/Fr mice that are genetically predisposed to develop CL/P, oxidative stress has shown to be important in affecting the incidence of CL/P (104). Under normal conditions, CL/Fr mice spontaneously develop CL/P in 37% of the fetuses. Interestingly, when these pregnant mice were exposed to hyperoxic conditions for 24h at day 10 of gestation, only 13% of their progeny developed CL/P, whereas exposure to hypoxia increased the incidence of CL/P to 89% (104). A similar experimental setup can be used to investigate the protective effects of RIPC on the incidence of CL/P.

RIPC treatment creates short-term hypoxic stress, which subsequently can protect against secondary stronger stresses (such as is experienced during CL/P formation). RIPC as preconditioning to prevent CL/P formation is still promising and needs further investigation, e.g., by applying RIPC shortly before the process of palatogenesis which finishes around day 15, thus e.g., sometime around day 10-14 in pregnant CL/Fr mice.

Molecular mechanisms of tissue protection

Following injury, the immune system is activated to eliminate pathogenic invaders (105). The “danger model” of Matzinger proposed that the immune system only becomes activated after a danger signal, such as nucleic acids, heat-shock proteins, or heme, is

detected by Toll-like receptors (TLR), which subsequently warn leukocytes (106-108). We propose here that there are also signals that can warn the tissue for upcoming danger, and act as tissue survival factor (TSF).

Therefore, in **Chapter 7** we proposed a “tissue survival theory” describing that heme scavenging is a discriminating factor between tissue survival and immune activation. We used RIPC as a model to present our theory. After RIPC treatment, heme levels are slightly but significantly elevated. We postulated that in the presence of hemopexin (hpx), heme is directly scavenged and this TSF then binds to the LRP-1 receptor, which via e.g., nrf2 can activate cytoprotective genes, such as HO-1 and PRDX1. RIPC indeed induced HO-1 mRNA and protein expression in the skeletal muscle, kidney, and heart, and HO-1 was co-expressed with LRP-1 in the cells of the heart. When hpx is exhausted, high levels of free heme can bind to TLR-4 and via NF-KB can induce pro-inflammatory genes, such as TNF- α and ICAM-1. This theory is further supported by various pathological conditions, including IRI, hemoglobinopathies, hematoma, hemorrhage, and muscle injury, where large amounts of free heme and heme-proteins are found after hemolysis or rhabdomyolysis and act harmful (109-112).

RIPC has shown to protect against several pathological conditions, such as heart failure, kidney injury and improves the outcome after organ transplantation (113-116). However, results are not always consistent (117-120), and not every tissue and organ is protected following RIPC, such as in our study during cutaneous wound repair (121). This tissue-specific protection may depend on the function of the tissue. Skin is most frequently affected by inflammation by continually being exposed to microbes, which may elevate tissue tolerance and make skin less responsive towards internal stressors (22, 122). However, this could not explain why RIPC improved wound repair of diabetic foot ulcers. A difference with excisional wound repair may be that short following injury heme is abundantly released, which results in a pro-inflammatory response that is necessary to attract leukocytes and clean up wound debris (123, 124). Hpx that is locally present will then quickly be exhausted and not cause fast enough tissue protection, because the excess of heme binds to TLR-4, acts pro-inflammatory and can cause damage. Our model is further supported by the observation that treatment with heme before renal ischemia-reperfusion injury reduced renal damage, while treatment after IRI worsened the renal damage (125). This suggests that small amounts of heme only act protectively when it can be in complex with hpx. When hpx is depleted, heme will activate TLR-4 and aggravate injuries.

In summary, heme scavenging discriminates between activating tissue survival or alerting the immune system. This theory may be relevant in a plethora of diseases, and therapies using administration of small amounts of heme as preconditioning strategy, or administration of hpx, which as TSF activate protective signaling and skews away from TLR-4-induced inflammation.

Solving part of the puzzle: Novel therapies to transform tissue repair into regeneration

Inflammatory and oxidative stress leads to the release of danger signals, also known as damage-associated molecular patterns (DAMPs), pathogen-associated molecular patterns (PAMPs), or alarmins, such as heme, heat shock proteins, and S100 proteins (126-128). These danger signals can activate the immune system, leading to the mobilization of for example granulocytes and macrophages (128). In addition, these danger signals can bind to

cell receptors, such as TLRs, and activate pro-inflammatory stress responses that damage the tissue (128, 129). Tissue can have different reactions against external stresses, and this originates from the difference in tolerance between individuals (Figure 8.1). Everybody has a different response (c.q. tolerance) to injurious stressors because of differences in genetic makeup, diseases, drug use, age, and behavior (122, 130). The difference in tolerance causes that each individual will respond differently to danger signals (122, 130). The use of gene knockout makes it possible to investigate the contribution of a specific gene (131). For example, it has been shown that the lack of HO activity makes tissue more prone to tissue damage, and thus less tolerant towards injurious stresses. Low tolerant cells may have less expression or are depleted of protective molecules and molecular protective pathways. Exposure of these low tolerant cells to inflammatory and oxidative stress results in tissue damage and disease predisposition. In contrast, high tolerant cells may have more expression of protective molecules, such as HO-1, making them less susceptible to tissue damage. Preconditioning strategies or activation of TSFs may enhance the tolerance of cells and make them better equipped to fight off injurious stressors (Figure 8.1A).

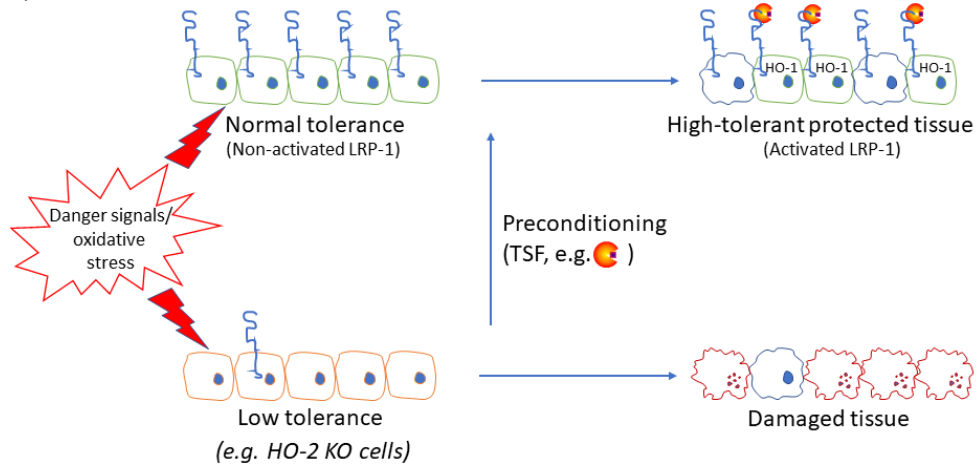
Preconditioning is a method to induce tolerance and prepare tissue against following stresses, in this way harnessing the stress signals and preventing tissue damage (130, 132). For example, stimulation of the heme-hpx complex formation can activate the LRP-1 receptor leading to the intracellular production of the cytoprotective HO-1. This protects the cell against damage and apoptosis. When cells get older, their repair strategies get easier exhausted, leading to cell damage and eventually apoptosis. Stem cells can be mobilized to the injured tissue and restore and rejuvenate the damaged cells (133). This offers therapeutic potential for (mesenchymal) stem cell therapy. However, the stringent microenvironment under inflammatory and oxidative stress makes the stem cells vulnerable to cell death (59, 78).

Therefore, preconditioning strategies may further improve the efficacy of stem cell therapy (Figure 8.1B). As discussed, this may be achieved by inducing protective pathways, such as HO-1, which enhances the protection against external stressors and thereby the cell survival (79-82). Moreover, these stem cells can also produce paracrine factors that protect their surroundings (61-63). Ideally, the tolerance of the cells must be elevated, preparing them for stress and leading to improved cell survival, with the ultimate outcome being tissue regeneration. Preconditioning strategies form an attractive option to induce tissue survival signals and obtain tissue regeneration.

Clinical relevance for CL/P patients?

Having presented these pre-clinical data, we will now address their possible clinical implications. We showed that the lack of protective enzyme systems can promote fetal malformations and hampered wound repair (134, 135). In contrast to animal studies using specific strains, patients have their own immune system, and the large differences in genetics and different exposure to environmental factors between patients make it difficult to translate data from animal experiments to the clinic directly (136-138). However, despite these translational drawbacks, having the same genetic background (e.g., HO-2 KO mice) and standardized environmental factors in animals and *in vitro* models, makes it possible to specifically study the mechanistic contribution of one or a couple of variables in a more causal manner (139).

A).



B).

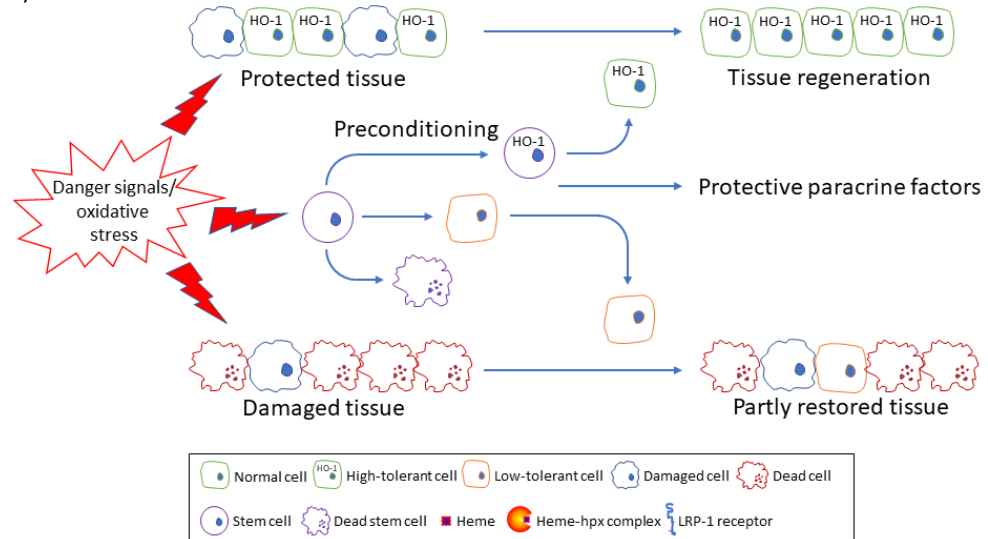


Figure 8.1: Tissue tolerance

A). Inflammatory and oxidative stress leads to the release of danger signals that can activate the immune system or directly bind to the cells of the tissue where it promotes injury. Every individual has a different genetic makeup and defense against oxidative and inflammatory stressors as a result of illness (e.g., diabetes, infections or age) resulting in differential tolerance towards injurious stressors. Cells with decreased tolerance towards oxidative and inflammatory stress because of depletion of anti-oxidant and anti-inflammatory molecules, such as in diabetes patients and aged people, are more prone to injury than cells with enough cell protective enzymes. Pre- and post-conditioning strategies or induction of tissue survival factors (TSFs) could restore tolerance against injurious stressors. For instance, RIPC results in the release of heme, which upon scavenging by hemopexin (hpx) forms the heme-hpx complex that as TSF can activate LRP-1 receptors, and lead to the production of the cytoprotective enzyme HO-1. **Note:** hpx should be present or co-administered to achieve cytoprotection. B). (Mesenchymal) stem cells produce protective paracrine factors and can renew damaged cells and improve tissue repair. Under stressful conditions (e.g., inflammatory or oxidative stress in the wound area), MSCs or tissue may die, or lead to low tolerant new cells. However, after preconditioning, cytoprotective systems as HO-1 are also induced in these stem cells, which may lead to high tolerant stem cells and increased production of protective paracrine factors. These high-tolerant stem cells will then replace damaged tissue and produce paracrine protective factors, resulting in tissue regeneration.

Preconditioning of stem cells by induction of HO-1 before inflicting oxidative stress resulted in improved stem cell survival (79). Although this data is based on *in vitro* evidence, enhanced survival of local stem cells in wound regions or after administration in stem cell therapy may offer better perspectives for the repair and regeneration of damaged tissue and could be promising as adjuvant therapy following CL/P surgery.

Our findings showed that RIPC did not directly contribute to enhanced cutaneous wound repair. However, we observed that HO-1 was remotely induced in different organs like the kidney and the heart (121). Interestingly, other studies showed that RIPC can act protectively in ischemia-reperfusion injury of these remote organs (113-116), and therefore we argued that local heme levels upon wounding may be too high to induce protective HO-1 expression in cutaneous excisional wound repair.

Our “tissue survival model” describes that heme can play the discriminating factor between tissue survival and immune activation. RIPC leads to the release of small amounts of heme, that scavenged by hpx form a tissue survival factor (TSF). This TSF can bind to LRP-1 and induce nrf2 responsive cytoprotective HO-1 signaling, which will warn the tissue against injurious stressors. When the scavenger hpx is exhausted, heme will be available for binding to TLR-4 and activate immune responses. Attracted leukocytes will excrete more pro-inflammatory signals that lead to collateral damage. Therefore, we propose hpx administration as novel therapeutic strategy that skews towards tissue protection via LRP-1 mediated HO-1 signaling for a diversity of pathologies, including heme-mediated diseases such as sickle cell disease, malaria, sepsis, fibrosis, but also during inflammation-mediated pathologies such as burn wounds, diabetes, pathological pregnancies, and after CL/P surgery. Since the TSF heme-hpx complex acts via induction of HO activity, it is also an option to pharmacologically induce HO-1 or administer HO-effector molecules, such as CO and bilirubin. Typically, treatments start after suffering from a disease, but when damage is expected, e.g., following a planned (CL/P) surgery, preconditioning strategies may be a better alternative to prevent (collateral) tissue damage. Also, preconditioning can be done in high-risk women for having a child with a cleft, and in such cases, the development of CL/P and its associated problems might be prevented. However, since our models are mainly based on animal studies, more research is needed first. Translational studies and clinical trials that further confirm our findings need to be performed.

There is evidence that the induction of cytoprotective pathways may protect tissue against oxidative and inflammatory stress and lead to tissue tolerance. Therefore, RIPC, MSC therapy, and the proposed novel pharmacological therapies mentioned above that harness inflammatory and oxidative stress during wound repair and palatogenesis should be further explored.

References

1. Papatthanasious E, Trotman CA, Scott AR, Van Dyke TE. Current and Emerging Treatments for Postsurgical Cleft Lip Scarring: Effectiveness and Mechanisms. *Journal of dental research*. 2017;96(12):1370-7.
2. van Beurden HE, Von den Hoff JW, Torensma R, Maltha JC, Kuijpers-Jagtman AM. Myofibroblasts in palatal wound healing: prospects for the reduction of wound contraction after cleft palate repair. *Journal of dental research*. 2005;84(10):871-80.
3. Brouwer KM, Lundvig DM, Middelkoop E, Wagener FA, Von den Hoff JW. Mechanical cues in orofacial tissue engineering and regenerative medicine. *Wound Repair Regen*. 2015;23(3):302-11.
4. Li J, Johnson CA, Smith AA, Salmon B, Shi B, Brunski J, et al. Disrupting the intrinsic growth potential of a suture contributes to midfacial hypoplasia. *Bone*. 2015;81:186-95.
5. Biggs LC, Goudy SL, Dunnwald M. Palatogenesis and cutaneous repair: A two-headed coin. *Dev Dyn*. 2015;244(3):289-310.
6. Jin JZ, Ding J. Analysis of cell migration, transdifferentiation and apoptosis during mouse secondary palate fusion. *Development*. 2006;133(17):3341-7.
7. Nawshad A. Palatal seam disintegration: to die or not to die? that is no longer the question. *Dev Dyn*. 2008;237(10):2643-56.
8. Vukojevic K, Kero D, Novakovic J, Kalibovic Govorko D, Saraga-Babic M. Cell proliferation and apoptosis in the fusion of human primary and secondary palates. *European journal of oral sciences*. 2012;120(4):283-91.
9. Iseki S. Disintegration of the medial epithelial seam: is cell death important in palatogenesis? *Development, growth & differentiation*. 2011;53(2):259-68.
10. Rousselle P, Braye F, Dayan G. Re-epithelialization of adult skin wounds: Cellular mechanisms and therapeutic strategies. *Adv Drug Deliv Rev*. 2018.
11. Shaw TJ, Kishi K, Mori R. Wound-associated skin fibrosis: mechanisms and treatments based on modulating the inflammatory response. *Endocrine, metabolic & immune disorders drug targets*. 2010;10(4):320-30.
12. Meyer M, Muller AK, Yang J, Sulcova J, Werner S. The role of chronic inflammation in cutaneous fibrosis: fibroblast growth factor receptor deficiency in keratinocytes as an example. *The journal of investigative dermatology Symposium proceedings / the Society for Investigative Dermatology, Inc [and] European Society for Dermatological Research*. 2011;15(1):48-52.
13. Spilson SV, Kim HJ, Chung KC. Association between maternal diabetes mellitus and newborn oral cleft. *Ann Plast Surg*. 2001;47(5):477-81.
14. Stott-Miller M, Heike CL, Kratz M, Starr JR. Increased risk of orofacial clefts associated with maternal obesity: case-control study and Monte Carlo-based bias analysis. *Paediatr Perinat Epidemiol*. 2010;24(5):502-12.
15. Bille C, Skytthe A, Vach W, Knudsen LB, Andersen AM, Murray JC, et al. Parent's age and the risk of oral clefts. *Epidemiology*. 2005;16(3):311-6.
16. Shahrukh Hashmi S, Gallaway MS, Waller DK, Langlois PH, Hecht JT, National Birth Defects Prevention S. Maternal fever during early pregnancy and the risk of oral clefts. *Birth Defects Res A Clin Mol Teratol*. 2010;88(3):186-94.
17. Redd MJ, Cooper L, Wood W, Stramer B, Martin P. Wound healing and inflammation: embryos reveal the way to perfect repair. *Philosophical transactions of the Royal Society of London Series B, Biological sciences*. 2004;359(1445):777-84.
18. Martin P, Parkhurst SM. Parallels between tissue repair and embryo morphogenesis. *Development*. 2004;131(13):3021-34.
19. Glim JE, van Egmond M, Niessen FB, Everts V, Beelen RH. Detrimental dermal wound healing: what can we learn from the oral mucosa? *Wound Repair Regen*. 2013;21(5):648-60.
20. Fernandez-Sanchez A, Madrigal-Santillan E, Bautista M, Esquivel-Soto J, Morales-Gonzalez A, Esquivel-Chirino C, et al. Inflammation, oxidative stress, and obesity. *Int J Mol Sci*. 2011;12(5):3117-32.
21. Ferrucci L, Fabbri E. Inflammageing: chronic inflammation in ageing, cardiovascular disease, and frailty. *Nat Rev Cardiol*. 2018;15(9):505-22.
22. Nathan C. Points of control in inflammation. *Nature*. 2002;420(6917):846-52.
23. Liu J, Bian Z, Kuijpers-Jagtman AM, Von den Hoff JW. Skin and oral mucosa equivalents: construction and performance. *Orthod Craniofac Res*. 2010;13(1):11-20.
24. Szpaderska AM, Zuckerman JD, DiPietro LA. Differential injury responses in oral mucosal and cutaneous wounds. *Journal of dental research*. 2003;82(8):621-6.

25. Johnson A, Francis M, DiPietro LA. Differential Apoptosis in Mucosal and Dermal Wound Healing. *Adv Wound Care (New Rochelle)*. 2014;3(12):751-61.
26. Ashcroft GS, Lei K, Jin W, Longenecker G, Kulkarni AB, Greenwell-Wild T, et al. Secretory leukocyte protease inhibitor mediates non-redundant functions necessary for normal wound healing. *Nat Med*. 2000;6(10):1147-53.
27. Angelov N, Moutsopoulos N, Jeong MJ, Nares S, Ashcroft G, Wahl SM. Aberrant mucosal wound repair in the absence of secretory leukocyte protease inhibitor. *Thromb Haemost*. 2004;92(2):288-97.
28. Turabelidze A, Guo S, Chung AY, Chen L, Dai Y, Marucha PT, et al. Intrinsic differences between oral and skin keratinocytes. *PLoS One*. 2014;9(9):e101480.
29. Torres P, Castro M, Reyes M, Torres VA. Histatins, wound healing and cell migration. *Oral Dis*. 2017.
30. Kapturczak MH, Wasserfall C, Brusko T, Campbell-Thompson M, Ellis TM, Atkinson MA, et al. Heme oxygenase-1 modulates early inflammatory responses: evidence from the heme oxygenase-1-deficient mouse. *The American journal of pathology*. 2004;165(3):1045-53.
31. Paine A, Eiz-Vesper B, Blasczyk R, Immenschuh S. Signaling to heme oxygenase-1 and its anti-inflammatory therapeutic potential. *Biochemical pharmacology*. 2010;80(12):1895-903.
32. Motterlini R, Foresti R. Heme oxygenase-1 as a target for drug discovery. *Antioxidants & redox signaling*. 2014;20(11):1810-26.
33. Grochot-Przeczek A, Lach R, Mis J, Skrzypek K, Gozdecka M, Sroczyńska P, et al. Heme oxygenase-1 accelerates cutaneous wound healing in mice. *PLoS One*. 2009;4(6):e5803.
34. Ahanger AA, Prawez S, Leo MD, Kathirvel K, Kumar D, Tandan SK, et al. Pro-healing potential of hemin: an inducer of heme oxygenase-1. *European journal of pharmacology*. 2010;645(1-3):165-70.
35. Bellner L, Martinelli L, Halilovic A, Patil K, Puri N, Dunn MW, et al. Heme oxygenase-2 deletion causes endothelial cell activation marked by oxidative stress, inflammation, and angiogenesis. *The Journal of pharmacology and experimental therapeutics*. 2009;331(3):925-32.
36. Seta F, Bellner L, Rezzani R, Regan RF, Dunn MW, Abraham NG, et al. Heme oxygenase-2 is a critical determinant for execution of an acute inflammatory and reparative response. *The American journal of pathology*. 2006;169(5):1612-23.
37. Halilovic A, Patil KA, Bellner L, Marrazzo G, Castellano K, Cullaro G, et al. Knockdown of heme oxygenase-2 impairs corneal epithelial cell wound healing. *Journal of cellular physiology*. 2011;226(7):1732-40.
38. Bellner L, Marrazzo G, van Rooijen N, Dunn MW, Abraham NG, Schwartzman ML. Heme oxygenase-2 deletion impairs macrophage function: implication in wound healing. *FASEB journal : official publication of the Federation of American Societies for Experimental Biology*. 2015;29(1):105-15.
39. Yates CC, Whaley D, Wells A. Transplanted fibroblasts prevents dysfunctional repair in a murine CXCR3-deficient scarring model. *Cell transplantation*. 2012;21(5):919-31.
40. Yates CC, Whaley D, Hooda S, Hebda PA, Bodnar RJ, Wells A. Delayed reepithelialization and basement membrane regeneration after wounding in mice lacking CXCR3. *Wound Repair Regen*. 2009;17(1):34-41.
41. Yates CC, Whaley D, Kulasekeran P, Hancock WW, Lu B, Bodnar R, et al. Delayed and deficient dermal maturation in mice lacking the CXCR3 ELR-negative CXC chemokine receptor. *The American journal of pathology*. 2007;171(2):484-95.
42. Tortelli F, Pisano M, Briquez PS, Martino MM, Hubbell JA. Fibronectin binding modulates CXCL11 activity and facilitates wound healing. *PLoS One*. 2013;8(10):e79610.
43. Huen AC, Wells A. The Beginning of the End: CXCR3 Signaling in Late-Stage Wound Healing. *Adv Wound Care (New Rochelle)*. 2012;1(6):244-8.
44. Ryter SW, Choi AM. Heme oxygenase-1/carbon monoxide: from metabolism to molecular therapy. *Am J Respir Cell Mol Biol*. 2009;41(3):251-60.
45. Zenclussen AC, Joachim R, Hagen E, Peiser C, Klapp BF, Arck PC. Heme oxygenase is downregulated in stress-triggered and interleukin-12-mediated murine abortion. *Scand J Immunol*. 2002;55(6):560-9.
46. Zenclussen AC, Lim E, Knoeller S, Knackstedt M, Hertwig K, Hagen E, et al. Heme oxygenases in pregnancy II: HO-2 is downregulated in human pathologic pregnancies. *Am J Reprod Immunol*. 2003;50(1):66-76.
47. Zenclussen AC, Sollwedel A, Bertoja AZ, Gerlof K, Zenclussen ML, Woiciechowsky C, et al. Heme oxygenase as a therapeutic target in immunological pregnancy complications. *Int Immunopharmacol*. 2005;5(1):41-51.
48. Seaton M, Hocking A, Gibran NS. Porcine models of cutaneous wound healing. *ILAR journal*. 2015;56(1):127-38.

49. Kim DJ, Mustoe T, Clark RA. Cutaneous wound healing in aging small mammals: a systematic review. *Wound Repair Regen.* 2015;23(3):318-39.
50. Zomer HD, Trentin AG. Skin wound healing in humans and mice: Challenges in translational research. *J Dermatol Sci.* 2018;90(1):3-12.
51. Vandamme TF. Use of rodents as models of human diseases. *J Pharm Bioallied Sci.* 2014;6(1):2-9.
52. Dunn L, Prosser HC, Tan JT, Vanags LZ, Ng MK, Bursill CA. Murine model of wound healing. *J Vis Exp.* 2013(75):e50265.
53. Galiano RD, Michaels Jt, Dobryansky M, Levine JP, Gurtner GC. Quantitative and reproducible murine model of excisional wound healing. *Wound Repair Regen.* 2004;12(4):485-92.
54. Ahanger AA, Prawez S, Kumar D, Prasad R, Amarpal, Tandan SK, et al. Wound healing activity of carbon monoxide liberated from CO-releasing molecule (CO-RM). *Naunyn Schmiedebergs Arch Pharmacol.* 2011;384(1):93-102.
55. Ram M, Singh V, Kumawat S, Kant V, Tandan SK, Kumar D. Bilirubin modulated cytokines, growth factors and angiogenesis to improve cutaneous wound healing process in diabetic rats. *Int Immunopharmacol.* 2016;30:137-49.
56. Ahanger AA, Leo MD, Gopal A, Kant V, Tandan SK, Kumar D. Pro-healing effects of bilirubin in open excision wound model in rats. *Int Wound J.* 2016;13(3):398-402.
57. Leung A, Crombleholme TM, Keswani SG. Fetal wound healing: implications for minimal scar formation. *Current opinion in pediatrics.* 2012;24(3):371-8.
58. Butler KL, Goverman J, Ma H, Fischman A, Yu YM, Bilodeau M, et al. Stem cells and burns: review and therapeutic implications. *Journal of burn care & research : official publication of the American Burn Association.* 2010;31(6):874-81.
59. Chen FM, Wu LA, Zhang M, Zhang R, Sun HH. Homing of endogenous stem/progenitor cells for in situ tissue regeneration: Promises, strategies, and translational perspectives. *Biomaterials.* 2011;32(12):3189-209.
60. Bertozzi N, Simonacci F, Grieco MP, Grignaffini E, Raposio E. The biological and clinical basis for the use of adipose-derived stem cells in the field of wound healing. *Ann Med Surg (Lond).* 2017;20:41-8.
61. Wei L, Fraser JL, Lu ZY, Hu X, Yu SP. Transplantation of hypoxia preconditioned bone marrow mesenchymal stem cells enhances angiogenesis and neurogenesis after cerebral ischemia in rats. *Neurobiology of disease.* 2012;46(3):635-45.
62. Malgieri A, Kantzari E, Patrizi MP, Gambardella S. Bone marrow and umbilical cord blood human mesenchymal stem cells: state of the art. *International journal of clinical and experimental medicine.* 2010;3(4):248-69.
63. Tse WT, Pendleton JD, Beyer WM, Egalka MC, Guinan EC. Suppression of allogeneic T-cell proliferation by human marrow stromal cells: implications in transplantation. *Transplantation.* 2003;75(3):389-97.
64. Jackson WM, Nesti LJ, Tuan RS. Concise review: clinical translation of wound healing therapies based on mesenchymal stem cells. *Stem cells translational medicine.* 2012;1(1):44-50.
65. Maxson S, Lopez EA, Yoo D, Danilkovitch-Miagkova A, Leroux MA. Concise review: role of mesenchymal stem cells in wound repair. *Stem cells translational medicine.* 2012;1(2):142-9.
66. Isakson M, de Blacam C, Whelan D, McArdle A, Clover AJ. Mesenchymal Stem Cells and Cutaneous Wound Healing: Current Evidence and Future Potential. *Stem cells international.* 2015;2015:831095.
67. Cerqueira MT, Pirraco RP, Marques AP. Stem Cells in Skin Wound Healing: Are We There Yet? *Adv Wound Care (New Rochelle).* 2016;5(4):164-75.
68. Madrigal M, Rao KS, Riordan NH. A review of therapeutic effects of mesenchymal stem cell secretions and induction of secretory modification by different culture methods. *Journal of translational medicine.* 2014;12:260.
69. Spees JL, Lee RH, Gregory CA. Mechanisms of mesenchymal stem/stromal cell function. *Stem cell research & therapy.* 2016;7(1):125.
70. Lee DE, Ayoub N, Agrawal DK. Mesenchymal stem cells and cutaneous wound healing: novel methods to increase cell delivery and therapeutic efficacy. *Stem cell research & therapy.* 2016;7:37.
71. Arno AI, Amini-Nik S, Blit PH, Al-Shehab M, Belo C, Herer E, et al. Human Wharton's jelly mesenchymal stem cells promote skin wound healing through paracrine signaling. *Stem cell research & therapy.* 2014;5(1):28.
72. Yew TL, Hung YT, Li HY, Chen HW, Chen LL, Tsai KS, et al. Enhancement of wound healing by human multipotent stromal cell conditioned medium: the paracrine factors and p38 MAPK activation. *Cell transplantation.* 2011;20(5):693-706.

73. Shin L, Peterson DA. Human mesenchymal stem cell grafts enhance normal and impaired wound healing by recruiting existing endogenous tissue stem/progenitor cells. *Stem cells translational medicine*. 2013;2(1):33-42.
74. Liang X, Ding Y, Zhang Y, Tse HF, Lian Q. Paracrine mechanisms of mesenchymal stem cell-based therapy: current status and perspectives. *Cell transplantation*. 2014;23(9):1045-59.
75. Maranda EL, Rodriguez-Menocal L, Badiavas EV. Role of Mesenchymal Stem Cells in Dermal Repair in Burns and Diabetic Wounds. *Current stem cell research & therapy*. 2016;12(1):61-70.
76. Brower J, Blumberg S, Carroll E, Pastar I, Brem H, Chen W. Mesenchymal stem cell therapy and delivery systems in nonhealing wounds. *Adv Skin Wound Care*. 2011;24(11):524-32; quiz 33-4.
77. Karp JM, Leng Teo GS. Mesenchymal stem cell homing: the devil is in the details. *Cell Stem Cell*. 2009;4(3):206-16.
78. Parekkadan B, Milwid JM. Mesenchymal stem cells as therapeutics. *Annu Rev Biomed Eng*. 2010;12:87-117.
79. Cremers NA, Lundvig DM, van Dalen SC, Schelbergen RF, van Lent PL, Szarek WA, et al. Curcumin-induced heme oxygenase-1 expression prevents H₂O₂-induced cell death in wild type and heme oxygenase-2 knockout adipose-derived mesenchymal stem cells. *Int J Mol Sci*. 2014;15(10):17974-99.
80. Cai C, Teng L, Vu D, He JQ, Guo Y, Li Q, et al. The heme oxygenase 1 inducer (CoPP) protects human cardiac stem cells against apoptosis through activation of the extracellular signal-regulated kinase (ERK)/NRF2 signaling pathway and cytokine release. *J Biol Chem*. 2012;287(40):33720-32.
81. Zarjou A, Kim J, Traylor AM, Sanders PW, Balla J, Agarwal A, et al. Paracrine effects of mesenchymal stem cells in cisplatin-induced renal injury require heme oxygenase-1. *Am J Physiol Renal Physiol*. 2011;300(1):F254-62.
82. Zeng B, Ren X, Lin G, Zhu C, Chen H, Yin J, et al. Paracrine action of HO-1-modified mesenchymal stem cells mediates cardiac protection and functional improvement. *Cell Biol Int*. 2008;32(10):1256-64.
83. Hou C, Shen L, Huang Q, Mi J, Wu Y, Yang M, et al. The effect of heme oxygenase-1 complexed with collagen on MSC performance in the treatment of diabetic ischemic ulcer. *Biomaterials*. 2013;34(1):112-20.
84. Yang JJ, Yang X, Liu ZQ, Hu SY, Du ZY, Feng LL, et al. Transplantation of adipose tissue-derived stem cells overexpressing heme oxygenase-1 improves functions and remodeling of infarcted myocardium in rabbits. *The Tohoku journal of experimental medicine*. 2012;226(3):231-41.
85. Liu H, McTaggart SJ, Johnson DW, Gobe GC. Original article anti-oxidant pathways are stimulated by mesenchymal stromal cells in renal repair after ischemic injury. *Cytotherapy*. 2012;14(2):162-72.
86. Sun CK, Chang CL, Lin YC, Kao YH, Chang LT, Yen CH, et al. Systemic administration of autologous adipose-derived mesenchymal stem cells alleviates hepatic ischemia-reperfusion injury in rats. *Critical care medicine*. 2012;40(4):1279-90.
87. Liang OD, Mitsialis SA, Chang MS, Vergadi E, Lee C, Aslam M, et al. Mesenchymal stromal cells expressing heme oxygenase-1 reverse pulmonary hypertension. *Stem cells*. 2011;29(1):99-107.
88. Tsubokawa T, Yagi K, Nakanishi C, Zuka M, Nohara A, Ino H, et al. Impact of anti-apoptotic and anti-oxidative effects of bone marrow mesenchymal stem cells with transient overexpression of heme oxygenase-1 on myocardial ischemia. *Am J Physiol Heart Circ Physiol*. 2010;298(5):H1320-9.
89. Zhang ZH, Zhu W, Ren HZ, Zhao X, Wang S, Ma HC, et al. Mesenchymal stem cells increase expression of heme oxygenase-1 leading to anti-inflammatory activity in treatment of acute liver failure. *Stem cell research & therapy*. 2017;8(1):70.
90. Grochot-Przeczek A, Dulak J, Jozkowicz A. Therapeutic angiogenesis for revascularization in peripheral artery disease. *Gene*. 2013;525(2):220-8.
91. Lin HH, Chen YH, Chang PF, Lee YT, Yet SF, Chau LY. Heme oxygenase-1 promotes neovascularization in ischemic heart by coinduction of VEGF and SDF-1. *J Mol Cell Cardiol*. 2008;45(1):44-55.
92. Tejada S, Manayi A, Daglia M, Nabavi SF, Suredda A, Hajheydari Z, et al. Wound Healing Effects of Curcumin: A Short Review. *Current pharmaceutical biotechnology*. 2016;17(11):1002-7.
93. Thangapazham RL, Sharma A, Maheshwari RK. Beneficial role of curcumin in skin diseases. *Advances in experimental medicine and biology*. 2007;595:343-57.
94. Cheppudira B, Fowler M, McGhee L, Greer A, Mares A, Petz L, et al. Curcumin: a novel therapeutic for burn pain and wound healing. *Expert opinion on investigational drugs*. 2013;22(10):1295-303.
95. Akbik D, Ghadiri M, Chrzanowski W, Rohanizadeh R. Curcumin as a wound healing agent. *Life sciences*. 2014;116(1):1-7.
96. Senger DR, Cao S. Diabetic Wound Healing and Activation of Nrf2 by Herbal Medicine. *Journal of nature and science*. 2016;2(11).

97. Ravingerova T, Farkasova V, Griecsova L, Carnicka S, Murarikova M, Barlaka E, et al. Remote preconditioning as a novel "conditioning" approach to repair the broken heart: potential mechanisms and clinical applications. *Physiol Res*. 2016;65 Suppl 1:S55-64.
98. Tapuria N, Kumar Y, Habib MM, Abu Amara M, Seifalian AM, Davidson BR. Remote ischemic preconditioning: a novel protective method from ischemia reperfusion injury--a review. *J Surg Res*. 2008;150(2):304-30.
99. Masaoka K, Asato H, Umekawa K, Imanishi M, Suzuki A. Value of remote ischaemic preconditioning in rat dorsal skin flaps and clamping time. *J Plast Surg Hand Surg*. 2016;50(2):107-10.
100. Kraemer R, Lorenzen J, Kabbani M, Herold C, Busche M, Vogt PM, et al. Acute effects of remote ischemic preconditioning on cutaneous microcirculation--a controlled prospective cohort study. *BMC Surg*. 2011;11:32.
101. Kolbenschlag J, Sogorski A, Kapalschinski N, Harati K, Lehnhardt M, Daigeler A, et al. Remote Ischemic Conditioning Improves Blood Flow and Oxygen Saturation in Pedicled and Free Surgical Flaps. *Plast Reconstr Surg*. 2016;138(5):1089-97.
102. Shaked G, Czeiger D, Abu Arar A, Katz T, Harman-Boehm I, Sebbag G. Intermittent cycles of remote ischemic preconditioning augment diabetic foot ulcer healing. *Wound Repair Regen*. 2015;23(2):191-6.
103. Epps JA, Smart NA. Remote ischaemic conditioning in the context of type 2 diabetes and neuropathy: the case for repeat application as a novel therapy for lower extremity ulceration. *Cardiovasc Diabetol*. 2016;15(1):130.
104. Millicovsky G, Johnston MC. Hyperoxia and hypoxia in pregnancy: simple experimental manipulation alters the incidence of cleft lip and palate in CL/Fr mice. *Proceedings of the National Academy of Sciences of the United States of America*. 1981;78(9):5722-3.
105. Chaplin DD. Overview of the immune response. *J Allergy Clin Immunol*. 2010;125(2 Suppl 2):S3-23.
106. Matzinger P. The danger model: a renewed sense of self. *Science*. 2002;296(5566):301-5.
107. Matzinger P. Tolerance, Danger, and the Extended Family. *Annu Rev Immunol*. 1994;12:991-1045.
108. Dutra FF, Bozza MT. Heme on innate immunity and inflammation. *Front Pharmacol*. 2014;5:115.
109. Alayash AI. Oxidative mechanisms of hemoglobin-based blood substitutes. Artificial cells, blood substitutes, and immobilization biotechnology. 2001;29(6):415-25.
110. Letarte PB, Lieberman K, Nagatani K, Haworth RA, Odell GB, Duff TA. Hemin: levels in experimental subarachnoid hematoma and effects on dissociated vascular smooth-muscle cells. *J Neurosurg*. 1993;79(2):252-5.
111. Nath KA, Grande JP, Haggard JJ, Croatt AJ, Katusic ZS, Solovey A, et al. Oxidative stress and induction of heme oxygenase-1 in the kidney in sickle cell disease. *The American journal of pathology*. 2001;158(3):893-903.
112. Belcher JD, Beckman JD, Balla G, Balla J, Vercellotti G. Heme degradation and vascular injury. Antioxidants & redox signaling. 2010;12(2):233-48.
113. Kharbanda RK, Mortensen UM, White PA, Kristiansen SB, Schmidt MR, Hoschitzky JA, et al. Transient limb ischemia induces remote ischemic preconditioning in vivo. *Circulation*. 2002;106(23):2881-3.
114. Lim SY, Hausenloy DJ. Remote ischemic conditioning: from bench to bedside. *Front Physiol*. 2012;3:27.
115. Wever KE, Masereeuw R, Wagener FA, Verweij VG, Peters JG, Pertijs JC, et al. Humoral signalling compounds in remote ischaemic preconditioning of the kidney, a role for the opioid receptor. *Nephrol Dial Transplant*. 2013;28(7):1721-32.
116. Wever KE, Warle MC, Wagener FA, van der Hoorn JW, Masereeuw R, van der Vliet JA, et al. Remote ischaemic preconditioning by brief hind limb ischaemia protects against renal ischaemia-reperfusion injury: the role of adenosine. *Nephrol Dial Transplant*. 2011;26(10):3108-17.
117. Hausenloy DJ, Candilio L, Evans R, Ariti C, Jenkins DP, Kolvekar S, et al. Remote Ischemic Preconditioning and Outcomes of Cardiac Surgery. *N Engl J Med*. 2015;373(15):1408-17.
118. Sukkar L, Hong D, Wong MG, Badve SV, Rogers K, Perkovic V, et al. Effects of ischaemic conditioning on major clinical outcomes in people undergoing invasive procedures: systematic review and meta-analysis. *BMJ*. 2016;355:i5599.
119. Garratt KN, Whittaker P, Przyklen K. Remote Ischemic Conditioning and the Long Road to Clinical Translation: Lessons Learned From ERICCA and RIPHeart. *Circ Res*. 2016;118(7):1052-4.
120. King N, Dieberg G, Smart NA. Remote ischaemic pre-conditioning does not affect clinical outcomes following coronary Artery bypass grafting. A systematic review and meta-analysis. *Clinical Trials and Regulatory Science in Cardiology*. 2016;17:1-8.
121. Cremers NA, Wever KE, Wong RJ, van Rheden RE, Vermeij EA, van Dam GM, et al. Effects of Remote Ischemic Preconditioning on Heme Oxygenase-1 Expression and Cutaneous Wound Repair. *Int J Mol Sci*. 2017;18(2).

122. Medzhitov R, Schneider DS, Soares MP. Disease tolerance as a defense strategy. *Science*. 2012;335(6071):936-41.
123. Koh TJ, DiPietro LA. Inflammation and wound healing: the role of the macrophage. *Expert Rev Mol Med*. 2011;13:e23.
124. Wagener FA, van Beurden HE, von den Hoff JW, Adema GJ, Figdor CG. The heme-heme oxygenase system: a molecular switch in wound healing. *Blood*. 2003;102(2):521-8.
125. Rossi M, Delbaue S, Wespes E, Roumeguere T, Leo O, Flamand V, et al. Dual effect of hemin on renal ischemia-reperfusion injury. *Biochem Biophys Res Commun*. 2018.
126. Rosin DL, Okusa MD. Dangers within: DAMP responses to damage and cell death in kidney disease. *J Am Soc Nephrol*. 2011;22(3):416-25.
127. Soares MP, Bozza MT. Red alert: labile heme is an alarmin. *Curr Opin Immunol*. 2016;38:94-100.
128. Castellheim A, Brekke OL, Espevik T, Harboe M, Mollnes TE. Innate immune responses to danger signals in systemic inflammatory response syndrome and sepsis. *Scand J Immunol*. 2009;69(6):479-91.
129. Barton GM. A calculated response: control of inflammation by the innate immune system. *J Clin Invest*. 2008;118(2):413-20.
130. Soares MP, Gozzelino R, Weis S. Tissue damage control in disease tolerance. *Trends Immunol*. 2014;35(10):483-94.
131. Bouabe H, Okkenhaug K. Gene targeting in mice: a review. *Methods Mol Biol*. 2013;1064:315-36.
132. Bhuiyan MI, Kim YJ. Mechanisms and prospects of ischemic tolerance induced by cerebral preconditioning. *Int Neurolog J*. 2010;14(4):203-12.
133. Rennert RC, Sorkin M, Garg RK, Gurtner GC. Stem cell recruitment after injury: lessons for regenerative medicine. *Regen Med*. 2012;7(6):833-50.
134. Suttorp CM, Cremers NA, van Rheden R, Regan RF, Helmich P, van Kempen S, et al. Chemokine Signaling during Midline Epithelial Seam Disintegration Facilitates Palatal Fusion. *Front Cell Dev Biol*. 2017;5:94.
135. Lundvig DM, Scharstuhl A, Cremers NA, Pennings SW, te Paske J, van Rheden R, et al. Delayed cutaneous wound closure in HO-2 deficient mice despite normal HO-1 expression. *J Cell Mol Med*. 2014;18(12):2488-98.
136. Shanks N, Greek R, Greek J. Are animal models predictive for humans? *Philos Ethics Humanit Med*. 2009;4:2.
137. Grada A, Mervis J, Falanga V. Research Techniques Made Simple: Animal Models of Wound Healing. *J Invest Dermatol*. 2018;138(10):2095-105 e1.
138. Justice MJ, Dhillon P. Using the mouse to model human disease: increasing validity and reproducibility. *Dis Model Mech*. 2016;9(2):101-3.
139. Grose R, Werner S. Wound-healing studies in transgenic and knockout mice. *Mol Biotechnol*. 2004;28(2):147-66.

Chapter 9

Summary

Chapter 1 introduces the topic of cleft lip and/ or palate (CL/P), its incidence and related problems, the process of palatogenesis, and the etiology and treatment strategies of CL/P. The close similarity between biological processes involved in palatogenesis and wound repair was discussed. We postulated that the balance between injurious and protective signaling determines wound repair, the level of scar formation, and the risk of congenital abnormalities, such as CL/P. Therefore, we split this thesis into three parts:

- I). Decreased protective mechanisms hamper tissue repair and craniofacial development,
- II). Activation of protective mechanisms to enhance tissue regeneration, and
- III). General discussion and Summary

Part I consists of three studies investigating the effects of decreased protective mechanisms on wound repair and palatogenesis.

Chapter 2 evaluated the contribution of the cytoprotective enzyme heme oxygenase (HO) during excisional wound repair using HO-2 knockout (KO) and wild-type (WT) mice. HO-1 has previously shown to be very important during wound repair and embryonic development, and lack of HO-1 results in severe problems. The mild phenotype in HO-2 KO animals results in attenuated corneal wound repair, but more data investigating the role of HO-2 in other morbidities is scarce. Here, we showed that lack of HO-2 expression resulted in hampered wound repair, and reduced collagen deposition and vessel density when compared to WT mice. Although there were no differences between the two genotypes in inflammation, HO-1 expression, and proliferation and differentiation of myofibroblasts, CXCL11 expression was delayed in HO-2 KO mice. Abnormal CXCL11 regulation has been linked to hampered wound repair and disturbed angiogenesis. This may help explain the observed hampered wound repair following HO-2 depletion.

In **Chapter 3**, the disappearance of the midline epithelial seam (MES), a crucial process during palatal fusion and CL/P formation, was investigated. During palatogenesis several processes are similar to wound repair processes, including mesenchymal-epithelial cross-talk, chemokine signaling, and cell proliferation, differentiation and apoptosis. Therefore, we postulated that chemokine CXCL11, its receptor CXCR3, and HO, which all are important factors during wound repair, also play a decisive role during palatogenesis. The contribution of HO-2 in this process was studied using HO-2 KO and WT mice. HO-2 KO embryos at day 15-16 of intrauterine gestation suffered from fetal growth restriction and craniofacial abnormalities, but had no problems with palatal fusion. In both WT and HO-2 KO mice, CXCR3-positive macrophages were recruited towards the CXCL11 expressing MES, and contained multiple apoptotic DNA fragments, supporting the hypothesis that the MES was disintegrated by epithelial apoptosis. Since macrophages located near the MES were HO-1 positive, and more HO-1 positive cells were present in HO-2 KO mice, HO-1 induction forms likely a compensatory mechanism to handle oxidative stressors. HO and CXCL11/CXCR3 signaling play thus also an important role in embryogenesis and palatal fusion.

In **Chapter 4**, since CL/P patients after cleft surgery experience mechanical stress during wound repair from myofibroblasts and the growing head, static mechanical stress was induced in a mouse model, to simulate the increased injurious environment and the effects of decreased protective pathways. Mechanical stress during wound repair was applied using a splinted excisional wound model. HO-1 is thought to orchestrate the defense

against inflammatory and oxidative insults that drive fibrosis, and therefore we investigated the activation of the HO-system in splinted and non-splinted excisional wound models using HO-1 luc transgenic mice. These mice co-express luciferase when HO-1 gets induced, which can be measured *in vivo* by administration of the substrate luciferin which results in the release of photons. After seven days, splinting had delayed cutaneous wound closure and HO-1 protein expression, whereas the number of F4/80-positive macrophages, α SMA-positive myofibroblasts, and pro-inflammatory signals IL-1 β , TNF- α , and COX-2 were increased after application of mechanical stress. The pro-inflammatory environment following splinting may explain the higher myofibroblast numbers and increased risk of fibrosis and scar formation when compared to non-splinted wounds.

Part II consists of three studies investigating the effects of activation of protective pathways using preconditioning strategies on mesenchymal stem cell (MSC) apoptosis, wound repair, and organs. In the latter study, we designed a novel “tissue survival theory” that could help explain how tissue gets first warned by tissue survival factors (TSFs) following injurious insults.

Chapter 5 investigated the effects of the cytoprotective HO-system on MSC survival following pharmacological preconditioning. MSC therapy is considered a promising strategy for a wide diversity of injuries and diseases. However, the survival of MSCs after administration is limited due to the hostile wound microenvironment displaying an accumulation of oxidative and inflammatory stressors. A prolonged MSC survival by preconditioning strategies could improve their therapeutic efficacy. In this study, the anti-oxidative and anti-apoptotic effects of HO-1, HO-2 and its effector molecules were investigated on adipose-derived MSC (ASC) survival. HO-1 was induced following curcumin treatment, and this provided potent protection against oxidative stress, which was mediated by hydrogen peroxide (H₂O₂). This protection was abrogated by simultaneous treatment with the selective HO-1 activity inhibitor QC15, supporting an HO-1-dependent protective mechanism. Also, exposure to anti-oxidant N-acetylcysteine protected against H₂O₂-induced ASC apoptosis, while the HO-effector molecules and anti-oxidants bilirubin and biliverdin did not have an effect. Interestingly, HO-effector molecule CO did also rescue H₂O₂-induced ASC death, suggesting that HO-1 provided protection against apoptosis via CO signaling. No differences were found between WT, and HO-2 KO derived ASCs in sensitivity towards H₂O₂, or curcumin and HO-effector molecules-mediated protection. Thus, induction of cytoprotective molecules by pharmacological preconditioning led to better protection against oxidative stress in an *in vitro* model of stem cell survival.

Next, in **Chapter 6**, we analyzed the effects of remote ischemic preconditioning (RIPC) on cutaneous tissue injury. RIPC has shown that transient occlusion of the blood flow to a limb will induce a stress response that protects the body against a secondary more harmful stress, e.g., transplantation and organ injuries. We aimed to improve excisional wound repair using early and late RIPC (respectively 5 min and 24h before wounding) and investigated the role of HO-1 using HO-1 *luc* transgenic mice. HO-1 promoter activity was induced dorsally, and locally in the kidneys, following RIPC treatment. On mRNA level, HO-1 was increased in the ligated muscle, heart, and kidneys, but surprisingly not in the skin. Early and late RIPC did not change HO-1 mRNA and protein levels in the wounds seven days after cutaneous injury, nor did it accelerate cutaneous wound closure or did it affect collagen deposition. Thus, the used RIPC protocol induces HO-1 expression in several

organs, but not the skin, and did not improve excisional wound repair, suggesting that the skin is insensitive to RIPC-mediated protection. However, other studies showed that RIPC improved transplanted skin flap survival and improved healing of diabetic ulcers. Possibly other signals play a decisive role.

Lastly, **Chapter 7** proposes a novel molecular mechanism that explains how the tissue is protected from injurious agents or collateral damage following the attack by an activated immune system. TSFs mediate tissue protection while danger signals alert the immune system. Hemopexin (hpx) can scavenge heme, and form the heme-hpx complex that can bind to LRP-1 having a protective effect. When hpx levels are exhausted or depleted, the excess of free heme can bind to TLR-4 and alarm the immune system resulting in a pro-inflammatory effect. We proposed that the presence of hpx is the discriminating factor between tissue repair and tissue damage, and provided a new concept of how RIPC can induce protective HO-1 signaling. RIPC led to the release of low levels of heme, and the induction of HO-1, which was co-expressed with LRP-1. We propose that systemic protection mediated by RIPC is orchestrated via binding of the heme-hpx complex, a tissue survival factor (TSF), to LRP-1, subsequently activating protective responses, including HO-1. Therefore, the binding of heme by hpx may regulate tissue protection or immune activation.

In **Part III**, the most important results of this thesis and their clinical relevance were summarized and discussed, and future perspectives for therapeutical approaches were proposed.

The induction of cytoprotective pathways, such as HO-1, by pharmacological therapy or by application of RIPC or administration of hpx, may harness inflammatory and oxidative insults. Therefore, these strategies may prevent CL/P formation and improve the outcome of tissue repair in patients with CL/P or burn wounds. However, more mechanistic and translational research is necessary before it can be used in the clinic.

In conclusion, decreased activity of protective pathways can hamper wound repair and craniofacial development, whereas induction of protective signaling cascades, with a focus on pathways that mediate the resolution of oxidative and inflammatory stress, may provide a regenerative microenvironment that improves wound repair and regeneration.

Chapter 10

Samenvatting

Hoofdstuk 1 introduceert het onderwerp schisis (gespleten lip/ gehemelte (CL/P)), de incidentie en gerelateerde problemen, de ontwikkeling van het palatum en de etiologie en behandelingsstrategieën van CL/P. De sterke overeenkomst tussen de biologische processen die betrokken zijn bij palatogenese en bij wondgenezing werden besproken. We veronderstelden dat de balans tussen schadelijke en beschermende factoren de wondgenezing, de mate van littekenvorming en de kans op aangeboren afwijkingen zoals CL/P bepaalt. Het proefschrift bestaat uit drie delen:

- I). Belemmering van weefselherstel en craniofaciale ontwikkeling door verminderde beschermende mechanismen,
- II). Verbetering van weefselregeneratie door activering van beschermende mechanismen,
- III). Algemene discussie en samenvatting

Deel I bestaat uit drie studies die de effecten van verminderde beschermende mechanismen bestuderen op wondgenezing en craniofaciale ontwikkeling.

Hoofdstuk 2 evalueerde de rol van het celbeschermende enzym heme oxygenase (HO) tijdens wondgenezing met behulp van HO-2 knockout (KO) en wild-type (WT) muizen. Eerder is aangetoond dat HO-1 zeer belangrijk is tijdens wondgenezing en embryologische ontwikkeling en dat het ontbreken van HO-1 resulteert in ernstige problemen. Het mildere fenotype in HO-2 KO muizen leidt tot vertraagde corneale wondgenezing, maar meer gegevens over de rol van HO-2 in andere morbiditeiten zijn schaars. Wij hebben hier in een excisioneel wondmodel aangetoond dat gebrek aan HO-2-expressie resulteert in vertraagde wondgenezing, verminderde collageenafzetting en een verlaagde vaatdichtheid. Hoewel er in vergelijking met WT muizen geen verschillen waren tussen de twee genotypes betreffende ontsteking, de expressie van HO-1 en proliferatie en differentiatie van myofibroblasten, was de expressie van CXCL11 wel vertraagd in HO-2 KO muizen. Abnormale CXCL11 regulatie is eerder in verband gebracht met belemmerde wondgenezing en verstoorde angiogenese. Dit geeft een mogelijke verklaring voor de vertraagde wondgenezing na HO-2 uitschakeling.

In **Hoofdstuk 3** werd de fusie van de epitheliale naad (MES) in het midden van het palatum onderzocht. Dit is een cruciaal proces tijdens palatale fusie en CL/P-vorming. Tijdens palatogenese zijn verschillende ontwikkelingsprocessen vergelijkbaar met wondgenezingsprocessen, waaronder mesenchymale-epitheliale communicatie, chemokine signalering en proliferatie, differentiatie en apoptose van cellen. Daarom veronderstelden we dat het chemokine CXCL11, zijn receptor CXCR3 en het celbeschermende HO, die alle belangrijk zijn tijdens wondgenezing, ook een beslissende rol spelen bij het samenvoegen van de MES. De rol van HO-2 in dit proces werd bestudeerd met behulp van HO-2 KO en WT muizen. HO-2 KO-embryo's op dag 15-16 van intra-uteriene ontwikkeling lijdten aan foetale groei beperking en craniofaciale afwijkingen, maar hadden geen problemen met palatale fusie. In zowel WT- als HO-2 KO-muizen werden CXCR3-positieve macrofagen aangetrokken door CXCL11 dat in de MES tot expressie komt. Deze palatale macrofagen bleken meerdere apoptotische DNA-fragmenten te bevatten. Dit ondersteunt de theorie dat de MES wordt gedesintegreerd door apoptose van het epitheel. Aangezien macrofagen dichtbij de MES HO-1-positief waren en er meer HO-1-positieve cellen aanwezig zijn in HO-2 KO-muizen, dient HO-1 inductie mogelijk als

compensatiemechanisme om oxidatieve stress te neutraliseren. HO- en CXCL11/CXCR3-signalerings spelen dus een belangrijke rol bij embryogenese en palatale fusie.

In **Hoofdstuk 4** werd statische mechanische stress geïnduceerd met behulp van een spalk als model voor de postoperatieve situatie in CL/P patiënten. Op deze manier werden de verhoogde schadelijke omgevingsfactoren en de effecten van verminderde beschermende processen tijdens wondgenezing gesimuleerd. Deze mechanische stress werd toegebracht met behulp van een spalk in een excisioneel wondmodel. HO-1 speelt een rol bij de verdediging tegen inflammatoire en oxidatieve insulten die op hun beurt fibrose en littekens veroorzaken en daarom onderzochten we de activering van het HO-systeem in gespalkte en niet-gespalkte excisionele wonden met behulp van HO-1 *luc* transgene muizen. Deze muizen brengen luciferase tot co-expressie wanneer HO-1 wordt geactiveerd. Dit kan *in vivo* worden gemeten door het substraat luciferine toe te dienen dat leidt tot het vrijkomen van fotonen. Na zeven dagen heeft het spalken van de wonden de wondsluiting en HO-1 eiwit inductie vertraagd, terwijl het aantal F4/80-positieve macrofagen, α SMA-positieve myofibroblasten en de pro-inflammatoire signalen IL-1 β , TNF- α en COX-2 verhoogd waren na blootstelling aan mechanische stress. De pro-inflammatoire omgeving die ontstaat ten gevolge van het spalken kan het toegenomen aantal myofibroblasten en het verhoogde risico op fibrose en littekens verklaren.

Deel II bestaat uit drie studies naar de effecten van activering van beschermende signalering met behulp van preconditioneringsstrategieën op celdood van mesenchymale stamcellen (MSC), wondgenezing en organen. In de laatstgenoemde studie hebben we een nieuwe “weefsel overlevingstheorie” ontworpen die zou kunnen helpen verklaren hoe weefsel eerst wordt gewaarschuwd door weefseloverlevingsfactoren (TSFs) na schadelijke prikkels.

Hoofdstuk 5 onderzoekt de effecten van het celbeschermende HO-systeem op MSC overleving na farmacologische preconditionering. MSC therapie wordt beschouwd als een veelbelovende behandeling voor een grote verscheidenheid van verwondingen en ziekten. De overleving van MSCs na toediening is echter beperkt door de vijandige wondomgeving met veel oxidatieve en inflammatoire stress. Een langdurige overleving van de MSCs door preconditioneringsstrategieën zou de therapeutische efficiëntie kunnen verbeteren. In deze studie werden de anti-oxidatieve en anti-apoptotische effecten van HO-1, HO-2 en hun effectormoleculen onderzocht op de overleving van MSCs afkomstig uit vetweefsel (ASCs). HO-1 werd geïnduceerd door behandeling met curcumine en dit bood bescherming tegen waterstofperoxide (H_2O_2) geïnduceerde oxidatieve stress. Deze bescherming werd voorkomen door gelijktijdige behandeling van curcumine met de HO-1 activiteitsremmer QC15. Deze bevinding ondersteunt een HO-1-afhankelijk beschermend mechanisme van curcumine. Ook de anti-oxidant N-acetylcysteïne beschermt tegen H_2O_2 -geïnduceerde ASC celdood, terwijl de HO-effectormoleculen en tevens anti-oxidanten bilirubine en biliverdine dat niet deden. Interessant is dat het koolstofmonoxide (CO) afgevend molecuul (CORM) ook H_2O_2 -geïnduceerde ASC-dood voorkwam, wat suggereert dat HO-1 bescherming kan bieden via zijn effector molecuul CO. Er werden geen verschillen gevonden tussen ASCs afkomstig van WT en HO-2 KO muizen in hun gevoeligheid voor H_2O_2 , of de bescherming door curcumine of de HO-effectormoleculen. De inductie van celbeschermende moleculen door farmacologische preconditionering leidt tot een betere bescherming tegen oxidatieve stress in een *in vitro* model van stamceloverleving.

Vervolgens onderzochten we in **Hoofdstuk 6** de effecten van ischemische preconditionering 'op afstand' (RIPC) op wondgenezing. Bij RIPC wordt door kortstondige afklemming van de bloedstroom naar een ledemaat een niet ernstige stressreactie teweeg gebracht. Deze lichte stress beschermt het lichaam tegen een secundaire meer schadelijke stress, zoals bijvoorbeeld tijdens transplantaties en orgaanletsel. We probeerden excisionele wondgenezing te verbeteren door het toepassen van een 'vroeg' of 'late' RIPC behandeling (respectievelijk 5 min en 24 uur voor verwonding) en onderzochten de rol van HO-1 hierop met behulp van HO-1 *luc* transgene muizen. HO-1-promotoractiviteit werd dorsaal en lokaal in de nieren geïnduceerd na de RIPC behandeling. Op mRNA niveau was HO-1 verhoogd in de afgeklemde spieren, het hart en de nieren, maar verrassend genoeg niet in de huid. Zowel 'vroeg' als 'late' RIPC veranderde de HO-1 mRNA en eiwitniveaus niet in de dorsale wonden 7 dagen na verwonding, noch beïnvloedde het de snelheid van de wondsluiting of de collageenafzetting. Aangezien RIPC de expressie van HO-1 verhoogt in verschillende organen, maar niet in de huid en RIPC de excisionele wondgenezing niet verbetert, wordt gesuggereerd dat de huid ongevoelig is voor RIPC-gemedieerde bescherming. Hoewel andere studies lieten zien dat RIPC de overleving van getransplanteerde huidflappen en de genezing van diabetische ulcers verbetert. Mogelijk spelen andere signalen een beslissende rol.

Tenslotte werd in **Hoofdstuk 7** een nieuw moleculair mechanisme voorgesteld voor de bescherming van het weefsel tegen schadelijke stoffen of tegen bijkomende schade als gevolg van een aanval door een geactiveerd immuunsysteem. TSFs veroorzaken weefselbescherming terwijl alarmsignalen het immuunsysteem activeren. Hemopexine (hpx) kan heme wegvangen en het haem-hpx complex vormen dat kan binden aan LRP-1 en een beschermend effect teweegbrengen. Wanneer hpx is uitgeput of uitgeschakeld, dan bindt het in overmaat zijnde vrije haem aan TLR-4 en wordt het immuunsysteem gealarmeerd, resulterend in een pro-inflammatoir effect. We stelden voor dat de aanwezigheid van hpx de onderscheidende factor is tussen weefselherstel en weefselbeschadiging en we komen tot een nieuw concept over hoe RIPC kan leiden tot beschermende HO-1 signalering. RIPC leidt tot het vrijkomen van lage hoeveelheden haem en de inductie van HO-1, dat samen met LRP-1 gelokaliseerd tot expressie komt. We stellen daarom voor dat systemische bescherming gemedieerd door RIPC wordt geregeld door binding van de TSF, het haem-hpx-complex, aan LRP-1 en vervolgens beschermende mechanisme, zoals HO-1, activeert. Zodoende kan de binding van haem door hpx het onderscheid maken tussen weefselbescherming of immuunactivatie.

In **Deel III** zijn de belangrijkste resultaten van dit proefschrift en wat ze betekenen voor de kliniek samengevat en besproken en werden toekomstige therapeutische strategieën voorgesteld.

De inductie van een celbeschermend mechanisme, zoals HO-1, door farmacologische behandeling met bijvoorbeeld curcumine of hpx of door toepassing van RIPC, kan inflammatoire en oxidatieve stress afwenden. Zodoende vormen deze opties interessante strategieën om schisis te voorkomen en de uitkomst van weefselgenezing te verbeteren bij patiënten met schisis of brandwonden. Er is echter meer mechanistisch en translationeel onderzoek nodig voordat dit klinisch kan worden toegepast.

Concluderend kan worden gesteld dat een verminderde activiteit van beschermende processen wondgenezing, craniofaciale ontwikkeling en palatogenese zal belemmeren, terwijl inductie van beschermende processen, met name degene die leiden tot de opheffing van oxidatieve en inflammatoire stress, een regeneratieve omgeving creëren die wondgenezing en regeneratie zal verbeteren.

Dankwoord

Naar aanleiding van mijn promotieonderzoek is dit proefschrift geschreven aan het Radboudumc op de afdeling Tandheelkunde, vakgroep Orthodontie en Craniofaciale Biologie te Nijmegen. Allen die hebben bijgedragen aan het tot stand komen van dit proefschrift wil ik van harte bedanken. Een aantal mensen verdienen een speciaal woord van dank, omdat zonder hun hulp en inzet dit proefschrift niet zijn huidige vorm had kunnen bereiken.

Mijn promotoren prof. dr. Carine Carels en em. prof. dr. Anne Marie Kuijpers-Jagtman, allereerst bedankt voor het in mij gestelde vertrouwen dat tot aanstelling van mijn PhD positie heeft geleid. Ik wil jullie beiden bedanken voor jullie inzet en begeleiding tijdens mijn proefschrift, het kritisch commentaar tijdens presentaties en op de manuscripten hebben geleid tot een mooi eindresultaat. Beste Carine, ik hoop dat alles goed met u gaat en ik wens u het allerbeste. Beste Anne Marie, fijn dat u als emeritus hoogleraar nog de tijd heeft om mij bij te staan tijdens deze promotie. Ik heb enorm veel respect voor wat u heeft bereikt als onderzoeker.

Beste dr. Frank Wagener, als co-promotor ben jij zonder twijfel degene die het meest intensief betrokken is geweest bij mijn promotietraject. Ik wil je dan ook van harte bedanken voor al je input. Zonder jouw hulp was dit proefschrift nooit tot stand gekomen en ik ben je hier erg dankbaar voor. Je onuitputbare bron van inspiratie, motivatie en ongekend positieve instelling zijn een uitstekend voorbeeld van hoe ik me als onderzoeker en persoon wil profileren.

Uiteraard wil ik ook alle collega's van de afdeling Orthodontie en Craniofaciale Biologie bedanken. Beste Jan Schols, Hans, Jaap, Ditte, Katrien, Bas, Sander, Corien, René, Pia, Coby, Aysel, Kriti, Marjon, Paola, Liesbeth, Doris, Roel, het secretariaat, de verschillende generaties orthodontisten in opleiding en de studenten tandheelkunde, allemaal hartelijk bedankt voor het stimulerende werkklimaat en de aangename sfeer op de afdeling. Ik waardeer de leuke en spontane momenten die op kantoor plaatsvonden. Collega's in het lab bedankt voor de collegiale instelling en prettige samenwerking met diverse experimenten. Graag betrek ik hierbij ook de afdeling biomaterialen en uit ik mijn dankbaarheid ook naar hen, aangezien het laboratorium gemeenschappelijk gedeeld is.

De leden van de promotiecommissie, bestaande uit prof. dr. G.J. Meijer, prof. dr. E. Middelkoop, dr. H.A.M. Mutsaers, prof. dr. I. Lambrichts, prof. dr. P.J. Sloomweg en dr. K.E. Wever, wil ik graag bedanken voor hun geïnvesteerde tijd bij het beoordelen van mijn proefschrift en voor hun bereidheid om zitting te nemen in mijn promotiecommissie. Rector Magnificus prof. dr. J.H.J.M. van Krieken, bedankt voor het voorzitten van mijn promotie.

In mijn experimenten is veelvuldig gebruik gemaakt van proefdieren. Helaas is proefdieronderzoek noodzakelijk om ziektebeelden en behandelingen beter in kaart te brengen. We zijn samen met de ethische toetsingscommissie van mening dat de belangen van deze medische kennis opwegen tegen het ongerief dat we toebrachten aan de dieren.

Graag wil ik het centraal dierenlaboratorium, met name de afdelingen SPF en PRIME van harte bedanken, beste Bianca, Daphne, Debbie, Helma en Jeroen, bedankt voor jullie hulp met de dierenexperimenten.

Na afronding van het experimenteel werk en het indienen van mijn artikelen bij wetenschappelijke tijdschriften ben ik bij de afdeling reumatologie aan het werk gegaan als onderzoeker. Beste Peter van Lent, ik ben blij dat ik onder jouw leiding in werkgroep 4 de rol van leukocyten op artrose heb mogen onderzoeken. Je bent een echte wetenschapper met passie en ik heb veel van je geleerd en een ander inzicht in wetenschappelijk onderzoek gekregen. Werkgroep 4, Edwin, Arjen, Martijn, Wouter, Annet, Stephanie, Irene, Giuliana en Nik, bedankt voor de leuke tijd. Beste werkgroepsleiders, Peter van der Kraan, Fons en Marije, ik heb veel van jullie geleerd tijdens de werkbesprekingen en de kritische vragen die jullie over mijn onderzoek hadden. Verder wil ik ook alle andere collega's van de afdeling reumatologie bedanken voor de leuke tijd en gemoedelijke sfeer op het laboratorium.

Gewaardeerde paranimfen, beste Maarten en Christian, bedankt voor het aanvaarden van deze belangrijke plechtige functie. Jullie zijn beiden echte clinici met interesse in het onderzoek. Los van het professionele contact hebben we privé ook gemeenschappelijke interesses. Maarten, samen met jou heb ik ons record op de zevenheuvelenloop gevestigd, of eigenlijk moet ik zeggen dankzij jou. Een tijd die ik graag nog eens samen met je zal verbreken. Christian, jij hebt me ingewijd in de Vlaamse manier van denken en doen. Beiden heel veel succes met jullie eigen proefschrift.

Lieve vrienden, familie en schoonfamilie, bedankt voor jullie steun en interesse in mijn onderzoek, maar vooral voor de fijne momenten samen! Fijn dat jullie bij de verdediging van mijn proefschrift aanwezig zijn.

Beste ouders, jullie hebben de grootste invloed gehad op mijn ontwikkeling. Allereerst bedankt voor de opvoeding, het stimuleren om hard te studeren en er altijd voor mij te zijn. Dit werpt nu z'n vruchten af. Hoewel een deel uit mijn proefschrift voor jullie mogelijk wat lastig te begrijpen is hielden jullie het enthousiasme om er toch alles over te willen weten. Ik weet dat jullie trots zijn op het resultaat.

Esther, de belangrijkste persoon in mijn leven, bedankt voor je onvoorwaardelijke steun en al je liefde. Je hebt me altijd weten te motiveren om door te zetten en nooit "af te geven". Hoewel ik dankzij die eigenschap jou ook heb weten te veroveren. Ik ben blij dat we na lange tijd op en neer pendelen gelukkig samenwonen. Wie weet ruil ik mijn Nederlandse paspoort ooit nog wel in voor een Belgische. Ik ben benieuwd wat de toekomst ons nog meer brengt en ga ieder avontuur graag met je aan. Ik houd van je!

Niels Creemers


Curriculum Vitae

Niels Cremers received his Bachelor's degree in biochemistry in June 2006 and started working as a research technician at the Department of Pathology of the Canisius-Wilhelmina Hospital in Nijmegen. At the same time, he started his Master's degree programme in Biomedical Sciences at the Radboud University Nijmegen. In 2008 he did his research internship for his first Major in Human Pathobiology at the Department of Biomedical Engineering at the University of Memphis in the USA. Here, he developed antibiotic loaded scaffolds to improve cutaneous wound healing. For his second Major in Toxicology he did an internship at the Department of Orthodontics and Craniofacial Biology (OCB) at the Radboud university medical center (Radboudumc), where he investigated cytoprotective mechanisms for cell-based therapies. In 2010 he completed his Master's degree and started his PhD project "Cytoprotective mechanisms, palatogenesis, and wound repair" at the department of OCB of which this thesis is the result. In 2015 he started to work as a post-doctoral researcher in the Department of Experimental Rheumatology of the Radboudumc where he investigated the role of inflammation and leucocytes on osteoarthritis. Currently, he works as a research associate on honey-based wound care products (L-Mesitran) at the company Triticum in Maastricht.

List of publications

Research articles

Curcumin-induced heme oxygenase-1 expression prevents H₂O₂-induced cell death in wild type and heme oxygenase-2 knockout adipose-derived mesenchymal stem cells, **Cremers NA**, Lundvig DM, van Dalen SC, Schelbergen RF, van Lent PL, Szarek WA, Regan RF, Carels CE, Wagener FA. *International Journal of Molecular Sciences*, 2014 Oct 8;15(10):17974-99.

Delayed cutaneous wound closure in HO-2 deficient mice despite normal HO-1 expression, Lundvig DM*, Scharstuhl A*, **Cremers NA**, Pennings SW, te Paske J, van Rheden R, van Run- van Breda C, Regan RF, Russel FG, Carels CE, Maltha JC, Wagener FA. *Journal of Cellular and Molecular Medicine*, 2014 Dec;18(12):2488-98. *contributed equally

Mechanical stress changes the complex interplay between HO-1, inflammation and fibrosis, during excisional wound repair, **Cremers NA**, Suttorp M, Gerritsen MM, Wong RJ, van Run- van Breda C, van Dam GM, Brouwer KM, Kuijpers-Jagtman AM, Carels CE, Lundvig DM, Wagener FA. *Frontiers in Medicine*, 2015 Dec 15;2:86.

Effects of Remote Ischemic Preconditioning on Heme Oxygenase-1 Expression and Cutaneous Wound Repair. **Cremers NA**, Wever KE, Wong RJ, van Rheden RE, Vermeij EA, van Dam GM, Carels CE, Lundvig DM, Wagener FA. *International Journal of Molecular Sciences*, 2017 Feb 17;18(2).

Chemokine signaling during midline epithelial seam disintegration facilitates palatal fusion, Suttorp CM, **Cremers NA**, van Rheden R, Regan RF, Helmich P, van Kempen S, Kuijpers- Jagtman AM, Wagener FADTG. *Frontiers in Cell and Developmental Biology*, 2017 Oct 30;5:94.

Heme scavenging discriminates between tissue survival and immune activation, **Cremers NAJ**, Wong RJ, Helmich P, Bilos A, Brouwer KM, van Dam GM, Carels CEL, Matzinger P, Kuijpers-Jagtman AM, Immenschuh S, Wagener FADTG. *To be submitted*.

S100A8/A9 increases the mobilization of pro-inflammatory Ly6Chigh monocytes to the synovium during experimental osteoarthritis, **Cremers NAJ**, van den Bosch MHJ, van Dalen S, Di Ceglie I, Ascone G, van de Loo F, Koenders M, van der Kraan P, Sloetjes A, Vogl T, Roth J, Geven EJW, Blom AB, van Lent PLEM. *Arthritis Research and Therapy*, 2017 Sep 29;19:217.

Fc gamma receptor-mediated influx of S100A8/A9-producing neutrophils as important determinant of bone erosion during antigen-induced arthritis, Di Ceglie I, Ascone G, **Cremers NAJ**, Sloetjes AW, Walgreen B, Vogl T, Roth J, Verbeek JS, van de Loo FAJ, Koenders MI, van der Kraan PM, Blom AB, van den Bosch MHJ, van Lent PLEM. *Arthritis Research and Therapy*, 2018 May 2;20:80.

The role of NOX2-derived reactive oxygen species in S100A8/A9-driven inflammatory osteoarthritis. van Dalen SCM, Kruisbergen NNL, Walgreen B, Helsen MMA, Slöetjes

AW, **Cremers NAJ**, Koenders MI, van de Loo FAJ, Roth J, Vogl T, Blom AB, van der Kraan PM, van Lent PLEM, van den Bosch MHJ. *Osteoarthritis Cartilage*, 2018 Sep 5. In press.

Book chapter

Effects of Remote Ischemic Preconditioning on Heme Oxygenase-1 Expression and Cutaneous Wound Repair. **Cremers NA**, Wever KE, Wong RJ, van Rheden RE, Vermeij EA, van Dam GM, Carels CE, Lundvig DM, Wagener FA. In: *Wound Repair and Regeneration*, Allison Cowin (Editor), MDPI, 2018 Mar, 98-115.

PhD Portfolio

Name PhD student:	<i>NAJ Cremers</i>	PhD period:	<i>01-09-2010 until 01-11-2018</i>	
Department:	<i>Dentistry</i>	Promotor(s):	<i>Prof.dr. AM Kuijpers-Jagtman,</i>	
Graduate school:	<i>Radboud Institute for Molecular Life Sciences</i>	Co-promotor(s):	<i>Prof.dr. CEL Carels Dr. FADTG Wagener</i>	
TRAINING ACTIVITIES			Year(s)	ECTS
a) Courses & Workshops				
- Graduate course (RIMLS)		2010	2	
- Orientation program PhD students (Radboudumc)		2011	0.15	
- Academic writing (RIMLS PhD course)		2011	3	
- Presenteren eigen onderzoek (Radboud University)		2011	1.5	
- BKO-introductie (basis kwalificatie onderwijs) (Radboud University)		2011	0.15	
- BKO-2: Effectieve individuele begeleiding van studenten (Radboud University)		2011	1	
- Workshop digital tools (Radboud University)		2012	0.3	
- Workshop cell labeling and tracking (ENCITE Leiden)		2012	0.25	
- Workshop Adobe InDesign (PON)		2013	0.1	
b) Seminars & Lectures				
- Research forum, dept. of Orthodontics and Craniofacial Biology*		2011-2014	3	
- RIMLS technical forum: statistics		2010/ 2012	0.4	
- RIMLS technical forum: bioinformatics		2012	0.2	
- RIMLS technical forum: metabolomics		2012	0.2	
- RIMLS technical forum: laboratory animal science		2012	0.2	
- RIMLS technical forum: tissue engineering		2012	0.2	
- RIMLS technical forum: epigenetics		2013	0.2	
- RIMLS technical forum: how to conquer the scientific journals		2013	0.2	
- RIMLS seminar: the myofibroblast during tissue repair and tissue destruction (Boris Hinz)		2010	0.1	
- RIMLS seminar: gene and cell therapy (Bakhos Tannous)		2010	0.1	
- RIMLS seminar: skingeneering (Ernst Reichmann)		2010	0.1	
- RIMLS seminar: artificial skin for burn wounds (Esther Middelkoop)		2010	0.1	
- RIMLS seminar: stem cells and skin cancer (Cedric Blanpain)		2011	0.1	
- RIMLS seminar: fluorescent tags in biological research (Dan Beacham)		2011	0.1	
- RIMLS seminar: gene expression in development and evolution (Pavel Tomancak)		2012	0.1	
- RIMLS seminar: biomaterials and growth factors in regenerative medicine (Jeffrey Hubel)		2012	0.1	
- RIMLS lunch seminar: small RNA in germ cells (Rene Ketting)		2011	0.1	
- RIMLS noon spotlight: genetic and epigenetic pathways of disease		2013	0.1	
- RIMLS noon spotlight: infection and inflammation		2013	0.1	
- RIMLS noon spotlight: regenerative medicine and microenvironment		2013	0.1	
c) (Inter)national Symposia & Congresses				
- NIRM (Netherlands Institute of Regenerative Medicine)/ ISSCR (International Symposium for Stem Cell Research), Amsterdam		2010	0.75	
- New frontiers symposium: Bioenergetics: live and let die (RIMLS), Nijmegen		2010	1	
- MOVE-ACTA meeting: Oral regenerative medicine, Amsterdam		2011	0.25	
- SAWC (Symposium on Advanced Wound Care)/ WHS (Wound Healing Society, Dallas *^)		2011	1	
- NVMB (Nederlandse Vereniging voor Matrix Biologie), Lunteren		2011	0.5	
- ETRS (European Tissue Regeneration Society), Amsterdam*		2011	0.75	
- NVMB: Symposium on inflammation, Amersfoort		2011	0.25	
- New frontiers symposium: Nobel channels (RIMLS), Nijmegen		2011	1	
- PhD retreat RIMLS, Wageningen^		2012	1	
- NVMB, Lunteren*		2012	1	
- Heme Oxygenase Conference, Edinburgh		2012	1.25	
- New frontiers symposium: Personal genomics (RIMLS), Nijmegen		2012	1	
- IOT Dental Research Meeting *, Lunteren		2013	1	
- PhD retreat RIMLS, Wageningen^		2013	1	
- Wetenschapsdag brandwondenstichting, Amersfoort		2013	0.25	
d) Other				
- Organisation of technical forum: tissue engineering		2013	1	
TEACHING ACTIVITIES			Year(s)	ECTS
e) Lecturing				
- Supervision of Bachelor and Master students		2010-2014	4	
TOTAL			31.25	

Oral and poster presentations are indicated with a * and ^ after the name of the activity, respectively.

About the cover: Originally, Da Vinci's Vitruvian man symbolizes an in proportionate human as the center of the universe. Here, a modern touch adds two dimensions. On the left, the individual is injured and suffering from impaired wound repair as visualized by a foot ulcer and scars on the lip and arm. On the right, diverse medical strategies (pharmacological induction of cytoprotective responses, stem cell therapy, and remote ischemic preconditioning by ligation of a limb) have attenuated injury and led to regenerated tissue.